UNIVERSITY OF SOUTHAMPTON

Faculty of Social Sciences
School of Mathematical Sciences

Second-Order Gravitational Self-Force in Kerr Spacetime

DOI: 10.5258/SOTON/T0051

Volume 1 of 1

by

Andrew Robert Clifford Spiers

Msci

ORCiD: 0000-0003-0222-7578

A thesis for the degree of
Doctor of Philosophy

September 2022

University of Southampton

Abstract

Faculty of Social Sciences
School of Mathematical Sciences

Doctor of Philosophy

Second-Order Gravitational Self-Force in Kerr Spacetime

by Andrew Robert Clifford Spiers

Gravitational-wave astronomy has been a burgeoning field of research since the first detection of a merging black hole binary in 2015 [3]. As gravitational-wave detector sensitivity improves, our models must keep pace. The planned space-based detector LISA will be sensitive to new gravitational wave sources, such as extreme-mass-ratio inspirals (EMRIs). Precise extraction of EMRI parameters from LISA data will require highly accurate waveform templates. These templates need models which include, among other things, the dissipative piece of the second-order self-force in Kerr. This thesis formulates methods to help calculate the second-order self-force in Kerr.

In the first part of the thesis, I develop a general framework for second-order calculations by deriving a new form of the second-order Teukolsky equation. I show that the source of this equation is well defined (in a highly regular gauge [151, 185]) for second-order self-force calculations. Additionally, I present methods for calculating second-order gauge-invariants. I produce an algebraic method for calculating a gauge-invariant. I also provide a formalism for calculating a gauge-invariant associated with the Bondi–Sachs gauge (with a fixed BMS frame). The asymptotically flat property of the Bondi–Sachs gauge is shown to circumvent infrared divergences that arise in generic second-order calculations.

Next, I calculate a general formula for the second-order source, decomposed into spherical harmonics, in Schwarzschild. Using this formula, I help to implement a framework for quasi-circular inspirals in Schwarzschild. I transform the source to a near-Bondi–Sachs gauge, increasing the asymptotic falloff by two orders in r. My collaborator Ben Leather integrates the resulting source. From the resulting quantity, we will extract fluxes and evolve inspirals to first post-adiabatic accuracy.

In the final part, I take a step toward implementation in Kerr by developing a new method of constructing a more regular first-order perturbation [183]. To help formulate this method, I implement Green–Hollands–Zimmerman metric construction [86] for a stationary point-mass in flat spacetime.

Contents

List of Figures

List of Tables

List of Additional Material

Mathematica notebook containing $\delta G_{ab}[h^{(1)}_{ab}]$ and $\delta^2 G_{ab}[h^{(1)}_{ab}]$ in the GHP formalism.

Mathematica notebook containing $\psi^{(2)}_{4Q}$ in the NP and GHP formalism (defined in Petrov type D spacetime with a principle null direction aligned background tetrad and a perturbed tetrad defined in App. A).

Mathematica notebook containing a formula for the decomposed modes of $\delta^2 G_{ab}[h^{(1)}_{ab}]$ in Schwarzschild in the Carter tetrad.

Mathematica notebook containing a formula for the decomposed modes of the jump in $\psi^{(2)}_{4L}$ due to the gauge transform from the Lorenz gauge to Bondi–Sachs gauge for quasi-circular orbits in Schwarzschild (this formula does not contain the slow-time derivative contribution).

Declaration of Authorship

I declare that this thesis and the work presented in it is my own and has been generated by me as the result of my own original research.

I confirm that:

1. This work was done wholly or mainly while in candidature for a research degree at this University;
2. Where any part of this thesis has previously been submitted for a degree or any other qualification at this University or any other institution, this has been clearly stated;
3. Where I have consulted the published work of others, this is always clearly attributed;
4. Where I have quoted from the work of others, the source is always given. With the exception of such quotations, this thesis is entirely my own work;
5. I have acknowledged all main sources of help;
6. Where the thesis is based on work done by myself jointly with others, I have made clear exactly what was done by others and what I have contributed myself;
7. Parts of this work have been published as:
   V. Toomani, P. Zimmerman, A. Spiers, S. Hollands, A. Pound, and S. R. Green. New metric reconstruction scheme for gravitational self-force calculations. *Classical and Quantum Gravity*, 39(1):015019, 2021
   A. Spiers, A. Pound, and B. Wardell. Second-order perturbation theory in Schwarzschild spacetime. in preparation,
   A. Spiers, J. Moxon, and A. Pound. Second-order Teukolsky formalism with applications to gravitational self-force theory. in preparation,

Signed:..... Date:.....

Acknowledgements

First and foremost, I thank my supervisor Adam Pound for his exceptional guidance and insights during my doctorate. I am incredibly grateful to have had the privilege to learn and work alongside him during the past four years.

I also would like to thank the many collaborators I have had the pleasure to work with during my PhD. They are, in alphabetical order: Leanne Durkan, Stephen R. Green, Stefan Hollands, Ben Leather, Jordan Moxon, Jonathan Thornburg, Vahid Toomani, Sam Upton, Niels Warburton, Barry Wardell, and Peter Zimmerman. Jordan Moxon provided the LaTeX for Eqs. (A.22) to (A.38), which I checked (and provided minor corrections for) independently.

I would also like to thank my co-supervisor, Leor Barack, for the many interesting discussions we have had and the valuable advice and suggestions he has offered.

Many individuals have offered their time to discuss physics with me during the last four years, I thank them all, and among them, I would like to mention Sam Dolan and Maarten van de Meent.

I would like to thank my examiners, Bernard F. Whiting and Oscar J. C. Dias, for taking the time to read this thesis. Their comments and feedback were warmly received and used to improve this work.

I thank the Royal Society for funding my PhD.

I want to acknowledge that a majority of this work was conducted during the COVID-19 pandemic. I was fortunate that I could conduct my research from home during this time. However, the pandemic brought many challenges that could not have been foreseen when I began this PhD.

Finally, I would like to thank my family and friends for their support. With special thanks to Kamilla Toewe who helped me countless times and made the past four years very special.

To Robert Spiers and Clifford Wormleighton...

Definitions and Abbreviations

BL	Boyer–Lindquist
BMS	Bondi–(van der Burg)–Metzner–Sachs
EFE	Einstein field equations
EMRI	extreme-mass-ratio inspiral
GHP	Geroch–Held–Penrose
IMRI	intermediate-mass-ratio inspiral
NP	Newman–Penrose
t, r, θ, ϕ	Boyer–Lindquist coordinates
u	retarded-time coordinate
v	advanced-time coordinate
$u, \hat{r}, \hat{\theta}, \hat{\phi}$	Bondi–Sachs coordinates
γ	worldline
z or x'	point on the worldline
z^α or x'^α	coordinate of point on the worldline
r_p	compact object radial Boyer–Lindquist coordinate
$\mathbf{r}$	radial distance from the worldline
δ^n	$(n-1)$-th post-linear operation
l^a, n^a, m^a, $\bar{m}^a$	Newman–Penrose tetrad
D, Δ, δ, $\bar{\delta}$	Newman–Penrose derivatives
Þ, Þ′, ð, ð′	Geroch–Held–Penrose derivatives
s, b	spin and boost weights
p, q	GHP weights
ℓ, $\mathtt{m}$	azimuthal and magnetic harmonic numbers
$\mathbf{g}_{ab}$	exact metric
g_{ab}	background metric
$h^{(n)}_{ab}$	n-th-order metric perturbation
h_{ab}	first-order metric perturbation
∇^a	covariant derivative (associated with g_{ab})
∂_a	partial derivative
$\mathcal{L}$	Lie derivative
$\mathcal{O}(a)$	of order a

$\mathcal{O}_s$	spin-s Teukolsky operator
$\mathcal{S}_s$	spin-s Teukolsky source operator
$\mathcal{T}_s$	spin-s Teukolsky field scalar operator
$\mathcal{E}$ or δG_{ab}	linearised Einstein operator
†	adjoint
μ	mass of the compact object
M	mass of the supermassive black hole
a	spin parameter of the supermassive black hole
${\mu^\ell}_n = \sqrt{(l-n)(l+n+1)}$	a coefficient in terms of ℓ and n

Preamble

This preamble endeavours to summarise my thesis for a non-expert audience (physics/applied mathematics undergraduates and well-informed members of the public).

The last century has shown General Relativity to be outstandingly successful at describing gravity. It has survived every physical measurement that experimentalists and astronomers have devised to test it. Improving on such tests will require probing more extreme regimes of spacetime curvature to assess whether and where General Relativity breaks down.

A new era for testing General Relativity began in 2015 when LIGO made the first detection of gravitational waves [3]. Gravitational waves propagate outward at the speed of light, expanding and contracting space and time as they pass. Einstein predicted their existence due to General Relativity in 1916 [66]. The gravitational waves LIGO first detected were produced billions of years ago by a merging binary black hole system. The detection marked the dawn of a new era for astronomy in two senses:

- the first detection of a whole new class of radiation with which to observe the universe,
- the first direct observation of black holes.

As gravitational wave signals are weak, they are usually hidden beneath detector noise. Extracting the wave signal from detector data requires matched filtering techniques. matched filtering matches signals in the data to waveform templates. This technique relies on using a bank of waveform templates from accurate source models.

Since 2015, there have been dozens of binary black hole detections (and a handful of black hole-neutron star binaries and neutron star binaries) by the LIGO/VIRGO/KAGRA collaboration. These detections have been rich in astrophysical information and produced constraints on alternative theories of gravity. Testing General Relativity further with gravitational wave astronomy will be possible as detectors increase in sensitivity. However, this will require more precise models of

the systems that produce gravitational waves. Improving the precision of binary models in General Relativity is the subject of this thesis.

Before I discuss the type of model I have improved, allow me to explain why I chose to pursue a Ph.D. as a relativist: General Relativity is undoubtedly a beautiful theory, birthed out of the simple notion that gravity is fundamentally a manifestation of the curvature of space and time. As the Einstein field equations (EFE) have proven challenging to solve, there is still much to learn and achieve. Lastly, the interaction of General Relativity with observations has just begun, and the next few decades of gravitational wave research have the potential to become a golden age in physics.

Techniques for modelling systems that emit gravitational waves have been of mathematical interest for over half a century. They have recently risen to prominence due to the first detection of gravitational waves. Modelling gravitational wave sources is not a simple task as the equations governing General Relativity, the EFE, are challenging to solve. The Schwarzschild and Kerr solutions are two of the most astrophysically relevant exact solutions to the EFE. These solutions describe stationary black holes; however, being stationary, they do not emit gravitational waves. To model gravitational waves-emitting systems, one must resort to solving the EFE numerically [17] or finding approximate solutions using techniques like perturbation theory [142]. This thesis concentrates on black hole perturbation theory which calculates small perturbations to the Schwarzschild or Kerr solutions to build approximate solutions to the EFE (which emit gravitational waves).

Models alone are insufficient to test physics; we also need observations to test them against. One of the next logical steps in gravitational wave astronomy is building a space-based interferometer. Current plans are for the Laser Interferometer Space Antenna (LISA) to be launched in 2034 [58]; China is also planning two space-based detectors [103, 165]. LISA will detect gravitational waves signals in the mHz frequency band (a significantly lower frequency than LIGO), opening up the possibility of detecting new types of gravitational waves sources. The primary application of the work in this thesis will be modelling a key source for LISA, *extreme-mass-ratio inspirals* (EMRIs). EMRIs occur when a compact stellar-mass object (such as a black hole or neutron star) slowly inspirals into a supermassive black hole.

The evolution of an EMRI from bound orbit to merger is driven by the emission of gravitational waves carrying energy and angular momentum away from the system. The perturbation caused by the presence of the inspiraling object produces these waves. The energy and angular momentum carried away by the waves correspond to the work done (by a force) on the inspiralling object. This force, effectively generated by the presence of the inspiraling object, acts on the object itself. Hence, the effect is known as gravitational *self-force*. As the self-force is a small effect, it can be calculated with high accuracy using black hole perturbation theory.

EMRIs offer excellent testing grounds for General Relativity. The compact object spends a long time ($\sim$ 2 years) near the supermassive black hole. In this region, the spacetime curvature is stronger (known as *strong-field*) than the regimes in which we usually test General Relativity (e.g., the solar system). Additionally, the compact object achieves relativistic velocities ($\sim 0.3c$) during an inspiral. Moreover, EMRIs are detectable for $\mathcal{O}(10^5)$ space-filling orbits before the inspiraling object plunges into the supermassive black hole. Hence, LISA observations of EMRIs will be excellent maps of the spacetime around a supermassive black hole. For a review of the possible tests of General Relativity and astrophysics that can be performed with EMRIs, see Refs. [27, 18, 14]. To summarize, EMRIs are expected to be sensitive to violations of the no-hair theorem, extra degrees of freedom beyond General Relativity, dark matter, and astrophysical effects.

Precise extraction of an EMRI's parameters from LISA measurements will require highly accurate waveform models. These models must be calculated to what is known as *post-adiabatic order* [69] accuracy. This high accuracy requirement can be understood by considering that an EMRI will typically be in the LISA frequency band for hundreds of thousands of orbits. Hence, even a small error in modelling a single orbit will cause the accumulation of a significant error throughout the whole inspiral. These highly accurate models require, amongst other things, contributions from the second-perturbative-order self-force [69].

This thesis presents methods to help calculate the second-order self-force. Recently, the first second-order self-force results have been published [156, 195, 194]. However, these results specialize to a Schwarzschild black hole (which has no spin). Astrophysical supermassive black holes are expected to have significant spin. Hence, astrophysically accurate self-force models need to be for a Kerr black hole. Here, I develop new second-order methods, applicable for self-force calculations in Kerr. I derive an equation for calculating a second-order quantity in Kerr, from which the self-force can likely be extracted. I also help solve this equation in Schwarzschild and will soon calculate the second-order self-force (and compare the results with Ref. [195]).

Chapter 1

Introduction

In this chapter, I review the astrophysical motivation for this work: producing high-accuracy waveform models of compact binaries for data analysis of gravitational detector observations. I then provide introductory material on the mathematical tools I will build on in later chapters. The premise is to motivate second-order self-force calculations clearly and include the necessary groundwork for the reader to follow the subsequent chapters.

1.1 Conventions

In this work, I use geometrical units where $c = G = 1$. I use a metric signature $(-,+,+,+)$ unless stated otherwise.

The index notation applies as follows:

- Lowercase Latin indices are abstract indices [191].
- Lowercase Greek indices are 4D tensor component indices (e.g., $\mu = \{0,1,2,3\}$).
- Capital Latin indices denote 2D components of tensors on the unit sphere (e.g., $B \in \{2,3\}$).
- Lowercase Latin indices in square brackets are tetrad indices (e.g., $[a] = \{[1],[2],[3],[4]\}$).

Subscript or superscript numbers in round parentheses are labels representing the order of the perturbation.

Generally, I am discussing vector and tensor *fields* but will drop the word *fields* for conciseness.

1.2 Gravitational-wave astronomy: state of play

Gravitational waves were predicted by Einstein using his theory of General Relativity in 1916 [67]. Almost a century later, in 2015, the LIGO collaboration made the first detection of gravitational waves [3]. The source of the signal LIGO detected was produced around a billion years ago when a black hole binary merged. The two black holes were initially of around 36 and 29 solar masses. During the inspiral and merger, about three solar masses of energy were emitted in gravitational waves. The peak power (for a few milliseconds) was greater than the electromagnetic luminosity of all the stars in the universe combined. Still, detecting this signal was an astounding feat as these waves changed the length of LIGO's four-kilometre detector arms by only a thousandth of a proton's width.

Over the last seven years, more gravitational wave detections of binary systems have steadily been made by the LIGO/VIRGO/KAGRA collaboration [5]. Fig. 1.1 [76] gives a visual representation of the detections made as of November 7, 2021. Achieving the incredible precision required to detect the gravitational waves produced by these binaries has been a scientific endeavour on three fronts: technology, data science, and modelling. Building the high precision detectors was a technological challenge. However, the signals measured by these detectors are (*usually*) hidden under the detector noise. Hence, extracting precision measurements from the detector's data requires using matched filtering with accurate waveform templates (of the source that produced the signal). The modelling community produces these waveform templates.

Fig. 1.1 [76] shows the range of binaries detected to date. Most detections have been black hole binaries; additionally, a few are neutron star-black hole binary and neutron star binary detections have been made. However, the range of sources is limited by the sensitivity of LIGO/VIRGO/KAGRA. Binaries with a black hole of mass > 200 solar masses produce gravitational waves with a frequency outside the sensitive region of the LIGO/VIRGO/KAGRA frequency band.

The grey arrows in Fig. 1.1 [76] represent the difference in masses of the two objects in the binary. Currently, the smallest mass ratio of a published LIGO/VIRGO/KAGRA detection is around 0.04 [6]. Detecting smaller mass ratios is limited by the frequency bandwidth of the LIGO/VIRGO/KAGRA detectors (as small mass ratio require the primary object to have significant mass, which results in lower frequency gravitational waves outside LIGO/VIRGO/KAGRA sensitivity bandwidth) and the modelling capabilities used to make the waveform templates.

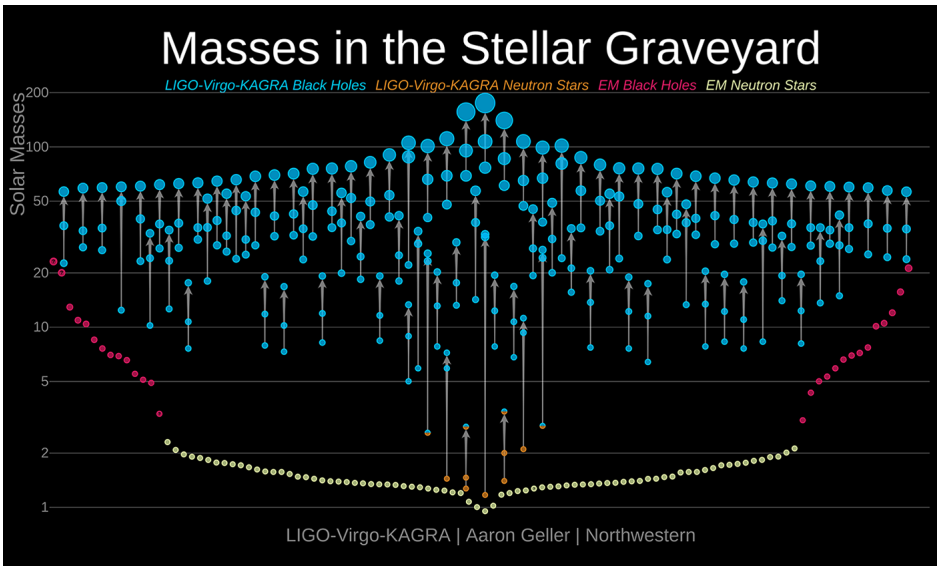

FIGURE 1.1: The stellar graveyard: black holes and neutron stars detected using electromagnetic and gravitational wave signals. This includes the binaries detected by LIGO/VIRGO/KAGRA as of November 7, 2021.[76]

1.3 Extreme-mass-ratio inspirals

Evidence shows that at the centre of each galaxy lies a supermassive black hole [161], with masses reaching up to $10^9 M_\odot$. Supermassive black holes were first indirectly observed half a century ago [196] by examining orbits of stars near the galactic center, and their existence astounded astronomers. In 2019 the Event Horizon Telescope collaboration published the first image of a supermassive black hole [54] (see Fig. 1.2), showing a ring generated by a hot, luminous accretion disk with a supermassive black hole at its centre. In 2022, the Event Horizon Telescope collaboration also published an image of Sagittarius A* [9]. The origin and evolution of supermassive black holes are still relatively unknown. They are expected to have a close connection to the origin and evolution of galaxies [161], and galactic centres are the only place where they have been found.

Supermassive black hole are not alone in galactic centres; a busy neighbourhood of orbiting stars surrounds them. Still, these stars rarely encroach close enough to merge with the supermassive black hole. Hence, when a stellar-mass object is captured into a sufficiently closely bound orbit around the supermassive black hole (e.g., see Fig. 1.3), the pair become effectively isolated from their surroundings. Such a binary system eventually is called an extreme-mass-ratio inspiral (EMRI).

General Relativity effects cause the dissipation of energy and angular momentum away from the system. Hence, the orbit of the compact object is not stable. Over the timescale years, the compact object evolves through progressively tighter bound orbits until it eventually plunges into its enormous neighbour's event horizon. The

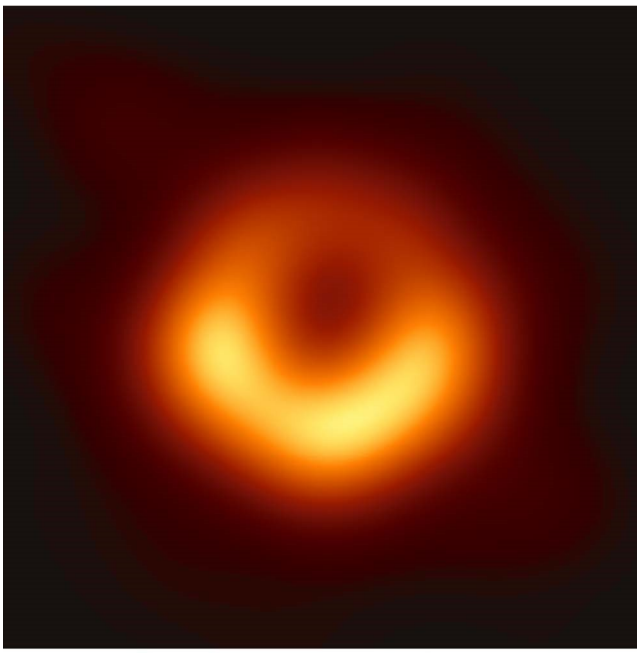

FIGURE 1.2: The first image of a supermassive black hole. Produced by the Event Horizon Telescope collaboration using radio telescope observations of the supermassive black hole M87* [54].

inspiralling object must be compact to prevent tidal forces from ripping it apart as it travels closer to the supermassive black hole before reaching the merger.

EMRIs are characterised by their mass ratio,

$$\varepsilon = \frac{\mu}{M}, \tag{1.1}$$

where μ is the mass of the stellar-mass compact object and M is the mass of the supermassive black hole. EMRIs are described as *extreme* due to the smallness of the mass ratio ($10^{-5} \gtrsim \varepsilon \gtrsim 10^{-8}$). They differ from the comparable mass binaries ($1 \gtrsim \varepsilon \gtrsim 10^{-1}$) which LIGO has detected [3]. A third class of binaries are intermediate mass-ratio inspirals (IMRIs) ($10^{-2} \gtrsim \varepsilon \gtrsim 10^{-4}$); these systems can occur when a stellar-mass object inspirals into an intermediate-mass black hole, or an intermediate-mass black hole inspirals into an supermassive black hole. Excitingly, improvements to ground-based gravitational-wave detectors will make LIGO/VIRGO/KAGRA more sensitive to IMRIs in future observation runs [11]. There is a further class of binaries, so-called *extremely-large mass-ratio inspirals* ($\varepsilon \lesssim 10^{-8}$) [12].

In EMRIs, spacetime is strongly curved, and the velocities are highly relativistic. Hence, even high-order post-Newtonian approximations do not achieve the required accuracy to model full inspirals [23]. An added complication is that astrophysical supermassive black holes are expected to have significant spin. The spacetime surrounding such black holes is described by the Kerr metric [97]. Bound orbits (geodesics) of Kerr spacetime are significantly more complicated than in the

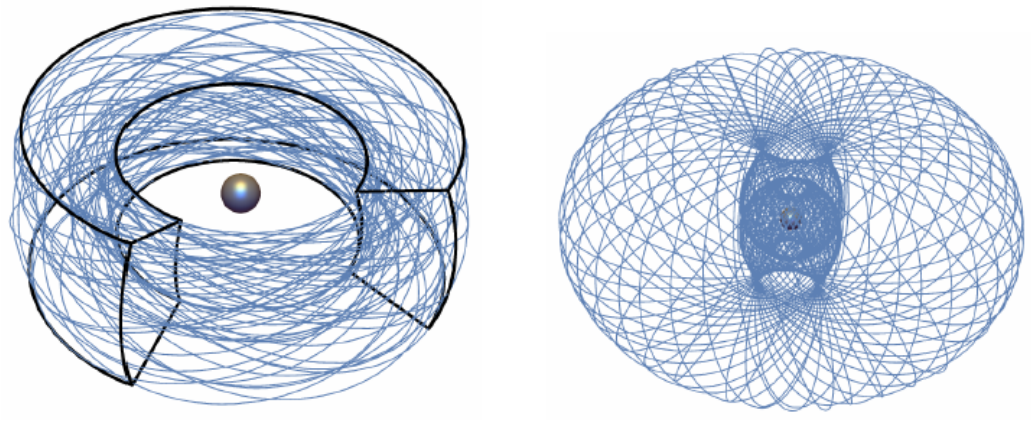

FIGURE 1.3: Examples of bound geodesics (blue lines) of a Kerr black hole. The orbit on the left is a typical geodesic, having three frequencies and being space filling (within a torus outlined in black). The orbit on the right is a 3 : 2 (r-θ) resonant orbit. Note how resonant orbits are non-space filling, which impacts orbital evolution. Picture taken from Ref. [23]

non-spinning black hole spacetime (Schwarzschild): in Kerr, to describe a generic orbit requires the knowledge of its radial, polar, and azimuthal frequencies [48]. The three fundamental frequencies correspond to three conserved quantities of Kerr geodesics: energy, angular momentum, and the Carter constant [46][1].

Kerr is stationary and axially symmetric; i.e., the Kerr metric g_{ab} has two "Killing vectors" Ξ^a_t and Ξ^a_ϕ which satisfy $\mathcal{L}^c_\Xi g_{ab} = 0$. Hence, the orbital energy and angular momentum of Kerr geodesics are well-defined conserved quantities. The Carter constant is a manifestation of the Kerr metric admitting a Killing tensor. The existence of three fundamental frequencies reflects that not all Kerr geodesics exist on a single plane; Kerr geodesics are generally space-filling in three dimensions, as illustrated by Fig. 1.3.

Over a sufficiently short timescale, a Kerr geodesic will approximate an EMRI orbit reasonably well. This is due to the curvature of the spacetime being dominated by the presence of the supermassive black hole. However, unlike a test particle on a Kerr geodesic, the mass of the compact object causes EMRIs to emit gravitational radiation. The radiation dissipates either infinitely away from the system (to future null infinity, $\mathcal{I}^+$) or into the supermassive black hole horizon (affecting the supermassive black hole's mass and spin). The loss of orbital energy and angular momentum results in an error growing with time if one assumes the compact object remains on a single Kerr geodesic. Instead, one can (roughly) consider the compact object to sit on a series of Kerr geodesics, corresponding to orbital constants that slowly evolve with time. The

[1] As three fundamental frequencies are present, resonant orbits are significantly more likely to occur. $r - \theta$ resonances (which are possible in Kerr) have the strongest impact on orbital evolution, see Fig. 1.3. Hence, resonance contributions are significant when modelling EMRIs. The problem of resonances [70, 29] is not addressed in this thesis; please see Refs. [186, 130] for the current progress.

evolution of two Kerr geodesic constants (the orbital energy and angular momentum) clearly corresponds to the energy and angular momentum dissipated away from the system and into the supermassive black hole. However, the evolution of the Carter constant is related to the emitted waves in a less obvious way (as I shall discuss in Sec. 1.7.4).

1.4 LISA and detecting EMRIs

The progression of telescope sensitivity to new bandwidths of the electromagnetic spectrum uncovered unseen sources of electromagnetic radiation. Similarly, new gravitational wave detectors, sensitive to different bandwidths of gravitational wave frequencies, will allow us to observe yet unseen gravitational wave sources. The LISA mission plans to observe unexplored gravitational wave frequency regimes.

Like LIGO, LISA will be a laser interferometer instrument designed to detect gravitational waves [58]. However, it will be housed in outer space rather than on Earth. LISA will consist of three satellites suspended in a Lagrange point (of the Earth-Sun binary system) trailing the Earth's solar orbit by 50 million km [16]. China is also planning two space-based detectors, TianQin [103] and Taiji [165].

Being situated in space brings many advantages. The lasers must travel in a vacuum to avoid atmospheric noise; LIGO requires large vacuum tubes with cutting-edge technology to produce the best possible vacuum [2] (whilst minimising thermal noise from any equipment). For LISA, the near-vacuum of space is a convenient medium to house a laser interferometer. With no need for tubes connecting the interferometer arms, LISA will be $\mathcal{O}(10^5)$ times longer than LIGO, with an arm length of 2.5×10^6 km. This will help LISA reach peak sensitivity in the mHz band, a much lower frequency than LIGO is sensitive to (as illustrated in Fig. 1.4 [44]). These lower-frequency gravitational waves are undetectable on earth due to seismic noise, another problem which LISA avoids by being in space. Within LISA's frequency band sit EMRIs with a mass ratio (ϵ) of 10^{-5} to 10^{-7} (amongst other binary signals and gravitational waves from the early universe) [58].

LISA is expected to be sensitive to EMRI signals out to a redshift of $z \approx 4$ [56]. While LISA will be in the range of a large population of supermassive black holes, the expected capture rate of compact stellar remnants into an EMRI system is low. Current estimates expect tens to hundreds of detectable EMRIs over the LISA mission lifetime [75].

When LISA begins to detect EMRIs, it will allow us to study the astrophysics of galactic centres and supermassive black holes to impressive precision. It is predicted that measurements of the mass and spin of the supermassive black hole can be

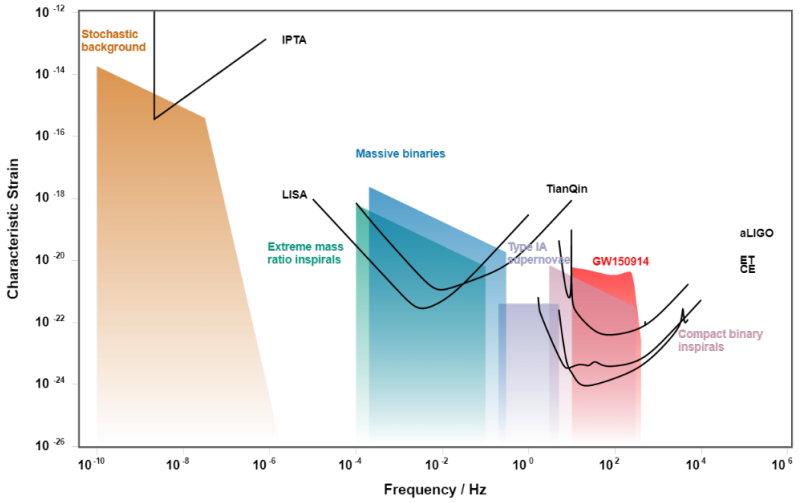

FIGURE 1.4: The sensitivity curves of a selection of planned and operating gravitational wave detectors (IPTA is International Pulsar Timing Array, CE is Cosmic Explorer, and ET is Einstein Telescope) and the sources they will be sensitive to. Produced using Ref. [44].

extracted from EMRI signals to a precision of 1 part in 10^4 [23]. Data will also be collected on the so-called stellar relics present near the centres of galaxies. Astronomers will observe the zoo of compact objects inspiraling into supermassive black holes. Eventually, data analysts will be able to construct a mass distribution of these compact objects. LISA will also be sensitive to IMRIs where an intermediate-mass black hole ($100\mathrm{M}_\odot - 10^4\mathrm{M}_\odot$) inspirals into a supermassive black holes. Hence, LISA could then test whether intermediate-mass black holes exist near galactic cores [58].

In addition, EMRI detections will be used to measure the universe's rate of expansion. EMRIs are potential standard sirens (the gravitational wave version of standard candles) as their detection can be used to measure distance [91]. There are currently two disagreeing measurements for the expansion of the universe (the Hubble constant) using electromagnetic radiation measurements [162]. EMRIs and other standard sirens could provide measurements to help resolve this tension.

EMRIs also offer a groundbreaking opportunity to test General Relativity. Measuring EMRI signals in LISA data to the planned precision would constrain General Relativity to one or more orders of magnitude higher than any other planned experiment [13]. As an EMRI is detectable over the timescale of $\mathcal{O}(1)$ year, and Kerr geodesics are space-filling, their signal allows us to produce a detailed map of the spacetime. This makes EMRIs an excellent laboratory to test the Kerr hypothesis (i.e., testing the no-hair theorem). Ref. [27] gives a review of the astrophysical and General Relativity effects to which LISA will be sensitive, highlighting how precise parameter extraction from EMRIs is a crucial component of LISA science.

However, EMRI signals will be dominated not only by LISA's instrumental noise [23], but by other types of astrophysical gravitational-wave signals, supermassive black hole binaries [27]. Matched filtering is necessary to extract EMRI signals. It is expected that detecting an EMRI within LISA data will only require so-called *Kludge* models [52]. These models do not describe the precise physics which drive the motion of EMRIs, but are quick to calculate and are probably sufficiently accurate to detect most EMRI signals. However, measuring an EMRI requires higher precision than detecting an EMRI. Waveform models must be highly accurate for precise parameter extraction, with significantly less than 1 radian orbital error throughout the whole inspiral. Kludge models are unable to achieve this level of accuracy.

1.5 Modelling EMRIs

Modeling EMRIs presents some distinct challenges as compared to modelling the comparable-mass binary mergers observed by LIGO [23]. The numerical relativity techniques utilised for comparable-mass binaries are not suitable for EMRIs because an EMRI is a system of such contrasting length scales. Post-Minkowski methods are not appropriate due to the strong field nature of EMRIs. Post-Newtonian methods suffer a double shortfall because they take both a weak-field and small-velocity limit. In contrast, the later stages of EMRIs are in the strong field and involve relativistic velocities. The strengths and limitations of these methods when modelling comparable-mass binaries and EMRIs are represented in Fig. 1.5. Additionally, effective one-body theory [43] combines the knowledge of all these theories to model binaries for all mass ratios and separations. As effective one-body theory is currently calibrated with Numerical Relativity data, it is most accurate and reliable in the comparable-mass regime.

The disparate mass scales in EMRIs provide a practical solution for modelling their spacetimes: perturbatively expanding the metric in powers of the mass ratio ε. In EMRIs, the background spacetime is Kerr, and the presence of the compact object produces perturbations. These perturbations, in turn, affect the compact object's motion. One can consider the deviation of the motion of the compact object away from a Kerr geodesic as the result of a force generated by the object's own gravitational field. Hence, this modelling method is known as *self-force* theory.

Before jumping into the details of self-force theory and black hole perturbation theory, I conclude this section with an argument on why calculating the dissipative piece of the second-order self-force is necessary for precise EMRI measurements.

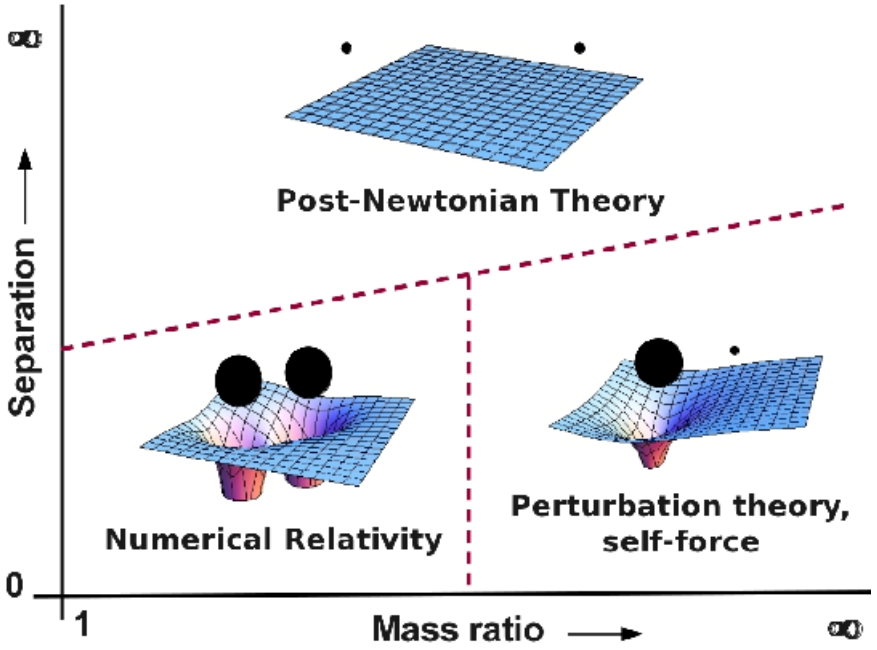

FIGURE 1.5: Visual representation of the regions of applicability for black hole binary modeling techniques (here "mass ratio" is the lager mass divided by the smaller mass). Taken from [21].

1.5.1 Why the second-order gravitational self-force is required

The self-force per unit mass (F^a_{SF}) the compact object experiences can be expanded in orders of the mass ratio,

$$F^a_{SF} = \varepsilon F^a_{(1)} + \varepsilon^2 F^a_{(2)} + \mathcal{O}(\varepsilon^3). \tag{1.2}$$

The effect of the self-force on the motion of the inspiraling object is described by the object's equation of motion,

$$u^b \nabla_b u^a = a^a = (\varepsilon F^a_{(1)} + \varepsilon^2 F^a_{(2)}) + \mathcal{O}(\varepsilon^3), \tag{1.3}$$

where u^a is the four-velocity of the compact object and ∇^b is the covariant derivative. Hence, due to the self-force, the compact object does not remain on a geodesic of Kerr spacetime.

Methods for calculating $F^a_{(1)}$ have been the subject of a great amount of research over the past few decades and are now at a mature stage. $F^a_{(1)}$ can now be calculated for generic orbits in Kerr [114]. However, precise parameter extraction will require models which account for the dissipative piece of $F^a_{(2)}$ [69]. Here, I give a brief scaling argument for why this is necessary:

To begin the scaling argument, I show the long timescale (t) of an EMRI is $\mathcal{O}(\frac{1}{\varepsilon})$. This can be understood by comparing the orbital energy with how quickly energy is

dissipated from the system through gravitational waves. The rate of energy dissipation scales as $\dot{E} = \frac{dE}{dt} \sim h_{ab}^{(1)2} \sim \varepsilon^2$ [15]. The orbital energy of the compact object is $E \sim \mu$. As $t \sim \frac{E}{\dot{E}}$ and $\frac{E}{\dot{E}} \sim \frac{\mu}{\varepsilon^2} \sim \frac{M}{\varepsilon}$; therefore, $t \sim \frac{1}{\varepsilon}$.

The error in the position (δz^μ) is related to the error in the acceleration (δa^μ) associated with the self-force on the long timescale of the whole inspiral [145],

$$\delta z^\mu \sim t^2 \delta a^\mu \sim \tfrac{1}{\varepsilon^2} \delta a^\mu. \tag{1.4}$$

For δz^μ to be small, $\delta a^\mu = \mathcal{O}(\varepsilon^3)$ is necessary. Hence, the equation of motion (a^μ) must be calculated through to second order to achieve an accurate model over an entire EMRI. That is the second-order self-force is required.

The self-force can be separated into a conservative piece (which conserves the orbital energy of the system over an averaged orbit) and a dissipative piece (which radiates orbital energy away from the system). Hinderer and Flanagan [69], through a more rigorous argument, describe why only the dissipative second-order self-force effects are required. To summarise, their key result is the following: the (radial, polar, and azimuthal) phases of the inspiral (ϕ_i), over long time scales, have the expansion

$$\phi_i(t, \varepsilon) = \frac{1}{\varepsilon} \phi_i^{\{0\}}(t, \varepsilon) + \phi_i^{\{1\}}(t, \varepsilon) + \mathcal{O}(\varepsilon), \tag{1.5}$$

where $\phi_i^{\{0\}}$ is dependent on dissipative first-order self-force and $\phi_i^{\{1\}}(t, \varepsilon)$ is dependent on the complete first-order self-force and the dissipative second-order self-force [69]. Hence, to calculate $\phi_i(t, \varepsilon)$ through order ε^0 the dissipative piece of the second-order self-force must be calculated. Calculations including $\phi_i^{\{0\}}$ are know as *adiabatic* accuracy, and calculations including up to and including $\phi_i^{\{1\}}$ are known as *first-post adiabatic* accuracy (the numbers in curly brackets denote the post adiabatic order).

Fig. 1.6 shows a numerical approximation of the regimes where various modelling methods are accurate. The data is produced by fitting Eq. (1.5) to Numerical Relativity waveforms, and then assessing how large an error would accumulate if only the first two terms are included. The Numerical Relativity waveforms are for quasi-circular orbits in Schwarzschild and provides evidence that first-post adiabatic waveforms have good accuracy in the $\sim 1:10$ mass ratio regime. This estimate has been shown to hold for first-post adiabatic waveforms for quasi-circular orbits in Schwarzschild in Refs. [156, 195, 194]. This plot (and the results in Refs. [156, 195, 194]) clarify the prediction of the regimes where methods are valid represented in Fig. 1.5.

1.6 Black hole perturbation theory and gravitational self-force

In this section, I review the key methods of self-force modelling. I describe a

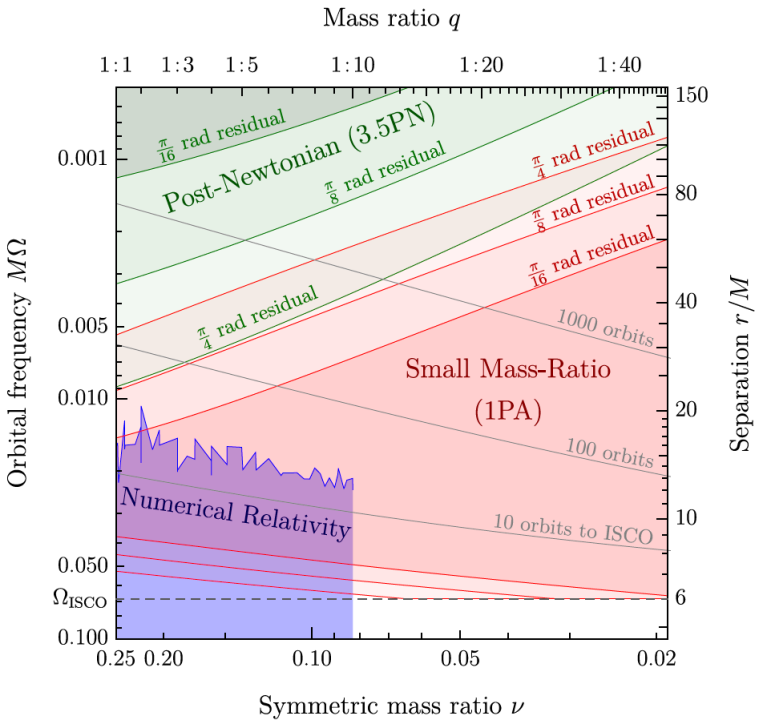

FIGURE 1.6: Estimates for the regions of applicability for black hole binary modeling techniques. In red onesees that first-post adiabatic models perform well even in the large mass-ratio regime. Taken from Ref. [188].

framework for black hole perturbation theory and summarise some first-order self-force methods, focusing on which methods need to be extended to second order. I then survey the current state of second-order self-force calculations and review the Newman–Penrose formalism and Teukolsky equation.

1.6.1 Black hole perturbation theory framework

In General Relativity, metrics of physical spacetime are solutions to the EFE,

$$G_{ab}[\mathbf{g}_{ab}] = 8\pi T_{ab}, \tag{1.6}$$

where G_{ab} is the Einstein tensor, $\mathbf{g}_{ab}$ is the metric, and T_{ab} is the stress-energy tensor. It is challenging to find physically interesting exact solutions to Eq. (1.6) as G_{ab} is infinitely non-linear in its argument $(\mathbf{g}_{ab})$. Also, as a tensor equation, Eq. (1.6) is equivalent to 10 real scalar equations (6 of which are independent and 4 are constraints corresponding to $\nabla^a G_{ab} = 0$). There are known analytical solutions to the EFE, and the astrophysically relevant black hole solutions are Schwarzschild and Kerr black holes. Finding these solutions relied on their temporal and axial symmetry. As these solutions are stationary, they do not emit gravitational waves. Finding exact solutions allowing for gravitational radiation is not feasible analytically. The desire for calculating solutions which admit gravitational waves led to Numerical Relativity, a method for solving Eq. (1.6) numerically. However, numerical solutions are

computationally expensive and a numerical error is introduced. Approximate solutions can also produce models of interesting physical phenomena and be compared to measurements (to a given precision that the approximation is valid). Perturbation theory can be used to find approximate solutions to Eq. (1.6) which emit gravitational waves.

Perturbative expansions involves approximating a quantity, such as a tensor $A_{a_1\ldots a_m}{}^{b_1\ldots b_n}$, with a series expansion (in terms of orders of a parameter λ). For example,

$$A_{a_1\ldots a_m}{}^{b_1\ldots b_n} = A^{(0)}_{a_1\ldots a_m}{}^{b_1\ldots b_n} + \lambda A^{(1)}_{a_1\ldots a_m}{}^{b_1\ldots b_n} + \lambda^2 A^{(2)}_{a_1\ldots a_m}{}^{b_1\ldots b_n} + \ldots \tag{1.7}$$

For this series to approximate $A_{a_1\ldots a_m}{}^{b_1\ldots b_n}$ accurately, it requires $|\lambda| \ll 1$. Therefore, each successive order in the expansion will be smaller than the previous. The disparate mass scales in an EMRI system make the mass ratio, ε, an ideal expansion parameter for self-force calculations. As the mass ratio for an EMRI is $\mathcal{O}(10^{-5}\text{-}10^{-7})$, even a perturbative expansion truncated at second order provides an accurate approximation.

The principal object in tensor geometry is the metric ($\mathbf{g}_{ab}$). A perturbative expansion of the metric is (conventionally) written as

$$\mathbf{g}_{ab} = g^{(0)}_{ab} + \varepsilon h^{(1)}_{ab} + \varepsilon^2 h^{(2)}_{ab} + \ldots + \varepsilon^n h^{(n)}_{ab} + \ldots \tag{1.8}$$

Here, $g^{(0)}_{ab}$ is the background metric and $h^{(n)}_{ab}$ are the nth-order metric perturbations. $g^{(0)}_{ab}$ is a solution to the EFE (Eq. (1.6)) and plays a special role in perturbative calculations as it is used for the raising and lowering of indices. Following convention [191], $g^{(0)}_{ab}$ is also associated to the covariant derivative ∇_a (i.e., $\nabla^c g^{(0)}_{ab} := g^{(0);c}_{ab} = 0$). For this work I shall use the Kerr metric for $g^{(0)}_{ab}$ (unless I specify otherwise). For visual elegance, I simplify my notation, writing Eq. (1.8) as

$$\mathbf{g}_{ab} = g^{(0)}_{ab} + h^{(1)}_{ab} + h^{(2)}_{ab} + \mathcal{O}(\varepsilon^3), \tag{1.9}$$

where the metric perturbations $h^{(n)}_{ab}$ have absorbed their corresponding power of the expansion parameter (ε^n). Throughout this work, (n) superscripts or subscripts on tensors indicate that they are $\mathcal{O}(\varepsilon^n)$. The superscript (0) on $g^{(0)}_{ab}$ is often dropped for succinctness.

Note, by enforcing $\mathbf{g}^{ab}\mathbf{g}_{bc} = \delta^a_c$ it is straight forward to show that the the contravariant metric takes the form,

$$\mathbf{g}^{ab} = g^{ab}_{(0)} - h^{ab}_{(1)} + h^{ac}_{(1)} h_{(1)c}{}^{b} - \frac{1}{2} h^{ab}_{(2)} + \mathcal{O}(\varepsilon^3). \tag{1.10}$$

Just as I have expanded tensors in orders of ε, one can expand the infinitely non-linear behaviour of G_{ab} as a series of tensors $\delta^n G_{ab}$. Achieving a explicit expansion for the

non-linear nature of G_{ab} requires an explicit background metric which satisfies the EFE

$$G_{ab}[g_{ab}] = 8\pi T^{(0)}_{ab}, \tag{1.11}$$

In this thesis, I assume g_{ab} satisfies the vacuum EFE (that is, $T^{(0)}_{ab} = 0$). Kerr spacetime satisfies this assumption. The EFE can then be expressed in orders of how many (n) arguments it takes [191],

$$G_{ab}[x_{ab}] = \delta G_{ab}[x_{ab}] + \delta^2 G_{ab}[x_{ab}, x_{ab}] + \delta^3 G_{ab}[x_{ab}, x_{ab}, x_{ab}] + ... \tag{1.12}$$

where $\delta^n \mathbf{A} := \frac{1}{n!}\frac{d^n}{d\lambda^n}\mathbf{A}\left[g^{(0)}_{ab} + \lambda h_{ab}\right]|_{\lambda=0}$ for any tensor $\mathbf{A}$ and x_{ab} is some two-tensor. Note, the form of $\delta^n G_{ab}$ depends on the background metric g_{ab}; but, as g_{ab} generally remains fixed during a perturbative analysis, my notation does not explicitly write $\delta^n G_{ab}$ as explicit functions of g_{ab}. δG_{ab} is called the *linearised Einstein tensor*, $\delta^2 G_{ab}$ the *quadratic Einstein tensor*, and so on.

I now express the left hand side of Eq. (1.6) using the expansions in Eq. (1.12) and Eq. (1.9), this gives

$$\begin{aligned} G_{ab}[\mathbf{g}_{ab}] =& \delta G_{ab}[g^{(0)}_{ab} + h^{(1)}_{ab} + h^{(2)}_{ab} + ...] \\ &+ \delta^2 G_{ab}[g^{(0)}_{ab} + h^{(1)}_{ab} + h^{(2)}_{ab} + ..., h^{(1)}_{ab} + h^{(2)}_{ab} + ...] + ... \end{aligned} \tag{1.13}$$

To express the right hand side of Eq. (1.6) the stress-energy tensor can be expanded in orders of ε. Eq. (1.6) therefore reads as

$$\delta G_{ab}[h^{(1)}_{ab}] + \delta G_{ab}[h^{(2)}_{ab}] + \delta^2 G_{ab}[h^{(1)}_{ab}, h^{(1)}_{ab}] = 8\pi(T^{(1)}_{ab} + T^{(2)}_{ab}) + \mathcal{O}(\varepsilon^3), \tag{1.14}$$

where I have used that $g^{(0)}_{ab}$ satisfies the vacuum EFE (that is, $\delta^n G_{ab}[g_{ab}] = 0$ and $T^{(0)}_{ab} = 0$).

Eq. (1.14) can be solved to a given $\mathcal{O}(\varepsilon^n)$ by re-expressing it as a series of n equations in ascending orders of ε:

$$\delta G_{ab}[h^{(1)}_{ab}] = 8\pi T^{(1)}_{ab} \tag{1.15}$$

$$\delta G_{ab}[h^{(2)}_{ab}] = 8\pi T^{(2)}_{ab} - \delta^2 G_{ab}[h^{(1)}_{ab}, h^{(1)}_{ab}] \tag{1.16}$$

$$\delta G_{ab}[h^{(3)}_{ab}] = ... \tag{1.17}$$

Hence, first-order perturbation theory involves finding a metric perturbation $h^{(1)}_{ab}$ which satisfies Eq. (1.15). Extending to second order boils down to finding a $h^{(2)}_{ab}$ satisfying Eq. (1.16) (for a $h^{(1)}_{ab}$ which satisfies Eq. (1.15)).

To understand the equations needed to be solved in black hole perturbation theory, I will express $\delta G_{ab}[h_{ab}]$ and $\delta^2 G_{ab}[h_{ab}, h_{ab}]$ in terms of h_{ab}. The Einstein tensor is the

trace-reverse of the Ricci tensor, $G_{ab} = \overline{R}_{ab}$ (an over-line represents a trace reversal; i.e., $\overline{R}_{ab} = R_{ab} - \frac{1}{2}\mathbf{g}_{ab}R$, where R is the Ricci scalar $R = \mathbf{g}^{cd}R_{cd}$). Hence, the linearised Einstein and quadratic Einstein tensors are

$$\begin{aligned}\delta G_{ab} =&\delta\left[R_{ab} - \frac{1}{2}\mathbf{g}_{ab}R\right]\\ =&\delta R_{ab} - \frac{1}{2}g_{ab}\delta R, \qquad (1.18)\\ \delta^2 G_{ab} =&\delta^2\left[R_{ab} - \frac{1}{2}\mathbf{g}_{ab}R\right]\\ =&\delta^2 R_{ab} - \frac{1}{2}\left(g_{ab}\left(g^{cd}\delta^2 R_{cd} - 2h^{cd}\delta R_{cd}\right) + 2h_{ab}g^{cd}\delta R_{cd}\right), \qquad (1.19)\end{aligned}$$

where I have used that $R^{(0)}_{ab} = 0$ (as Kerr is vacuum)[2]. δR_{ab} and $\delta^2 R_{ab}$ can be expressed as [152, 110]

$$\begin{aligned}\delta R_{ab}[h_{ab}] =&\frac{1}{2}\left(2h^{c}{}_{(a;b)c} - h_{ab}{}^{;c}{}_{c} - h^{c}{}_{c;ab}\right), \qquad (1.20)\\ \delta^2 R_{ab}[h_{ab}] =&\frac{1}{2}\Bigg(h^{cd}\left(h_{ab;cd} + h_{cd;ab} - 2h_{c(a;b)d}\right) + \left(\frac{1}{2}h^{d}{}_{d;c} - h_{c}{}^{d}{}_{;d}\right)\left(2h^{c}{}_{(a;b)} - h_{ab}{}^{;c}\right)\\ &+ h_{a}{}^{c;d}h_{b[c;d]} + \frac{1}{2}h^{cd}{}_{;a}h_{cd;b}\Bigg), \qquad (1.21)\end{aligned}$$

in a vacuum background spacetime. By combining Eq. (1.18) and Eq. (1.20) one finds an expression for the linearised Einstein tensor in terms of h_{ab}.

The complexity of $\delta^n G_{ab}$ increases significantly as one extends to higher orders in n. Nevertheless, Eqs. (1.15), (1.16), and (1.17) show that every order of metric perturbation can be calculated by solving the linear EFE with a source containing the lower-order metric perturbations. That is, the hierarchical structure of Eqs. (1.15), (1.16) and (1.17) places the increase in complexity into the source term (on the right hand side). Because δG_{ab} is a linear operator, solving for a metric perturbation is much more straightforward than solving the full EFE (Eq. (1.6)) for the full metric.

In a Kerr background spacetime, solving the linearised EFE is still challenging as it reduces to a non-separable set of coupled PDEs. Solving Eq. (1.15) directly is possible with numerical techniques [136]; however, these methods are generally slow due to the disparate length scales and long inspiral timescales of EMRIs. In Secs. 1.7.3 and 1.8, I will review the commonly used method to indirectly solve the linearised EFE in Kerr by using the Teukolsky equation and CCK metric reconstruction.

[2]Similarly, for self-force calculations $\delta R_{cd}[h^{(1)}_{ab}] = 0$ away from the worldline γ.

1.6.2 Gauge freedom and perturbation theory

Before discussing self-force theory, I review the role of gauge freedom in General Relativity and perturbation theory. Here, I discuss how gauge freedom manifests itself in General Relativity and subsequently at each order in perturbation theory.

General Relativity admits four gauge degrees of freedom. These freedoms correspond to diffeomorphisms on the spacetime manifold (in the so-called *active view* [148]). Alternatively, one can consider them as the freedom to choose a coordinate system (in the so-called *passive view* [148]).

The freedoms are permissible due to the EFEs, Eq. (1.6), being underdetermined [191]. There are ten EFEs (1.6), which admit four constraint equations ($\nabla^a G_{ab} = 0$), leaving six evolution equations; whereas a generic metric, $\mathbf{g}_{ab}$, has ten independent components. Hence, the system is underdetermined. The four degrees of freedom in the metric left unconstrained by the EFE are gauge freedoms.

Additionally, General Relativity is locally Lorentz-invariant. That is, the theory is covariant under the three boosts and three spatial rotations of local Lorentz frames [48].

When one solves the field equations perturbatively, the background metric $g^{(0)}_{ab}$ is generally associated with a specific gauge. I refer to the gauge of the background spacetime as the choice in coordinates. Each nth-order perturbation is accompanied by a further four infinitesimal gauge degrees of freedom. The term *infinitesimal* denotes that these are $\mathcal{O}(\varepsilon^n)$ gauge freedoms of $h^{(n)}_{ab}$. As ε is small, the infinitesimal gauge freedoms are near identity transforms of the background coordinates [148]. For succinctness, I refer to the infinitesimal gauge as simply the gauge (as is common in self-force literature). Methods for calculating the metric perturbations are often associated with particular gauge choices. These gauges may not be fully specified (e.g., the Lorenz gauge, which I will define in Sec. 4.1.1, has some residual gauge freedom).

The number of gauge freedoms, and complexity of gauge transformations, become more involved the higher the order of the perturbation. This can be seen by examining how each metric perturbation transforms under gauge transformations [148],

$$h^{(1)}_{ab} \to h^{(1)}_{ab} + \mathcal{L}_{\vec{\xi}_{(1)}} g^{(0)}_{ab} \tag{1.22}$$

$$h^{(2)}_{ab} \to h^{(2)}_{ab} + \mathcal{L}_{\vec{\xi}_{(2)}} g^{(0)}_{ab} + \mathcal{L}_{\vec{\xi}_{(1)}} h^{(1)}_{ab} + \frac{1}{2}\mathcal{L}_{\vec{\xi}_{(1)}}\mathcal{L}_{\vec{\xi}_{(1)}} g^{(0)}_{ab} \tag{1.23}$$

$$h^{(3)}_{ab} \to ...,$$

where $\vec{\xi}_{(1)}$ and $\vec{\xi}_{(2)}$ are the first- and second-order gauge vectors respectively.

One must also consider the limitations of individual gauges and the desire to calculate measurable quantities easily. The extensivity of gauge freedom in General Relativity accommodates gauges that obscure the physical geometry in certain regimes. For example, using Schwarzschild coordinates to describe the Schwarzschild black hole introduces coordinate singularities at the black hole horizon. As the coordinate singularities are confined to a particular region, Schwarzschild coordinates can be used to study physics away from the horizon. However, at the horizon, the singular nature of the coordinates may obscure physical phenomena, such as a particle passing through the horizon. Therefore, one must use a different gauge to probe the physical geometry at the horizon. This example illustrates the meaning of describing a gauge as *bad*; that is, a gauge that obscures the physical geometry in a region one is interested in studying. *Bad* choices of gauge is a problem that occurs regularly in generic self-force calculations. If a gauge is well behaved in a region of interest, then it is said to be *good*. In this thesis I commonly tailor second-order self-force calculations to be working in a *good* gauge.

1.6.2.1 Future null infinity and asymptotically flat gauges

Here, I review the definition of future null infinity ($\mathscr{I}^+$), explaining what I mean by a *good* gauge there, and discuss why such gauges are said to be *asymptotically flat*.

Examining future null infinity poses a challenge as physical spacetimes are unbounded. To overcome this difficulty, one can use Penrose compactification [137]. That is, use a conformal transformation to produce a bounded, nonphysical metric, which contains a region representing asymptotic infinity of the physical spacetime [191, 107]. The region, known as conformal infinity, can span all asymptotic endpoints of the physical spacetime. A section of the asymptotic boundary of interest for gravitational-wave emitting systems is $\mathscr{I}^+$, the surface of endpoints of outgoing null geodesics (where energy and angular momentum are dissipated to). It is also convenient to probe $\mathscr{I}^+$ using a retarded time coordinate (u) [140], reaching $\mathscr{I}^+$ by taking $r \to \infty$ whilst constraining $u = constant$.

The form of the metric at $\mathscr{I}^+$ establishes whether the gauge is *good* there. If all curvature terms appear at orders in r below that of Minkowski (flat spacetime), then the gauge is said to be *good* at $\mathscr{I}^+$. This is equivalent to saying the gauge is "asymptotically flat" as the spacetime asymptotes to flat spacetime. Repeating this definition explicitly, first consider the metric of flat spacetime, the Minkowski metric

$$g^M_{\mu\nu} = \begin{pmatrix} -1 & 0 & 0 & 0 \\ 0 & 1 & 0 & 0 \\ 0 & 0 & r^2 & 0 \\ 0 & 0 & 0 & r^2 \sin[\theta] \end{pmatrix}, \tag{1.24}$$

expressed in inertial polar coordinates. Hence, for a gauge to be asymptotically flat the metric must satisfy

$$\mathbf{g}_{\mu\nu} - g^{M}_{\mu\nu} = \begin{pmatrix} \mathcal{O}(r^{-1}) & \mathcal{O}(r^{-1}) & \mathcal{O}(r^{0}) & \mathcal{O}(r^{0}) \\ \mathcal{O}(r^{-1}) & \mathcal{O}(r^{-1}) & \mathcal{O}(r^{0}) & \mathcal{O}(r^{0}) \\ \mathcal{O}(r^{0}) & \mathcal{O}(r^{0}) & \mathcal{O}(r^{1}) & \mathcal{O}(r^{1}) \\ \mathcal{O}(r^{0}) & \mathcal{O}(r^{0}) & \mathcal{O}(r^{1}) & \mathcal{O}(r^{1}) \end{pmatrix}, \tag{1.25}$$

(in similar coordinates), and derivatives of $\mathbf{g}_{\mu\nu}$ with respect to r (at fixed u) decay one order more rapidly with r. Often, one talks about the metric perturbation being asymptotically flat. This means $h^{(n)}_{\mu\nu}$ satisfies

$$h^{(n)}_{\mu\nu} = \begin{pmatrix} \mathcal{O}(r^{-1}) & \mathcal{O}(r^{-1}) & \mathcal{O}(r^{0}) & \mathcal{O}(r^{0}) \\ \mathcal{O}(r^{-1}) & \mathcal{O}(r^{-1}) & \mathcal{O}(r^{0}) & \mathcal{O}(r^{0}) \\ \mathcal{O}(r^{0}) & \mathcal{O}(r^{0}) & \mathcal{O}(r^{1}) & \mathcal{O}(r^{1}) \\ \mathcal{O}(r^{0}) & \mathcal{O}(r^{0}) & \mathcal{O}(r^{1}) & \mathcal{O}(r^{1}) \end{pmatrix}, \tag{1.26}$$

and the derivative of $h_{\mu\nu}$ with respect to r (at fixed u) decays at least one order more rapidly with r.

1.6.3 First-order self-force methods

I now turn my attention to self-force. Here, I cover some of the essential methods for calculating first-order self-force.

1.6.3.1 Matched asymptotic expansions

In Sec. 1.6, I outlined how EMRIs are modelled using black hole perturbation theory where the expansion parameter, ε, is the mass ratio and the background spacetime is the Kerr spacetime of the supermassive black hole. This model, known as the *outer expansion*, is applicable in regions where the presence of the supermassive black hole dominates the curvature of the spacetime. However, in a region significantly close to the compact object, $\mathbf{r} \sim \mu$ (where $\mathbf{r}$ is the distance from the compact object) [146], the curvature generated by the presence of the compact object dominates. Hence, the outer expansion breaks down (the outer expansion is only valid for $\mathbf{r} \gg \mu$).

In the region where spacetime curvature is dominated by the presence of the compact object, known as the inner region, a new perturbative expansion is required. An appropriate background spacetime for the so-called *inner expansion* is the metric of the compact object. In this thesis, I assume the compact object is a non-spinning and described by the Schwarzschild metric outside the object (but the methods here also extend to a spinning compact object [193, 112]).

Crucially, the same expansion parameter, ε, is used in the inner expansion as used in the outer expansion. This allows for matching the two asymptotic expansions in the region where they meet (the *buffer region*).

For the inner expansion, $\frac{\mathbf{r}}{\varepsilon}$ is held fixed while the expansion is calculated in orders of ε. The resulting metric expansion is

$$\mathbf{g}_{ab} = g_{ab}^{CO(0)} + H_{ab}^{(1)} + H_{ab}^{(2)} + \mathcal{O}(\varepsilon^3), \tag{1.27}$$

where $H_{ab}^{(n)}$ are the nth-order metric perturbations (which are produced by the presence of the supermassive black hole) and $g_{ab}^{CO(0)}$ is the metric of the compact object in isolation (Schwarzschild metric with mass μ). This expansion is valid in the region $\mathbf{r} \sim \mu$.

The region $\mu \ll \mathbf{r} \ll M$, known as the buffer region, seemingly lies outside the domains of validity of both expansions [23]. However, one can assume the *matching condition*; that is, when re-expanding each expansion into the buffer region, the two expansions must agree term by term in powers of $\mathbf{r}$ and ε (since they both are expansions of the same metric [147]). The form of the metric in the buffer region also provides information on the multipole moments of the compact object it surrounds as the buffer region effectively lies at asymptotic infinity in the local spacetime of the compact object [147]. One concludes that at distances $\mu \ll \mathbf{r}$ (in the outer region), the only significant properties of the compact object are its multipole moments.

Matched asymptotic expansions have been used to derive definitions of the stress-energy tensor of the compact object in the outer expansion. For the case of the compact object being a Schwarzschild black hole, the stress-energy tensor is a point mass (Eq. (1.31)). Matched asymptotic expansions have also been used to derive equations of motion for the compact object.

1.6.3.2 The MiSaTaQuWa equation

A significant stride forward into first-order self-force was made in 1997 by Mino, Sasaki and Tanaka [197] and Quinn and Wald [159]; they each derived a first-order equation of motion for the compact object in terms of the first-order metric perturbation. This is equivalent to providing an equation for the first-order self-force. The equation of motion, known as the MiSaTaQuWa equation, can be written as [147]

$$a^a = u^b u^a{}_{;b} = -\frac{1}{2} P^{ab} (2h^{(1)tail}_{bc;d} - h^{(1)tail}_{cd;b}) u^c u^d + \mathcal{O}(\varepsilon^2), \tag{1.28}$$

where a^a is the acceleration (away from geodesic motion) of the compact object, u^α is the four-velocity of the compact object, and $P^{ab} = g^{ab} + u^a u^b$. $h^{(1)tail}_{ab}$ is the piece of $h^{(1)}_{ab}$

that has propagated from points in the past of the compact object's worldline, γ (with coordinates z^μ).

1.6.3.3 The split into the regular and singular fields

As seen in the MiSaTaQuWa equation, Eq. (1.28), the motion of the compact object does not depend on the entire metric perturbation $h^{(1)}_{ab}$. Detweiler and Whiting [59, 62] showed that there is an alternative method to split $h^{(1)}_{ab}$ (which is consistent with the MiSaTaQuWa equation). This new split stemmed from a fundamental question which initiated self-force research: what part of an object's field affects its motion?

In electromagnetic theory, the importance of properly handling the *self-field* has long been apparent. Radiation reaction is a clear manifestation of an object interacting with its own field. That is, when a charged particle experiences a jerk (change in acceleration) in a vacuum, it spontaneously emits electromagnetic radiation. The radiation must derive from an interaction; hence, the jerked charge has interacted with its own field. However, it is not immediately clear how to describe this interaction as charged particles produce a singular electrostatic field at their position. Directly calculating a force with a singular field would result in a singular self-interaction. Theorists explained how a particle could interact with its own field by splitting the field into a regular and singular piece, and proving that the object does not interact with the singular piece [63]. The self-interaction with the regular part of the field results in a regular self-force. Similarly, in General Relativity, one must consider which (regular) part of the field an object interacts with and what singular part it does not [23].

The regular part of the field can be described as part of an effective external field which the object moves through. The effectively external metric compromises the background metric and a regular piece of the metric perturbation. Detweiler and Whiting applied this concept to the gravitational self-force problem by splitting the metric perturbation into a regular ($h^{(1)R}_{ab}$) and self-field ($h^{(1)S}_{ab}$, or singular) piece [59, 62],

$$h^{(1)}_{ab} = h^{(1)S}_{ab} + h^{(1)R}_{ab}. \tag{1.29}$$

Where $\delta G[h^{(1)S}_{ab}] = 8\pi T^{(1)}_{ab}$ and $\delta G[h^{(1)R}_{ab}] = 0$ [147]. To make the choice in split unique constraints are required: $h^{(1)S}_{ab}$ depends only on the instantaneous state and position of the particle and $h^{(1)R}_{ab}$ is causal, depending only on the particle's causal past [62]. The split allows one to define an effective metric,

$$\tilde{g}_{ab} = g^{(0)}_{ab} + h^{(1)R}_{ab}. \tag{1.30}$$

It has been shown that the compact object moves as a test particle in (on a geodesic of) $\tilde{g}_{ab}$, the effective metric, to first-order [197, 60, 62]. That is, Eq. (1.28) is equivalent to

the geodesic equation in $\tilde{g}_{ab}$. However, in practice, one calculates the self-force, with Eq. (1.28) (replacing $h^{(1)tail}_{ab}$ with $h^{(1)R}_{ab}$), that the compact object experiences as it moves through the background metric ($g^{(0)}_{ab}$). The particular choice of the regular and singular piece is a useful degree of freedom in self-force, subject to constraints that $\mathcal{E}[h^{(1)S}_{ab}] = 8\pi T^{(1)}_{ab}$ and $\mathcal{E}[h^{(1)R}_{ab}] = 0$.

1.6.3.4 The perturbed stress-energy tensor

Matched asymptotic expansions demonstrate that the appropriate stress-energy tensor is a point-mass for a compact object that produces a Schwarzschild metric when in isolation in its exterior. The point-mass stress-energy tensor is

$$T^{ab}_{(1)} = \mu \int_\gamma u^a u^b \delta^4(x,z) d\tau, \tag{1.31}$$

where τ is proper time (in the background spacetime), $u^\mu = dz^\mu/d\tau$ is the four-velocity of the compact object, and $\delta^4(x,z) = \frac{\delta^4(x^\alpha - z^\alpha)}{\sqrt{-g}}$.

The second-order stress-energy tensor was first conjectured by Detweiler [61] as

$$T^{ab}_{(2)} = -\frac{\mu}{2} \int_\gamma u^a u^b (g^{cd}_{(0)} - u^c u^d) h^{(1)R}_{cd} \delta^4(x,z) d\tau, \tag{1.32}$$

and has recently been shown to hold in the highly regular and Lorenz gauge by Ref. [185].

1.6.3.5 Puncture schemes

The singular nature of the stress-energy tensor relates to the singular behaviour in the metric perturbation on the worldline ($h^{(n)S}_{ab}$). Singularities can make equations ill-defined, cause integrals not to converge, or cause numerical calculations to be very slow. One method of handling singularities is subtracting singular behaviour away. To do so, one can derive a *puncture* analytically, which approximates the singular behaviour.

Here I will briefly describe using a puncture schemes to account for the singular behaviour in the stress-energy tensor through second-order. For a more detailed description see [23, 147]. The singular behaviour of $h^{(1)}_{ab}$ results from the stress-energy tensor, $T^{(1)}_{ab}$. For $h^{(2)}_{ab}$, the singular behaviour derives from both $h^{(1)}_{ab}$ and $T^{(2)}_{ab}$. The field equations for the puncture scheme can be formulated by extending the field-equations

away from the worldline

$$\delta G_{ab}[h^{(1)}_{ab}] = 0 \quad \forall\, x^{\alpha} \notin \gamma, \tag{1.33}$$

$$\delta G_{ab}[h^{(2)}_{ab}] = -\delta^2 G_{ab}[h^{(1)}_{ab}, h^{(1)}_{ab}] \quad \forall\, x^{\alpha} \notin \gamma, \tag{1.34}$$

$$\delta G_{ab}[h^{(3)}_{ab}] = ..., \tag{1.35}$$

Instead of using the singular stress-energy tensor on the worldline, one can introduce a singular puncture which approximates $h^{(n)S}_{ab}$. Such a puncture can be calculated analytically in an expansion in orders of $\mathbf{r}$, and attenuated to zero outside of some finite region containing the worldline. I label the puncture $h^{(n)\mathcal{P}}_{ab}$, with $h^{(n)\mathcal{P}}_{ab} \approx h^{(n)S}_{ab}$. $h^{(n)\mathcal{P}}_{ab}$ can be found by truncating the extension of the outer expansion of $h^{(n)S}_{ab}$ at some finite order of $\mathbf{r}$. One can then define a "residual" field, $h^{(n)\mathcal{R}}_{ab} := h^{(n)}_{ab} - h^{(n)\mathcal{P}}_{ab}$, which approximates the regular field $h^{(n)\mathcal{R}}_{ab} \approx h^{(n)R}_{ab}$.

If $h^{(n)\mathcal{P}}_{ab}$ approximates $h^{(n)S}_{ab}$ to a sufficiently high order in r, then the Taylor expansion of $h^{(n)\mathcal{R}}_{ab}$ and $h^{(n)R}_{ab}$ can be made to be identical to any finite order [23]. $h^{(1)\mathcal{R}}_{ab}$ can therefore be used in place of $h^{(1)tail}_{ab}$ in the MiSaTaQuWa equation, Eq. (1.28), to calculate the first-order self-force.

Using punctures, one can rewrite the field equations (Eqs. (1.15) and (1.16)) to solve for the residual field as

$$\delta G_{ab}[h^{(1)\mathcal{R}}_{ab}] = -\delta G_{ab}[h^{(1)\mathcal{P}}_{ab}], \tag{1.36}$$

$$\delta G_{ab}[h^{(2)\mathcal{R}}_{ab}] = -\delta^2 G_{ab}[h^{(1)}_{ab}, h^{(1)}_{ab}] - \delta G_{ab}[h^{(2)\mathcal{P}}_{ab}]. \tag{1.37}$$

Eqs. (1.36) and (1.37) are smooth on the particle, making them well defined as a distribution and straightforward to solve numerically. Eqs. (1.36) and (1.37) have been defined by treating the derivatives as ordinary derivatives. If one treats the derivatives as distributional, one obtains

$$\delta G_{ab}[h^{(1)\mathcal{R}}_{ab}] = T^{(1)}_{ab} - \delta G_{ab}[h^{(1)\mathcal{P}}_{ab}], \tag{1.38}$$

$$\delta G_{ab}[h^{(2)\mathcal{R}}_{ab}] = T^{(2)}_{ab} - \delta^2 G_{ab}[h^{(1)}_{ab}, h^{(1)}_{ab}] - \delta G_{ab}[h^{(2)\mathcal{P}}_{ab}], \tag{1.39}$$

where the stress-energy perturbations (defined in Sec. 1.6.3.4) will cancel with the distributional behaviour in $\delta G_{ab}[h^{(n)\mathcal{P}}_{ab}]$. However, to make Eq. (1.39) well defined, one must work in a gauge where $\delta^2 G_{ab}[h^{(1)}_{ab}, h^{(1)}_{ab}]$ and $T^{(2)}_{ab}$ are well defined (such as the highly regular gauge and Lorenz gauge [185]).

Alternatively to using a puncture scheme, one could work in a highly regular gauge where Eq. (1.16) is well defined and integrable. Ref. [185] also showed $\delta^2 G_{ab}[h^{(1)}_{ab}, h^{(1)}_{ab}]$ is well defined as a distribution in the Lorenz gauge using the definition of the puncture $\delta G_{ab}(h^{(2)\mathcal{P}}_{ab})$.

1.6.3.6 The self-consistent and Gralla-Wald approximations

So far, I have discussed how to calculate the self-force from $h^{(1)}_{ab}$. Nevertheless, to model an EMRI, one must evolve the worldline of the compact object under the influence of this force. The metric perturbation and worldline are interconnected. The metric perturbation depends on the position of the compact object, and the worldline depends on the self-force and, therefore, the metric perturbation. Two standard approximations for the worldline's evolution are the self-consistent approximation and the Gralla-Wald approximation. I will summarise both approximations here (for a detailed review, see [147]) and comment on their suitability for full EMRI calculations. In the following section, I summarise the most promising evolution approximation for modelling EMRIs, the two-timescale approximation.

The Gralla-Wald approximation: In the Gralla-Wald approximation the worldline (γ) is expanded in orders of ε [85],

$$\gamma = \gamma_{(0)} + \gamma_{(1)} + \gamma_{(2)} + ..., \tag{1.40}$$

$$z^{\mu}(s,\varepsilon) = z^{\mu}_{(0)}(s) + z^{\mu}_{(1)}(s,\varepsilon) + z^{\mu}_{(2)}(s,\varepsilon) + ..., \tag{1.41}$$

where $\gamma_{(0)}$ is the zeroth-order worldline (a geodesic of the background spacetime), $\gamma_{(1)}$ can be considered as the first-order deviation from the zeroth-order worldline ($\gamma_{(0)}$) and so on.

As the metric perturbations arise from the presence of the compact object, they have a dependence on the objects' position ($z^{\mu}(s,\varepsilon)$) and velocity ($\dot{z}^{\mu}(s,\varepsilon) = \frac{dz^{\mu}}{ds}$), where s is a generic time variable. That is, in the Gralla-Wald approximation, the metric is expressed as [147]

$$\mathbf{g}_{\mu\nu}(x,\varepsilon;z,\dot{z}) = g^{(0)}_{\mu\nu}(x) + \sum_{n>0} \varepsilon^n \check{h}^{(n)}_{\mu\nu}(x,\varepsilon;z_{(0)},...,z^a_{(n-1)},\dot{z}_{(0)},...,\dot{z}_{(n-1)}). \tag{1.42}$$

The issue with this approximation is that over the large time scales on which EMRI inspirals occur, the deviation vectors $z^{\mu}_{(n)}(s,\varepsilon)$ (for $n \geq 1$) grow at least quadratically with time, meaning this approximation breaks down well before modelling a whole EMRI inspiral. This breakdown is apparent when you consider that the initial geodesic, $\gamma_{(0)}$, is an inappropriate approximation for the late inspiral geodesics.

The self-consistent approximation: In the self-consistent approximation, to avoid growing errors, one does not expand the worldline, leaving it exact. It is known as an *accelerated worldline*, as it is not a geodesic in the background spacetime. The exact worldline is labelled γ_{ε} with coordinates z^{μ}_{ε}. In the self-consistent approximation, the

metric expansion can be written as

$$\mathbf{g}_{\mu\nu}(x^a, \varepsilon; z^a_\varepsilon, \dot{z}^a_\varepsilon) = g^{(0)}_{\mu\nu}(x^a) + \sum_{n>0} \varepsilon^n h^{(n)}_{\mu\nu}(x^a; z^a_\varepsilon, \dot{z}^a_\varepsilon). \tag{1.43}$$

Note, in this approximation the ε dependence of the coefficients $h^{(n)}_{ab}$ comes only through z^a_ε and $\dot{z}^a_\varepsilon$.

The approximation's self-consistency comes from the process that at each time-step z^a_ε must being calculated simultaneously with $h^{(n)}_{\mu\nu}(x^a; z_\varepsilon, \dot{z}^a_\varepsilon)$. The MiSaTaQuWa equation was first derived in the first-order self-consistent approximation. More recently, Pound [144] extended the self-consistent expansion to second order with a systematic method that could be taken to any order.

The self-consistent approximation is more appropriate for modelling systems that evolve through a worldline that eventually changes significantly from the initial geodesic. However, the expansion does not capitalise on the slow evolution of an EMRI inspiral [23], which effectively makes each EMRI orbit approximately geodesic on the orbital time scale [119].

1.6.3.7 The two-timescale approximation

The two-timescale expansion takes advantage of the near periodicity of EMRI inspirals whilst evolving the orbit without accumulating growing errors [98]. Quantities, such as the metric perturbation, are expressed in terms of both a slow-time ($\tilde{t}$, which evolves at the speed of the whole inspiral) and fast times (the three orbital phases φ_i). The slow timescale is related to the radiation reaction time, $t_{rr} \sim \frac{M}{\varepsilon}$[119]; hence, the slow timescale on which the orbit evolves due to radiation reaction is $\tilde{t} \sim \varepsilon t$ [69]. Here I overview how the two-timescale approximation is implemented for generic orbits in Kerr [154, 119].

Before describing the two-timescale approximation I first introduce the frequency-domain approach (which will have some similarities). The dependence on the fast timescale can be expressed using the three orbital frequencies, $\Omega_i := \{\Omega_r, \Omega_\theta, \Omega_\phi\}$ [154, 119]. This results in a leading order metric perturbation of the form

$$h^{(1)}_{ab} = \sum_{p,q,m} h^{(1),\omega_{p,q,m}}_{ab}(x^i) e^{-i(p\Omega_r + q\Omega_\theta + m\Omega_\phi)t}, \tag{1.44}$$

where $\omega_{p,q,m} = p\Omega_r + q\Omega_\theta + m\Omega_\phi$ and $x^i := \{r, \theta, \phi\}$. Eq. (1.44) is a time Fourier series of the metric perturbation and is used in the self-force frequency-domain approach [26]. The two-timescale approach appears similar to the frequency-domain approach at leading order; however, to express the fast time dependency at higher

orders requires replacing the t dependency (in Eq. (1.44)) with t dependent orbital phases φ_i. The three phases are defined as [119]

$$\varphi_i := \int \Omega_i dt, \tag{1.45}$$

where Ω_i now depend on the slow time $\tilde{t}$. The phases are called "fast times" as they evolve on the orbital timescale. In the two-timescale approach the metric perturbations are expressed as

$$h^{(n)}_{ab} = \sum_{p,q,m} h^{(n),\omega_{p,q,m}}_{ab}(\tilde{t}, x^i) e^{-i(p\varphi_r + q\varphi_\theta + m\varphi_\phi)}. \tag{1.46}$$

Eq. (1.46) is a discrete Fourier series in terms of the phases. Eq. (1.46) differs from the conventional frequency domain approach (Eq. (1.44)) as t does not appear explicitly and the frequencies (Ω_i) and $h^{(n),\omega_{p,q,m}}_{\mu\nu}(\tilde{t}, x^i)$ evolve on the slow timescale.

Putting Eq. (1.46) into the first- and second-order linearised EFE splits the equations into frequency-domain like equations for $h^{(n),\omega_{p,q,m}}_{\mu\nu}(\tilde{t}, x^i)$ for fixed $\tilde{t}$, and evolution equations for $h^{(n),\omega_{p,q,m}}_{\mu\nu}(\tilde{t}, x^i)$ and Ω_i as functions of $\tilde{t}$ [119]. The first-order linearised EFE in the two-timescale approximation is in a similar form to the first-order frequency-domain approach. Whereas, the two timescale approximation introduces slow time derivative terms to the right hand side of the second-order linearised EFE. Once these terms are included, the second-order linearised EFE can be solved similarly to the frequency-domain method. In Sec. 4.1.2, I describe how the two-timescale approximation is implemented for quasi-circular orbits in Schwarzschild (which illustrates how slow-time derivative terms appear in the general case).

1.6.4 Second-order self-force: state of play

I return to the desire to calculate the dissipative piece of second-order self-force (to produce accurate EMRI inspiral models). Before reviewing the current state of the art in second-order self-force results, I briefly review the progress in calculating second-order perturbations in gravity outside of self-force research.

The general formalism for perturbations to generic background spacetimes has been developed [180, 182, 42, 173]. There has been a significant scheme of work on second-order calculations in cosmology [125, 111, 7, 181, 128, 139, 184, 30]. And there have also been calculations on the second-order perturbations to Schwarzschild spacetime relevant to collapsing stars [39, 40, 41]. There has also been progress for second-order calculations restricted to vacuum perturbations [141, 80, 79, 81, 132, 92, 129, 198]. Tangentially, there has also been a success in formulating the post-Minkowski expansion to the nth-order [35, 34, 142], with a recent resurgence of interest in scattering orbits [57]. Post-Newtonian methods have also

been taken to a very high order [142, 32, 49]. Finally, there has been recent success in calculating quasinormal modes to second-order [102, 163] using a form of the second-order Teukolsky equation [45] (which I will discuss in Chap. 2).

The majority of self-force research has concerned developing and implementing first-order methods, delivering important results and methods that will be used to help model EMRIs. First-post adiabatic models require the full first-order self-force. However, first-post adiabatic models also require the dissipative piece of the second-order self-force [69]. Second-order self-force methods had been largely left unexplored until the last decade. Preliminary work on the second-order calculations began in 2006 by Rosenthal [164]. Ref. [61] also presents work on the subject. Rigorous, complete results emerged in 2012, with the derivation of the second-order equations of motion (an extension of the MiSaTaQuWa equation to second-order), independently derived by Pound [146] and Gralla [84], using the self-consistent and Gralla-Wald approximations respectively. These two derivations produce comparable results, but a detailed analysis of their equivalence has not yet been produced. In Ref. [146] the second-order equation of motion is given as

$$a^a = u^b u^a_{;b} = -\frac{1}{2} P^{ac} (g^{(0)d}_c - h^{\mathcal{R}d}_c)(2h^{\mathcal{R}}_{d(b;e)} - h^{\mathcal{R}}_{be;d}) u^b u^e + \mathcal{O}(\varepsilon^3), \tag{1.47}$$

where $P^{ab} = g^{(0)ab} + u^a u^b$ and $h^{\mathcal{R}}_{ab} = h^{(1)\mathcal{R}}_{ab} + h^{(2)\mathcal{R}}_{ab}$. Eq. (1.47) is equivalent to the geodesic motion in $g^{(0)}_{ab} + h^{\mathcal{R}}_{ab}$. In Ref. [146] Pound showed Eq. (1.47) is valid in any gauges smoothly related to the Lorenz gauge, and in Ref. [150] Pound showed the validity extends to the highly regular class of gauges.

Eq. (1.47) is only consistent if the compact object is spherical and non-spinning. Realistic post adiabatic models will require an equation of motion that includes the spin and quadrupole moments of the compact object [23]. Attempting such a derivation might lead to the issue of having more than one acceptable definition for the centre of mass of the compact object.

A toy model implementation of second-order calculations was made in Ref. [101], where some fictitious second-order modes were calculated (sourced by a handful of $h^{(1)}_{ab}$ modes) in the limited case of a head-on collision in a Schwarzschild background. Recently, more realistic second-order calculations were made, modelling EMRIs for quasi-circular orbits in Schwarzschild [156, 194, 195]. Precisely, the binding energy of an EMRI was calculated to second order [156], followed by the energy flux [194], and finally, waveforms were produced [195]. This breakthrough in second-order self-force calculations took the best part of a decade to implement. However, astrophysically realistic EMRI models will require a Kerr background (as supermassive black holes are expected to have spin), so much work is needed.

Ref. [195] shows compelling evidence that first-post adiabatic waveforms are accurate well outside of the EMRI regime. The first-post adiabatic models in Ref. [195] show good agreement with Numerical Relativity waveforms for mass-ratio as large as 1/10 (up to two orbits before the merger). This is encouraging news in the endeavour for modelling IMRIs. Also, the first-post adiabatic waveforms take just seconds to generate (and will be orders of magnitude faster once the code is converted from Mathematica to C++) as the self-force data has been precomputed. Hence, the waveform modelling calculations only need to call the self-force data to produce waveforms. Numerical Relativity techniques cannot match this speed, a typical Numerical Relativity binary simulation takes days to months to compute a waveform. Additionally, first-post adiabatic waveform modelling can be achieved whilst leaving the mass-ratio as a free parameter (see the 1PAT2 and 1PAF1 models in Ref. [195]). The mass-ratio agnostic models do compromise on accuracy but could be used to speed up data analysis.

1.7 The Newman–Penrose formalism and the Teukolsky equation

Introductory courses to General Relativity generally introduce the theory using tensor fields (such as the Riemann and Einstein tensors) and Christoffel symbols. Alternatively, one can re-express geometric quantities as a school of scalar fields. This can be achieved by defining a set of four basis vectors and contracting each tensor index with said basis vectors. Choosing the set of basis vectors to be orthonormal, with two real and two complex vectors, turns out to be particularly useful for expressing and calculating perturbed quantities in Kerr spacetime [191].

1.7.1 The Newman–Penrose formalism

The Newman–Penrose (NP) formalism [131] constructs a basis spanning $3+1$ spacetime using null vectors. A null vector (k^a) satisfies

$$g_{ab}k^a k^b = 0. \tag{1.48}$$

Note, here I have defined the null vector relative to the background metric g_{ab}; k^a is therefore a background quantity. While the definitions in this section can be promoted to the full spacetime metric $\mathbf{g}_{ab}$, the NP formalism generally makes definitions using the background metric. Perturbed NP quantities are then defined using the background NP quantities and the metric perturbations. Hence, a null vector in the full spacetime $\mathbf{k}^a = k^a + k^a_{(1)} + k^a_{(2)} + ...$, where $k^a_{(1)}$ is a function of $h^{(1)}_{ab}$ and the

background NP quantities, and $k^a_{(2)}$ is a function of $h^{(1)2}_{ab}$, $h^{(2)}_{ab}$, and the background NP quantities.

The NP basis vectors are labeled $e^a_{[a]} = \{e^a_{[1]}, e^a_{[2]}, e^a_{[3]}, e^a_{[4]}\} := \{l^a, n^a, m^a, \bar{m}^a\}$ (where indices in square brackets are tetrad indices) and are collectively referred to as a *tetrad* (or *tetrad legs*). The vectors have the chosen properties that l^a and n^a are real and m^a is complex. Over-bars ($\bar{m}^a$) denote a complex conjugate. Conventionally, using a positive metric signature, the orthonormal relationship of the tetrad takes the form

$$l^a n_a = -1, m^a \bar{m}_a = 1, \tag{1.49}$$

where all other combinations of contracted tetrad vectors $= 0$ [3]. This implies the existence of a fundamental matrix, $\eta_{[a][b]} := g_{ab} e^a_{[a]} e^b_{[b]}$, for raising and lowering tetrad indices, which takes the form,

$$\eta_{[a][b]} = \begin{pmatrix} 0 & -1 & 0 & 0 \\ -1 & 0 & 0 & 0 \\ 0 & 0 & 0 & 1 \\ 0 & 0 & 1 & 0 \end{pmatrix}. \tag{1.50}$$

Hence, $e^{[a]a} = \{e^{[1]a}, e^{[2]a}, e^{[3]a}, e^{[4]a}\} := \{-n^a, -l^a, \bar{m}^a, m^a\}$.

Similarly, $g_{ab} = e^{[a]}_a e^{[b]}_b \eta_{[a][b]}$ [131]; that is,

$$g_{ab} = -2 l_{(a} n_{b)} + 2 m_{(a} \bar{m}_{b)}, \tag{1.51}$$

where curved brackets denote symmetrisation.

1.7.1.1 Ricci rotation coefficients

Instead of using Christoffel symbols to describe the metric connection, the NP formalism uses Ricci rotation coefficients [191],

$$\gamma_{[c][a][b]} = e^k_{[c]} e_{[a]k;i} e^i_{[b]}. \tag{1.52}$$

By expressing the covariant derivative using the tetrad partial derivative ($\mathbf{D}$) and the connection ($\tilde{\Gamma}$), one obtains

$$e^k_{[c]} e_{[a]k;i} e^i_{[b]} = e^k_{[c]} e^i_{[b]} (\mathbf{D}_i e_{[a]k} + \tilde{\Gamma}^j_{ik} e_{[a]j}) \tag{1.53}$$

[3] Originally [131], the NP formalism was formulated with the metric having a negative signature, where $l^a n_a = 1$ and $m^a \bar{m}_a = -1$. However, as current convention for modern research in General Relativity is largely with a positive metric signature, I work with the positive signature convention (with NP conventions consistent with Ref. [118]).

Using the definition of the tetrad partial derivatives ($\mathbf{D}_i e_{[a]k} = 0$), one finds

$$\gamma_{[c][a][b]} = e^{k}_{[c]} e^{i}_{[b]} \tilde{\Gamma}^{j}_{ik} e_{[a]j}. \tag{1.54}$$

That is, Ricci rotation coefficients are the metric connection (of the tetrad basis) contracted with tetrad vectors. Note, as the tetrad basis is non-holonomic ($\mathcal{L}_{e^{a}_{[c]}} e^{b}_{[d]} \neq 0$) and null, the Ricci rotation coefficients have different symmetry properties to the Christoffel symbols (the connection coefficients for holonomic/coordinate bases) [121]. Specifically, whereas Christoffel symbols are symmetric in the second two indices, Ricci rotation coefficients are antisymmetric in the first two indices:

$$\gamma_{[c][a][b]} = -\gamma_{[a][c][b]}. \tag{1.55}$$

Eq. (1.55) can be derived from $\eta_{[a][b],c} = (e_{[a]d} e^{d}_{[b]})_{;c} = 0$ [48].

1.7.1.2 Spin coefficients

The (non-trivially zero by Eq. (1.55)) tetrad components of the Ricci-rotation coefficients are conventionally represented using 12 complex scalars:

$$\kappa = -\gamma_{[3][1][1]},\ \tau = -\gamma_{[3][1][2]}, \sigma = -\gamma_{[3][1][3]},\ \rho = -\gamma_{[3][1][4]},$$

$$\pi = -\gamma_{[2][4][1]},\ \nu = -\gamma_{[2][4][2]}, \mu = -\gamma_{[2][4][3]}, \lambda = -\gamma_{[2][4][4]},$$

$$\epsilon = -\frac{\gamma_{[2][1][1]} + \gamma_{[3][4][1]}}{2}, \gamma = -\frac{\gamma_{[2][1][2]} + \gamma_{[3][4][2]}}{2},$$

$$\beta = -\frac{\gamma_{[2][1][3]} + \gamma_{[3][4][3]}}{2}, \alpha = -\frac{\gamma_{[2][1][4]} + \gamma_{[3][4][4]}}{2}], \tag{1.56}$$

known as *spin coefficients*. Note, ϵ, γ, β, and α contain two Ricci-rotation coefficients because one of their Ricci-rotation coefficients is purely real, whilst the other is purely complex. For example, by using the complex conjugate operation, $\{l \to l, n \to n, m \to \bar{m}, \bar{m} \to m\}$ ($\{[1] \to [1], [2] \to [2], [3] \to [4], [4] \to [3]\}$). Hence, for ϵ, $\overline{\gamma_{[2][1][1]}} = \gamma_{[2][1][1]} \Rightarrow \mathrm{Im}[\gamma_{[2][1][1]}] = 0$ and $\overline{\gamma_{[3][4][1]}} = \gamma_{[4][3][1]} = -\gamma_{[3][4][1]} \Rightarrow \mathrm{Re}[\gamma_{[3][4][1]}] = 0$. Therefore, the sum of these two Ricci rotation coefficients gives a single complex scalar (ϵ).

I write the covariant derivative contracted with a tetrad vector as

$$e^{a}_{[b]} \nabla_a \eta := \eta_{|[b]}, \tag{1.57}$$

Alternatively, the tetrad components of the covariant derivative is written as

$$\begin{aligned} D\eta &:= \eta_{|[1]} := l^a \nabla_a \eta, \quad \Delta\eta := \eta_{|[2]} := n^a \nabla_a \eta, \\ \delta\eta &:= \eta_{|[3]} := m^a \nabla_a \eta, \quad \bar{\delta}\eta := \eta_{|[4]} := \overline{m}^a \nabla_a \eta. \end{aligned} \tag{1.58}$$

1.7.1.3 Ricci and Weyl curvature scalars

Another key curvature quantity in differential geometry is the Riemann tensor, which can be split into the Ricci tensor and Weyl tensor. The Ricci tensor is the trace piece of the Riemann tensor,

$$R_{ab} = R^c{}_{acb}. \tag{1.59}$$

In general, the Ricci tensor is related to the stress-energy tensor via the EFE, Eq. (1.6); therefore, the Ricci tensor represents non-vacuum curvature.

The Weyl tensor (C_{abcd}) is defined as the trace-free part of the Riemann tensor (i.e., the non-Ricci piece) and represents the vacuum curvature. Explicitly, it is expressed as

$$\begin{aligned} C_{abcd} =& R_{abcd} - \frac{1}{2}(\mathbf{g}_{ac}R_{bd} - \mathbf{g}_{bc}R_{ad} - \mathbf{g}_{ad}R_{bc} + \mathbf{g}_{bd}R_{ac}) \\ &+ \frac{1}{6}(\mathbf{g}_{ac}\mathbf{g}_{bd} - \mathbf{g}_{ad}\mathbf{g}_{bc})R. \end{aligned} \tag{1.60}$$

In the NP formalism one contracts the Weyl tensor with the various tetrad legs. The ten degrees of freedom of the Weyl tensor can be expressed as five complex scalars (known as Weyl scalars),

$$\psi_0 = C_{[1][3][1][3]}, \tag{1.61}$$

$$\psi_1 = C_{[1][3][1][2]}, \tag{1.62}$$

$$\psi_2 = C_{[1][3][4][2]}, \tag{1.63}$$

$$\psi_3 = C_{[1][2][4][2]}, \tag{1.64}$$

$$\psi_4 = C_{[2][4][2][4]}. \tag{1.65}$$

One can similarly express the Ricci tensor as a set of four real scalars and three complex scalars labeled Φ_{ij} [48]. However, for the purpose of understanding their physical significance, I instead replace components of the Ricci tensor with tetrad components of the stress-energy tensor. The EFE informs us that $R_{[a][b]} = 8\pi T_{[a][b]}$ except $R_{[1][2]} = 8\pi T_{[3][4]}$ and $R_{[3][4]} = 8\pi T_{[1][2]}$ (as $8\pi T_{ab}$ is the trace-reverse of R_{ab} using the EFE).

1.7.1.4 The Ricci and Bianchi identities in the NP formalism

The usefulness of the NP formalism becomes apparent when the Riemann tensor and Bianchi identities are expressed using the NP scalars. Similarly to how the Riemann tensor can be constructed from Christoffel symbols, it can also be expressed in terms of spin coefficients, as follows. As a preliminary step, I express the Riemann tensors using Ricci rotation coefficients by contracting the Riemann tensor with the tetrad basis vectors,

$$e^{a}_{[a]}e^{b}_{[b]}e^{c}_{[c]}e^{d}_{[d]}R_{abcd} = R_{[a][b][c][d]} = -\gamma_{[a][b][c],[d]} + \gamma_{[a][b][c],[d]} \tag{1.66}$$

$$+\gamma_{[b][a][f]}(\gamma_{[c]}{}^{[f]}{}_{[d]} - \gamma_{[d]}{}^{[f]}{}_{[c]}) \tag{1.67}$$

$$+\gamma_{[f][a][c]}\gamma_{[b]}{}^{[f]}{}_{[d]} - \gamma_{[f][a][d]}\gamma_{[b]}{}^{[f]}{}_{[c]}. \tag{1.68}$$

Deriving this relation uses the Ricci identity ($R_{abcd}e^{a}_{[a]} = e_{[a]b;c;d} - e_{[a]b;d;c}$) [48]. One can then choose particular tetrad vectors for $[a]$, $[b]$, $[c]$ and $[d]$ in Eq. (1.66); e.g.,

$$R_{[1][3][1][3]} = (D - \rho - \bar{\rho} - 3\epsilon + \bar{\epsilon})\sigma - (\delta - \tau + \bar{\pi} - \bar{\alpha} - 3\beta)\kappa. \tag{1.69}$$

This form of the Riemann tensor is useful when equated with the Riemann tensor deconstructed into its Ricci and Weyl tensor parts. In vacuum,

$$R_{[1][3][1][3]} = C_{[1][3][1][3]} = \psi_0. \tag{1.70}$$

Hence, Eq. (1.69) can be written as the equality

$$\psi_0 = (D - \rho - \bar{\rho} - 3\epsilon + \bar{\epsilon})\sigma - (\delta - \tau + \bar{\pi} - \bar{\alpha} - 3\beta)\kappa. \tag{1.71}$$

There are 36 linearly independent equalities one can derive from the Riemann tensor, these are called *Ricci identities*. One can also express tetrad parallel derivatives acting on the Riemann tensor (e.g., $R_{[a][b][c][d]||[f]}$) in terms of NP spin coefficients. Hence, one can also express the Bianchi identities, $R_{[a][b]\{[c][d]||[f]\}} = 0$ (where the enclosed curly bracket represent antisymmetrisation), in NP form, of which there are 20 independent equations. See Ref. [48] for a full list of the Ricci and Bianchi identities in NP form.

1.7.1.5 Infinitesimal tetrad rotations

In the NP formalism, the choice of tetrad accounts for 6 degrees of freedom. These freedoms are associated with the three local boosts and three local spatial rotations of the tetrad [48] (as General Relativity is a locally Lorentz-invariant theory). In the context of tetrad transformations, one refers to all six of these local Lorentz transformations as *tetrad rotations*, and the choice of the tetrad is known as the *tetrad frame*.

As one moves to a perturbation set-up, the tetrad frame grows in complexity. Similarly to how introducing perturbations introduces (infinitesimal) gauge degrees of freedom, perturbations also introduce infinitesimal tetrad rotation degrees of freedom. Keeping track of the tetrad frame and infinitesimal tetrad frame can be challenging, so it is essential to be precise with one's language when referring to the tetrad frame.

1.7.1.6 The Petrov type D nature of Kerr spacetime

The NP formalism is very convenient for describing spacetimes with coinciding principle null vectors. Principle null vectors (k^a) satisfy [191]

$$k^b k^c k_{\{e} C_{a\}bc\{d} k_{f\}} = 0. \tag{1.72}$$

Generally, spacetimes have four principle null vectors. Whether a spacetime's principle null vectors coincide or not characterises their so-called Petrov type [48].

Kerr spacetime is Petrov type D as it has two principle null vectors (two pairs of principle null vectors which coincide). The tetrad can be chosen such that l^a and n^a are tangent to the principle null directions (l^a and n^a then represent the outgoing and ingoing null geodesics from the black hole, respectively). Choosing such a tetrad basis (in a Petrov type D background spacetime) causes four of the Weyl scalars and 4 of the NP spin coefficients to vanish [48],

$$\psi_0 = 0, \psi_1 = 0, \psi_3 = 0, \psi_4 = 0, \tag{1.73}$$

$$\kappa = 0, \lambda = 0, \nu = 0, \sigma = 0. \tag{1.74}$$

ϵ can also be made to vanish by using the remaining tetrad rotation degree of freedom (that is, choosing a Kinnersley tetrad) [99]. This choice, however, destroys the symmetry between n^a and l^a. To maintain this symmetry, one can use the Carter tetrad [47] (with $\epsilon \neq 0$).

Note, $\kappa = 0, \lambda = 0, \nu = 0, \sigma = 0$ is equivalent to l^a and n^a being shear free [48]. The Goldberg-Sachs theorem [82] states that these conditions are also equivalent to the spacetime being of Petrov type D [48]. In this work, I am interested in the Kerr metric, which is Petrov type D. I will always use principle-null direction aligned tetrads, so throughout the remainder of this thesis, the simplifications in Eq. (1.73) will generally be made without comment.

1.7.2 The GHP formalism

Shortly after the NP formalism became popular, Geroch, Held and Penrose (GHP) made a significant simplification to the method in Petrov type D spacetimes [77]. This

simplification relies on symmetries of NP formalism while choosing two null vectors to align with the principle null directions. Two degrees of tetrad rotation freedom remain while constraining l^a and n^a to point in the principle null directions. These freedoms can be associated with two constants (spin s and boost b weight) for (most) NP quantities. The $\{b, s\}$ weights of the tetrad vectors are, $\{1, 0\}$, $\{-1, 0\}$, $\{0, 1\}$ and $\{0, -1\}$ for l^a, n^a, m^a and $\bar{m}^a$ respectively.

Additionally, there is a freedom to interchange l^a and n^a, for which GHP introduced a prime notation. Hence, half of the NP spin coefficients can be related to the other half by the prime notation,

$$\kappa' := -\nu,\ \sigma' := -\lambda,\ \rho' := -\mu,\ \tau' := -\pi,\ \beta' := -\alpha,\ \epsilon' := -\gamma. \tag{1.75}$$

Introducing a spin and boost weight highlights that four of the NP spin coefficients do not have a well defined spin and boost weight (ϵ, ϵ', β, and β', the four spin coefficients which consist of two Ricci rotation coefficients each). Additionally, the NP derivatives do not have a well defined spin and boost weight. Instead, these quantities can be combined to produce the *GHP derivatives* (which have well-defined spin and boost weights),

$$\begin{aligned} \text{Þ}\eta &= (D - p\epsilon - q\bar{\epsilon})\eta,\ \text{Þ}'\eta = (\Delta + p\epsilon' + q\bar{\epsilon}')\eta, \\ \text{ð}\eta &= (\delta - p\beta + q\bar{\beta})\eta,\ \text{ð}'\eta = (\bar{\delta} + p\beta' - q\bar{\beta}')\eta, \end{aligned} \tag{1.76}$$

where p and q are *GHP weights* of the generic tensor η with spin-weight $s = \frac{1}{2}(p - q)$ and boost-weight $b = \frac{1}{2}(p + q)$.

The $\{p, q\}$ weights of the tetrad vectors are $\{1, 1\}$, $\{-1, -1\}$, $\{1, -1\}$ and $\{-1, 1\}$ for l^a, n^a, m^a and $\bar{m}^a$ respectively (and for Þ, Þ′, ð and ð′ respectively). The product of a scalar of type $\{p, q\}$ with a scalar of type $\{r, s\}$ is a scalar of type $\{p + r, q + s\}$. For most of this thesis I work in the NP formalism, but in some sections the GHP formalism will prove more useful.

1.7.3 The Teukolsky equation

At first appearance, the NP equations, the Ricci and Bianchi identities in NP form (e.g., Eq. (1.71)), may look quite cumbersome. Manipulating such equations by hand is a challenging task, and it is quite hard to believe that someone could find a useful equation from this swamp of NP spin coefficients, yet that is precisely what Teukolsky achieved. In the context of perturbation theory in Kerr, the Teukolsky equation is of primary importance, as it is a separable hyperbolic differential equation for a quantity containing the gauge-invariant content of the metric perturbation. Here I will present

a brief outline of how the Teukolsky equation was derived. See Refs. [178, 48] for complete derivations.

Deriving the Teukolsky equation involves manipulating a selection of perturbed Bianchi and Ricci identities. For example, perturbing Eq. (1.71) gives

$$\psi_0^{(1)} = (D^{(1)} - \rho^{(1)} - \bar{\rho}^{(1)} - 3\epsilon^{(1)} + \bar{\epsilon}^{(1)})\sigma^{(0)} - (\delta^{(1)} - \tau^{(1)} + \bar{\pi}^{(1)} - \bar{\alpha}^{(1)} - 3\beta^{(1)})\kappa^{(0)} + (D^{(0)} - \rho^{(0)} - \bar{\rho}^{(0)} - 3\epsilon^{(0)} + \bar{\epsilon}^{(0)})\sigma^{(1)} - (\delta^{(0)} - \tau^{(0)} + \bar{\pi}^{(0)} - \bar{\alpha}^{(0)} - 3\beta^{(0)})\kappa^{(1)}. \tag{1.77}$$

I rewrite Eq. (1.77) whilst making the simplifications of working in Petrov type D and omitting (0) labels for succinctness (they will generally be omitted in the rest of this thesis), this gives

$$\psi_0^{(1)} = (D - \rho - \bar{\rho} - 3\epsilon + \bar{\epsilon})\sigma^{(1)} - (\delta - \tau + \bar{\pi} - \bar{\alpha} - 3\beta)\kappa^{(1)}. \tag{1.78}$$

One can combine certain perturbed Bianchi and Ricci identities in NP form [48] (using either Petrov type D Eq. (1.73) or Petrov Type-II simplifications) to eliminate all first-order perturbed quantities except for $\psi_4^{(1)}$ (and $T^{(1)}_{[a][b]}$ which is assumed to be known). This results in the Teukolsky equation,

$$[(\Delta + 3\gamma - \bar{\gamma} + 4\mu + \bar{\mu})(D + 4\epsilon - \rho) - (\bar{\delta} - \bar{\tau} + \bar{\beta} + 3\alpha + 4\pi)(\delta - \tau + 4\beta) - 3\psi_2]\psi_4^{(1)} = T_4, \tag{1.79}$$

where T_4 is

$$\begin{aligned} T_4 :&= \mathcal{S}_4[8\pi T^{(1)}_{ab}] \\ &= 4\pi\left[\bar{d}_4^{(0)}\left[(\bar{\delta} - 2\bar{\tau} + 2\alpha)T^{(1)}_{n\bar{m}} - (\Delta + 2\gamma - 2\bar{\gamma} + \bar{\mu})T^{(1)}_{\bar{m}\bar{m}}\right]\right. \\ &\left. + \bar{d}_3^{(0)}\left[(\Delta + 2\gamma + 2\bar{\mu})T^{(1)}_{n\bar{m}} - (\bar{\delta} - \bar{\tau} + 2\bar{\beta} + 2\alpha)T^{(1)}_{nn}\right]\right], \end{aligned} \tag{1.80}$$

where $\bar{d}_4^{(0)} := \Delta + 3\gamma - \bar{\gamma} + 4\mu + \bar{\mu}$ and $\bar{d}_3^{(0)} := \bar{\delta} - \bar{\tau} + \bar{\beta} + 3\alpha + 4\pi$. $\mathcal{S}_4$ is known as the spin -2 Teukolsky source operator. In Type-D spacetimes, there is a similar spin $+2$ equation for ψ_0, which can be derived by taking the GHP prime operation ($l^a \to n^a$ and $m^a \to \bar{m}^a$) [77].

In a concise notation, I write Eq. (1.79) as

$$\mathcal{O}_4\psi_4^{(1)} = \mathcal{S}_4[8\pi T^{(1)}_{ab}], \tag{1.81}$$

which defines the spin -2 Teukolsky operator ($\mathcal{O}_4$).

The Teukolsky equation has two remarkable properties. Firstly, as I mentioned, $\psi_4^{(1)}$ decouples from the other (unknown) first-order quantities. Secondly, the Teukolsky equation is separable. Eq. (1.81), in Boyer–Lindquist (BL) coordinates (and using the Kinnersley tetrad [99][4]), can be written in terms of the spin -2 master Teukolsky equation (where $\hat{\mathcal{O}}_4$ denotes the master Teukolsky operator, for spin -2) [177],

$$\hat{\mathcal{O}}_4[\rho^{-4}\psi_4^{(1)}] = -\Sigma\rho^{-4}\mathcal{S}_4[8\pi T_{ab}^{(1)}], \tag{1.82}$$

where $\Sigma = r^2 + a^2\cos^2[\theta]$. By using a Fourier transform (where the t and ϕ dependencies become trivial as Kerr is stationary and axially symmetric), the master Teukolsky operator is separable into a radial ODE and an angular (θ) ODE [177]. The angular part of the master Teukolsky equation has an eigenbasis of solutions, the spin-weighted spheroidal harmonics [177] (which reduce to spin-weighted spherical harmonics when $a = 0$).

A desirable characteristic for quantities is gauge (and local Lorentz frame) invariance, allowing for a simple comparison of results. $\psi_4^{(1)}$ is gauge (and infinitesimal tetrad rotation invariant) [48] because $\psi_4^{(0)} = 0$ (and $\psi_3^{(0)} = 0$) in a principle-null-direction aligned tetrad. $\psi_4^{(1)}$ also contains all the information about the vacuum piece of the metric perturbation [190] (up to perturbations towards other Kerr solutions). $\psi_4^{(1)}$ includes the gravitational waves being emitted to $\mathcal{I}^+$ [178, 45] and into the Kerr black hole horizon.

1.7.4 Balance laws

Obtaining the full first-order self-force requires calculating the first-order metric perturbation ($h_{ab}^{(1)}$). However, the dissipative piece of the first-order self-force can be obtained from $\psi_4^{(1)}$ directly. This is useful as adiabatic EMRI models only require the dissipative piece of the first-order self-force.

From $\psi_4^{(1)}$, one can extract the gravitational wave fluxes being dissipated out to $\mathcal{I}^+$and into the supermassive black hole horizon. At $\mathcal{I}^+$the formula for the power per unit solid angle is [178]

$$\frac{d^2E}{dtd\Omega} = \lim_{r\to\infty}\frac{r^2}{4\pi\omega^2}|\psi^2_{4(1)}|. \tag{1.83}$$

Using Eq. (1.83) and balance laws, one can calculate the corresponding change in orbital energy. Similar equations hold at the horizon and for the angular momentum dissipation [87]. Calculating the change in the Carter constant is more involved, but it

[4]There exists a separable master Teukolsky equation for all principle-null-direction aligned tetrads. For the Carter tetrad Eq. (1.82) changes only by replacing $\rho^{-4}\psi_4^{(1)} \to \rho^{-2}\Delta\psi_4^{(1)}$ and $\rho^{-4}T_{ab}^{(1)} \to \rho^{-2}\Delta T_{ab}^{(1)}$ [154], where $\Delta = r^2 - 2Mr + a^2$

can also be extracted from $\psi_4^{(1)}$ [134, 68]. The change in the energy, angular momentum, and Carter constant is equivalent to the dissipative piece of the first-order self-force. From the evolution of the three constants of geodesic motion, one can calculate the evolution of the fundamental frequencies of the orbit (similarly to the two-timescale approximation) to adiabatic accuracy.

A similar shortcut may hold at second order. This would streamline post adiabatic EMRI models as only the dissipative piece of the second-order self-force is required (as well as the full first-order self-force). Concerning energy and angular momentum, the second-order gravitational wave fluxes can be calculated from $\psi_4^{(2)}$. Hence, to calculate the dissipative piece of the second-order self-force, one only needs to provide second-order flux balance laws. Recent, currently unpublished work [123], has produced second-order flux balance laws for the energy and angular momentum, but they are not yet in a form practical for application.

Additionally, a method for extracting the second-order evolution of the Carter constant from $\psi_4^{(2)}$ will be necessary. This will require extending the methods in Refs. [134, 68] to second-order. Alternatively, one could derive a Carter constant balance law at first order and extend it to second-order. Assuming these efforts are successful, the dissipative piece of the second-order self-force will be calculable from $\psi_4^{(2)}$.

1.8 CCK metric reconstruction.

Calculating $\psi_4^{(1)}$ is useful for obtaining the first-order gravitational waves and the dissipative piece of the self-force, but calculating the conservative self-force requires the complete metric perturbation. Also, as $h_{ab}^{(1)}$ is an input in Eq. (1.16), one needs the first-order metric perturbation to source second-order calculations.

In the past decade, the first-order self-force in Kerr has been obtained [114] by calculating the metric perturbation using the Chrzanowski, Cohen, and Kegeles (CCK) procedure of metric reconstruction [50, 53, 94]. This method reconstructs $h_{ab}^{(1)}$ from $\psi_4^{(1)}$ (or $\psi_0^{(1)}$) using a Hertz potential as an intermediary step. Wald [190] succinctly described the CCK metric reconstruction in a way that makes clear how it stems from the Teukolsky equation and the linearised EFE. Here, I summarise Wald's description.

To express the Wald identity, first I define the operator which takes one from $h_{ab}^{(1)}$ to $\psi_4^{(1)}$ as $\mathcal{T}_4$,

$$\mathcal{T}_4[h_{ab}^{(1)}] = \psi_4^{(1)}. \tag{1.84}$$

Hence, using the definition of $\mathcal{E}$, the linearised EFE operator (equivalent to δG_{ab} in Eq. (1.15)), the (spin -2) Teukolsky equation, Eq. (1.79), can be expressed as

$$\mathcal{O}_4\mathcal{T}_4[h_{ab}] = \mathcal{S}_4\mathcal{E}[h_{ab}]. \tag{1.85}$$

As h_{ab} can be an arbitrary symmetric rank 2 tensor in Eq. (1.85), Eq. (1.85) is an operator identity

$$\mathcal{O}_4\mathcal{T}_4 = \mathcal{S}_4\mathcal{E}, \tag{1.86}$$

known as the spin -2 *Wald identity* [190]. A prime operation gives the spin $+2$ Wald identity,

$$\mathcal{O}_0\mathcal{T}_0 = \mathcal{S}_0\mathcal{E}, \tag{1.87}$$

where I have used $\mathcal{O}_0 \equiv \mathcal{O}_4'$, $\mathcal{T}_0 \equiv \mathcal{T}_4'$, and $\mathcal{S}_0 \equiv \mathcal{S}_4'$. Note, $\mathcal{E}$ is unaffected by the prime operation.

The key step in CCK metric reconstruction is to utilise the adjoint of the Wald identity,

$$\mathcal{T}_4^\dagger\mathcal{O}_0 = \mathcal{E}\mathcal{S}_4^\dagger, \tag{1.88}$$

Where $\mathcal{E} = \mathcal{E}^\dagger$ and $\mathcal{O}_4^\dagger = \mathcal{O}_0$ has been used [190]. Suppose there exists a *Hertz potential*, Φ, which satisfies $\mathcal{O}_0[\Phi] = 0$; then, acting Eq. (1.88) on Φ gives

$$\mathcal{E}\mathcal{S}_4^\dagger[\Phi] = 0. \tag{1.89}$$

Hence, $\mathcal{S}_4^\dagger[\Phi]$ satisfies the vacuum linearised EFE. Therefore, one can obtain a real metric perturbation ($\hat{h}_{ab}$) from Φ,

$$\hat{h}_{ab} = \mathrm{Re}[\mathcal{S}_4^\dagger[\Phi]]_{ab}. \tag{1.90}$$

Crucially this proof only holds in vacuum (as Eq. (1.89) is homogeneous).

Calculating a vacuum metric perturbation in this way requires a Hertz potential. To find an appropriate Hertz potential, one can use $\mathcal{T}_4[\hat{h}_{ab}] = \psi_4^{(1)}$. Assuming $\psi_4^{(1)}$ is known (calculated from the Eq. (1.81)), one can solve the fourth-order differential equation

$$\mathcal{T}_4[\mathrm{Re}[\mathcal{S}_4^\dagger[\Phi]]] = \psi_4^{(1)}, \tag{1.91}$$

for Φ. Similarly, one can calculate Φ from $\psi_0^{(1)}$ using

$$\mathcal{T}_0'[\mathrm{Re}[\mathcal{S}_4^\dagger[\Phi]]] = \psi_0^{(1)}. \tag{1.92}$$

By using the GHP prime operation, one can produce an analogous spin $+2$ CCK procedure, where the metric is calculated from a Hertz potential satisfying $\mathcal{O}_4[\Phi] = 0$ and $\hat{h}_{ab} = \mathrm{Re}[\mathcal{S}_0^\dagger[\Phi]]_{ab}$.

The CCK procedure may seem like a circuitous method for finding a solution to the linearised EFE. However, all the equations involved are separable, whereas the linearised EFE in Kerr are non-separable. Hence, CCK metric reconstruction is less numerically expensive. This method has already been successfully used for first-order self-force calculations in Kerr [114]. However, the vacuum condition makes it inconsistent at second order. In Chap. 5, I discuss the extension of CCK metric reconstruction to non-vacuum and second order[86].

1.8.1 The radiation gauges

The CCK procedure yields a metric perturbation in a radiation gauge. I will analyse the metric perturbation produced by the spin $+2$ form of CCK metric reconstruction to describe the radiation gauge. For this, I require the explicit form of $\mathcal{S}_0^\dagger[\Phi]$,

$$\begin{aligned}(S_0^\dagger\Phi)_{ab} =& \frac{1}{2}\Big[- l_a l_b(\eth - \tau)(\eth + 3\tau) - m_a m_b(\text{Þ} - \rho)(\text{Þ} + 3\rho) \\ &+ l_{(a}m_{b)}\big\{(\text{Þ} - \rho + \bar{\rho})(\eth + 3\tau) + (\eth - \tau + \bar{\tau}')(\text{Þ} + 3\rho)\big\}\Big]\Phi. \end{aligned} \tag{1.93}$$

As $(S_0^\dagger\Phi)_{ab}$ has no n_a components, the metric perturbation satisfies [118]

$$\hat{h}_{ab}l^a = 0; \tag{1.94}$$

this gauge is known as the outgoing radiation gauge as conventionally l^a is aligned with the outgoing principal null direction. For spin -2 CCK metric reconstruction, the resulting metric is in the ingoing radiation gauge, $\hat{h}_{ab}n^a = 0$.

Price, Shankar, and Whiting [158] showed that any metric perturbation (satisfying the linearised EFE) can be transformed into the radiation gauge by using gauge degrees of freedom. However, by again analysing the form of Eq. (1.93), one can clearly see there is a further condition on the spin $+2$ (and spin -2) CCK metric perturbation:

$$\hat{h}_{ab}m^a\bar{m}^b = 0. \tag{1.95}$$

In the context of the radiation gauge, where $h_{ln} = 0$ by definition, Eq. (1.95) is equivalent to the *trace-free* condition, $g^{ab}h_{ab} = 0$.

Satisfying Eqs. (1.95) and (1.95) for a generic non-vacuum metric perturbations cannot, in general, be achieved with a gauge transformation [158]. A trace-free radiation gauge metric perturbation satisfies $\mathcal{E}_{ll} = 0$ (see appendix A of Ref. [86]); hence, the stress-energy tensor must satisfy $T_{ll} = 0$. Therefore, the existence of a

trace-free radiation gauge metric perturbation cannot be achieved with gauge constraints alone; physical constraints on the stress-energy are also required. This property is consistent with CCK metric reconstruction being derived under the restriction of the perturbation being vacuum.

The vacuum condition may seem stringent. However, first-order self-force calculations *nearly* satisfy this condition. The source (T_{ab}) is vacuum everywhere except on the worldline. Hence, CCK metric reconstruction can be used everywhere off the worldline consistently. One can extend CCK metric reconstruction to include the worldline, but the resulting metric perturbation does not satisfy the linearised EFE on the worldline. The resulting metric perturbation must be "completed", as I describe in Sec 1.8.2.

In the presence of the particle, the radiation gauge suffers from pathological (gauge) singularities. These can come in four forms. The first three are string-like singularities, either emanating from the worldline of the particle out to infinity, from the worldline to the supermassive black hole horizon, or both (see Fig. 1.7). The final, most useful form restricts the singularity to a sphere (of constant BL radius) that intersects the particle at each instant. Pound, Merlin, and Barack [116] formulated the no-string radiation gauge to calculate the first-order self-force. They built the no-string solution by effectively gluing together the smooth halves of two half-string gauges. This process introduces a step function and delta function (with an unknown coefficient) on the surface where the two gauges meet. However, one can still calculate the first-order self-force by taking limits from both sides of the sphere. The radiation no-string gauge were first used by Refs. [95, 96, 170, 171] for self-force calculations. Building on this approach, the first-order self-force for generic orbits in Kerr has been calculated by van de Meent and Shah [115, 113, 114]). In Ref. [115] the self-force results were used to calculate some unknown high order Post-Newtonian terms.

As products of the first-order metric perturbation source second-order calculations, the gauge singularities that arises in CCK metric reconstruction are problematic. Products of radiation gauge singularities cause second-order equations to have ill-defined sources. This major obstacle for second-order calculations is addressed in Chap. 5.

1.8.2 Metric reconstruction completion piece

Initially, one may question how a perturbed Weyl scalar could contain sufficient information to reconstruct an entire metric. Wald's theorem [189] states that $\psi_4^{(1)}$ ($\psi_0^{(1)}$) contains all the information in vacuum metric perturbations apart from mass and angular momentum perturbations. Consequently, CCK metric reconstruction recovers the entire metric perturbation, up to the mass and spin contributions. The mass and

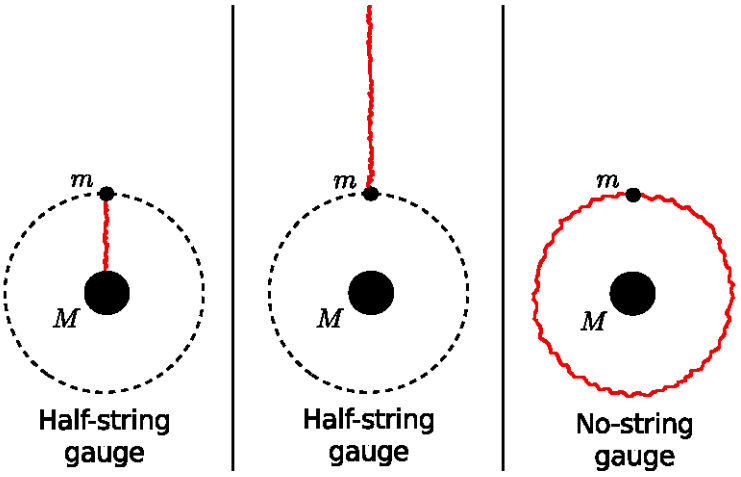

FIGURE 1.7: The various types of pathological singularities in the metric perturbations produced from CCK metric reconstruction with a point particle source. All these solutions are in the trace-free radiation gauge and do not satisfy the EFE on the particle. Image courtesy of Adam Pound.

spin in the metric perturbation does not contribute to $\psi_4^{(1)}$, corresponding to $\mathcal{T}_4$ having a kernel.

The mass and spin perturbations are known as the *completion piece*. For globally vacuum perturbations, the completion piece can be absorbed into the background mass and spin parameters. Self-force perturbations are non-vacuum on the particle, this effectively divides the spacetime into two vacuum regions (similarly to the no-string gauge in Fig. 1.7), with different completion pieces in each region. One must determine the relative difference between these two regions' mass and angular momentum content. Merlin et al. [118] developed a method for calculating the completion piece by constructing gauge-invariant fields using the complete metric perturbation. Imposing continuity off the particle (for these gauge-invariant fields) constrained the mass and angular-momentum degrees of freedom, producing the metric perturbation completion piece. Ref. [115] also provided a method for calculating the completion piece. The completion piece is necessary to obtain a solution to the EFE on the particles radius.

Additionally, there is a "gauge completion piece" [187]. This piece is required to ensure that the coordinate frequencies have the same meaning on either side of the no-string solution [104, 169, 31, 183]. The gauge completion piece is calculated by imposing continuity of certain metric components at $r = r_p$ [104]. In Cap. 5, I give a simpler method, with a more physical motivation, for calculating the gauge completion piece (and completion piece).

Nevertheless, their remains a missing radial delta function in the no-string solution (to completely satisfy the EFE). In Chap. 5 I show how the missing radial delta function can be obtained using Ref. [86].

1.9 Goals and summary of this thesis

A key ingredient in achieving LISA science goals is calculating the dissipative piece of second-order self-force in Kerr. In the following chapters, I formulate methods to help accomplish this, and I implement some of them in the simpler case of a Schwarzschild background. The second-order methods are derived mainly from the extension of first-order methods I have reviewed in this chapter. Whilst this work does not encompass a complete formulation for calculating the second-order self-force in Kerr, the methods provided show key progress and will likely perform crucial roles in future efforts.

In Chap. 2, I analyse the second-order Teukolsky equation. I review the known extension of the Teukolsky equation to second order [45], and discuss why it does not appear to have a source that is well defined as a distribution for self-force calculations (in a region containing the worldline). I then derive a new form of the second-order Teukolsky equation and show its source to be integrable for self-force calculations (in a highly regular gauge [151]). This new second-order Teukolsky equation solves for a quantity similar to $\psi_4^{(2)}$, which can be used as a starting point for second-order metric reconstruction [86]. Alternatively, if it can be shown that the evolution of the Carter constant can be extracted from $\psi_4^{(2)}$ (Sec. 1.7.4), the dissipative piece of the second-order self-force could be extracted directly from $\psi_4^{(2)}$. I round this chapter off by deriving a *quadratic Wald identity*.

In Chap. 3, I present methods for calculating second-order gauge invariants. I formalise practical methods for gauge fixing at first order. Using the valuable property that $\psi_4^{(2)}$ transforms more simply than a generic second-order quantity, I develop techniques for constructing second-order gauge-invariant quantities using first-order gauge-fixing schemes. Further, I discuss how gauge invariants will be helpful for EMRI calculations when they are associated with a *good* gauge. I provide a method for gauge fixing to the Bondi–Sachs gauge and formulate a gauge-invariant[5] asymptotically flat quantity by producing an algorithm to fix the BMS frame. By working with these quantities that respect the spacetime's physical asymptotic flatness, this procedure entirely sidesteps one of the major hurdles in second-order self-force calculations, infrared divergences [149].

Chap. 4 describes my role in a collaboration solving the second-order Teukolsky equation in Schwarzschild for quasi-circular orbits. I present my key contributions, summarise the full calculation, and discuss the significance of this work in the field of self-force and gravitational wave science. I derive a general formula for calculating the modes of the second-order Teukolsky source from the first-order metric perturbation

[5] The quantity is gauge invariant up to gauge transformations along the Killing vectors of Kerr spacetime. The remaining gauge freedoms will be constrained using the transformation of the first-order stress-energy tensor in future work.

in Schwarzschild. I then present the second-order Teukolsky source calculated from a Lorenz gauge metric perturbation for quasi-circular orbits in Schwarzschild. I show how the convergence of the source near $\mathcal{I}^+$ can be improved by transforming towards the Bondi–Sachs gauge. This improved convergence makes our method for solving the radial Teukolsky equation viable with trivial boundary conditions (using hyperboloidal slicing and spectral methods [106]). I also describe the mode decompositions I have calculated for the slow-time-derivative piece of the source and the correction to the puncture near the worldline. Finally, I summarise the remaining pieces of the source that need including; once complete we will be able to calculate fluxes, evolve inspirals and generate waveforms to first-post adiabatic accuracy.

In Chap. 5, I discuss the recent extension of CCK metric reconstruction to non-vacuum perturbations [86] by Greens, Hollands, and Zimmerman (GHZ). I comment on Ref. [86]'s prospect for helping second-order self-force calculations. I also summarise my paper (with collaborators) [183] which formalises how to best implement GHZ for self-force calculations. I present my major contribution to this work, implementing GHZ at first order for a stationary perturbation in flat spacetime. This analysis gave useful insights into implementing the method for non-stationary point mass in Kerr. It also helped us to formalise a method for calculating a regular metric perturbation using gauge transforms and a puncture scheme.

Finally, in Chap. 6, I conclude this thesis, summarising the significant results and their effect on second-order self-force modelling. I also describe future avenues for progress and exploration in second-order self-force.

Chapter 2

Second-Order Teukolsky Equations

2.1 Introduction

The most direct method to perform second-order black hole perturbation theory is solving the second-order linearised EFE, Eq. (1.16), for $h^{(2)}_{ab}$. However, in Kerr, Eq. (1.16) is a set of ten non-separable equations (similarly to the first-order linearised EFE equation, Eq. (1.15), as discussed in the previous chapter). Solving non-separable PDEs directly for $h^{(2)}_{ab}$ is computationally expensive. Methods are being developed to integrate such r-θ (the t and ϕ dependencies separate trivially due to the symmetries of the Kerr black hole) PDEs in the self-force problem. Recently, results have been obtained for a scalar charge on a circular orbit around a Kerr black hole at first order by solving the r-θ PDE numerically [136].

Alternatively, a natural approach to second-order calculations is extending the separable first-order methods in Kerr. The Teukolsky equation (Eq. (1.79)) seems the auspicious route forward, as it solves for a single variable and is separable into ODEs. Their are two different extensions of the Teukolsky equation at second order: one by Campanelli and Lousto [45], and one to be published in my work [174]. The second case also appeared implicitly in the non-linear metric reconstruction formalism of Ref. [86], which I refer to as *GHZ metric reconstruction*).

This chapter is split into three sections. In the first, I review the second-order Teukolsky equation derived by Campanelli and Lousto [45] (providing minor corrections to their expressions for the perturbed spin coefficients [102]). I also discuss why its form is not integrable for general second-order self-force calculations. In the second section, I present my derivation of the new form of the second-order Teukolsky equation [174], which I show, in principle, has a well-defined source for self-force calculations. In the final section, I derive a *quadratic Wald identity* by combining the two second-order Teukolsky equations. The work in this chapter will be published in Ref. [174] in the near future.

2.2 The Campanelli–Lousto–Teukolsky equation

2.2.1 Overview

Campanelli and Lousto [45] successfully extended the Teukolsky equation to second order in 1999. As described in Sec. 1.7.3, Teukolsky derived his eponymous equation by manipulating certain first order perturbed Ricci and Bianchi identities within the NP formalism. Campanelli and Lousto repeated this procedure up to any given order (n) by using analogous manipulations. Crucially, they move all quantities of an order less than n to the right-hand side (RHS), treating them as source terms. This produces an nth-order Teukolsky equation,

$$\mathcal{O}_4[\psi_4^{(n)}] = \mathcal{S}_{4CL}^{(n)}[h_{ab}^{(1)},\ldots,h_{ab}^{(n-1)},h_{ab}^{(1)},\ldots,h_{ab}^{(n-1)}] + \mathcal{S}_4^{(n)}[T_{ab}^{(1)},\ldots,T_{ab}^{(n)},h_{ab}^{(1)},\ldots,h_{ab}^{(n-1)}]. \tag{2.1}$$

As the same operator, $\mathcal{O}_4$, appears on the left-hand side as in the first order Teukolsky equation (Eq. (1.81)) the Campanelli–Lousto–Teukolsky equation is separable. The equation is for a quantity ($\psi_4^{(n)}$) which contains all the information about the second-order gravitational waves [45].

The Campanelli–Lousto–Teukolsky source terms are given by

$$\begin{aligned}\mathcal{S}_{4CL}^{(n)}[h_{ab}^{(1)},\ldots,h_{ab}^{(n-1)},h_{ab}^{(1)},\ldots,h_{ab}^{(n-1)}] = \sum_{p=1}^{n-1}\Bigg(&\Big[\bar{d}_3^{(0)}(\delta+4\beta-\tau)^{(n-p)}\\ &-\bar{d}_4^{(0)}(D+4\epsilon-\rho)^{(n-p)}\Big]\psi_4^{(p)} - \Big[\bar{d}_3^{(0)}(\Delta+4\mu+2\gamma)^{(n-p)} - \bar{d}_4^{(0)}(\bar{\delta}+4\pi+2\alpha)^{(n-p)}\Big]\psi_3^{(p)}\\ &+3\Big[\bar{d}_3^{(0)}\nu^{(n-p)} - \bar{d}_4^{(0)}\lambda^{(n-p)}\Big]\psi_2^{(p)} + 3\Big[(\bar{d}_3^{(0)}-3\pi)^{(n-p)}\nu^{(p)} - (\bar{d}_4^{(0)}-3\mu)^{(n-p)}\lambda^{(p)}\Big]\Bigg),\end{aligned} \tag{2.2}$$

(note, $\mathcal{S}_{4CL}^{(n)}$ is a non-linear operator) and

$$\begin{aligned}\mathcal{S}_4^{(n)}[T_{ab}^{(1)},...T_{ab}^{(n)},h_{ab}^{(1)},..h_{ab}^{(n-1)}] = 4\pi\Bigg[\sum_{p=1}^{n}\Bigg(&\bar{d}_4^{(0)}\Big[(\bar{\delta}-2\bar{\tau}+2\alpha)^{(n-p)}T_{n\bar{m}}^{(p)}\\ &-(\Delta+2\gamma-2\bar{\gamma}+\bar{\mu})^{(n-p)}T_{\bar{m}\bar{m}}^{(p)}\Big] + \bar{d}_3^{(0)}\Big[(\Delta+2\gamma+2\bar{\mu})^{(n-p)}T_{n\bar{m}}^{(p)}\\ &-(\bar{\delta}-\bar{\tau}+2\bar{\beta}+2\alpha)^{(n-p)}T_{nn}^{(p)}\Big]\Bigg)\Bigg].\end{aligned} \tag{2.3}$$

I present here some minor corrections to Ref. [45]: the sum in Eq. (2.6) runs to n (rather than to $n-1$), and corrected expressions for the perturbed spin coefficients ($\kappa^{(1)}$, $\sigma^{(1)}$,...) are given in Appendix A.

For clarity, and to analyse the behaviour of the source, I explicitly express the second-order Campanelli–Lousto–Teukolsky equation as

$$\mathcal{O}_4[\psi_4^{(2)}] = \mathcal{S}^{(2)}_{4CL}[h^{(1)}_{ab}, h^{(1)}_{ab}] + \mathcal{S}^{(2)}_4[T^{(1)}_{ab}, T^{(2)}_{ab}, h^{(1)}_{ab}], \tag{2.4}$$

where

$$\begin{aligned}
&\mathcal{S}^{(2)}_{4CL}[h^{(1)}_{ab}, h^{(1)}_{ab}] = \\
&\Bigg(\Big[\bar{d}_3^{(0)}(\delta + 4\beta - \tau)^{(1)} - \bar{d}_4^{(0)}(D + 4\epsilon - \rho)^{(1)}\Big]\psi_4^{(1)} - \\
&\Big[\bar{d}_3^{(0)}(\Delta + 4\mu + 2\gamma)^{(1)} - \bar{d}_4^{(0)}(\bar{\delta} + 4\pi + 2\alpha)^{(1)}\Big]\psi_3^{(1)} \\
&+ 3\Big[\bar{d}_3^{(0)}\nu^{(1)} - \bar{d}_4^{(0)}\lambda^{(1)}\Big]\psi_2^{(1)} + 3\Big[(\bar{d}_3 - 3\pi)^{(1)}\nu^{(1)} - (\bar{d}_4 - 3\mu)^{(1)}\lambda^{(1)}\Big] \Bigg),
\end{aligned} \tag{2.5}$$

and

$$\begin{aligned}
&\mathcal{S}^{(2)}_4[T^{(1)}_{ab}, T^{(2)}_{ab}, h^{(1)}_{ab}] = \\
&4\pi \Bigg[\sum_{p=1}^{2} \Bigg(\bar{d}_4^{(0)} \Big[(\bar{\delta} - 2\bar{\tau} + 2\alpha)^{(2-p)} T^{(p)}_{n\bar{m}} - (\Delta + 2\gamma - 2\bar{\gamma} + \bar{\mu})^{(2-p)} T^{(p)}_{\bar{m}\bar{m}} \Big] \\
&\quad + \bar{d}_3^{(0)} \Big[(\Delta + 2\gamma + 2\bar{\mu})^{(2-p)} T^{(p)}_{n\bar{m}} - (\bar{\delta} - \bar{\tau} + 2\bar{\beta} + 2\alpha)^{(2-p)} T^{(p)}_{nn} \Big] \Bigg) \Bigg].
\end{aligned} \tag{2.6}$$

To understand how $\mathcal{S}_4^{(n)}$ relates to the Teukolsky source operator $\mathcal{S}_4$ in (1.79), one can observe how $\mathcal{S}_4^{(2)}$ naturally splits up into $\mathcal{S}_4$-like pieces. To show this, I define

$$\begin{aligned}
\tilde{\mathcal{S}}_4[T^{(1)}_{ab}, h^{(1)}_{ab}] :=& 4\pi \Bigg(\bar{d}_4^{(0)} \Big[(\bar{\delta} - 2\bar{\tau} + 2\alpha)^{(1)} T^{(1)}_{n\bar{m}} - (\Delta + 2\gamma - 2\bar{\gamma} + \bar{\mu})^{(1)} T^{(1)}_{\bar{m}\bar{m}} \Big] \\
&+ \bar{d}_3^{(0)} \Big[(\Delta + 2\gamma + 2\bar{\mu})^{(1)} T^{(1)}_{n\bar{m}} - (\bar{\delta} - \bar{\tau} + 2\bar{\beta} + 2\alpha)^{(1)} T^{(1)}_{nn} \Big] \Bigg),
\end{aligned} \tag{2.7}$$

which is identical to $\mathcal{S}_4[T^{(1)}_{ab}]$ except some of the zeroth-order quantities are now first-order quantities (due to the dependence on $h^{(1)}_{ab}$). I can now write Eq. (2.6) as

$$\mathcal{S}^{(2)}_4[T^{(1)}_{ab}, T^{(2)}_{ab}, h^{(1)}_{ab}] = \mathcal{S}_4[T^{(2)}_{ab}] + \tilde{\mathcal{S}}_4[T^{(1)}_{ab}, h^{(1)}_{ab}]. \tag{2.8}$$

Note, in the first-order Teukolsky equation (Eq. (1.79)) $\mathcal{S}_4$ acts on $T^{(1)}_{ab}$; in the second-order Campanelli–Lousto–Teukolsky equation, $\mathcal{S}_4$ acts on $T^{(2)}_{ab}$.

Ref. [45] also noted how $\psi_4^{(2)}$ contains both a linear-in-$h_{ab}^{(2)}$ piece and a quadratic-in-$h_{ab}^{(1)}$ piece; that is,

$$\begin{aligned}\psi_4^{(2)} &= \mathcal{T}_4[h_{ab}^{(2)}] + \delta^2\psi_4[h_{ab}^{(1)}, h_{ab}^{(1)}] \\ &= \psi_{4L}^{(2)} + \psi_{4Q}^{(2)},\end{aligned} \tag{2.9}$$

where $\psi_{4L}^{(2)} = \mathcal{T}_4[h_{ab}^{(1)}]$ and $\psi_{4Q}^{(2)} = \delta^2\psi_4[h_{ab}^{(1)}, h_{ab}^{(1)}]$. Eq. (2.9) defines the quadratic Weyl scalar operator $\delta^2\psi_4$ which I give in terms of NP quantities in a Mathematica notebook in the supplementary materials (to derive this expression I used the perturbed tetrad defined in App. A).

2.2.2 Utility in self-force calculations

For Eq. (2.4) to be solvable, its source must be well defined. The solution to Eq. (2.4) can always be written as a four-dimensional integral of the source against a Green's function. But, for the solution to exist, $\mathcal{S}_{4CL}^{(2)}[h_{ab}^{(1)}, h_{ab}^{(1)}]$ must be well defined as a distribution, such that its integral against a Green's function is well defined. Here I show, that for generic second-order self-force calculations, the singular nature of $h_{ab}^{(1)}$ and $T_{ab}^{(1)}$ near the worldline (γ) causes the source to be ill-defined.

As a preliminary investigation, I first show that $\mathcal{S}_{4CL}^{(2)}[h_{ab}^{(1)}, h_{ab}^{(1)}]$ is not locally integrable (if it were locally integrable it would be well defined). In self-force, near the worldline, generally, $h_{ab}^{(1)} \sim \frac{1}{\mathbf{r}}$ (where again $\mathbf{r}$ is the proper spatial distance from γ). The second-order Campanelli–Lousto source, $\mathcal{S}_{4CL}^{(2)}[h_{ab}^{(1)}, h_{ab}^{(1)}]$ in Eq. (2.5), is a complicated fourth-order differential operator, quadratic in $h_{ab}^{(1)}$. Hence, one can expect its most singular scaling to be

$$\begin{aligned}\mathcal{S}_{4CL}^{(2)}[h_{ab}^{(1)}, h_{ab}^{(1)}] &\sim (\partial_r\partial_r h_{ab}^{(1)})(\partial_r\partial_r h_{ab}^{(1)}) \\ &\sim \mathbf{r}^{-6}.\end{aligned} \tag{2.10}$$

Next, I check if $\mathcal{S}_{4CL}^{(2)}[h_{ab}^{(1)}, h_{ab}^{(1)}]$ is locally integrable by attempting to integrate within a small region near the worldline ($\mathbf{r} < R$),

$$\int_0^R \mathcal{S}_{4CL}^{(2)}[h_{ab}^{(1)}, h_{ab}^{(1)}]\mathbf{r}^2 d\Omega \tag{2.11}$$

$$\sim \int_0^R \mathbf{r}^{-6} r^2 d\Omega = \left[-\frac{4\pi}{3\mathbf{r}^3} \right]_0^R. \tag{2.12}$$

Clearly $-\frac{4\pi}{3\mathbf{r}^3}$ evaluated at $\mathbf{r} = 0$ is not defined; hence, $\mathcal{S}_{4CL}^{(2)}[h_{ab}^{(1)}, h_{ab}^{(1)}]$ is not locally integrable. This suggests Eq. (2.4) may not be well defined as a distribution on any domain that includes $\mathbf{r} = 0$.

A lack of local integrability is not sufficient to show $\mathcal{S}^{(2)}_{4CL}[h^{(1)}_{ab}, h^{(1)}_{ab}]$ is ill-defined. It could still be well defined as a distribution if it could be expressed as a linear operator acting on a well-defined distribution. However, $\mathcal{S}^{(2)}_{4CL}[h^{(1)}_{ab}, h^{(1)}_{ab}]$ is expressed as a quadratic operator acting on a singular distribution in Ref. [45], and hence, appears to be not well defined. Terms may cancel, leaving a well-defined source (in certain gauges), but this seems unlikely and challenging to prove due to the source being highly convoluted and involving a quadratic operator.

There is an even more problematic part of the source, $\tilde{\mathcal{S}}_4[T^{(1)}_{ab}, h^{(1)}_{ab}]$, which is ill defined as $T^{(1)}_{ab}$ and $h^{(1)}_{ab}$ are both singular on γ. $T^{(1)}_{ab}$ contains a Dirac delta function, and $h^{(1)}_{ab}$ behaves as $\sim \frac{1}{\mathbf{r}}$. Hence, the general form of $\tilde{\mathcal{S}}_4[T^{(1)}_{ab}, h^{(1)}_{ab}]$ is a differential operator acting on $\frac{1}{|x^i - x^i_p|^2}\delta^3(x^i - x^i_p)$ (where x^i_p is the spatial position of the worldline) near γ. The quantity $\frac{1}{|x^i - x^i_p|^2}\delta^3(x^i - x^i_p)$ is manifestly ill-defined. Hence, this piece of the source is very problematic, and it seems unlikely to be ameliorated by a gauge transform.

The remaining part of the source, $\mathcal{S}_4[T^{(2)}_{ab}]$, is well defined in specific gauges. $\mathcal{S}_4[T^{(2)}_{ab}]$ can be shown to be well defined as a distribution as $\mathcal{S}$ is a smooth linear operator and Ref. [185] has shown that in a highly regular gauge (and any gauge smoothly related to the Lorenz gauge) $T^{(2)}_{ab}$ is well defined as a distribution. Hence, $\mathcal{S}_4[T^{(2)}_{ab}]$ is well defined as a distribution in such gauges.

The issue of an ill-defined source is not exclusive to self-force. It can appear for any second-order black hole perturbation theory calculation where there exists a point (or set of points) where $h^{(1)}_{ab}$ is singular. In Sec 2.3, I derive a second-order Teukolsky equation with a source that is well defined as a distribution for any problem in which $\delta^2 G_{ab}[h^{(1)}_{ab}, h^{(1)}_{ab}]$ and $T^{(2)}_{ab}$ is well defined (which includes the self-force problem in a highly regular gauge [185]).

Alternatively, one could avoid the problem of an ill-defined source by implementing a puncture scheme (see Sec. 1.6.3.5). To describe such a puncture scheme, I first consider points close to but off the worldline. This region is vacuum, with $T^{(1)}_{ab} = 0$ and $T^{(2)}_{ab} = 0$. To isolate the regular piece of $\psi^{(2)}_4$, I introduce a puncture and residual split for $h^{(1)}_{ab}$ and $h^{(2)}_{ab}$. That is, $h^{(1)}_{ab} = h^{(1)\mathcal{R}}_{ab} + h^{(1)\mathcal{P}}_{ab}$ and $h^{(2)}_{ab} = h^{(2)\mathcal{R}}_{ab} + h^{(2)\mathcal{P}}_{ab}$. The puncture pieces $h^{(1)\mathcal{P}}_{ab}$ and $h^{(2)\mathcal{P}}_{ab}$ contain the singular behaviour and can be calculated analytically [153]. I can define $\psi^{(2)\mathcal{P}}_4$ as

$$\begin{aligned}\psi^{(2)\mathcal{P}}_4 &= \mathcal{T}[h^{(2)\mathcal{P}}_{ab}] + \delta^2\psi_4[h^{(1)\mathcal{P}}_{ab}, h^{(1)\mathcal{P}}_{ab}] + \delta^2\psi_4[h^{(1)\mathcal{P}}_{ab}, h^{(1)\mathcal{R}}_{ab}] + \delta^2\psi_4[h^{(1)\mathcal{R}}_{ab}, h^{(1)\mathcal{P}}_{ab}] \\ &= \psi^{(2)\mathcal{P}}_{4L} + \psi^{(2)\mathcal{P}}_{4Q}. \end{aligned} \tag{2.13}$$

Now one can solve Eq. (2.4) directly for the residual piece $\psi^{(2)\mathcal{R}}_4$, using

$$\mathcal{O}[\psi^{(2)\mathcal{R}}_4] = \mathcal{S}^{(2)}_{4CL}[h^{(1)}_{ab}, h^{(1)}_{ab}] + \mathcal{S}_4[T^{(2)}_{ab}] + \tilde{\mathcal{S}}_4[T^{(1)}_{ab}, h^{(1)}_{ab}] - \mathcal{O}[\psi^{(2)\mathcal{P}}_4]. \tag{2.14}$$

This equality can be extended down to the worldline such that one can solve for a $\psi_4^{(2)\mathcal{R}}$ valid for any point in spacetime. The singular behaviour in $\psi_{4Q}^{(2)\mathcal{P}}$ will cancel with the singular behaviour in $\mathcal{S}^{(2)}_{4CL}[h^{(1)}_{ab}, h^{(1)}_{ab}]$, $\mathcal{S}_4[T^{(2)}_{ab}]$, and $\tilde{\mathcal{S}}_4[T^{(1)}_{ab}, h^{(1)}_{ab}]$ making the expression well defined distributionally.

2.2.3 Infinitesimal tetrad-rotation and gauge dependence of $\psi_4^{(2)}$

Note, $\psi_4^{(2)}$ (unlike $\psi_4^{(1)}$) is not infinitesimal tetrad rotation invariant. This can be seen from the form of an infinitesimal tetrad rotation of type I , under which $\psi_4^{(2)}$ transforms as [48]

$$\psi_4'^{(2)} = \psi_4^{(2)} + 4a\psi_3 + 6a^2\psi_2 + \mathcal{O}(\varepsilon^3), \tag{2.15}$$

where a is a complex function and $a = \mathcal{O}(\varepsilon)$. Given that ψ_3 and ψ_2 are also given as an expansion in ε, one can write,

$$\psi_4'^{(2)} = \psi_4^{(2)} + 4a(\psi_3^{(0)} + \psi_3^{(1)}) + 6a^2\psi_2^{(0)} + \mathcal{O}(\varepsilon^3) \tag{2.16}$$

$$= \psi_4^{(2)} + 4a\psi_3^{(1)} + 6a^2\psi_2^{(0)} + \mathcal{O}(\varepsilon^3), \tag{2.17}$$

where I have used $\psi_3^{(0)} = 0$ in a Petrov type D background (with the tetrad basis vectors l^a and n^a aligned with the principle null directions). As $\psi_3^{(1)}$ and $\psi_2^{(0)}$ are non-zero, $\psi_4^{(2)}$ is not infinitesimal tetrad rotation invariant. Campanelli and Lousto [45] give a method for constructing a infinitesimal tetrad rotation invariant quantity from $\psi_4^{(2)}$.

Similarly, unlike $\psi_4^{(1)}$, $\psi_4^{(2)}$ is not (infinitesimal) gauge invariant. $\psi_4^{(2)}$ transforms under a second-order gauge transformation (defined by the gauge vector $\xi^a = \xi^a_{(1)} + \xi^a_{(2)}$) as

$$\psi_4'^{(2)} = \psi_4^{(2)} + \mathcal{L}_{\vec{\xi}_{(1)}}\psi_4^{(1)} + \frac{1}{2}\mathcal{L}_{\vec{\xi}_{(1)}}\mathcal{L}_{\vec{\xi}_{(1)}}\psi_4^{(0)} + \mathcal{L}_{\vec{\xi}_{(2)}}\psi_4^{(0)} \tag{2.18}$$

$$= \psi_4^{(2)} + \mathcal{L}_{\vec{\xi}_{(1)}}\psi_4^{(1)}, \tag{2.19}$$

where I have used $\psi_4^{(0)} = 0$ in a Petrov type D background (again with the tetrad basis null vectors l^a and n^a aligned with the principle null directions). This second-order gauge transform is significantly simpler than an arbitrary second-order quantity transformation, especially since there is no $\xi^a_{(2)}$ dependence. This is a property which I will take advantage of in Chap. 3). However, as $\xi^a_{(1)}$ appears in Eq. (2.19), $\psi_4^{(2)}$ is not gauge invariant. Campanelli and Lousto [45] also gave a method for constructing an gauge-invariant quantity from $\psi_4^{(2)}$; however, their method involves solving PDEs, so it is not ideal for practical application.

2.3 The *reduced* second-order Teukolsky equation

2.3.1 Overview

Here I present a new form of the second-order Teukolsky equation. For want of a better name, I shall call it the *reduced second-order Teukolsky equation*, to differentiate it from the Campanelli–Lousto–Teukolsky Eq. (2.4). The reasoning for this name is that it solves for a field variable that is purely dependent on $h^{(2)}_{ab}$ (i.e., the field variable has no direct dependence on $h^{(1)}_{ab}$).

Like the Campanelli–Lousto–Teukolsky equation, Eq. (2.4), the reduced second-order Teukolsky equation is separable; but, dissimilarly, it solves for a naturally infinitesimal tetrad rotation invariant quantity. The significant advantage of the reduced second-order Teukolsky equation is that its source is well defined as a distribution for self-force calculations in a highly regular gauge [151] (as I will show in Sec. 2.3.2) and hence is solvable without requiring a puncture scheme.

The derivation of the reduced second-order Teukolsky equation is straightforward and can be trivially extended to any order. I begin with Wald's operator identity [190], Eq. (1.86). Applying this identity to $h^{(2)}_{ab}$, one obtains

$$\begin{aligned} &\mathcal{O}_4\mathcal{T}_4[h^{(2)}_{ab}] = \mathcal{S}_4\mathcal{E}[h^{(2)}_{ab}], \\ \Rightarrow\ &\mathcal{O}_4[\psi^{(2)}_{4L}] = \mathcal{S}_4\big[T^{(2)}_{ab} - \delta^2 G[h^{(1)}_{ab}, h^{(1)}_{ab}]\big], \end{aligned} \tag{2.20}$$

the reduced second-order Teukolsky equation, where $\psi^{(2)}_{4L} := \mathcal{T}_4[h^{(2)}_{ab}]$ (see Eq. (2.9)) and I have used Eq. (1.16).

Similarly to Eq. (2.4), the operator on the LHS of Eq. (2.20) is the Teukolsky operator. However, the Teukolsky operator is acting not on the complete $\psi^{(2)}_4$, but only on $\psi^{(2)}_{4L}$ (the linear piece of $\psi^{(2)}_4$, see Eq. (2.9)). No information is lost about $h^{(2)}_{ab}$ by solving for $\psi^{(2)}_{4L}$ rather than $\psi^{(2)}_4$, as they contain identical $h^{(2)}_{ab}$ content. Subsequently, given that $h^{(1)}_{ab}$ is known, one can easily construct $\psi^{(2)}_4$ from $\psi^{(2)}_{4L}$ using Eq. (2.9), if required. In many gravitational wave contexts this will likely be unnecessary due to the leading order asymptotic behaviour (as $r \to \infty$, where r is the global radial coordinate) of $\psi^{(2)}_4$ and $\psi^{(2)}_{4L}$ being identical in asymptotically flat gauges. As $\psi^{(2)}_{4Q}$ is quadratic in $h^{(1)}_{ab}$, assuming $h^{(1)}_{ab}$ is in an asymptotically gauge, then $\psi^{(2)}_{4Q}$ must be $\mathcal{O}_4(r^{-2})$; hence, $\psi^{(2)}_4 = \psi^{(2)}_{4L} + \mathcal{O}(r^{-2})$.

The existence of the reduced second-order Teukolsky equation is implicit in the non-linear metric reconstruction of Ref. [86] (which I will review in Chap. 5). It was derived independently by myself and presented at GR22 in July 2019 [176], and will be explicitly presented in the literature in my paper Ref. [174]. Next, I discuss the infinitesimal tetrad rotation invariant nature of ψ^2_{4L} and its gauge dependence.

Following that, I analyse the advantages of Eq. (2.20) compared to Eq. (2.4), showing its source is well defined in a highly regular gauge.

2.3.2 Enhanced utility in self-force calculations

The important difference between Eq. (2.4) and Eq. (2.20) is the form of their respective sources. As discussed in Sec. 2.2.2, due to the singular behaviour of $h^{(1)}_{ab}$ (and $T^{(1)}_{ab}$) on γ, the source in Eq. (2.4) is not, in general, well defined for self-force calculations. Now I shall show that the source of Eq. (2.20) is distributionally well defined in a highly regular gauge.

First note, the Teukolsky source operator $\mathcal{S}_4$ (Eq. (1.80)), which appears on the RHS of Eq. (2.20), is linear. Using distribution theory [74] one can prove that $\mathcal{S}_4\big[T^{(2)}_{ab} - \delta^2 G[h^{(1)}_{ab}, h^{(1)}_{ab}]\big]$ is well defined as a distribution if $T^{(2)}_{ab}$ and $\delta^2 G[h^{(1)}_{ab}, h^{(1)}_{ab}]$ are both well defined as distributions (as $\mathcal{S}_4$ is linear and a linear operator acting on a well defined distribution is well defined [74],).

First, I analyse if $\delta^2 G[h^{(1)}_{ab}, h^{(1)}_{ab}]$ is well defined in a self-force context. In a generic gauge $\delta^2 G[h_{ab}, h_{ab}] \sim \frac{1}{\mathbf{r}^4}$ and not well defined as a distribution. Ref. [151, 185] show that in the highly regular gauge $\delta^2 G_{ab}[h^{(1)}_{ab}, h^{(1)}_{ab}]$ is well defined. Pound [151] showed, in a highly regular gauge, the most problematic part of $\delta^2 G_{ab}$ behaves as,

$$\delta^2 G_{ab}[h^{HRS}_{ab}, h^{HRS}_{ab}] \sim \frac{1}{\mathbf{r}^2}, \tag{2.21}$$

near γ where h^{HRS}_{ab} is the singular part of the metric perturbation in the highly regular gauge. Such a function *is* locally integrable, the $\mathbf{r}^2$ factor in $\sqrt{\det(g_{\mu\nu})}$ in Eq. (2.11) makes the integral non-singular. That is, Pound [151] showed $\delta^2 G[h^{HR}_{ab}, h^{HR}_{ab}]$ is well defined as a distribution; hence, $\mathcal{S}_4\big[\delta^2 G[h^{HR}_{ab}, h^{HR}_{ab}]\big]$) is well defined as distribution.

There is, however, the issue of obtaining h^{HR}_{ab}. Current first-order self-force calculations for generic orbits in Kerr [114] use CCK metric reconstruction [50], which puts the metric perturbation in the no-string radiation gauge. This results in $h^{(1)}_{ab}$ containing a delta function (with an unknown coefficient) and jump singularities on the sphere containing the worldline. Chapter 5 discusses ameliorating these singularities. Additionally, a method for performing a local gauge transformation from the Lorenz gauge to a highly regular gauge is given in Sec. 3.7.

Ref. [185] has shown that $T^{(2)}_{ab}$ is also well defined as a distribution in a highly regular gauge (and gauges smoothly related to the Lorenz gauge). Hence, in a highly regular gauge (and gauges smoothly related to the Lorenz gauge) Eq. (2.20) has a well-defined source and is solvable without requiring a puncture scheme.

Whilst a puncture scheme may not be necessary to solve Eq. (2.20), it could still be implemented to provide some advantages. A punctured source is less singular, making the equation easier and faster to solve numerically. Also, a puncture scheme equation will solve directly for a residual field. To calculate the full self-force residual (or regular) fields are necessary. However, the dissipative piece of the second-order self-force can likely be extracted from $\psi^{(2)}_{4L}$ or its residual field (once appropriate flux balance laws are derived). The disadvantage of a puncture scheme is it is challenging and time consuming to implement.

Next, I summarise how to implement a puncture scheme with Eq. (2.20). First note, off the worldline (γ) spacetime is vacuum; in this region Eq. (2.20) reduces to

$$\mathcal{O}_4[\psi^{(2)}_{4L}] = \mathcal{S}_4\big[-\delta^2 G[h^{(1)}_{ab}, h^{(1)}_{ab}]\big] \quad \forall\, x^\alpha \notin \gamma.$$

The goal of a puncture scheme is to approximate the regular metric perturbation on γ without introducing non-distributional singularities. Implementing a puncture scheme (see Sec. 1.6.3.5) defines

$$h^{(2)}_{ab} = h^{(2)\mathcal{R}}_{ab} + h^{(2)\mathcal{P}}_{ab}, \tag{2.22}$$

where $h^{(2)\mathcal{R}}_{ab}$ is the residual field and $h^{(2)\mathcal{P}}_{ab}$ the puncture field. The residual field satisfies the second-order EFE equation

$$\mathcal{E}[h^{(2)\mathcal{R}}_{ab}] = -\delta^2 G[h^{(1)}_{ab}, h^{(1)}_{ab}] - \mathcal{E}[h^{(2)\mathcal{P}}_{ab}]. \tag{2.23}$$

Returning to my derivation of the reduced second-order Teukolsky equation (Eq. (2.20)), instead of applying the Wald operator identity (1.86) to $h^{(2)}_{ab}$, one can apply it to $h^{(2)\mathcal{R}}_{ab}$, giving

$$\begin{aligned}
&\mathcal{O}_4\mathcal{T}_4[h^{(2)\mathcal{R}}_{ab}] = \mathcal{S}_4\mathcal{E}[h^{(2)\mathcal{R}}_{ab}],\\
\Rightarrow&\mathcal{O}_4[\psi^{(2)\mathcal{R}}_{4L}] = \mathcal{S}_4\big[-\delta^2 G[h^{(1)}_{ab}, h^{(1)}_{ab}] - \mathcal{E}[h^{(2)\mathcal{P}}_{ab}]\big],\\
\Rightarrow&\mathcal{O}_4[\psi^{(2)\mathcal{R}}_{4L}] = \mathcal{S}_4\big[-\delta^2 G[h^{(1)}_{ab}, h^{(1)}_{ab}]\big] - \mathcal{O}_4[\psi^{2\mathcal{P}}_{4L}] \quad \forall\, x^\alpha.
\end{aligned} \tag{2.24}$$

By the definition of the puncture, the source of Eq. (2.24) is well defined as a distribution (in any gauge); i.e., one can solve for a well defined $\psi^{(2)\mathcal{R}}_{4L}$.

Far away from the worldline, $\psi^{(2)}_{4L} = \psi^{(2)\mathcal{R}}_{4L}$. That is, the second-order gravitational waves being dissipated away from the system are also contained in $\psi^{(2)\mathcal{R}}_{4L}$. Hence, if appropriate balance laws are derived, one expects that the dissipative piece of the second-order self-force could be extracted from $\psi^{(2)\mathcal{R}}_{4L}$ directly. This could be used to produce waveforms at first post-adiabatic accuracy. As discussed in Sec. 1.7.4, work on deriving balance laws has already begun. If balance laws are unobtainable, one

could instead use $\psi_{4L}^{(2)}$ as a vital first step in second-order metric reconstruction, as I discuss in Chap. 5.

2.3.3 The infinitesimal tetrad-rotation invariance and gauge dependence of ψ_{4L}^2

Solving the reduced second-order Teukolsky equation for $\psi_{4L}^{(2)}$ offers the advantage that $\psi_{4L}^{(2)}$ is infinitesimal tetrad rotation invariant, unlike $\psi_4^{(2)}$. This can be proved by first noting that $\psi_4^{(1)}$ is infinitesimal tetrad rotation invariant [48] and $\psi_4^{(1)} := \mathcal{T}_4[h_{ab}^{(1)}]$. Since $h_{ab}^{(1)}$ has no tetrad dependencies, $\mathcal{T}_4$ must also be infinitesimal tetrad rotation invariant. Hence, $\psi_{4L}^{(2)} := \mathcal{T}_4[h_{ab}^{(2)}]$ is also infinitesimal tetrad rotation invariant (as $h_{ab}^{(2)}$, similarly, has no tetrad dependence). The infinitesimal tetrad dependence of $\psi_4^{(2)}$ comes solely in $\psi_{4Q}^{(2)}$. To derive the expression for $\psi_{4Q}^{(2)}$ in the supplementary material I used the perturbed tetrad defined in App. A.

The property of infinitesimal tetrad rotation invariance is beneficial because it is equivalent to local Lorentz frame invariance [48], allowing for a straightforward comparison of results and a freedom to choose an advantageous tetrad.

An adverse property of $\psi_{4L}^{(2)}$, like $\psi_4^{(2)}$, is its (infinitesimal) gauge dependence (unlike $\psi_4^{(1)}$, which is gauge independent). Here, I analyse the precise gauge dependence of $\psi_{4L}^{(2)}$, showing that (like $\psi_4^{(2)}$) its gauge dependence is significantly simpler than a generic second-order scalar. This will lead us naturally onto Chapter 3, where I will use this simplification to construct a gauge-independent version of $\psi_{4L}^{(2)}$ (via gauge fixing).

Using the definition of a gauge transformation in Sec. 1.6.2, and denoting quantities in the new gauge with a prime, one finds that $\psi_{4L}^{(2)}$ transforms as

$$\begin{aligned}\psi_{4L}^{\prime(2)} &= \mathcal{T}_4[h_{ab}^{\prime(2)}] \\ &= \mathcal{T}_4[h_{ab}^{(2)} + \mathcal{L}_{\xi_{(2)}^c} g_{ab} + \mathcal{L}_{\xi_{(1)}^c} h_{ab}^{(1)} + \frac{1}{2}\mathcal{L}_{\xi_{(1)}^c}\mathcal{L}_{\xi_{(1)}^c} g_{ab}] \\ &= \psi_{4L}^{(2)} + \mathcal{T}_4[\mathcal{L}_{\xi_{(1)}^c} h_{ab}^{(1)} + \frac{1}{2}\mathcal{L}_{\xi_{(1)}^c}\mathcal{L}_{\xi_{(1)}^c} g_{ab}]. \end{aligned} \tag{2.25}$$

Here, I have used $\mathcal{T}_4[\mathcal{L}_{\xi_{(2)}^c} g_{ab}] = 0$ (equivalent to $\psi_4^{(1)}$ being gauge invariant [48]). Hence, no second-order gauge vector appears in this second-order gauge transformation for $\psi_{4L}^{(2)}$. That is, $\psi_{4L}^{(2)}$ is invariant under a second-order gauge transformation. This is a significant simplification to the gauge transformation; but, $\psi_{4L}^{(2)}$ is still gauge dependent due to the presence of $\xi_{(1)}^a$ in Eq. (2.25).

2.4 The quadratic Wald identity

To finish the analysis of second-order Teukolsky equations, I show that the existence of two distinct second-order Teukolsky equations implies the existence of a *quadratic Wald identity*. Here I derive a quadratic Wald identity and discuss its relevance in second-order calculations.

The derivation begins from the second-order Campanelli–Lousto-Teukolsky equation (Eq. (2.4)), which I can express as

$$\mathcal{O}_4[\psi^{(2)}_{4L}] + \mathcal{O}_4[\psi^{(2)}_{4Q}] = \mathcal{S}^{(2)}_{4CL}[h^{(1)}_{ab}, h^{(1)}_{ab}] + \mathcal{S}_4[T^{(2)}_{ab}] + \tilde{\mathcal{S}}_4[T^{(1)}_{ab}, h^{(1)}_{ab}], \tag{2.26}$$

where I have used Eqs (2.8) & (2.9). I can replace $\mathcal{O}[\psi^{(2)}_{4L}]$ using the reduced second-order Teukolsky equation (Eq. (2.20)), giving

$$\mathcal{S}_4\big[T^{(2)}_{ab} - \delta^2 G[h^{(1)}_{ab}, h^{(1)}_{ab}]\big] + \mathcal{O}_4[\psi^{(2)}_{4Q}] = \mathcal{S}^{(2)}_{4CL}[h^{(1)}_{ab}, h^{(1)}_{ab}] + \mathcal{S}_4[T^{(2)}_{ab}] + \tilde{\mathcal{S}}_4[T^{(1)}_{ab}, h^{(1)}_{ab}]. \tag{2.27}$$

Moving $\delta^2 G[h^{(1)}_{ab}, h^{(1)}_{ab}]$ to the right hand side, and cancelling the $\mathcal{S}_4\big[T^{(2)}_{ab}\big]$ terms gives

$$\mathcal{O}_4[\psi^{(2)}_{4Q}] = \mathcal{S}_4\big[\delta^2 G[h^{(1)}_{ab}, h^{(1)}_{ab}]\big] + \mathcal{S}^{(2)}_{4CL}[h^{(1)}_{ab}, h^{(1)}_{ab}] + \tilde{\mathcal{S}}_4[T^{(1)}_{ab}, h^{(1)}_{ab}]. \tag{2.28}$$

This is nearly an operator identity except for the $T^{(1)}_{ab}$ input. $T^{(1)}_{ab}$ can be replaced using the linearised Einstein field equation, $\mathcal{E}[h^{(1)}_{cd}]_{ab} = T^{(1)}_{ab}$. Therefore, I can define $\check{\mathcal{S}}_4[h^{(1)}_{ab}, h^{(1)}_{ab}]$ as

$$\check{\mathcal{S}}_4[h^{(1)}_{ab}, h^{(1)}_{ab}] := \tilde{\mathcal{S}}_4[\mathcal{E}[h^{(1)}_{cd}]_{ab}, h^{(1)}_{ab}] = \tilde{\mathcal{S}}_4[T^{(1)}_{ab}, h^{(1)}_{ab}]. \tag{2.29}$$

Inputting Eq. (2.29) into Eq. (2.28), noting $\psi^{(2)}_{4Q} := \psi^{(2)}_{4Q}[h^{(1)}_{ab}, h^{(1)}_{ab}]$, gives a quadratic operator identity

$$(\mathcal{O}_4\psi^{(2)}_{4Q})[h^{(1)}_{ab}, h^{(1)}_{ab}] = (\mathcal{S}_4\big[\delta^2 G\big] + \mathcal{S}^{(2)}_{4CL} + \check{\mathcal{S}}_4)[h^{(1)}_{ab}, h^{(1)}_{ab}]. \tag{2.30}$$

That is,

$$\mathcal{O}_4\psi^{(2)}_{4Q} = \mathcal{S}_4\big[\delta^2 G\big] + \mathcal{S}^{(2)}_{4CL} + \check{\mathcal{S}}_4. \tag{2.31}$$

I name Eq. (2.31) the *quadratic Wald identity* due to its similarities with the (linear) Wald identity, Eq. (1.86). Eq. (2.31) is far less elegant than the Wald identity, which suggests it will be less useful for perturbative calculations. To understand the implications of Eq. (2.31) on non-linear perturbation theory, $\mathcal{S}^{(2)}_{4CL}$ and $\check{\mathcal{S}}$ need to be studied further.

Naively, one might have expected the Wald identity to extend to a quadratic form as

$$\mathcal{O}_4\psi_{4\mathrm{Q}}^{(2)} = \mathcal{S}_4\big[\delta^2 G\big]. \tag{2.32}$$

But it seems unlikely this would hold as Eq. (2.31) informs one that this requires $\mathcal{S}_{4CL}^{(2)} + \check{\mathcal{S}}_4 = 0$. The cancellations between $\mathcal{S}_{4CL}^{(2)}$ and $\check{\mathcal{S}}_4$ have not yet been studied, but if $\mathcal{S}_{4CL}^{(2)} + \check{\mathcal{S}}_4 = 0$ this would have huge implications on the Campanelli-Lousto-Teukolsky equation, which would become

$$\mathcal{O}_4[\psi_4^{(2)}] = \mathcal{S}_4[T_{ab}^{(2)}], \tag{2.33}$$

which seems unlikely as generic second-order calculations are sourced by $h_{ab}^{(1)}$.

Chapter 3

Gauge Fixing

In second-order perturbation theory, finding a gauge-invariant quantity is more challenging than at first order. Gauge-invariants help compare results. They can also help avoid problems that come from poor gauge choices and give straightforward access to physical and geometrical information. Poor gauge choices can cause severe problems in the self-force problem, such as increased singular behaviour on the worldline and infrared divergences near $\mathcal{I}^+$and the horizon. A gauge-invariant can exhibit undesirable behaviour as well, meaning it is insufficient to simply find a generic gauge-invariant.

In this chapter, I develop methods for calculating gauge-invariants that are equal to $\psi_{4L}^{(2)}$ in fixed gauges. These invariants satisfy the reduced second-order Teukolsky equation. I consider several such invariants. Ultimately, by choosing fixed gauges that reflect the geometry of the perturbed spacetime (specifically, the null structure and asymptotic structure), I ensure that the invariants have clear geometrical meaning and manifestly represent the second-order waveform. The work in this chapter was completed in collaboration with Jordan Moxon and will be published in Ref. [174] shortly.

3.1 Gauge fixing second-order curvature scalars

As described in the previous chapter, should practical balance laws be derived, Eq. (2.20) can be used to calculate the dissipative piece of the second-order self self-force. However, $\psi_{4L}^{(2)}$ is gauge dependent, meaning a poor choice in gauge may obscure the gravitational wave (and therefore the dissipative piece of the second-order self self-force) content in $\psi_{4L}^{(2)}$.

To avoid this issue, one can design a quantity $\psi_{4L}^{\prime(2)}[h_{ab}^{(1)}]$ that, no matter which gauge $h_{ab}^{(1)}$ is in, always takes the value $\psi_{4L}^{(2)}$ would have in some specific well-behaved

gauge. This method for calculating a gauge-invariant is equivalent to *gauge fixing* [108]. Using gauge fixing to construct a gauge-invariant at second order has been utilised before in cosmology modelling [126, 127, 128]. As $\xi^a_{(2)}$ does not appear in the gauge transformation equation of $\psi^{(2)}_{4L}$, it is much simpler to implement a gauge fixing algorithm. Only the first-order gauge requires fixing to calculate a (gauge-fixed) gauge-invariant $\psi'^{(2)}_{4L}$.

I re-express Eq. (2.25), writing $\xi^a_{(1)}$ as a function of $h^{(1)}_{ab}$,

$$\psi'^{(2)}_{4L}[h^{(2)}_{ab}, h^{(1)}_{ab}] := \mathcal{T}_4[h^{(2)}_{ab}] + \mathcal{T}_4\Big[\mathcal{L}_{\xi^a_{(1)}[h^{(1)}_{ab}]} h^{(1)}_{ab} + \frac{1}{2}\mathcal{L}_{\xi^a_{(1)}[h^{(1)}_{ab}]}\mathcal{L}_{\xi^a_{(1)}[h^{(1)}_{ab}]} g_{ab}\Big]. \tag{3.1}$$

I define the first-order gauge vector ($\xi^a_{(1)}[h^{(1)}_{ab}]$) such that it takes one from any first-order gauge to a specific, fully specified first-order gauge (labelled with a prime). $\xi^a_{(1)}$ can be calculated from $h^{(1)}_{ab}$ through

$$h'^{(1)}_{ab} := h^{(1)}_{ab} + \mathcal{L}_{\xi^c_{(1)}} g_{ab}, \tag{3.2}$$

where $h'^{(1)}_{ab}$ takes a fully specified, predetermined form.

Eq. (3.2) cannot fully specify $\xi^c_{(1)}$ as g_{ab} admits Killing vectors. That is, the time and azimuthal Killing vectors of Kerr spacetime satisfy $\mathcal{L}_{\xi^c_{(1)}} g_{ab} = 0$. To remove the Killing vector degrees of freedom from $\xi^c_{(1)}$ one can use the gauge transformation of the stress energy tensor

$$T'^{(1)}_{ab} := T^{(1)}_{ab} + \mathcal{L}_{\xi^c_{(1)}} T^{(0)}_{ab}. \tag{3.3}$$

Assuming $T^{(0)}_{ab}$ does not admit the same Killing vectors as the background metric, Eq. (3.3) can be used to constrain the Killing vector content in $\xi^c_{(1)}$ from $T^{(1)}_{ab}$ (assuming $T'^{(1)}_{ab}$ is predetermined).

The resulting $\psi'^{(2)}_{4L}[h^{(1)}_{ab}]$ in Eq. (3.1) will be, by definition, gauge invariant if the gauge conditions uniquely specify $\xi^a_{(1)}$. That is, identical results are acquired regardless of which gauge the calculation is made in (if $\xi^a_{(1)}$ is fully specified).

Ref. [45] sketched gauge fixing methods for $\psi^{(2)}_4$ and the Campanelli–Lousto–Teukolsky equation (Eq. (2.4)). Here, I show how gauge fixing is implemented for $\psi^{(2)}_{4L}$ and the reduced second-order Teukolsky equation (Eq. (2.20)). For the rest of this chapter, as I am only working with first-order gauge transformations, I drop the superscript (1) on $h^{(1)}_{ab}$ and $\xi^a_{(1)}$, instead writing h_{ab} and ξ^a. By implementing a gauge transform of the inputs for Eq. (2.20), one can calculate $\psi^{(2)}_{4L}$

in the fixed gauge ($\psi^{\prime(2)}_{4L}$) using

$$\begin{aligned}\mathcal{O}_4[\psi^{\prime(2)}_{4L}] &= \mathcal{S}_4\big[T^{\prime(2)}_{ab} - \delta^2 G[h'_{ab}, h'_{ab}]\big] \\ &= \mathcal{S}_4\Big[T^{(2)}_{ab} + \mathcal{L}_{\xi^a} T^{(1)}_{ab} - \delta^2 G\big[(h_{ab} + \mathcal{L}_{\xi^c} g_{ab}), (h_{ab} + \mathcal{L}_{\xi^c} g_{ab})\big]\Big]. \end{aligned} \tag{3.4}$$

Hence, calculating $\psi^{\prime(2)}_{4L}$ requires knowledge of both h_{ab} and ξ^c. I want to construct a method such that ξ^c can be calculated from h_{ab} (in any gauge) and is associated with a specific final gauge (with no residual gauge freedom). Ideally, the final gauge should be *good*. In the context of EMRIs, I will discuss what properties make a gauge *good* in specific regions of spacetime (in Sec. 3.2).

I present multiple methods for calculating a uniquely determined $\xi^c[h_{ab}]$. I give a method to compute ξ^c algebraically from first-order quantities, but the resulting final gauge is not asymptotically flat. Following that, I present a method for calculating the gauge vector into the Bondi–Sachs gauge (an asymptotically flat gauge) by solving ODEs along out-going null rays. To fully fix the Bondi–Sachs gauge, I also provide a method for fixing the BMS frame. These methods can be implemented to calculate a $\psi^{\prime(2)}_{4L}$ associated with a fully fixed asymptotically flat gauge. The resulting $\psi^{\prime(2)}_{4L}$ is an invariant measure of the second-order radiation along the outgoing null rays of the physical, perturbed spacetime.

3.2 Good gauge fixing for an EMRI

Gauge fixing to any fully fixed gauge helps compare results. However, problems may have multiple physically significant regions where gauge-invariants associated with *good* gauges (see Sec. 1.6.2) would be advantageous. For an EMRI, three physically significant regions are evident: near the worldline (γ) of the inspiralling object, the future horizon of the supermassive black hole ($\mathcal{H}^+$), and future null infinity ($\mathscr{I}^+$). These three regions (and the required well-behaved gauges) are illustrated in Fig. 3.1.

The significance of the region near the compact object is the singularity on the worldline; a highly regular gauge reduces the singular behaviour and makes the source of Eq. (3.4) well defined. $\mathcal{H}^+$ and $\mathcal{I}^+$ share their reasoning for significance: gravitational waves (i.e., energy and angular momentum) are emitted into both these regions. Hence, extracting the energy and angular momentum dissipated into these regions is aided by using a *good* gauge there (known as *horizon regular* or *asymptotically flat* gauges respectively). In this thesis, I am primarily interested in transformations to a *good* gauge at $\mathscr{I}^+$. In Sec. 3.6, I present a method to transform into the Bondi–Sachs gauge (an asymptotically flat gauge, adapted to the null structure at $\mathscr{I}^+$).

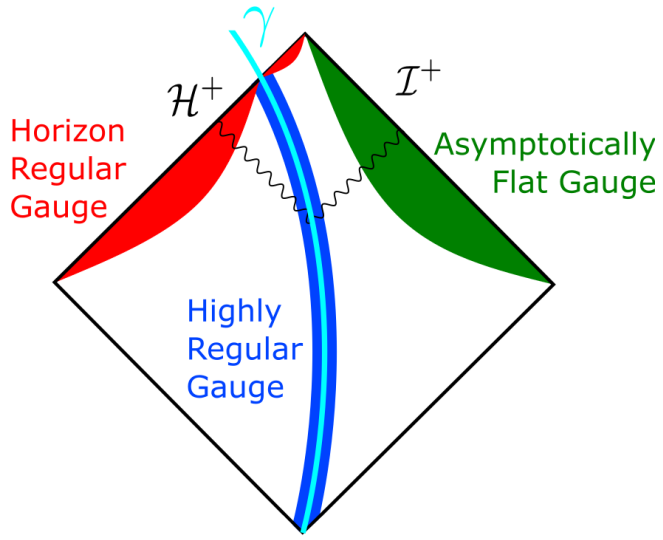

FIGURE 3.1: A Penrose diagram depicting an EMRI (and the gauges designed to help model an ERMI). γ is the worldline of the inspiraling object; it is surrounded by a highly regular gauge (to make second-order equations integrable). The black wave lines emanating from γ to the future supermassive black hole horizon ($\mathcal{H}^+$) and future null-infinity ($\mathcal{I}^+$) represent gravitational waves emitted to these regions. Each region is partnered with a well-behaved gauge there: *horizon regular* and *asymptotically flat* gauges, respectively.

3.3 Asymptotically regular gauge vectors

Before formulating methods to calculate ξ^a, I develop a method for assessing whether a given ξ^a takes one from one asymptotically flat gauge to another. I do this by assuming the initial and final gauges are asymptotically flat and use this assumption to constrain the form of ξ^a. To begin, note that the metric perturbation transforms as

$$\Delta h_{ab} = \mathcal{L}_{\xi^c} g_{ab} = \xi^c g_{ab,c} + 2\xi^c{}_{,(a} g_{b)c} \,, \tag{3.5}$$

where $\Delta h_{ab} := h'_{ab} - h_{ab}$. I constrain h'_{ab} and h_{ab} to be asymptotically flat; i.e., they must both be consistent with Eq. (1.26) near $\mathscr{I}^+$. I can now derive the expected asymptotic behaviour of ξ^a. For example, examining the Δh_{tt} component, one finds

$$\begin{aligned} \Delta h_{tt} &= \xi^c g_{tt,c} + 2\xi^c{}_{,t} g_{tc} \\ &= \xi^r g_{tt,r} + \xi^\theta g_{tt,\theta} + 2\xi^t{}_{,t} g_{tt} + 2\xi^\phi{}_{,t} g_{t\phi} \\ \Rightarrow \mathcal{O}(r^{-1}) &= \xi^r \mathcal{O}(r^{-2}) + \xi^\theta \mathcal{O}(r^{-3}) + \xi^t \mathcal{O}(r^0) + \xi^\phi \mathcal{O}(r^{-1}), \end{aligned} \tag{3.6}$$

Where I have inputted the Kerr metric in BL coordinate for g_{ab}, and assumed $\partial_t \xi^\alpha = \mathcal{O}(\xi^\alpha)$.

From Eq. (3.6) one can conclude that if $\xi^r = \mathcal{O}(r^1)$, $\xi^\theta = \mathcal{O}(r^2)$, $\xi^t = \mathcal{O}(r^{-1})$, $\xi^\phi = \mathcal{O}(r^0)$ and the initial gauge is asymptotically flat, then the component h_{tt} in the final gauge is also asymptotically flat. This is a strong constraint because there could

be gauge transformation where the components of ξ^μ do not satisfy these conditions but, due to cancellations in Eq. (3.6), h_{tt} is asymptotically flat in the final gauge.

If one repeats this analysis for the other components of Δh_{ab}, one finds the constraints presented in Table 3.1. Underlined in Table 3.1 are the strongest constraints: $\xi^t = \mathcal{O}(r^{-1})$, $\xi^r = \mathcal{O}(r^{-1})$, $\xi^\theta = \mathcal{O}(r^{-2})$ and $\xi^\phi = \mathcal{O}(r^{-2})$. Therefore, if a gauge vector satisfies these constraints (in BL coordinates with a Kerr background spacetime), and one starts in an asymptotically flat gauge, then all the metric perturbation components in the final gauge are asymptotically flat; that is, the final gauge is asymptotically flat.

Δh_{tt}	$\underline{\xi^t = \mathcal{O}(r^{-1})}$, $\xi^r = \mathcal{O}(r^1)$, $\xi^\theta = \mathcal{O}(r^2)$ and $\xi^\phi = \mathcal{O}(r^0)$
Δh_{tr}	$\xi^t_{,r} = \mathcal{O}(r^{-1})$,$\underline{\xi^r = \mathcal{O}(r^{-1})}$ and $\xi^\phi_{,r} = \mathcal{O}(r^0)$
$\Delta h_{t\theta}$	$\xi^t{}_{,\theta} = \mathcal{O}(r^0)$, $\underline{\xi^\theta = \mathcal{O}(r^{-2})}$ and $\xi^\phi{}_{,\theta} = \mathcal{O}(r^1)$
$\Delta h_{t\phi}$	$\xi^t = \mathcal{O}(r^0)$, $\xi^r = \mathcal{O}(r^2)$, $\xi^\theta = \mathcal{O}(r^1)$ and $\underline{\xi^\phi = \mathcal{O}(r^{-2})}$
Δh_{rr}	$\xi^r{}_{,r} = \mathcal{O}(r^{-1})$ and $\xi^\theta = \mathcal{O}(r^1)$
$\Delta h_{r\theta}$	$\xi^r{}_{,\theta} = \mathcal{O}(r^0)$, $\xi^\theta{}_{,r} = \mathcal{O}(r^{-2})$
$\Delta h_{r\phi}$	$\xi^t{}_{,r} = \mathcal{O}(r^1)$, $\xi^r = \mathcal{O}(r^0)$ and $\xi^\phi{}_{,r} = \mathcal{O}(r^{-2})$
$\Delta h_{\theta\theta}$	$\xi^r = \mathcal{O}(r^0)$, $\xi^\theta{}_{,\theta} = \mathcal{O}(r^{-1})$
$\Delta h_{\theta\phi}$	$\xi^\phi{}_{,\theta} = \mathcal{O}(r^2)$, $\xi^\theta = \mathcal{O}(r^{-1})$, $\xi^\phi{}_{,\theta} = \mathcal{O}(r^{-1})$
$\Delta h_{\phi\phi}$	$\xi^t = \mathcal{O}(r^2)$, $\xi^r = \mathcal{O}(r^0)$, $\xi^\theta = \mathcal{O}(r^{-1})$ and $\xi^\phi = \mathcal{O}(r^{-1})$

TABLE 3.1: Constraints on the leading, large-r form of components of the gauge vector at $\mathcal{I}^+$, calculated using the assumption that the gauge vector transforms from one asymptotically flat gauges to another (with a Kerr background in BL coordinates). The strongest constraints are underlined.

An interesting conclusion derivable from the constraints $\xi^t = \mathcal{O}(r^{-1})$, $\xi^r = \mathcal{O}(r^{-1})$, $\xi^\theta = \mathcal{O}(r^{-2})$ and $\xi^\phi = \mathcal{O}(r^{-2})$ is that the leading order expansion (in r at $\mathcal{I}^+$) of $\psi_4^{(2)}$ is invariant under such gauge transformations. This can be shown by considering spacetimes emitting gravitational waves in asymptotically flat gauges are expected to have $\psi_4^{(2)} = \mathcal{O}(r^{-1})$ (using the peeling theorem [191]). Further, I analyse the

transformation of $\psi_4^{(2)}$ under ξ^a obeying the constraints above:

$$\begin{aligned}\psi_4'^{(2)} &= \psi_4^{(2)} + \mathcal{L}_{\vec{\xi}}\psi_4^{(1)} + \mathcal{L}_{\vec{\xi}_{(2)}}\psi_4^{(0)} + \mathcal{L}_{\vec{\xi}}\mathcal{L}_{\vec{\xi}}\psi_4^{(0)} \\ &= \psi_4^{(2)} + \mathcal{L}_{\vec{\xi}}\psi_4^{(1)} \\ &= \psi_4^{(2)} + \xi^a\psi_{4\,,a}^{(1)} \\ &= \psi_4^{(2)} + \mathcal{O}(r^{-2}),\end{aligned} \tag{3.7}$$

where I have used $\psi_4^{(0)} = 0$ (as Kerr is Petrov type D [48]) and $\psi_4^{(1)} = \mathcal{O}(r^{-1})$. Hence, I can conclude from Eq. (3.7) that the leading-order large-r behaviour is invariant under such transformations. This suggests the leading-order behaviour of $\psi_4^{(2)}$ is invariant in all asymptotically flat gauges, but the proof is incomplete because the constraints on ξ^a are strong. Still, this proof aligns with my expectations as the $\sim r^{-1}$ piece of $\psi_4^{(2)}$ should contain only gravitational waves in asymptotically flat gauges. As gravitational waves are measurable they should be gauge independent (up to the subtlety of the BMS frame which I discuss in Sec. 3.6.2).

3.4 "Constrained metric components" gauges

By reversing the analysis in Sec. 3.3, one could calculate the gauge vector components by constraining metric perturbation in the final gauge to have specific component values. A fully constrained gauge (and associated gauge vector) would require constraints on four independent metric perturbation components (as there are four gauge freedoms). This section discusses how to calculate such a gauge vector. The resulting gauge vector corresponds to an asymptotically flat final gauge (if the initial gauge is asymptotically flat) but involves solving a coupled set of linear PDEs. Solving PDEs numerically is inefficient and the method does not address specifying a unique solution. In the following section, I build on this method, finding a gauge vector that can be calculated algebraically (in the frequency domain); however, this method results in a non-asymptotically flat gauge.

Here, I assume one works in the frequency domain (i.e., any tensor can be written as $\propto e^{i(m\phi-\omega t)}$). This makes the t and ϕ derivatives trivial.

First, I examine how the components h_{tt}, $h_{t\phi}$, and $h_{\phi\phi}$ transform:

$$h'_{tt} = h_{tt} + \xi^r g_{tt,r} + \xi^\theta g_{tt,\theta} - 2i\omega\xi^t g_{tt} - 2i\omega\xi^\phi g_{t\phi}, \tag{3.8}$$

$$h'_{t\phi} = h_{t\phi} + \xi^r g_{t\phi,r} + \xi^\theta g_{t\phi,\theta} - i\omega\xi^t g_{\phi t} - i\omega\xi^\phi g_{\phi\phi} + im\xi^t g_{tt} + im\xi^\phi g_{t\phi}, \tag{3.9}$$

$$h'_{\phi\phi} = h_{\phi\phi} + \xi^r g_{\phi\phi,r} + \xi^\theta g_{\phi\phi,\theta} + 2im\xi^t g_{\phi t} + 2im\xi^\phi g_{\phi\phi}, \tag{3.10}$$

these are algebraic equations as all the remaining derivatives act on the background metric. These equations can be used to solve for ξ^μ algebraically, assuming $h_{\alpha\beta}$ is known and h'_{tt}, $h'_{t\phi}$ and $h'_{\phi\phi}$ are being set to specific functions (in order to constrain the gauge). However, there are four unknowns (in ξ^μ) and only three equations to solve; hence, the solution for ξ^μ will be under-constrained.

For a fully constrained ξ^μ a fourth equation is required. Unfortunately, the remaining metric perturbation components transformations result in either ODEs or PDEs for ξ^μ, making them more challenging to solve. For example, one of the simplest remaining component transformations is that of $h_{\theta\theta}$,

$$h'_{\theta\theta} = h_{\theta\theta} + \xi^r g_{\theta\theta,r} + \xi^\theta g_{\theta\theta,\theta} + 2\xi^\theta{}_{,\theta} g_{\theta\theta}. \tag{3.11}$$

Similarly, assuming $h_{\theta\theta}$ is known, and $h'_{\theta\theta}$ is being constrained, one can now solve simultaneously Eqs. (3.8), (3.9), (3.10) and (3.11) for a unique ξ^μ (up to a θ independent integration constant). Finding ξ^μ now involves solving a linear ODE ($\xi^\theta_{,\theta}$) numerically (with appropriate boundary conditions). However, the resulting final gauge is not asymptotically flat (as I show next).

If one were to specify the form of h'_{tt}, $h'_{t\phi}$, $h'_{\theta\theta}$ and $h'_{\phi\phi}$ in order to make the final gauge asymptotically flat, naively, according to Eq. (1.26), one would choose: $h'_{tt} = \mathcal{O}(r^{-1})$, $h'_{t\phi} = \mathcal{O}(r^0)$, $h'_{\theta\theta} = \mathcal{O}(r^1)$ and $h'_{\phi\phi} = \mathcal{O}(r^1)$. However, these constraints do not constrain the other metric perturbation components to be asymptotically-flat. From Table. 3.1, one sees the strongest constraints on ξ^t, ξ^r, ξ^θ, and ξ^ϕ come from Δh_{tt}, Δh_{tr} $\Delta h_{t\theta}$, and $\Delta h_{t\phi}$ respectively. By constraining h'_{tt} and $h'_{t\phi}$ in the calculation for ξ^α, I can expect $\xi^t = \mathcal{O}(r^{-1})$ and $\xi^\phi = \mathcal{O}(r^{-2})$, which is sufficiently asymptotically-flat. However, the strongest constraints on ξ^r and ξ^θ by constraining h^B_{tt}, $h^B_{t\phi}$, $h^B_{\theta\theta}$, and $h^B_{\phi\phi}$ are $\xi^r = \mathcal{O}(r^0)$ and $\xi^\theta = \mathcal{O}(r^{-1})$, these are not sufficient fall offs for the final gauge to be asymptotically flat (as $\xi^r = \mathcal{O}(r^{-1})$ and $\xi^\theta = \mathcal{O}(r^{-2})$ is required, see Table. 3.1). Hence, it appears that this method does not necessarily result in an asymptotically flat gauge. Of course, as $\xi^t = \mathcal{O}(r^{-1})$, $\xi^r = \mathcal{O}(r^{-1})$, $\xi^\theta = \mathcal{O}(r^{-2})$ and $\xi^u = \mathcal{O}(r^{-2})$ are sufficient but not necessary conditions for the final gauge to be asymptotically-flat, it is possible that due to some terms cancelling the final gauge may be asymptotically-flat, but this could only be tested by explicitly calculating the metric perturbation in the final gauge.

If one were to repeat the above method for calculating ξ^α, instead using the transformations of the components h_{tt}, h_{tr}, $h_{t\theta}$ and $h_{t\phi}$, which provide the strongest constraints in Table 3.1, then one can expect the resulting gauge to be asymptotically flat (providing the initial gauge and the constraints on h'_{tt}, h'_{tr}, $h'_{t\theta}$ and $h'_{t\phi}$ are

asymptotically flat). h_{tr} and $h_{t\theta}$ transform as

$$h'_{tr} = h_{tr} - i\omega\xi^r g_{rr} + \xi^t{}_{,r} g_{tt} + \xi^\phi{}_{,r} g_{t\phi}, \tag{3.12}$$

$$h'_{t\theta} = h_{t\theta} - i\omega\xi^\theta g_{\theta\theta} + \xi^t{}_{,\theta} g_{tt} + \xi^\phi{}_{,\theta} g_{t\phi}. \tag{3.13}$$

Clearly, this choice makes the equations to solve for ξ^α much more challenging. The previous components were chosen to minimise the number of r and θ derivatives acting on ξ^α (to just one). Here, Eqs. (3.12) and (3.13) have a total of four (r or θ) derivatives acting on ξ^α. Hence, solving Eqs. (3.8), (3.9), (3.12) and (3.13) simultaneously results in a coupled system of two linear PDEs (and two coupled algebraic equations). I have been unable to simplify the coupled PDEs; hence, strenuous numerical methods would be required. The practical limitations of this method motivated me to devise alternative schemes for finding a gauge vector to a specific gauge. In the next subsection, I produce a method to algebraically calculate a (non-asymptotically flat) gauge vector. In Sec. 3.6 I present a method for calculating the gauge vector to the Bondi–Sachs gauge (which is asymptotically flat), which only involves solving ODEs along out-going null rays.

3.5 Chandrasekhar-like gauges

Chandrasekhar introduced the concept of using a gauge transform to set $\psi_2^{(1)} = 0$ [48]. This choice was designed to separate certain Bianchi identities. Here, however, I am not motivated by these simplifications. Instead, I am motivated by how such a gauge conditions can be used to calculate a fully constrained gauge vector (complementing the methods in Sec. 3.4).

The Chandrasekhar gauge has been used before for similar motivations. Ref. [187] used it to help calculate the periapsis advance. Also, Ref. [117] used the Chandrasekhar class of gauges to construct first-order gauge-invariants. For constructing a second-order gauge-invariant, I require a first-order gauge that is fully constrained. Additional constraints are required since the Chandrasekhar gauge is not fully constrained (fixing only two of the four gauge freedoms, as I shall show). Here, I combine the Chandrasekhar gauge with constraints on certain metric perturbation components to produce simultaneous equations for ξ^α. These equations can be solved algebraically and result in a fully constrained final gauge.

Again, the Chandrasekhar gauge condition is $\psi_2'^{(1)} = 0$, where $\psi_2'^{(1)} = \psi_2^{(1)} + \mathcal{L}_{\vec{\xi}}\psi_2^{(0)}$. Here I discuss a more general class of gauges, where ψ_2 is replaced with any generic scalar, ψ, for which $\psi^{(0)} \neq 0$.

First, I observe how $\psi^{(1)}$ transforms,

$$\psi'^{(1)} = \psi^{(1)} + \xi^{\mu}\psi^{(0)}_{,\mu}. \tag{3.14}$$

Specialising to a Kerr background, $\psi^{(0)}_{,t} = \psi^{(0)}_{,\phi} = 0$ (as the spacetime is stationary and axially symmetric). Hence,

$$\psi'^{(1)} = \psi^{(1)} + \xi^{r}\psi^{(0)}_{,r} + \xi^{\theta}\psi^{(0)}_{,\theta}. \tag{3.15}$$

If $\psi^{(1)}$ is complex then one can write a second, independent equation by taking the complex conjugate (noting ξ^{α} is real),

$$\bar{\psi}'^{(1)} = \bar{\psi}^{(1)} + \xi^{r}\bar{\psi}^{(0)}_{,r} + \xi^{\theta}\bar{\psi}^{(0)}_{,\theta}, \tag{3.16}$$

where over-bars denote the complex conjugate.

Assuming $\psi^{(1)}$ is known and $\psi'^{(1)}$ is being constrained (to a chosen function in the resulting gauge), then Eq. (3.15) and Eq. (3.16) can be solved simultaneously for ξ^{r} and ξ^{θ}, giving

$$\xi^{r} = \frac{\Delta\bar{\psi}^{(1)} - \frac{\bar{\psi}^{(0)}_{,\theta}}{\psi^{(0)}_{,\theta}}\Delta\psi^{(1)}}{\bar{\psi}^{(0)}_{,r} - \frac{\bar{\psi}^{(0)}_{,\theta}}{\psi^{(0)}_{,\theta}}\psi^{(0)}_{,r}}, \tag{3.17}$$

$$\tag{3.18}$$

$$\xi^{\theta} = \frac{\Delta\bar{\psi}^{(1)} - \frac{\bar{\psi}^{(0)}_{,r}}{\psi^{(0)}_{,r}}\Delta\psi^{(1)}}{\bar{\psi}^{(0)}_{,\theta} - \frac{\bar{\psi}^{(0)}_{,r}}{\psi^{(0)}_{,r}}\psi^{(0)}_{,\theta}}, \tag{3.19}$$

where $\Delta\psi^{(1)} = \psi'^{(1)} - \psi^{(1)}$. These equalities are defined for any complex scalar that is perturbatively well defined and whose background value has both an r and θ derivative which are non-zero (and at least one of which is complex).

This method for constraining ξ^{r} and ξ^{θ} is possible because the Kerr metric is a function of r and θ. Due to the time and axial symmetry of Kerr spacetime, I cannot constrain ξ^{t} and ξ^{ϕ} using this method. To constrain ξ^{t} and ξ^{ϕ} I can return to the transformations of the metric perturbation components (Sec. 3.4). Analysing which components can be solved algebraically for ξ^{t} and ξ^{ϕ} tells us Eq. (3.8) and (3.9) are suitable. Additionally, from Table 3.1, I know that Δh_{tt} and $\Delta h_{t\phi}$ produce the strongest constraints on ξ^{t} and ξ^{ϕ}, so these equations are ideal choices to attempt to achieve a final asymptotically flat gauge. However, the Chandrasekhar like gauge constraints seemingly result in a final gauge that is generally not asymptotically flat (as I show Sec. 3.5.1).

Eq. (3.8) and (3.9) solved simultaneously for ξ^t and ξ^ϕ give

$$\xi^t = \frac{-\Delta h_{tt} + \frac{\Delta h_{t\phi}}{\frac{g_{\phi\phi}}{g_{t\phi}} - \frac{m}{\omega}} + \xi^r\left(g_{tt,r} - \frac{g_{t\phi,r}}{\frac{g_{\phi\phi}}{g_{t\phi}} - \frac{m}{\omega}}\right) + \xi^\theta\left(g_{tt,\theta} - \frac{g_{t\phi,\theta}}{\frac{g_{\phi\phi}}{g_{t\phi}} - \frac{m}{\omega}}\right)}{i\omega(g_{tt} + g_{t\phi}) - img_{tt}}, \tag{3.20}$$

$$\xi^\phi = \frac{-\Delta h_{t\phi} + (\frac{g_{t\phi}}{g_{tt}} - \frac{m}{\omega})\Delta h_{tt} + \xi^r\left(g_{t\phi,r} - (\frac{g_{t\phi}}{g_{tt}} - \frac{m}{\omega})g_{tt,r}\right) + \xi^\theta(g_{t\phi,\theta} - (\frac{g_{t\phi}}{g_{tt}} - \frac{m}{\omega})g_{tt,\theta}}{i\omega g_{\phi\phi} - img_{t\phi} - i(\frac{g_{t\phi}}{g_{tt}} - \frac{m}{\omega})\omega g_{t\phi}}. \tag{3.21}$$

Note that these equations are not defined for stationary, axially symmetric modes ($m = \omega = 0$). I can insert ξ^r and ξ^θ calculated from Eqs. (3.17) and (3.19) into Eqs. (3.20) and (3.21). This results in algebraic equations for a fully constrained gauge vector.

ψ_2 is an appropriate choice of scalar ψ: on a Kerr background it takes the form $\psi_2^{(0)} = -\frac{M}{(r-ia\cos[\theta])^3}$ in BL coordinates coordinates [48], which is complex and has complex, non-zero r and θ derivatives. I note, the NP spin coefficients ρ, β, π, τ, μ, γ and α (also ϵ when not specifying to a Kinnersly tetrad) also obey these properties. That is, there are many choices of gauges with which one can use this method, each using a different scalar quantity; I call this class of gauges *Chandrasekhar-like*. However, ψ_2 has an additional benefit, making it the preferred scalar for gauge fixing. In Petrov type-D spacetime (with a principal null direction aligned background tetrad) $\psi_2^{(1)}$ is infinitesimal tetrad rotation invariant [48]. If one uses a non-infinitesimal tetrad rotation invariant scalar for gauge fixing, then the gauge will only be fixed for identical tetrads. Therefore, $\psi := \psi_2$ is the ideal choice for gauge fixing (unless one concurrently uses a technique for tetrad fixing at first order [45]).

There is also unbounded freedom in choosing the form the scalar field takes in the final gauge ($\psi'^{(1)}$). One might wish to exploit this freedom to calculate a gauge vector such that the final gauge is asymptotically flat. However, in general, Chandrasekhar-like gauges appear non-asymptotically flat for whatever choice of scalar and function the perturbed scalar takes in the final gauge (unless the perturbed scalar possesses a very unusual property), as I show in the next section.

3.5.1 The asymptotic irregularity of Chandrasekhar-like gauges

I shall analyse what form ξ^r and ξ^θ take when transforming to a Chandrasekhar-like gauge, and compare to Table 3.1, providing evidence that the final gauge is not, in general, asymptotically flat.

Examining Eq. (3.17), taking $\frac{\bar{\psi}^{(0)}_{,\theta}}{\psi^{(0)}_{,\theta}} = \mathcal{O}(r^0)$, this gives

$$\begin{aligned} \xi^r &= \mathcal{O}\left(\frac{\Delta\bar{\psi}^{(1)} - \Delta\psi^{(1)}}{\bar{\psi}^{(0)}_{,r} - \psi^{(0)}_{,r}}\right) \\ \Rightarrow \mathcal{O}(\frac{1}{r}) &= \mathcal{O}\left(\frac{\psi^{(1)}}{\psi^{(0)}_{,r}}\right) \\ \Rightarrow \mathcal{O}(\frac{1}{r}) &= \mathcal{O}\left(\frac{r\psi^{(1)}}{\psi^{(0)}}\right) \\ \Rightarrow \psi^{(1)} &= \mathcal{O}\left(\frac{\psi^{(0)}}{r^2}\right), \end{aligned} \tag{3.22}$$

where, in the second line I have assumed $\xi^r = \mathcal{O}(r^{-1})$ to achieve an asymptotically flat gauge transformation (see Sec. 3.3). Also, I have assumed $\psi'^{(1)}$ falls off quickly (as one is free to choose $\psi'^{(1)}$). Eq. (3.22) appears to hold an impossible constraint: it would be challenging for the first-order perturbation of a scalar to behave a factor of r^2 orders less than its zeroth-order form near $\mathcal{I}^+$. From this, I can conclude that generally Chandrasekhar-like gauges are non-asymptotically flat (regardless of what form one chooses $\psi'^{(1)}$ to take in the final gauge). This analysis produces similar results when analysing Eq. (3.19). Of course, there will exist choices for $\psi'^{(1)}$ which result in an asymptotically flat final gauge; however, there is no obvious way to predetermine an appropriate $\psi'^{(1)}$.

Whilst generic Chandrasekhar-like gauges are non-asymptotically flat, the algebraic nature of finding its gauge vector makes it an excellent tool for comparing results. Inputting the gauge vector into Eq. (3.1) results in a gauge invariant $\psi'^{(2)}_{4L}$ up to gauge transformations along the Killing vectors of Kerr spacetime.

3.6 The Bondi–Sachs gauge and fixing the BMS frame

So far, I have presented methods with limited success for calculating gauge vectors to fixed asymptotically flat gauges. My only applicable method involves solving coupled PDEs which is impractical for application. I will now present a method for calculating the gauge vector to the Bondi–Sachs gauge (an asymptotically flat gauge), which involves solving ODEs along out-going null-rays. Following this, to achieve a gauge-invariant $\psi^{(2)}_{4L}$, I produce a method for fixing the Bondi–Metzner–Sachs (BMS) frame at $\mathcal{I}^+$ (the remaining freedom in the Bondi–Sachs gauge). First, I outline basic introductions to the Bondi–Sachs formalism, BMS transformations, and vector spherical harmonics to familiarise the reader and present my notation.

3.6.1 The Bondi–Sachs formalism

A well-studied asymptotically flat gauge is that of the Bondi–Sachs formalism. The Bondi–Sachs gauge was designed specifically to analyse gravitational radiation at $\mathcal{I}^+$ [107], constructing spacetime out of successive out-going null hypersurfaces. I.e., working in Bondi–Sachs coordinates $\hat{x}^\mu = (u, \hat{r}, \hat{x}^A)$ (where $\hat{x}^A = (\hat{\theta}, \hat{\phi})$), the null hypersurfaces are of constant u. Additionally, the angular coordinates are chosen such that out-going null geodesics are of constant $\hat{x}^A$ (as well as constant u). $\hat{r}$ is therefore a parameter on the null geodesics and is chosen such that (near $\mathcal{I}^+$) the surface element on a two-surface of constant u and $\hat{r}$ is identical to the surface element on a geometrical sphere of radius $\hat{r}$ [33, 71]. These four gauge conditions can be written as $\mathbf{g}^{uu} = 0$, $\mathbf{g}^{uA} = 0$ (or $\mathbf{g}_{\hat{r}\hat{r}} = \mathbf{g}_{\hat{r}A} = 0$) and $\partial_{\hat{r}} \det[f_{AB}] = 0$ (where f_{AB} is the angular metric, per unit $\hat{r}^2$, on surfaces of constant u and $\hat{r}$) for a totally generic asymptotically flat metric $\mathbf{g}_{ab}$. Asymptotic flatness requirements [191] also require the leading-order large-$\hat{r}$ behaviour of f_{AB} to be q_{AB}, the unit 2-sphere metric [71].

Applying these gauge conditions, a metric in the Bondi–Sachs gauge takes the form

$$\mathbf{g}_{ab} d\hat{x}^a d\hat{x}^b = -\frac{V}{\hat{r}} e^{2\beta} du^2 - 2e^{2\beta} du d\hat{r} + \hat{r}^2 f_{AB} (d\hat{x}^A - U^A du)(d\hat{x}^B - U^B du), \tag{3.23}$$

where V, β, U^A and f_{AB} are all functions of $(u, \hat{r}, \hat{x}^A)$. The functions V, β, U^A and f_{AB} have six degrees of freedom (accounting for the gauge condition which restricts the freedom of f_{AB} and that f_{AB} is symmetric). They accommodate the six physical degrees of freedom of General Relativity, whilst the Bondi–Sachs gauge conditions constrain all four gauge degrees of freedom (up to the BMS transformations, see Sec. 3.6.2).

For physical solutions, one must also enforce that the metric satisfies the EFE (Eq. (1.6)). For a stress-energy tensor with an appropriate fall off, the EFE constrains the fall off at large r of the metric functions to be [71]

$$\begin{aligned} V &= \hat{r} - 2M_B - \frac{2Z}{\hat{r}} + \mathcal{O}(\hat{r}^{-2}), \quad \beta = \mathcal{O}(\hat{r}^{-2}) \\ f_{AB} &= q_{AB} + \frac{C_{AB}}{\hat{r}} + \mathcal{O}(\hat{r}^{-2}), \\ U^A &= \frac{-D^B C_{AB}}{\hat{r}^2} + \frac{1}{\hat{r}^3}\Big[-\frac{2}{3} N^A + \frac{1}{16} D^A (C_{BC} C^{BC}) \\ &\quad + \frac{1}{2} C^{AB} D^C C_{BC} \Big] + \mathcal{O}(\hat{r}^{-4}), \end{aligned} \tag{3.24}$$

where D_A is the covariant derivative corresponding to q_{AB}, M_B is the Bondi mass aspect, and N^A is the angular momentum aspect. C_{AB} is related to the the Bondi News tensor ($N_{AB} := \partial_u C_{AB}$), which contains the information about the gravitational waves emitted to $\mathcal{I}^+$. Z relates to the BMS frame (as I will show in Sec. 3.6.7).

3.6.2 The BMS symmetry group

Whilst most of the gauge freedom of General Relativity is constrained by working in the Bondi–Sachs gauge, there is still residual freedom left corresponding to the choice of coordinates on $\mathcal{I}^+$. $\mathcal{I}^+$ is preserved under diffeomorphisms of the BMS symmetry group [107] and these transformations affect the form of the metric. The BMS group contains not only the Poincare symmetry group of flat spacetime, but also an infinite-dimensional subgroup known as *supertranslations*[1]. Here, I give a brief overview of the BMS transformation. For more detailed, recent explanations please see Refs. [71, 107, 55]. Alternatively, one can study the original work of Bondi, Van de Burg and Metzner [36] and Sachs [167, 166].

The BMS symmetry group becomes apparent through examining the freedom within the Bondi–Sachs gauge at $\mathcal{I}^+$. That is, analysing which transformations preserve both the Bondi–Sachs gauge conditions ($g_{rr} = g_{rA} = 0$ and $\partial_r \det[f_{AB}] = 0$) and the asymptotic fall offs of the Bondi–Sachs metric functions (Eq. (3.24)). Naively (as physicists originally supposed [166]), one may expect $\mathcal{I}^+$ to have identical symmetries in General Relativity as in Special Relativity. The motivation behind this expectation is asymptotically flat spacetimes asymptote to Minkowski spacetime near $\mathcal{I}^+$. However, as Refs. [36, 167, 166] found, the symmetries of $\mathcal{I}^+$ in General Relativity has a more novel structure than Special Relativity.

The symmetries of $\mathcal{I}^+$in Special Relativity are the global symmetries of the Minkowski spacetime. The symmetries of $\mathcal{I}^+$in General Relativity are the asymptotic symmetries of asymptotically flat spacetimes in General Relativity. After a full analysis of the symmetries of $\mathcal{I}^+$, the transformation vector ($\vec{\xi}$) does take similar forms in both General Relativity and Special Relativity [166],

$$\vec{\xi} = \left[\alpha(\theta^A) + \frac{1}{2} u D_A Y^A(\theta^B)\right]\partial_u + Y^A(\theta^B)\partial_A, \tag{3.25}$$

where $Y^A(\theta^B)$ satisfies

$$2D_{(A}Y_{B)} - D_C Y^C q_{AB} = 0, \tag{3.26}$$

and has the general solution

$$Y^A = D^A\chi - \epsilon^{AB}D_B\kappa, \tag{3.27}$$

where χ and κ are $\ell = 1$ spherical harmonics [71] (accounting for the three rotational and three boost degrees of freedom). However, there is a crucial difference between the Special Relativity and General Relativity transformation vectors. This manifests

[1]There are extensions of the BMS symmetry group which include an additional infinite-dimensional subgroup, known as *superrotations* [28]. I omit superrotations in my analysis as they involve singular coordinates which I do not expect to occur in the perturbative calculation I am considering

itself in the form of $\alpha(\theta^A)$. In Special Relativity $\alpha(\theta^A)$ is constrained to be a linear combination of the $l \in \{0, 1\}$ spherical harmonics (corresponding to the time and three spatial translations). In General Relativity, $\alpha(\theta^A)$ can be any linear combination of twice differentiable functions of θ^A [166] (i.e., a linear combination of spherical harmonics). This coined the term *supertranslations*, an infinite subgroup of the BMS group corresponding to the infinite freedom to choose $\alpha(\theta^A)$ (which includes the ordinary time and spatial translations).

3.6.3 Vector spherical harmonics

During my analysis of the BMS frame in perturbation theory, I shall find it useful to decompose vectors on the unit 2-sphere into vector spherical harmonics. I follow the conventions (but not the notation) of Martel and Poisson [109]. Vector spherical harmonics come in two types, even (Z^{lm}_A) and odd (X^{lm}_A) parity, defined for $l \geq 1$. Vector harmonics are related to spherical harmonics (Y_{lm}),

$$\begin{aligned} Z^{lm}_A &= D_A Y_{lm}, \\ X^{lm}_A &= -\epsilon_A{}^B D_B Y_{lm}, \end{aligned} \tag{3.28}$$

where ϵ_{AB} is Levi–Civita tensor on the unit two-sphere [140].

3.6.4 Gauge fixing to the Bondi-Sachs gauge

Here, I give a method for calculating the gauge vector ($\vec{\xi}$) which takes the metric perturbation into the (infinitesimal) Bondi–Sachs gauge from any initial gauge. The gauge vector is calculated by solving an explicit, hierarchical set of ODEs, written in NP form. The resulting metric perturbation $\hat{h}_{ab}$ ($\hat{h}_{ab} = h_{ab} + 2\nabla_{(a}\xi_{b)}$) is in the Bondi–Sachs gauge and hence is asymptotically flat and fully gauge fixed up to the BMS freedoms (which I fix in Sec. 3.6.7). I assume that $g^{(0)}_{ab}$ is the Kerr metric.

This scheme requires a tetrad where l^a is radial, and m^a is angular in some coordinates. For example, the Carter and Kinnersley tetrads obey these conditions in Bondi-Sachs coordinates. Such a tetrad allows one to express the Bondi–Sachs infinitesimal gauge conditions as $\hat{h}_{ll} = \hat{h}_{lm} = \hat{h}_{m\bar{m}} = 0$. The conditions $\hat{h}_{ll} = \hat{h}_{lm} = 0$ are trivial to derive by contracting l^a and m^a with the metric perturbation of the form Eq. (3.23). $\hat{h}_{m\bar{m}} = 0$ derives from Jacobi's formula [140, 143] and $\partial_r \det[f_{AB}] = 0$.

Note that these infinitesimal gauge conditions are coordinate invariant. I, again, use the Petrov type D simplifications in this section.

I introduce the decomposition of the gauge vector ξ^α into its null tetrad components,

$$\xi^\alpha = -l^\alpha \xi_n - n^\alpha \xi_l + m^\alpha \xi_{\bar{m}} + \bar{m}^\alpha \xi_m. \tag{3.29}$$

Using the constraints of the Bondi–Sachs infinitesimal gauge I solve for each component of the gauge vector.

The conditions $\hat{h}_{ll} = \hat{h}_{lm} = 0$ simplify to a hierarchical pair of radial ordinary differential equations in NP form,

$$2D\xi_l - 2(\epsilon + \bar{\epsilon})\xi_l = -h_{ll} \tag{3.30}$$

$$D\xi_m + (-\epsilon + \bar{\epsilon} + \bar{\rho})\xi_m = -h_{lm} - \delta\xi_l + (\beta + \bar{\alpha} + \bar{\pi})\xi_l. \tag{3.31}$$

Eqs. (3.31) and (3.29) determine the components ξ_l and ξ_m up to integration constants which correspond to choosing ξ_l and ξ_m on a single $r =$ constant surface (a convenient choice of surface is $\mathcal{I}^+$).

The angular trace free condition ($\hat{h}_{m\bar{m}} = 0$) expressed in NP form results in an algebraic equation for ξ_n,

$$(\rho + \bar{\rho})\xi_n = -h_{m\bar{m}} + (\mu + \bar{\mu})\xi_l + (\alpha - \bar{\beta})\xi_m + (\bar{\alpha} - \beta)\xi_{\bar{m}} - \delta\xi_{\bar{m}} - \bar{\delta}\xi_m. \tag{3.32}$$

The u dependence of ξ_l and ξ_m (at $\mathcal{I}^+$) is constrained by the asymptotic falloff conditions $\lim_{r\to\infty} \hat{h}_{ru} = 0$ and $\lim_{r\to\infty} \hat{h}_{uA} = 0$, written in tetrad form as $h_{ln}|_{\mathcal{I}^+} = h_{nm}|_{\mathcal{I}^+} = 0$. These conditions result in simple ODEs along future null infinity (further constraining ξ_l and ξ_m),

$$(\Delta\xi_l - (\gamma + \bar{\gamma})\xi_l)|_{\mathcal{I}^+} = (-h_{ln} - D\xi_n - (\epsilon + \bar{\epsilon})\xi_n + (\pi - \bar{\tau})\xi_m + (\bar{\pi} - \tau)\xi_{\bar{m}})\,|_{\mathcal{I}^+}, \tag{3.33a}$$

$$(\Delta\xi_m + (\bar{\gamma} - \gamma - \mu)\xi_m)|_{\mathcal{I}^+} = (-h_{nm} - \delta\xi_n - (\beta + \bar{\alpha} + \tau)\xi_n)|_{\mathcal{I}^+}. \tag{3.33b}$$

This (and Eq. (3.31)) fixes the remaining freedom of ξ_l and ξ_m, up to choosing a (u independent) $\sim r^0$ piece of ξ_l and (u independent) $\sim r^1$ piece of ξ_m on a single sphere at constant u (at $\mathcal{I}^+$). When working in the frequency domain, the above equations constrain the oscillatory part of the gauge vector, and the zero frequency contribution remains unfixed (corresponding to initial data).

I must also apply the condition $\hat{h}_{AB} \to 0$ at $\mathcal{I}^+$. This constrains the trace-free piece of $\hat{h}_{AB}$. The condition can be expressed as $\hat{h}_{mm}|_{\mathcal{I}^+} = 0$ and results in the ODE (assuming the ϕ dependence of ξ^a and h_{ab} can be written as $\propto e^{im\phi}$)

$$2(\delta\xi_m + (\bar{\alpha} - \beta)\xi_m)|_{\mathcal{I}^+} = (-h_{mm})|_{\mathcal{I}^+}. \tag{3.34}$$

Eq. (3.34) is only applied at a single u_0 because the only remaining freedom in ξ_m is on a single surface of $\mathcal{I}^+$at a single u_0. This completes the collection of infinitesimal gauge conditions. The remaining freedom to set the (u independent) r^0 piece of ξ_l and (u independent) r^1 piece of ξ_m at a single cut of $\mathcal{I}^+$, corresponds to the BMS freedoms as I will show in Sec. 3.6.7.

It is worth emphasising that this method uses a tetrad which has particular properties when expressed in Bondi–Sachs coordinates, but one does not have to use Bondi–Sachs coordinates when solving the above equations because the NP formalism is coordinate covariant. In Appendix B I give a similar derivation that was completed in Bondi–Sachs coordinates and motivated finding this covariant method.

3.6.5 Gauge fixing to the radiation gauge

At this point, I note the similarities between the (infinitesimal) Bondi–Sachs gauge and the radiation gauge. The difference being, the Bondi–Sachs gauge imposes $h_{m\bar{m}} = 0$ whereas the radiation gauge imposes $h_{ln} = 0$ instead (both gauges impose $h_{ll} = h_{lm} = 0$).

Therefore, it is straightforward to alter the infinitesimal gauge transformation in Sec. 3.6.4 to give a transformation to the radiation infinitesimal gauge. One simply solves Eqs. (3.30) and (3.31) for ξ_l and ξ_m, followed by

$$D\xi_n + (\epsilon + \bar{\epsilon})\xi_n = -h_{ln} - \Delta\xi_l + (\gamma + \bar{\gamma})\xi_l + (\pi - \bar{\tau})\xi_m + (\bar{\pi} - \tau)\xi_{\bar{m}}, \tag{3.35}$$

for ξ_n. The resulting gauge vector will take one to the radiation infinitesimal gauge.

3.6.6 Kerr in Bondi-Sachs form and its associated BMS frame

The BMS symmetries are not unique to the Bondi–Sachs gauge. All generic asymptotically flat gauges transform under the BMS group (as the group corresponds to deformations of $\mathcal{I}^+$). However, here, I analyse the BMS symmetries of perturbations to Kerr through the lens of Bondi–Sachs coordinates. Before I discuss the BMS frame of a perturbed Kerr metric, I analyse the form of the Kerr metric in the Bondi–Sachs gauge and its associated BMS frame. This analysis will provide useful expressions relating the Bondi–Sachs coordinates to BL coordinates in Kerr (which I will use in Sec. 3.6.7). It will inform me which BMS transformations (and their infinitesimal counterparts) affect the form of the Kerr metric and which symmetries are intrinsic to Kerr spacetime.

Multiple works have already expressed Kerr in Bondi–Sachs form. I comment on them here: Fletcher [73] expresses the Kerr metric in generalized Bondi–Sachs form (where

the angular metric gauge condition is not imposed). Bishop and Venter [33] express an analytical form for the Kerr metric in Bondi–Sachs form. However, their expression for their metric is highly non-trivial, containing integrals which must be evaluated numerically. There also appear to be errors in Eqs. (35) and (36) of Ref. [33], which become apparent upon evaluating their respective asymptotic limits (one would expect $j_{11} = 1 + \mathcal{O}(\hat{r}^{-1})$ and $j_1 = \mathcal{O}(\hat{r}^{-1})$, but evaluating their expression gives $j_{11} = \frac{1}{2} + \mathcal{O}(\hat{r}^{-1})$ and $j_1 = \mathcal{O}(\hat{r}^3)$ respectively). Finally, Bai et al. [19] calculate an asymptotic expansion for the Kerr metric in the BS gauge. Whilst the expansion is incomplete (but can be evaluated to an arbitrarily high order iteratively), their results are to a sufficiently high order for my analysis of the Kerr BMS frame.

The expansion for the Kerr metric in BS coordinates $\{u, \hat{r}, \hat{\theta}, \hat{\phi}\}$ in Ref. [19] is not uniform in the order in $\hat{r}$ (beyond Minkowski). Here, I restate their expansion up to a consistent order:

$$\begin{aligned} ds^2 = &-\left(1 - \frac{2M}{\hat{r}} + \frac{Ma^2(2\cos^2[\hat{\theta}] - \sin^2[\hat{\theta}])}{\hat{r}^3}\right) du^2 - 2du d\hat{r} \\ &+ \frac{6Ma^2 \sin[\hat{\theta}]\cos[\hat{\theta}]}{\hat{r}^2} du d\hat{\theta} - \frac{4Ma\sin^2[\hat{\theta}]}{\hat{r}} du d\hat{\phi} + \left(\hat{r}^2 - \frac{Ma^2\sin^2[\hat{\theta}]}{\hat{r}}\right) d\hat{\theta}^2 \\ &+ \left(\hat{r}^2 \sin^2[\hat{\theta}] + \frac{Ma^2 \sin[\hat{\theta}]}{\hat{r}}\right) d\hat{\phi}^2 + \mathcal{O}(\hat{r}^{M-4}), \end{aligned} \tag{3.36}$$

where $\mathcal{O}(\hat{r}^{M-4})$ denotes that all additional terms are 4-th order in $\hat{r}$ post Minkowski. Note, Bai et al. [19] listed the $du d\phi$ term as having an $\mathcal{O}(r^{-2})$ error. I have checked, using the coordinate transformations as given in Bai, that the $\mathcal{O}(r^{-2})$ term vanishes, leaving an $\mathcal{O}(r^{-3}) = \mathcal{O}(r^{M-4})$ error, consistent with the other components.

The coordinate transform in Ref. [19] from the Bondi–Sachs coordinates (corresponding to the metric Eq. (3.36)) to BL coordinates $\{t, r, \theta, \phi\}$ is

$$\begin{aligned} u &= t + r + 2M\log\left[\frac{r}{2M}\right] - \frac{4M^2 - \frac{1}{2}a^2\sin^2[\theta]}{r} \\ &\quad - \frac{4M^3 - Ma^2}{r^2} + \mathcal{O}(r^{-3}), \\ \hat{r} &= r + \frac{a^2\sin^2[\theta]}{2r} + \frac{a^2 M \sin^2[\theta]}{2r^2} + \mathcal{O}(r^{-3}), \\ \hat{\theta} &= \theta + \frac{a^2\cos[\theta]\sin[\theta]}{2r^2} + \mathcal{O}(r^{-4}), \\ \hat{\phi} &= \phi + \frac{Ma}{r^2} + \frac{4M^2 a}{3r^3} + \mathcal{O}(r^{-4}). \end{aligned} \tag{3.37}$$

And the coordinate transformation from BL to these Bondi–Sachs coordinates is

$$\begin{aligned}
t &= u - \hat{r} - 2M\log\left[\frac{\hat{r}}{2M}\right] + \frac{4M^2}{\hat{r}} \\
&\quad + \frac{4M^3 - Ma^2 + \frac{3}{2}Ma^2\sin^2\left[\hat{\theta}\right]}{\hat{r}^2} + \mathcal{O}(\hat{r}^{-3}), \\
r &= \hat{r} - \frac{a^2\sin^2\left[\hat{\theta}\right]}{2\hat{r}} - \frac{Ma^2\sin^2\left[\hat{\theta}\right]}{2\hat{r}^2} + \mathcal{O}(\hat{r}^{-3}), \\
\theta &= \hat{\theta} - \frac{a^2\cos\left[\hat{\theta}\right]\sin\left[\hat{\theta}\right]}{2\hat{r}^2} + \mathcal{O}(\hat{r}^{-4}), \\
\phi &= \hat{\phi} - \frac{Ma}{\hat{r}^2} - \frac{4M^2a}{3\hat{r}^3} + \mathcal{O}(\hat{r}^{-4}).
\end{aligned} \tag{3.38}$$

Eq. (3.36) is not a unique form of the Kerr metric in the Bondi–Sachs gauge. It is transformable under the BMS freedoms.

From Eq. (3.36), it is clear that the Bondi–Sachs metric quantities (Eq. (3.24)) take the form

$$C_{AB} = 0,\ M_B = M,\ N^A = \{0, -3Ma\}, \tag{3.39}$$

in Kerr in this BMS frame. Another conclusion one can take from Eq. (3.36) is how similar it is to the Kerr metric in BL coordinates: the Bondi mass aspect is simply the Kerr mass and the angular momentum is (similarly to BL form) purely associated with the azimuthal coordinate in this BMS frame. Also, as Kerr is stationary, no gravitational waves are emitted from the system; hence, C_{AB} must be independent of u. As $C_{AB} = 0$, the u independence holds and C_{AB} is as simple as possible (making this form preferable).

As I am concerned with BMS frame fixing, it is necessary to ask whether there are residual BMS freedoms associated with Eq. (3.36); i.e., is the BMS frame fully fixed by this expression for the metric. The answer presents itself by considering the symmetries of Kerr spacetime: time and azimuthal symmetry. Time translations and azimuthal rotations are BMS transformations which leave the form of Eq. (3.36) invariant. Therefore, the frame is not fully fixed by the form of the metric. Later, I shall prove that the other BMS degrees of freedom (two further rotations, three Lorentz boosts, and the supertranslations) are fully constrained by the form of the Kerr metric in Eq. (3.36). I achieve this by proving that their respective infinitesimal transformations leave Eq. (3.36) non-invariant.

3.6.7 Fixing the BMS frame at first order

I now turn my attention to the BMS frame of a perturbation to Kerr in the infinitesimal Bondi–Sachs gauge ($\hat{h}_{ab}$, as calculated in Sec. 3.6). I.e., the infinitesimal BMS frame of

the Bondi–Sachs infinitesimal gauge. The BMS freedoms correspond to the remaining gauge freedoms within the family of Bondi–Sachs gauges. If one fully fixes the BMS frame in a Bondi–Sachs gauge, one has a fully constrained the gauge.

The infinitesimal BMS frame fixing method I present is derived using similar methods to how I fixed the infinitesimal gauge freedoms in earlier sections. I define a gauge vector ξ^c (consistent with BMS vector form, Eq. (3.25)) such that $\hat{h}'_{ab} = \hat{h}_{ab} + \mathcal{L}_{\xi^c_{(1)}} g_{ab}$ transforms to a fully specified infinitesimal gauge ($\hat{h}'_{ab}$). For now, I assume the background metric and Bondi–Sachs coordinates are consistent with the Bai et al. Bondi–Sachs form [19] (discussed in the previous section). However, later, I convert my resulting method to NP form, making it covariant. In this subsection, I use the definitions and conventions given for BMS transformations in Sec. 3.6.2 and vector spherical harmonics in Sec. 3.6.3.

In order to analyse the form of $\hat{h}'^{(1)}_{ab}$, one can express $\hat{h}'^{(1)}_{ab}$ near $\mathcal{I}^+$ in orders of $\hat{r}$. As I do not want to analyse the metric perturbation directly at $\mathcal{I}^+$ (because this would require a conformal transformation), instead I will analyse the form near $\mathcal{I}^+$. Hence, I need to extend ξ^c (Eq. (3.25)) into the interior of the spacetime; Ref. [71] provides such an expression in Bondi–Sachs coordinates,

$$\begin{aligned}\vec{\xi} = f_{(1)}\partial_u + \Big[Y^A_{(1)} - \frac{1}{\hat{r}}D^A f_{(1)} + \frac{1}{2\hat{r}^2}C^{AB}_{(0)}D_B f_{(1)} + \mathcal{O}(\hat{r}^{-3},\varepsilon^2)\Big]\partial_A \\ - \Big[\frac{1}{2}\hat{r}D_A Y^A_{(1)} - \frac{1}{2}D^2 f_{(1)} - \frac{1}{2\hat{r}}U^A_{(0)}D_A f_{(1)} + \frac{1}{4\hat{r}}D_A(D_B f_{(1)}C^{AB}_{(0)}) + \mathcal{O}(\hat{r}^{-2},\varepsilon^2)\Big]\partial_{\hat{r}},\end{aligned} \tag{3.40}$$

where $f_{(1)} := \alpha_{(1)}(\theta^A) + \frac{1}{2}uD_A Y^A_{(1)}(\theta^B)$. Using the Bondi–Sachs Kerr metric given by Bai et al. [19], I can make the simplifications $C^{(0)}_{\mu\nu} = 0$ and $U^{(0)}_A = 0$ (see Eq. (3.36)). Hence, Eq. (3.40) simplifies to

$$\vec{\xi} = f_{(1)}\partial_u + \Big[Y^A_{(1)} - \frac{1}{\hat{r}}D^A f_{(1)} + \mathcal{O}(\hat{r}^{-3})\Big]\partial_A - \Big[\frac{1}{2}\hat{r}D_A Y^A_{(1)} - \frac{1}{2}D^2 f_{(1)} + \mathcal{O}(\hat{r}^{-2})\Big]\partial_{\hat{r}}. \tag{3.41}$$

This is still a complicated gauge vector, with multiple types of BMS transformations affecting each component. To associate $h'^{(1)}_{ab}$ to a specific infinitesimal BMS frame, I must separate these degrees of freedom. This can be achieved by finding quantities which transforms in such a way as to isolate each transformation, allowing each degree of freedom to be fixed individually. To find conveniently transforming

quantities, I begin by examining how the $\hat{h}_{uu}$ component transforms,

$$\begin{aligned}\Delta\hat{h}_{uu} &= \xi^c g_{uu,c} + 2\xi^c{}_{,u} g_{uc} \\ &= \xi^{\hat{r}} g_{uu,\hat{r}} + 2\xi^u{}_{,u} g_{uu} + 2\xi^{\hat{r}}{}_{,u} g_{u\hat{r}} + 2\xi^A{}_{,u} g_{uA} \\ &= \frac{3M}{\hat{r}} D_A Y^A_{(1)} + \frac{M}{\hat{r}^2}\Big(2a^{(0)}\sin^2[\hat{\theta}] D^{\hat{\phi}} D_A Y^A_{(1)} - D^2\alpha_{(1)} - \frac{u}{2} D^2 D_A Y^A_{(1)}\Big) + \mathcal{O}(\hat{r}^{-3}).\end{aligned} \tag{3.42}$$

By isolating each order in $\hat{r}$ of Δh_{uu}, one finds

$$\Delta M^{(1)} = \frac{3M}{2} D_A Y^A_{(1)}, \tag{3.43}$$

$$\Delta Z^{(1)} = -\frac{1}{\hat{r}^2}\Big[M D^2\alpha_{(1)} + \frac{Mu}{2} D^2 D_A Y^A_{(1)} - 2Ma^{(0)}\sin^2[\hat{\theta}] D^{\hat{\phi}} D_A Y^A_{(1)}\Big], \tag{3.44}$$

where $\Delta M^{(1)} = M_B'^{(1)} - M_B^{(1)}$ and $\Delta Z = Z'^{(1)} - Z^{(1)}$ (and M_B and Z are defined in Eq. (3.23)). Note, Eq. (3.43) is identical to Eq. (2.18a) in Ref. [71] when $C^{(0)}_{ab} = 0$ is imposed.

Immediately one sees Eq. (3.43) isolates the boosts, in Eqs. (3.25) and (3.27), from the other BMS transformations as $D_A Y^A_{(1)} = D_A D^A \chi_{(1)}$ (i.e., $D_A \epsilon^{AB} D_B \kappa = 0$). Also, by fixing the boost frame using Eq. (3.43), one can isolate the supertranslations ($\alpha_{(1)}$) in Eq. (3.44). To fix the boost frame I express $Y^A_{(1)}$ in terms of modes. Eq. (3.27) becomes

$$Y^A_{(1)} = \sum_{m=-1}^{+1} D_A D^A \chi^{(1)}_{1,\mathtt{m}} Y_{\ell,\mathtt{m}} - \epsilon^{AB} D_B \kappa_{1,\mathtt{m}} Y_{\ell,\mathtt{m}}. \tag{3.45}$$

Similarly, one can express $\alpha^{(1)}$, $\Delta M^{(1)}$, and $\Delta Z^{(1)}$ in terms of spherical harmonics. Eq. (3.43) can now be rearranged to give an equation for $\chi^{(1)}_{1,\mathtt{m}}$

$$\begin{aligned} D^2\chi^{(1)}_{1,\mathtt{m}} Y_{1,\mathtt{m}} &= -\frac{2\Delta M^{(1)}_{1,\mathtt{m}} Y_{1,\mathtt{m}}}{3M}, \\ \Rightarrow \chi^{(1)}_{1,\mathtt{m}} &= -\frac{\Delta M^{(1)}_{1,\mathtt{m}}}{3M}, \end{aligned} \tag{3.46}$$

where in the second line I have used that D^2 is the Laplacian on the unit two-sphere; i.e., $D^2 Y_{\ell,\mathtt{m}} = -\ell(\ell+1) Y_{\ell,\mathtt{m}}$.

By using Eq. (3.46), Eq. (3.44) can be rearranged to solve for $\alpha^{(1)}_{\ell,\mathtt{m}}$ in terms of $\Delta Z^{(1)}_{\ell,\mathtt{m}}$ and $\Delta M^{(1)}_{1,\mathtt{m}}$,

$$\alpha^{(1)}_{\ell,\mathtt{m}} = \frac{2}{M\ell(\ell+1)}\Delta Z^{(1)}_{\ell,\mathtt{m}} - \frac{4ia\mathtt{m}}{3M\ell(\ell+1)}\Delta M^{(1)}_{1,\mathtt{m}} - \frac{u}{3M}\Delta M^{(1)}_{1,\mathtt{m}}. \tag{3.47}$$

Where I have again used that D^2 is the unit two-sphere Laplacian. I have solved for $\chi^{(1)}_{1,\mathtt{m}}$ and $\alpha^{(1)}_{\ell,\mathtt{m}}$ (for $\ell > 1$) algebraically in terms of $\Delta M^{(1)}_{1,\mathtt{m}}$ and $\Delta Z^{(1)}_{\ell,\mathtt{m}}$. One is therefore free

to choose $M'^{(1)}_{1,\mathtt{m}}$ and $Z'^{(1)}$ as they are purely BMS frame dependent. For simplicity, one can choose $M'^{(1)}_{1,\mathtt{m}} = 0$ and $Z'^{(1)} = 0$ (i.e., $\Delta M^{(1)}_{1,\mathtt{m}} = -M^{(1)}_{1,m}$ and $\Delta Z^{(1)}_{\ell,\mathtt{m}} = -Z^{(1)}_{\ell,\mathtt{m}}$). These choices, respectively, put the coordinate system into the center of momentum frame and set the position of the origin to the center of mass of the first-order perturbation.

The remaining BMS transformations are the time translation ($\alpha_{0,0}$) and the three rotations ($\kappa_{1,\mathtt{m}}$). I expect to be unable to constrain $\alpha_{0,0}$ and $\kappa_{1,0}$ using the metric perturbation as they correspond to the time and axial symmetry of Kerr spacetime respectively. Alternatively, these freedoms could be fixed using the transformation of the first-order stress-energy tensor, Eq. (3.3). The other rotations, as I will show, can be constrained by fixing the form of $N^{(1)}_A$. The transformation of $N^{(1)}_A$ is given in Eq. (2.18c) of Ref. [71] (and can be also derived from the transformation of h_{uA} expanded in r). Setting $C^{(0)}_{ab} = 0$ and $U^{(0)}_A = 0$ in that equation gives

$$\Delta N^{(1)}_A = 3M^{(0)} D_A f_{(1)} + \mathcal{L}_{\vec{Y}_{(1)}} N^{(0)}_A + D_B Y^A_{(1)} N^{(0)}_A. \tag{3.48}$$

I can isolate the BMS rotations by splitting the Lie derivative into the even and odd piece, $Y^A_{(1)} = Y^A_{(1)e} + Y^A_{(1)o}$ (where $Y^A_{(1)o}$ corresponds to the rotations), equivalently to Eq. (3.27). Rearranging Eq. (3.48) for $\mathcal{L}_{\vec{Y}_{(1)o}} N^{(0)}_A$ (as $Y^A_{(1)e}$ has already been fixed by fixing $\chi^{(1)}_{1,m}$) gives

$$\mathcal{L}_{\vec{Y}_{(1)o}} N^{(0)}_A = \Delta N^{(1)}_A - 3M D_A f_{(1)} - \mathcal{L}_{\vec{Y}_{(1)e}} N^{(0)}_A - D_B Y^A_{(1)} N^{(0)}_A. \tag{3.49}$$

This equation simplifies significantly when implementing a vector spherical harmonic decomposition [88, 172]. Noting $N^{(0)}_A = \{0, -3Ma\sin^2[\hat{\theta}]\} \propto X^{1,0}_A$, $Y^A_{(1)e} \propto Z^A_{1,m}$ and $Y^A_{(1)o} \propto X^A_{1,m}$, one finds

$$\mathcal{L}_{\vec{Y}_{(1)o}} N^{(0)}_A \propto X^{1,\pm1}_A; \tag{3.50}$$

$$\mathcal{L}_{\vec{Y}_{(1)e}} N^{(0)}_A \propto X^{2,\pm1}_A, X^{2,0}_A; \tag{3.51}$$

$$D_A f_{(1)} \propto Z^{\ell,\mathtt{m}}_A; \tag{3.52}$$

$$D_B Y^A_{(1)} N^{(0)}_A \propto Z^{1,\pm1}_A, X^{2,\pm1}_A, X^{2,0}_A; \tag{3.53}$$

$$\Delta N^{(1)}_A \propto Z^{\ell,\mathtt{m}}_A, X^{\ell,\mathtt{m}}_A. \tag{3.54}$$

Here, I have used Eq. (3.28) to replace the vector harmonics with spherical harmonics, converted the Lie and covariant derivatives to partial derivatives, explicitly evaluated the angular derivatives, and then compared the resulting spherical harmonic expression with Eq. (3.28) to deduce the vector harmonic content. As $\mathcal{L}_{\vec{Y}_{(1)o}} N^{(0)}_A$ is purely $X^{1,\pm1}_A$, and the only other term which contains $X^{1,\pm1}_A$ elements is $\Delta N^{(1)}_A$, one

finds the equality

$$\mathcal{L}_{\vec{Y}^{1,\pm1}_{(1)o}} N^{(0)}_A = \Delta N^{(1)o1,\pm1}_A := \Delta N^{(1)o}_{1,\pm1} X^{1,\pm1}_A, \tag{3.55}$$

where $\Delta N^{(1)o1,\pm1}_A$ is the $X^{1,\pm1}_A$ piece of $\Delta N^{(1)}_A$. As expected due to axial symmetry of Kerr, $\vec{Y}^{10}_{(1)o}$ does not contribute. By evaluating the Lie derivative (using $Y^A_{(1)o} = -\varepsilon^{AB} D_B \kappa^{(1)}_{1,\mathtt{m}} Y_{1,\mathtt{m}}$), defining N such that $N^{(0)}_A = N X^{1,0}_A$ and decomposing into vector spherical harmonics, one finds

$$\pm 2\sqrt{\frac{3}{2\pi}} \kappa^{(1)}_{1,\pm1} N i X^{1,\pm1}_A = \Delta N^{(1)}_{o1,\pm1} X^{1,\pm1}. \tag{3.56}$$

Noting that $N = 2\sqrt{3\pi} Ma$ (from Eq. (3.36)), I can now solve for $\kappa^{(1)}_{1,\pm1}$, giving

$$\kappa^{(1)}_{1,\pm1} = \mp \frac{i \Delta N^{(1)}_{o1,\pm1}}{3\sqrt{2} Ma}. \tag{3.57}$$

That is, one can fix the BMS frame with respect to the rotations about the x- and y-axes (corresponding to $\kappa^{(1)}_{1,\pm1}$). Again, for simplicity, one can chose $N'^{(1)}_{o1,\pm1} = 0$, resulting in $\Delta N^{(1)}_{o1,\pm1} = -N^{(1)}_{o1,\pm1}$. This choice can be understood as aligning the angular momentum of the first-order perturbation along the z-axis.

In summary, one can solve for the gauge vector to a maximally fixed BMS frame by solving Eqs. (3.47), (3.46) and (3.57) for $\alpha^{(1)}_{\ell\geq1,\mathtt{m}}$, $\chi^{(1)}_{1,\mathtt{m}}$ and $\kappa^{(1)}_{1,\pm1}$ respectively. The gauge vector Eq. (3.41) can be expressed as

$$\begin{aligned}\vec{\xi} = f_{(1)}\partial_u &+ \Big[(D^A \chi^{(1)}_{1,\mathtt{m}} - \varepsilon^{AB} D_B \kappa^{(1)}_{1,\mathtt{m}}) Y_{1,\mathtt{m}} - \frac{1}{\hat{r}} D^A f_{(1)} + \mathcal{O}(\hat{r}^{-3})\Big]\partial_A \\ &- \Big[\frac{1}{2}\hat{r} D_A (D^A \chi^{(1)}_{1,\mathtt{m}} - \varepsilon^{AB} D_B \kappa^{(1)}_{1,\mathtt{m}}) Y_{1,\mathtt{m}} - \frac{1}{2} D^2 f_{(1)} + \mathcal{O}(\hat{r}^{-2})\Big]\partial_{\hat{r}},\end{aligned} \tag{3.58}$$

with

$$f_{(1)} := \alpha^{(1)}_{\ell,\mathtt{m}} Y^{\ell,\mathtt{m}}(\hat{\theta}^A) + \frac{1}{2} u D_A (D^A \chi^{(1)}_{1,\mathtt{m}} - \varepsilon^{AB} D_B \kappa^{(1)}_{1,\mathtt{m}}) Y_{1,\mathtt{m}}. \tag{3.59}$$

Eqs. (3.57), (3.46) and (3.47) fully fixes the infinitesimal supertranslation frame, the infinitesimal boost frame, and two of the infinitesimal rotation frames to first order. However, it leaves $\alpha_{0,0}$ and $\kappa_{1,0}$ (the time translation and rotation around the z-axis respectively) unconstrained. These freedoms could be fixed using Eq. (3.3). For a self-force calculation, this would be equivalent to fixing the infinitesimal position of the compact object at a given infinitesimal time, whilst remaining consistent with the BMS frame fixing. This method is consistent for a Kerr background and any background satisfying $C^{(0)}_{AB} = 0$ and $N^{(0)}_A = N X^{1,0}_A$.

3.6.8 Implementing BMS fixing in the Bondi–Sachs fixing method

The infinitesimal BMS fixing scheme described in Section 3.6.7 can be used to provide boundary conditions for the Bondi–Sachs infinitesimal gauge fixing method in Sec. 3.6. The resulting gauge vector calculation has no residual freedom (up to a time translation and axial rotation), resulting in a fully fixed infinitesimal gauge. That is, an infinitesimal Bondi–Sachs gauge with a fully fixed infinitesimal BMS frame.

The remaining freedom in the gauge vector calculation in Sec. 3.6.4 is in Eqs. (3.33a) and (3.33b). There remains the freedom to choose the (u independent) $\sim \hat{r}^0$ piece of ξ_l on a single cut on $\mathcal{I}^+$(which I label $\xi_l|_{\mathcal{I}^+,\,\hat{r}^0,\,u^0}$) and the freedom to choose the $\ell = 1$ (u independent) $\sim r^1$ piece of ξ_m on a single cut on $\mathcal{I}^+$(which I label $\xi_m^{\ell=1}|_{\mathcal{I}^+,\,\hat{r}^0,\,u^0}$). Implementing the BMS frame fixing method to apply boundary conditions gives (in Bondi–Sachs coordinates)

$$\begin{aligned}\xi_l|_{\mathcal{I}^+,\,\hat{r}^0,\,u^0} &= -A(\alpha^{(1)}_{\ell,\mathtt{m}}Y^{\ell,\mathtt{m}} + \frac{1}{2}uD^AY_A),\\ \xi_m^{\ell=1}|_{\mathcal{I}^+,\,\hat{r}^0,\,u^0} &= -\frac{\hat{r}}{\sqrt{2}}(Y^\theta + iY^\phi),\end{aligned} \tag{3.60}$$

with $Y^A_{(1)} = \sum_{\mathtt{m}=-1}^{1}\chi^{(1)}_{1,\mathtt{m}}D^AY_{\ell,\mathtt{m}} - \kappa_{1,\mathtt{m}}\epsilon^{AB}D_BY_{\ell,\mathtt{m}}$ and A is a factor corresponding to the choice of tetrad (in the Carter tetrad $A = 1$ and in the Kinnersley tetrad $A = \frac{1}{\sqrt{2}}$). I have used that $l^\mu = \{0, A, 0, 0\} + \mathcal{O}(r^{-1})$ and $m^\mu = \frac{1}{\sqrt{2}\hat{r}}\{0, 0, 1, \frac{i}{\sin[\hat{\theta}]}\} + \mathcal{O}(r^{-2})$ in Bondi–Sachs coordinates.

The strength of the tetrad transform method is its coordinate covariance. Transforming between coordinate schemes is straightforward as ξ^l and ξ^m are scalars. Also Eq. (3.60) only constrains the leading-order $\hat{r}$ dependency, plus retarded BL coordinates (with $u \to t + r$) are equivalent to Bondi–Sachs coordinates to leading order in r in Kerr (see Eq. (3.37)). Hence, Eq. (3.60) is the same in retarded BL coordinates and BS coordinates.

I now have expressions for the boundary conditions in the infinitesimal Bondi–Sachs gauge fixing method in BL coordinates. The required inputs are $\alpha^{(1)}_{\ell\geq 1,\mathtt{m}}$, $\chi^{(1)}_{1,\mathtt{m}}$ and $\kappa^{(1)}_{1,\pm 1}$. Currently the explicit expressions for $\alpha^{(1)}_{\ell\geq 1,\mathtt{m}}$, $\chi^{(1)}_{1,\mathtt{m}}$ and $\kappa^{(1)}_{1,\pm 1}$ (Eqs. (3.47), (3.46) and (3.57)) require working in BS coordinates. I will now show how $\alpha^{(1)}_{\ell\geq 1,\mathtt{m}}$, $\chi^{(1)}_{1,\mathtt{m}}$ and $\kappa^{(1)}_{1,\pm 1}$ can be obtained from BL coordinate metric perturbation. Again, this is straightforward as the Bondi–Sachs coordinates are equivalent to retarded BL coordinates to leading order in r in Kerr.

$\alpha^{(1)}_{\ell\geq 1,\mathtt{m}}$, $\chi^{(1)}_{1,\mathtt{m}}$ and $\kappa^{(1)}_{1,\pm 1}$ are obtained from $\Delta M^{(1)}$, $\Delta Z^{(1)}$ and $\Delta N^{(1)}_A$ in Eqs. (3.47), (3.46) and (3.57). As $\Delta M^{(1)} = M'^{(1)}_B - M^{(1)}_B$, finding $\Delta M^{(1)}$ requires choosing $M'^{(1)}_B$; an obvious choice in self-force calculations is $M'^{(1)}_B = \mu$ (for quasi-normal mode calculations, there is no additional mass in the system, making the obvious choice

$M_B'^{(1)} = 0$). Similarly, choosing $Z'^{(1)} = 0$ (placing the first-order center of mass at the origin) and $N_\theta'^{(1)} = 0$ (aligning the angular momentum with the z-axis) are obvious choices.

Additionally, to obtain $\Delta M^{(1)}$, $\Delta Z^{(1)}$ and $\Delta N_A^{(1)}$ one needs $M^{(1)}$, $Z^{(1)}$ and $N_A^{(1)}$. Such functions are acquired from the components of the metric perturbation in Bondi–Sachs coordinates, specifically, the components $\hat{h}_{uu}^{(1)BS}$ and $\hat{h}_{uA}^{(1)BS}$ (the superscript BS denotes a quantity expressed in Bondi–Sachs coordinates), see Eq. (3.24). As I want to relate these quantities to a metric perturbation in BL coordinates, I transform the components using the BL to Bondi–Sachs coordinate transform in Bai et al. [19] (Eq. (3.37)). This informs us that

$$\begin{aligned}\hat{h}_{uu}^{(1)BS} &= \hat{h}_{tt}^{(1)BL} + \mathcal{O}(r^{-3}),\\ \hat{h}_{uA}^{(1)BS} &= \hat{h}_{tA}^{(1)BL} + \mathcal{O}(r^{-2}),\end{aligned} \tag{3.61}$$

where $\hat{h}_{\mu\nu}^{(1)BL}$ is the metric perturbation in the infinitesimal Bondi–Sachs gauge expressed in BL coordinates. Therefore,

$$\begin{aligned}\hat{h}_{tt}^{(1)BL} &= \frac{M_{BL}^{(1)}}{r} + \frac{Z_{BL}^{(1)}}{r^2} + \mathcal{O}(r^{-3}),\\ \hat{h}_{tA}^{(1)BL} &= U_A^{(1)BL} - \frac{2N_A^{(1)BL}}{3r} + \mathcal{O}(r^{-2});\end{aligned} \tag{3.62}$$

that is, $M^{(1)} = M_{BL}^{(1)}$, $Z^{(1)} = Z_{BL}^{(1)}$ and $N_A^{(1)} = N_A^{(1)BL}$. Hence, I can write Eqs. (3.47), (3.46) and (3.57) as

$$\alpha_{\ell,\mathtt{m}}^{(1)} = \frac{2}{M\ell(\ell+1)}\Delta Z_{BL\ell,\mathtt{m}}^{(1)} - \frac{4ia\mathtt{m}}{3M\ell(\ell+1)}\Delta M_{BL1,\mathtt{m}}^{(1)} - \frac{u}{3M}\Delta M_{BL1,\mathtt{m}}^{(1)},$$

$$\chi_{1,\mathtt{m}}^{(1)} = -\frac{\Delta M_{BL1,\mathtt{m}}^{(1)}}{3M}, \tag{3.63}$$

$$\kappa_{1,\pm1}^{(1)} = \mp\frac{i\Delta N_{BL\ o1,\pm1}^{(1)}}{3\sqrt{2}Ma}. \tag{3.64}$$

These are the required inputs for Eq. (3.60) in BL coordinates.

This completes my formalism for transforming to an infinitesimal Bondi–Sachs gauge with a fully fixed infinitesimal BMS frame. The methods in Secs. 3.6.4, 3.6.7, and 3.6.8 combine to produce a practical way of calculating a gauge vector (ξ^a). This gauge vector can be inputted into Eq. (3.4) to solve for a fully fixed asymptotically flat infinitesimal gauge-invariant quantity (up to time translations and z-axis rotations).

3.6.9 Demonstrating gauge invariance up to Killing symmetries

In this section, I demonstrate that the Bondi–Sachs gauge fixing method with BMS frame fixing, and Chandrasekhar-like gauge fixing, produces a gauge invariant $\psi_{4L}^{\prime(2)}$ up to the Killing symmetries of Kerr spacetime. To achieve this I examine how $\psi_{4L}^{\prime(2)}$ transforms under a generic gauge transformation associated to the gauge vector $\zeta^a_{(1)}$ [37]. Quantities in this new gauge will be labelled with a tilde.

Under such a gauge transform, the metric perturbations transform as

$$h^{(1)}_{ab} \to \tilde{h}^{(1)}_{ab} = h^{(1)}_{ab} + \mathcal{L}_{\zeta^c_{(1)}} g^{(0)}_{ab} \tag{3.65}$$

$$h^{(2)}_{ab} \to \tilde{h}^{(2)}_{ab} = h^{(2)}_{ab} + \mathcal{L}_{\zeta^c_{(2)}} g^{(0)}_{ab} + \mathcal{L}_{\zeta^c_{(1)}} h^{(1)}_{ab} + \frac{1}{2}\mathcal{L}_{\zeta^c_{(1)}}\mathcal{L}_{\zeta^c_{(1)}} g^{(0)}_{ab} \tag{3.66}$$

Using the scheme in Sec. 3.6 with the boundary conditions in Eq. (3.60) and (3.63) one can calculate the vector $\xi^a_{(1)}$ in the new gauge, $\tilde{\xi}^a_{(1)}$. It can be shown that $\xi^a_{(1)}$ in the new gauge is

$$\xi^a_{(1)} \to \tilde{\xi}^a_{(1)} = \xi^a_{(1)} - \zeta^a_{(1)} + \Xi^a_{(1)}, \tag{3.67}$$

where $\Xi^a_{(1)}$ is the part of $\zeta^a_{(1)}$ that is tangent to the Killing vectors of Kerr spacetime.

Next, I want to assess the form of $\psi_{4L}^{\prime(2)}$ in the new gauge. By gauge transforming Eq. (3.1) to the new gauge, $\psi_{4L}^{\prime(2)}$ transforms as

$$\begin{aligned}\psi_{4L}^{\prime(2)} \to \tilde{\psi}_{4L}^{\prime(2)} = \mathcal{T}_4\Big[&h^{(2)}_{ab} + \mathcal{L}_{\zeta^c_{(2)}} g^{(0)}_{ab} + \mathcal{L}_{\zeta^c_{(1)}} h^{(1)}_{ab} + \frac{1}{2}\mathcal{L}_{\zeta^c_{(1)}}\mathcal{L}_{\zeta^c_{(1)}} g^{(0)}_{ab} \\ &+ \Big[\mathcal{L}_{(\xi^a_{(1)} - \zeta^a_{(1)} + \Xi^a_{(1)})}\left(h^{(1)}_{ab} + \mathcal{L}_{\zeta^c_{(1)}} g^{(0)}_{ab}\right) + \frac{1}{2}\mathcal{L}_{(\xi^a_{(1)} - \zeta^a_{(1)} + \Xi^a_{(1)})}\mathcal{L}_{(\xi^a_{(1)} - \zeta^a_{(1)} + \Xi^a_{(1)})} g_{ab}\Big].\end{aligned} \tag{3.68}$$

Expanding $\mathcal{L}_{(\xi^a_{(1)} - \zeta^a_{(1)} + \Xi^a_{(1)})} = \mathcal{L}_{\xi^a_{(1)}} - \mathcal{L}_{\zeta^a_{(1)}} + \mathcal{L}_{\Xi^a_{(1)}}$, using $\mathcal{L}_{\Xi^c_{(1)}} g_{ab} = 0$, and $\mathcal{T}_4[\mathcal{L}_{X^c} g_{ab}] = 0$ (for any vector X^c), one finds some terms cancel, giving

$$\begin{aligned}\tilde{\psi}_{4L}^{\prime(2)} = \mathcal{T}_4\Big[&h^{(2)}_{ab} + \mathcal{L}_{\xi^c_{(1)}} h^{(1)}_{ab} + \frac{1}{2}\mathcal{L}_{\xi^c_{(1)}}\mathcal{L}_{\xi^c_{(1)}} g_{ab} \\ &+ \frac{1}{2}\left(\mathcal{L}_{\xi^c_{(1)}}\mathcal{L}_{\zeta^c_{(1)}} g_{ab} - \mathcal{L}_{\zeta^c_{(1)}}\mathcal{L}_{\xi^c_{(1)}} g_{ab}\right) \\ &+ \mathcal{L}_{\Xi^c_{(1)}} h^{(1)}_{ab} + \frac{1}{2}\mathcal{L}_{\Xi^c_{(1)}}\mathcal{L}_{\xi^c_{(1)}} g_{ab}\Big].\end{aligned} \tag{3.69}$$

The second line in Eq. (3.69) is equal to $\frac{1}{2}\mathcal{T}_4\left[\mathcal{L}_{[\xi^c, \zeta^d]^e} g_{ab}\right] = 0$, where I have used the property of the Lie derivative that $\mathcal{L}_{\xi^c_{(1)}}\mathcal{L}_{\zeta^c_{(1)}} g_{ab} - \mathcal{L}_{\zeta^c_{(1)}}\mathcal{L}_{\xi^c_{(1)}} g_{ab} = \mathcal{L}_{[\xi^c, \zeta^d]^c}$ [157] and $\mathcal{T}_4[\mathcal{L}_{X^c} g_{ab}] = 0$ (for any vector X^c). Hence, noting that the top line in Eq. (3.69) is equal

to $\psi^{\prime(2)}_{4L}$,

$$\tilde{\psi}^{\prime(2)}_{4L} = \psi^{\prime(2)}_{4L} + \mathcal{T}_4\Big[\mathcal{L}_{\Xi^c_{(1)}} h^{(1)}_{ab} + \frac{1}{2}\mathcal{L}_{\Xi^c_{(1)}}\mathcal{L}_{\xi^c_{(1)}} g_{ab}\Big]. \tag{3.70}$$

Note, $\zeta^a_{(1)}$ does not appear in Eq. (3.3) except in its contribution to $\Xi^a_{(1)}$ (its Killing vector content). Therefore, I have shown that $\psi^{\prime(2)}_{4L}$ is gauge invariant up to gauge transformations along the Killing vectors of Kerr spacetime.

By fixing the Killing vector freedom using Eq. (3.3), the resulting $\xi^a_{(1)}$ will transform as $\xi^a_{(1)} \to \hat{\xi}^a_{(1)} = \xi^a_{(1)} - \zeta^a_{(1)}$ and Eq. (3.69) will become $\tilde{\psi}^{\prime(2)}_{4L} = \psi^{\prime(2)}_{4L}$. That is, this analysis shows that once I have fixed the Killing vector freedom using Eq. (3.3), $\psi^{\prime(2)}_{4L}$ will be completely gauge invariant for the Bondi–Sachs gauge with BMS fixing scheme and the Chandrasekhar-like gauge fixing scheme.

3.6.10 Asymptotic behaviour of the reduced second-order Teukolsky source in the Bondi–Sachs gauge

To complete my analysis on how the Bondi–Sachs gauge will aid second-order calculations, I analyse the form of the reduced second-order Teukolsky source in the Bondi–Sachs gauge near $\mathcal{I}^+$. I am interested in the leading-order-in-r falloff to determine the behaviour of the retarded solution of the reduced second-order Teukolsky equation (defined as an integral against the retarded Green's function). In summary, I show that source in the Bondi–Sachs gauge converges two orders in r faster than the source in a generic gauge. I also show how the leading-order piece of $\psi^{(2)}_{4L}$, which contains the gravitational waves being emitted to $\mathcal{I}^+$, manifestly behaves as a gravitational wave (in the sense of being a homogeneous perturbation of flat spacetime) in the Bondi–Sachs gauge.

In order to achieve a separable reduced second-order Teukolsky equation, one must express the equation in master Teukolsky form (similarly to Eq. (1.82)). In the Kinnersley tetrad, it takes the form

$$\hat{\mathcal{O}}_4\left[\rho^{-4}\psi^{(2)}_{4L}\right] = 2\rho^{-4}\Sigma\,\mathcal{S}_4\left[T^{(2)}_{ab} - \delta^2 G_{ab}\left[h^{(1)}_{cd}, h^{(1)}_{ef}\right]\right], \tag{3.71}$$

$$\sim r^6 \mathcal{S}_4\left[\delta^2 G_{ab}\left[h^{(1)}_{cd}, h^{(1)}_{ef}\right]\right], \tag{3.72}$$

where in the second line I have expressed the leading-order asymptotic behaviour near $\mathcal{I}^+$(using that $T^{(2)}_{ab} = 0$ away from the worldline, $\rho \sim \frac{1}{r}$, and $\Sigma \sim r^2$).

In a generic gauge, asymptotically flat gauge the leading-order asymptotic behaviour of $\delta^2 G_{ab}\left[h^{(1)}_{cd}, h^{(1)}_{ef}\right] \sim r^{-2}$ [152, 185]. This can be shown from $h^{(1)}_{\alpha\beta} \sim \frac{z_{\alpha\beta}[u,\theta,\phi]}{r}$ in an

asymptotically flat gauge, noting that u derivatives of $h^{(1)}_{\alpha\beta}$ also behave as $\sim r^{-1}$, and $\delta^2 G_{ab}\left[h^{(1)}_{cd}, h^{(1)}_{ef}\right] \sim \partial_u \partial_u h^{(1)}_{cd} h^{(1)}_{cd}$.

As $\mathcal{S}_4$ contains terms which behave as $\sim \partial_u$, $\mathcal{S}_4\left[\delta^2 G_{ab}\left[h^{(1)}_{cd}, h^{(1)}_{ef}\right]\right] \sim r^{-2}$. Hence, the source of the master Teukolsky equation (Eq. (3.71)) behaves as $\sim r^4$.

As $\hat{\mathcal{O}}_4 \sim r^2(-\partial_u^2 + \partial_r^2)$, and $\rho^{-4} \sim r^4$, sourcing the master Teukolsky equation with $\sim r^4$ is equivalent to sourcing $\psi^{(2)}_{4L}$ at $\mathcal{O}(r^{-2})$,

$$\hat{\mathcal{O}}_4\left[\rho^{-4}\psi^{(2)}_{4L}\right] \sim r^4 \Rightarrow (-\partial_u^2 + \partial_r^2)\psi^{(2)}_{4L} \sim r^{-2}. \tag{3.73}$$

This is problematic as the solution to this equation will contain $\psi^{(2)}_{4L} \sim \frac{\log[r]}{r}$ terms caused by the source. Additionally, the retarded greens function integral may not converge [149]. The divergence makes determining the correct boundary conditions highly non-trivial. This is known as the infrared divergence problem in self-force [149]. In Refs. [156, 194, 195], to calculate the boundary conditions a time-domain post-Minkowski solution at large r was used (similarly to Ref. [149]).

In a physically motivated gauge, I conjecture that the $\sim \frac{1}{r}$ behaviour in $\psi^{(2)}_{4L}$ is source-free. My reasoning, according to the Peeling theorem [138], the leading-order behaviour of $\psi^{(2)}_{4L}$ will appear at $\mathcal{O}(r^{-1})$, which is where the gravitational waves appear. Gravitational waves are vacuum solutions. Hence, the order in r where gravitational waves appear should be source free. A source present at $\mathcal{S}_4 = \mathcal{O}(r^{-2})$ will obscure the gravitational waves in $\psi^{(2)}_{4L}$ in a generic gauge, making it more challenging to extract the gravitational wave information.

Next, I show how working in the Bondi–Sachs gauge (a "physically motivated" gauge) avoids the infrared divergence problem. I show that in the Bondi–Sachs gauge the source is more regular, behaving as $\mathcal{S}_4 = \mathcal{O}(r^{-4})$ (and sourcing $(-\partial_u^2 + \partial_r^2)\psi^{(2)}_{4L}$ at $\mathcal{O}(r^{-4})$, meaning gravitational waves alone appear in the $\sim r^{-1}$ piece of $\psi^{(2)}_{4L}$).

I begin by analysing the behaviour of $\mathcal{S}_4$ in GHP form,

$$\begin{aligned}\mathcal{S}_4[\delta^2 G_{ab}] = &\frac{1}{2}\left(\eth' - \bar{\tau} - 4\tau'\right)\left(\left(\text{Þ}' - 2\bar{\rho}'\right)\delta^2 G_{n\bar{m}} - \left(\eth' - \bar{\tau}\right)\delta^2 G_{nn}\right)\\ &+ \frac{1}{2}\left(\text{Þ}' - 4\rho - \bar{\rho}'\right)\left(\left(\eth' - 2\bar{\tau}'\right)\delta^2 G_{n\bar{m}} - \left(\text{Þ}' - \bar{\rho}'\right)\delta^2 G_{\bar{m}\bar{m}}\right).\end{aligned} \tag{3.74}$$

Note, only $\delta^2 G_{\bar{m}\bar{m}}$, $\delta^2 G_{n\bar{m}}$ and $\delta^2 G_{nn}$ appear in the source. Also, the time derivatives in $\text{Þ}' \sim \partial_u$ contribute to the leading-order behaviour, while all other terms contribute a factor of at-least r^{-1}. That is, the source behaves as,

$$\mathcal{S}_4[\delta^2 G_{ab}] \sim \delta^2 G_{\bar{m}\bar{m}} + \frac{\delta^2 G_{n\bar{m}}}{r} + \frac{\delta^2 G_{nn}}{r^2}. \tag{3.75}$$

I now want to find what gauge conditions produce a maximally regular $\mathcal{S}_4\left[\delta^2 G_{ab}\right]$. In an asymptotically flat gauge $\delta^2 G_{ab}$ behaves as $\mathcal{O}(r^{-2})$. Hence, from Eq. (3.75), one can expect $\mathcal{S}_4\left[\delta^2 G_{ab}\right] \sim r^{-4}$ at best, in a well behaved gauge. To achieve $\mathcal{S}_4\left[\delta^2 G_{ab}\right] \sim r^{-4}$ requires

$$\begin{aligned} \delta^2 G_{nn} \sim r^{-2},\ \delta^2 G_{n\bar{m}} \sim r^{-3}, \\ \delta^2 G_{\bar{m}\bar{m}} \sim r^{-4}. \end{aligned} \tag{3.76}$$

This fall off can be understood by analysing the order at which one expects gravitational radiation to arise in $\delta^2 G\left[h^{(1)}_{ab}, h^{(1)}_{ab}\right]$. This is achieved by comparing $\delta^2 G\left[h^{(1)}_{ab}, h^{(1)}_{ab}\right]$ to a stress-energy tensor containing gravitational waves. Energy dissipated by gravitational waves appears at $\mathcal{O}(r^{-2})$ and is transmitted along the outgoing null direction l^a near $\mathcal{I}^+$; hence, energy dissipated will appear at leading order in the $\delta^2 G_{nn}\left[h^{(1)}_{ab}, h^{(1)}_{ab}\right]$ component. The angular momentum carried by gravitational waves will appear at $\mathcal{O}(r^{-3})$, and will appear (at leading order) in $G_{n\bar{m}}\left[h^{(1)}_{ab}, h^{(1)}_{ab}\right]$ but not $G_{\bar{m}\bar{m}}\left[h^{(1)}_{ab}, h^{(1)}_{ab}\right]$. Hence, in a well-behaved gauge, I expect $G_{\bar{m}\bar{m}}\left[h^{(1)}_{ab}, h^{(1)}_{ab}\right]$ behaves at $\mathcal{O}(r^{-4})$.

By analysing the form of $\delta^2 G_{ab}\left[h^{(1)}_{cd}, h^{(1)}_{ef}\right]$, one can derive the necessary gauge conditions on h_{ab} to obtain the appropriate falloffs in Eq. (3.76). The results of the analysis is that the first-order metric perturbation being asymptotically flat ($h^{(1)}_{ab}$ satisfies Eq. (1.26)) is insufficient to ensure Eq. (3.76) holds. Additional constraints are required: $h_{ln} \sim h_{lm} \sim h_{m\bar{m}} \sim \mathcal{O}(r^{-2})$ and $h_{ll} \sim \mathcal{O}(r^{-3})$. To derive these constraints, I analysed the form of $\delta^2 G_{ab}$ as a large r expansion in Mathematica; here, I will sketch the argument.

First, note as the trace piece of $\delta^2 G$ does not appear in $\mathcal{S}_4 \delta^2 G_{ab}$, and the first-order perturbation is vacuum away from the worldline; hence, $\mathcal{S}_4[\delta^2 G_{ab}] = \mathcal{S}_4[\delta^2 R_{ab}]$ (see Eq. (1.19)). Therefore, analysing the fall off of $\delta^2 R_{ab}\left[h^{(1)}_{cd}, h^{(1)}_{ef}\right]$ is sufficient. I express the quadratic Ricci tensor, Eq. (1.21), as [153]

$$\begin{aligned} \delta^2 R_{ab}\left[h^{(1)}_{ab}, h^{(1)}_{ab}\right] = &-\frac{1}{2}\bar{h}^{cd}{}_{;d}(2h_{c(a;b)} - h_{ab;c}) + \frac{1}{4}h^{cd}{}_{;a}h_{cd;b} + \frac{1}{2}h^{c}{}_{b}{}^{;d}(h_{ca;d} - h_{da;c}) \\ &- \frac{1}{2}h^{cd}(2h_{c(a;b)d} - h_{ab;cd} - h_{cd;ab}), \end{aligned} \tag{3.77}$$

where a bar denotes the trace reverse ($\bar{h}_{ab} := h_{ab} - \frac{1}{2}g^{(0)}_{ab}g^{(0)cd}$) and on the right hand side I have dropped the (1) superscript on the metric perturbation for legibility.

To determine the leading-order behaviour of $\delta^2 R_{ab}$, I analyse the fall off of $h_{\mu\nu}$, $h_{\mu\nu;\gamma}$ and $h_{\mu\nu;\gamma\delta}$ in the Bondi–Sachs gauge. The first is simply $h_{\mu\nu} \sim \frac{z_{\alpha\beta}[u,\theta,\phi]}{r}$. Next,

expressing the covariant derivative in NP form,

$$\begin{aligned} h_{\mu\nu;\gamma} &= -n_\gamma D h_{\mu\nu} - l_\gamma \Delta h_{\mu\nu} + \bar{m}_\gamma \delta h_{\mu\nu} + m_\gamma \bar{\delta} h_{\mu\nu} \\ &\sim \frac{a_{\mu\nu}[u,\theta,\phi]}{r} l_\gamma + \mathcal{O}(r^{-2}), \end{aligned} \tag{3.78}$$

This follows from noting $D \sim \partial_r + \mathcal{O}(r^{-1})$, $\Delta \sim \partial_u + \partial_r \mathcal{O}(r^{-1})$, and $\delta \sim \partial_u + \partial_r \mathcal{O}(r^{-1})$ and all the spin coefficients behave as $\mathcal{O}(r^{-1})$ [154]. Hence, the Δ derivative is leading order in r.

Similarly, a double covariant derivative can be written as

$$h_{\mu\nu;\gamma\delta} = -n_\delta D h_{\mu\nu;\gamma} - l_\delta \Delta h_{\mu\nu;\gamma} + \bar{m}_\delta \delta h_{\mu\nu;\gamma} + m_\delta \bar{\delta} h_{\mu\nu;\gamma} = \mathcal{O}(r^{-2}). \tag{3.79}$$

Using Eqs. (3.78) & (3.79) it is straightforward (but tedious) to show that $\delta^2 G_{nn} \sim r^{-2}$, $\delta^2 G_{n\bar{m}} \sim r^{-3}$ and $\delta^2 G_{\bar{m}\bar{m}} \sim r^{-3}$ if $h_{ln} \sim h_{lm} \sim h_{m\bar{m}} \sim \mathcal{O}(r^{-2})$ and $h_{ll} \sim \mathcal{O}(r^{-3})$.

By taking this analysis to a further order in r, it is possible to show $\delta^2 G_{\bar{m}\bar{m}} \sim r^{-4}$ if $h_{ln} \sim h_{lm} \sim h_{m\bar{m}} \sim \mathcal{O}(r^{-2})$ and $h_{ll} \sim \mathcal{O}(r^{-3})$. That is, in the Bondi–Sachs gauge $\mathcal{S}_4[\delta^2 G_{ab}[h_{ab}, h_{ab}]] \sim r^{-4}$, sourcing $(-\partial_u^2 + \partial_r^2)\psi_{4L}^{(2)}$ at $\mathcal{O}(r^{-4})$ (that is, only the gravitational waves appear in $\psi_{4L}^{(2)}$ at $\sim r^{-1}$). Crucially, the resulting source is not plagued by the infrared divergence problem that appears in generic second-order self-force calculations.

3.7 Highly regular gauge fixing

In this final section on gauge fixing, I present a method for deriving a local gauge transform to a *highly regular* gauge. Such a gauge transform reduces the singular nature of the source near the worldline in second-order self-force calculations, making the source of Eq. (2.20) well defined as a distribution (see Sec. 2.3.2). Here, I limit myself to a method for calculating the gauge vector ($\xi^a(x)$, at position x, with coordinates x^μ) which takes one from the Lorenz gauge (a commonly used gauge in self-force calculations) to the highly regular gauge, near the worldline. The highly regular gauge condition is

$$h_{ab}^{HR} k^a = 0, \tag{3.80}$$

where h_{ab}^{HR} is the metric perturbation in the highly regular gauge, and k^a is the set of null vectors corresponding to the set of future-directed null geodesics β emanating from the worldline (i.e., the object's future light cone). For each point (x^μ) near γ there is a unique geodesic (β_{x^μ}, which is a member of β) connecting the point to γ. I show in

Appendix C that I can approximate k^a near γ as

$$k^a = k^a_{\parallel} + k^a_{\perp} = u^a + \frac{P^a{}_b \Delta x^b}{\sqrt{P_{cd}\Delta x^c \Delta x^d}} + \mathcal{O}(\lambda). \tag{3.81}$$

where $\Delta x^\nu = x^\nu - x'^\nu$, x'^ν is the coordinate of the point where β_{x^μ} intercepts γ, u^a is again the four-velocity of γ (at x'^ν, $P_{ab} = g_{ab} + u_a u_b$ (the projection operator that projects onto the plane orthogonal to u^a) and λ is spatial distance from the worldline.

From Eq. (3.80), a gauge transformation from the Lorenz gauge to a highly regular gauge satisfies

$$(h^L_{ab} + \mathcal{L}_{\xi^a} g_{ab})k^a = 0, \tag{3.82}$$

which I solve to find ξ^a given the initial metric perturbation is in the Lorenz gauge (h^L_{ab}). To do so requires a form for the metric perturbation in the Lorenz gauge (at point x^μ). An expansion near the worldline (λ) for h^L_{ab} is given in Ref. [143],

$$h^L_{ab}[x^\mu] = \frac{2\mu}{\rho}(g_{ab} + 2u_a u_b) + \mathcal{O}(\lambda^0), \tag{3.83}$$

where $\rho := \sqrt{P_{\mu\nu}\Delta x^\mu \Delta x^\nu} = \mathcal{O}(\lambda)$.

The full derivation for $\xi_a(x)$ is given in Appendix C. Here, I state the result for solving Eq. (3.82) for $\xi_a(x^\mu)$ as an expansion in distance from the worldline,

$$\xi_a(x^\mu) = -2\mu \hat{u}_a \log[\hat{\rho}] + Y_a + A\hat{P}_{ab}\frac{\Delta \hat{x}^b}{\hat{\rho}} + \mathcal{O}(\lambda), \tag{3.84}$$

where $\hat{x}$ is the point on γ with the same BL time coordinate as x, $\hat{u}_a$ is the four velocity of the worldline at $\hat{x}$, $\Delta \hat{x}^\nu = x^\nu - \hat{x}^\nu$, $\hat{\rho} := \sqrt{P_{\mu\nu}\Delta \hat{x}^\mu \Delta \hat{x}^\nu}$, $\hat{P}_{ab} = \hat{g}_{ab} - \hat{u}_a \hat{u}_b$, Y_a is an arbitrary set of four constants, and A is an arbitrary constant. For simplicity, one can freely set $Y_a = 0_a$ and $A = 0$, which gives

$$\xi_a = -2\mu \hat{u}_a \log[\hat{\rho}] + \mathcal{O}(\lambda). \tag{3.85}$$

This method transforms into a useful gauge for second-order self-force calculations (making the source of Eq. (2.20) well defined as a distribution on γ). This formalism is the first step towards a highly regular gauge fixing scheme. To achieve such a scheme, constraining the remaining degrees of freedom, similarly to how I constrained the BMS freedoms in Sec. 3.6.7 in the Bondi–Sachs gauge will be necessary. I leave this extension to future work.

Chapter 4

Solving the Reduced Second-Order Teukolsky Equation in Schwarzschild

After finding the reduced second-order Teukolsky equation, Eq. (2.20), a natural progression is solving the equation. A collaboration has been formed to solve Eq. (2.20) for quasi-circular orbits in Schwarzschild. This project is a simplification of the ultimate generic orbit in Kerr goal. Nevertheless, as this will be the first time the reduced second-order Teukolsky equation will be solved, it will produce novel results and help develop the best methods for implementing further calculations. The collaboration contains Leanne Durkan, Ben Leather, Adam Pound, Sam Upton, Niels Warburton, and Barry Wardell.

We solve Eq. (2.20) for $\psi_{4L}^{(2)}$ for a point-mass on a quasi-circular orbit in Schwarzschild. Note, this is the reduced second-order Teukolsky equation with no gauge fixing, so the resulting $\psi_{4L}^{(2)}$ is not gauge independent. Nevertheless, energy and angular momentum fluxes radiated by a given orbit can be extracted from $\psi_{4L}^{(2)}$. We can use the two-timescale expansion (see Sec. 1.6.3.7) to evolve an inspiral through successively smaller orbits. This evolution will produce waveforms for quasi-circular inspirals in Schwarzschild to first-post adiabatic accuracy.

The project promises exciting results as we will compare the waveforms against the recent results of Ref. [195]. A successful comparison will be an important consistency check, as waveforms from Ref. [195] could be used for LIGO data analysis shortly. Additionally, solving the reduced second-order Teukolsky equation has three advantages to the methods used in Ref. [195]: only one complex scalar is solved for (rather than ten metric perturbation components), it is easier to extend to eccentric orbits, and most importantly, it naturally extends to Kerr.

In the next section, I summarise the calculation. The following sections present my contribution, including the form of the complete source (up to two pieces which will be added shortly). I also derive source coupling formulas which can be used for any second-order calculations in Schwarzschild (in the Carter tetrad). The formulas' applicability is not limited to self-force calculations and will be published in Ref. [175] shortly. The formulas express each mode of the second-order source as a sum of products of first-order modes. To finish the chapter I outline the final steps that are required to solve the reduced second-order Teukolsky equation, obtain fluxes, and waveforms.

4.1 Summarising the calculation

4.1.1 Tailoring the calculation to the Lorenz gauge

Solving the reduced second-order Teukolsky equation requires a well behaved first-order metric perturbation ($h^{(1)}_{ab}$) as an input. $h^{(1)}_{ab}$ in the Lorentz gauge is regular (except on the worldline, which can be handled with a puncture scheme, see Sec. 4.1.3). Calculating the Lorentz gauge first-order metric perturbation is straightforward in Schwarzschild [192] as the Einstein field equations are separable in the Lorenz gauge. Niels Warburton supplies retarded Lorenz gauge $h^{(1)}_{ab}$ data to the collaboration (as used in Refs [195, 194, 156]).

Throughout the implementation of the reduced second-order Teukolsky equation calculation we have, in places, used existing data and architecture from Refs. [195, 194, 156]. This is because second-order self-force calculations are incredibly time consuming. Refs [195, 194, 156] worked for the majority of a decade on their project before publishing results. With LISA fast approaching, we do not have the luxury of time, so leveraging previous work is necessary to obtain timely results. Nevertheless, the implementation described here does make many significant divergences to the methods in Refs [195, 194, 156], and the new methods show significant progress, as I shall highlight in this chapter.

To tailor our calculation to the Lorenz gauge, I will re-express the linearised EFE (Eq. (1.15)). The Lorenz gauge condition is

$$Z_a[h^{(1)}_{cd}] := \nabla^b \bar{h}^{(1)}_{ab} = 0. \tag{4.1}$$

where, over-bars denote a trace reverse (e.g., $\bar{h}^{(1)}_{ab} := h^{(1)}_{ab} - \frac{1}{2} g_{ab} g^{cd} h^{(1)}_{cd}$). In this calculation instead of applying Eq. (4.1), we apply $Z_a[h^{(1)}_{cd} + h^{(2)}_{cd} + ...] := \nabla^b(\bar{h}^{(1)}_{ab} + \bar{h}^{(2)}_{ab} + ...) = 0$; that is, the total perturbation satisfies the Lorenz gauge condition (I will clarify this distinction in Eqs. (4.26) and (4.27)).

One can rewrite the linearised Einstein field equation (Eq. (1.15)) in a convenient form

$$\delta G_{ab}[h^{(1)}_{cd}] = -\frac{1}{2}E_{ab}[h^{(1)}_{cd}] + \overline{\nabla_{(a}Z_{b)}}[h^{(1)}_{cd}], \tag{4.2}$$

where

$$E_{ab}[h^{(1)}_{ab}] := \Box\bar{h}^{(1)}_{ab} + 2R_a{}^c{}_b{}^d\bar{h}^{(1)}_{cd}, \tag{4.3}$$

and $\Box := g^{ab}\nabla_a\nabla_b$ (the d'Alembertian operator).

In Lorenz-gauge calculations, solving a gauge-damped linearised operator is more practical numerically because it partially decouples the field equations [22]. The gauge damped $\check{E}_{ab}$ reads

$$\check{E}_{ab} := E_{ab} - \frac{4M}{r^2}t_{(a}\check{Z}_{b)}, \tag{4.4}$$

where $t_a := \partial_a t$ and

$$\check{Z}_a = (Z_r, 2Z_r, Z_\theta, Z_\phi), \tag{4.5}$$

in BL coordinates (t, r, θ, ϕ). The linearised Einstein field equation is therefore written as

$$\delta G_{ab} = -\frac{1}{2}\check{E}_{ab} - \frac{2M}{r^2}t_{(a}\check{Z}_{b)} + \overline{\nabla_{(a}Z_{b)}}. \tag{4.6}$$

4.1.2 Implementing a two-timescale approximation

In order to evolve an inspiral to first-post-adiabatic accuracy, a two timescale approximation is implemented [69, 119, 154] (see Sec. 1.6.3.7). The field equations are re-expressed in a two-timescale expansion. First, the metric perturbation needs to be expressed as dependent on the two timescales. Note, I have previously been expressing $h^{(1)}_{ab}$ as implicitly dependent on the coordinates $x^\mu = \{t, r, \theta, \phi\}$. I select a time-foliation function

$$s = s[t, r] := t - k[r^*]. \tag{4.7}$$

where $k[r^*]$ is an arbitrary function of $r^* = r + 2M\ln|\frac{r}{2M} - 1|$. In the hyperboloidal method, s is chosen such that it asymptotes to advanced time, v, at the horizon and retarded time, u, at infinity. This greatly improves the behaviour of the slow-time-derivative terms in the field equations. An additional advantage is that the boundary conditions become trivial in a sufficiently regular gauge (like the Bondi–Sachs gauge, see Sec. 4.2.5.1) because the resulting source is sufficiently smooth at the boundaries; the field equations themselves automatically impose boundary

conditions [106]. We specifically adopt the height function k from Ref. [106], referred to as the "minimal gauge", and transform to a compact radial coordinate $\sigma = \frac{2M}{r}$. However, in this chapter I use BL coordinates ($k(r^*) = 0$, $s = t$, and I use r rather than σ) as the first-order data used as input is provided in these coordinates. The resulting reduced second-order Teukolsky source is then transformed to compactified hyperboloidal coordinates prior to solving the equation. s is also referred to as the so-called *fast-time* (on which the orbital phases evolve) and $\tilde{s} = \varepsilon s$ will be the *slow-time* (on which the frequencies of the inspiral evolve).

Rather than expressing $h^{(n)}_{ab}$ explicitly in terms of s and $\tilde{s}$, $h^{(n)}_{ab}$ is expressed in terms of the orbital phase $\phi_p = \phi_p(\varepsilon s, \varepsilon)$ and orbital frequency $\Omega = \Omega(\varepsilon s, \varepsilon) := \frac{d\phi_p}{ds}$. There is further expressed dependence of $h^{(n)}_{ab}$ on
$\varepsilon\delta M_A = \varepsilon\delta M_A(\varepsilon s, \varepsilon) := \{\varepsilon\delta M(\varepsilon s, \varepsilon), \varepsilon\delta J(\varepsilon s, \varepsilon)\}$, corrections to the central black hole's mass and spin (with an overall factor of ε pulled out to make δM_A order unity). That is [154],

$$h^{(1)}_{ab} = h^{(1)}_{ab}[x^i, \phi_p, \Omega, \delta M_A], \tag{4.8}$$
$$h^{(2)}_{ab} = h^{(2)}_{ab}[x^i, \phi_p, \Omega, \delta M_A], \tag{4.9}$$

where $x^i := \{r, \theta, \phi\}$. In contrast to Sec. 1.6.3.7 and Eq. (1.46), where I write the amplitudes as functions of the slow time $\tilde{t}$ explicitly, in Eq. (4.8) I have written the amplitudes as functions of Ω and δM_A, which are themselves functions of the slow time $\tilde{s}$. Explicitly, the slow and fast time dependence appears as

$$\phi_p(\tilde{s}, \varepsilon) = \varepsilon^{-1}\phi_p^{\{0\}}(\tilde{s}) + \phi_p^{\{1\}}(\tilde{s}) + \mathcal{O}(\varepsilon), \tag{4.10}$$
$$\Omega(\tilde{s}, \varepsilon) = \Omega^{\{0\}}(\tilde{s}) + \varepsilon\,\Omega^{\{1\}}(\tilde{s}) + \mathcal{O}(\varepsilon^2), \tag{4.11}$$
$$\delta M_A(\tilde{s}, \varepsilon) = M_A^{\{1\}}(\tilde{s}) + \mathcal{O}(\varepsilon), \tag{4.12}$$

where $\Omega^{\{n\}} = d\phi_p^{\{n\}}/d\tilde{s}$ and number labels in curly brackets again denote the post-adiabatic order at which the quantity enters [154, 119].

The expansions in Eqs. (4.10), (4.11), and (4.12) in powers of ε at fixed slow time are only used at the waveform-generation stage [154]. Whilst modeling the inspiral evolution ϕ_p, Ω, and δM_A are treated as independent coordinates of the orbital phase-space. The rates of change of these quantities (expanded in powers of ε) at fixed phase-space coordinate values are

$$\dot{\phi}_p = \Omega, \tag{4.13}$$
$$\dot{\Omega} = \varepsilon F_\Omega^{\{0\}}(\Omega) + \varepsilon^2 F_\Omega^{\{1\}}(\Omega, \delta M_A) + \mathcal{O}(\varepsilon^3), \tag{4.14}$$
$$\delta\dot{M}_A = \varepsilon F_A^{\{1\}}(\Omega) + \mathcal{O}(\varepsilon^2), \tag{4.15}$$

where a dot denotes d/ds and $F_i^{\{n\}}(\Omega)$ are nth-post adiabatic-order self-force coefficients.

The two-timescale coordinates result in a two-timescale partial derivative using the chain rule,

$$\frac{\partial}{\partial x^\alpha} = e^i_\alpha \frac{\partial}{\partial x^i} + s_\alpha \left(\frac{d\phi_p}{ds}\frac{\partial}{\partial \phi_p} + \frac{d\mathcal{J}_i}{ds}\frac{\partial}{\partial \mathcal{J}_i} \right), \tag{4.16}$$

where $e^i_\alpha := \frac{\partial x^i}{\partial x^\alpha}$, $s_\alpha := \partial_\alpha s$, and $\mathcal{J}_i := (\Omega, \delta M_A)$. This implies the covariant derivative expressed in the two-timescale formalism is

$$\nabla_\alpha = e^i_\alpha \frac{\partial}{\partial x^i} + s_\alpha \left(\frac{d\phi_p}{ds}\frac{\partial}{\partial \phi_p} + \frac{d\mathcal{J}_i}{ds}\frac{\partial}{\partial \mathcal{J}_i} \right) + \text{Christoffel terms.} \tag{4.17}$$

As the coordinates depend on ε, the covariant derivative is no longer a purely $\mathcal{O}(\varepsilon^0)$ quantity. It can be expressed as a series expansion in ε,

$$\nabla_\alpha = \nabla^{(0)}_\alpha + \nabla^{(1)}_\alpha + \mathcal{O}(\varepsilon^2). \tag{4.18}$$

The zeroth-order covariant derivative is

$$\nabla^{(0)}_\alpha = e^i_\alpha \frac{\partial}{\partial x^i} + s_\alpha \Omega \frac{\partial}{\partial \phi_p} + \text{Christoffel terms.} \tag{4.19}$$

The first-order covariant derivative is

$$\nabla^{(1)}_\alpha = \varepsilon s_\alpha \vec{\partial}_{\mathcal{V}}, \tag{4.20}$$

where $\vec{\partial}_{\mathcal{V}}$ is a directional derivative in the parameter space,

$$\vec{\partial}_{\mathcal{V}} := \mathcal{V}_i \frac{\partial}{\partial J_i} = F^{(0)}_\Omega \frac{\partial}{\partial \Omega} + F^{(1)}_A \frac{\partial}{\partial \delta M_A} \tag{4.21}$$

and $\mathcal{V}_i = (F^{\{0\}}_\Omega, F^{\{1\}}_A)$ is the leading-order "velocity through parameter space." I will refer to $\vec{\partial}_{\mathcal{V}}$ as a slow-time derivative as it only contributes over the long timescale of the inspiral. It is useful to count and collect slow-time derivatives. Hence, I re-write the covariant derivative to count powers of ε that come from the slow-time derivatives, labeling with numbers in angular brackets,

$$\nabla_\alpha = \nabla^{\langle 0\rangle}_\alpha + \nabla^{\langle 1\rangle}_\alpha + \mathcal{O}(\varepsilon^2); \tag{4.22}$$

note, $\nabla^{\langle n\rangle} \equiv \nabla^{(n)}$. Substituting the two-timescale metric perturbation expansion (Eq. (4.8)) into the first- and second-order linearised EFE (Eq. (1.15) and (1.16)), plus expressing the covariant derivative as the expansion in Eq. (4.22) (using the chain

rule), results in

$$\delta G^{\langle 0\rangle}_{ab}[h^{(1)}_{cd}] = 8\pi T^{(1)}_{ab}, \tag{4.23}$$

$$\delta G^{\langle 0\rangle}_{ab}[h^{(2)}_{cd}] = 8\pi T^{(2)}_{ab} - \delta^2 G^{\langle 0\rangle}_{ab}[h^{(1)}_{cd}, h^{(1)}_{cd}] - \delta G^{\langle 1\rangle}_{ab}[h^{(1)}_{cd}]. \tag{4.24}$$

Note, Eq. (4.23) is unchanged by the two timescale approximation except derivatives with respect to time have been replaced with ϕ_p derivatives. However, Eq. (4.24) contains an additional term involving slow-time derivatives of the first-order metric perturbation ($\vec{\partial}_{\mathcal{V}} h^{(1)}_{ab}$).

In a Teukolsky formalism, one does not solve the linearised EFE directly. Instead, implementing a two-timescale formalism in the reduced second-order Teukolsky equation, Eq. (2.20) becomes

$$\mathcal{O}^{(0)}_4[\psi^{(2)}_{4L}] = \mathcal{S}^{(0)}_4\left[8\pi T^{(2)}_{ab} - \delta^2 G^{\langle 0\rangle}_{ab}[h^{(1)}_{cd}, h^{(1)}_{cd}] - \delta G^{\langle 1\rangle}_{ab}[h^{(1)}_{cd}]\right] := S. \tag{4.25}$$

Here, I have defined S, the source of the reduced second-order Teukolsky equation in a two-timescale formalism. To see how $\vec{\partial}_{\mathcal{V}} h^{(1)}_{ab}$ appears in Eq (4.25) explicitly, see Sec. 4.2.6.

Using the expansion in Eq. (4.22), the Lorenz gauge condition, $Z_a[h^{(1)}_{cd} + h^{(2)}_{cd} + ...] := \nabla^b \bar{h}_{ab} = 0$, becomes

$$Z^{\langle 0\rangle}_a[h^{(1)}_{cd}] = \nabla^b_{\langle 0\rangle} \bar{h}^{(1)}_{ab} = 0, \tag{4.26}$$

and

$$Z^{\langle 1\rangle}_a[h^{(1)}_{cd}] + Z^{\langle 0\rangle}_a[h^{(2)}_{cd}] = \nabla^b_{\langle 1\rangle} \bar{h}^{(1)}_{ab} + \nabla^b_{\langle 0\rangle} \bar{h}^{(2)}_{ab} = 0. \tag{4.27}$$

The radial position of the particle in the two-timescale approximation for quasi-circular inspirals is given by

$$r_p = r_0[\Omega] + \varepsilon r_1[\Omega, \delta M_A] + O(\varepsilon^2), \tag{4.28}$$

where $r_0[\Omega] = M(M\Omega)^{-2/3}$.

4.1.3 Effective source and puncture scheme

Ref. [185] showed $T^{(2)}_{ab}$ and $\delta^2 G[h^{(1)}_{ab}, h^{(1)}_{ab}]$ are well defined in a highly regular gauge. Implementation of a gauge transform to the highly regular gauge (using Eq. (3.85)) is currently being worked on by Sam Upton. The resulting source to the reduced second-order Teukolsky equation will be well defined. Until the gauge transformation is ready, our current approach is using a puncture scheme to produce a well-defined

and regular reduced second-order Teukolsky equation source in the Lorenz gauge. A (sufficiently high order) puncture scheme removes the singular behaviour in $T^{(2)}_{ab}$ and $\delta^2 G[h^{(1)}_{ab}, h^{(1)}_{ab}]$, producing a well-defined equation solving for a residual field which approximates the regular field.

Additionally, there is the issue of obtaining $\delta^2 G[h^{(1)}_{ab}, h^{(1)}_{ab}]$ from modes of $h^{(1)}_{ab}$ near the particle. As a sum of input ℓ modes $\delta^2 G[h^{(1)}_{ab}, h^{(1)}_{ab}]$ does not converge on the worldline, and converges slowly near the worldline (when the retarded solution $h^{(1)}_{ab}$ modes are used as input). To overcome this issue Ref. [120] formalised an effective source approach which calculates the modes of $\delta^2 G[h^{(1)}_{ab}, h^{(1)}_{ab}]$ using the split of $h^{(1)}_{ab}$ into a 4D puncture, the corresponding modes of the 4D puncture, and the residual field. In Refs. [195, 194, 156] the effective source approach has been utilised and we build on their effective source for our reduced second-order Teukolsky equation calculation.

We require a puncture for the second-order metric perturbation of a point particle stress-energy tensor, $h^{(2)\mathcal{P}}_{ab}$. We then construct the puncture for the linearised second-order fourth Weyl scalar using

$$\psi^{(2)\mathcal{P}}_{4L} := \mathcal{T}^{\langle 0\rangle}_4[h^{(2)\mathcal{P}}]. \tag{4.29}$$

The puncture for the reduced second-order Teukolsky equation is, therefore, $\mathcal{O}^{\langle 0\rangle}[\psi^{(2)\mathcal{P}}_{4L}]$. That is, the effective source for the residual field ($\psi^{(2)\mathcal{R}}$) is

$$\mathcal{O}^{\langle 0\rangle}_4[\psi^{(2)\mathcal{R}}_{4L}] = S - \mathcal{O}^{\langle 0\rangle}_4[\psi^{(2)\mathcal{P}}_{4L}]. \tag{4.30}$$

Equivalently, one can introduce the puncture into the right-hand side of Eq. (4.25), giving

$$\mathcal{O}^{\langle 0\rangle}_4[\psi^{(2)\mathcal{R}}_{4L}] = \mathcal{S}^{\langle 0\rangle}_4\left[8\pi T^{(2)\text{eff}}_{ab}\right] := S_{\text{eff}}, \tag{4.31}$$

where S_{eff} is the effective source and

$$8\pi T^{(2)\text{eff}}_{ab} := 8\pi T^{(2)}_{ab} - \delta^2 G^{\langle 0\rangle}_{ab}[h^{(1)}_{cd}, h^{(1)}_{cd}] - \delta G^{\langle 1\rangle}_{ab}[h^{(1)}_{cd}] - \delta G^{\langle 0\rangle}_{ab}[h^{(2)\mathcal{P}}_{cd}]. \tag{4.32}$$

Note, $T^{(2)}_{ab}$ is only supported on the worldline and its singular distributional behaviour cancels with the puncture. Additionally, the effective stress-energy, $T^{(2)\text{eff}}_{ab}$, contains the modes of $\delta^2 G^{\langle 0\rangle}_{ab}[h^{(1)}_{cd}, h^{(1)}_{cd}]$ which have been calculated for Refs. [195, 194, 156] using the method described in Ref. [120].

Sufficiently far away from the worldline, the puncture scheme is unnecessary, and the reduced second-order Teukolsky equation reduces to

$$\mathcal{O}^{\langle 0\rangle}_4[\psi^{(2)}_{4L}] = \mathcal{S}^{\langle 0\rangle}_4\left[-\delta^2 G^{\langle 0\rangle}_{ab}[h^{(1)}_{cd}, h^{(1)}_{cd}] - \delta G^{\langle 1\rangle}_{ab}[h^{(1)}_{cd}]\right] := S_{\text{vac}}. \tag{4.33}$$

In practice, we solve Eq. (4.32) in a finite world-tube around the particle. The world-tube is the region $r_0 - d \leq r \leq r_0 + d$ where d is some finite length smaller than r_0. Outside of the world-tube Eq. (4.33) is solved. Across the boundaries of the world-tube we impose the matching conditions $\psi^{(2)}_{4L} = \psi^{(2)\mathcal{R}}_{4L} + \psi^{(2)\mathcal{P}}_{4L}$ and $\partial_r \psi^{(2)}_{4L} = \partial_r \psi^{(2)\mathcal{R}}_{4L} + \partial_r \psi^{(2)\mathcal{P}}_{4L}$.

4.1.3.1 Converting the known effective source

Calculating $\delta^2 G^{\langle 0\rangle}_{ab}[h^{(1)}_{cd}, h^{(1)}_{cd}]$ in the effective source is a numerically strenuous task and the current bottleneck for second-order calculations. Our collaboration chose to leverage an existing effective source to help solve the reduced second-order Teukolsky equation. Refs. [195, 194, 156] have provided the effective source they use to solve the linearised EFE in the Lorenz gauge. However, $T^{(2)\text{eff}}_{ab}$ (Eq. (4.32)) differs from the effective source used in Refs. [195, 194, 156], so our collaboration also adds a correction piece.

Refs. [195, 194, 156] have obtained an effective source of the form

$$-16\pi \breve{T}^{(2)\text{eff}}_{ab} := -16\pi T^{(2)}_{ab} + 2\delta^2 \breve{G}^{\langle 0\rangle}_{ab}[h^{(1)}, h^{(1)}] - \breve{E}^{\langle 1\rangle}_{ab}[h^{(1)}] - \breve{E}^{\langle 0\rangle}_{ab}[h^{(2)\mathcal{P}}]. \tag{4.34}$$

Hence,

$$S_{\text{eff}} = \mathcal{S}^{\langle 0\rangle}\left[8\pi \breve{T}^{(2)\text{eff}}_{ab}\right] + \mathcal{S}^{\langle 0\rangle}\left[8\pi \Delta T^{(2)\text{eff}}_{ab}\right], \tag{4.35}$$

where $\Delta T^{(2)\text{eff}}_{ab} := T^{(2)\text{eff}}_{ab} - \breve{T}^{(2)\text{eff}}_{ab}$. If $h^{(1)}_{ab}$ is in the Lorenz gauge, then

$$\Delta T^{(2)\text{eff}}_{ab} = -\overline{\nabla^{\langle 0\rangle}_{(a} Z^{\langle 1\rangle}_{b)}}[h^{(1)}_{cd}] - \overline{\nabla^{\langle 0\rangle}_{(a} Z^{\langle 0\rangle}_{b)}}[h^{(2)\mathcal{P}}_{cd}] + \frac{2M}{r^2} t_{(a}\left(\breve{Z}^{\langle 1\rangle}_{b)}[h^{(1)}_{cd}] + \breve{Z}^{\langle 0\rangle}_{b)}[h^{(2)\mathcal{P}}_{cd}]\right). \tag{4.36}$$

Eq. (4.36) would identically vanish if the puncture identically satisfied the second-order Lorenz gauge condition Eq. (4.27). However, since the puncture does not satisfy that equation (except to some order in a local expansion around the particle), there is no obvious reason for $\mathcal{S}^{(0)}\left[\Delta T^{(2)\text{eff}}_{ab}\right]$ to vanish. Hence, $\Delta T^{(2)\text{eff}}_{ab}$ is calculated and added to $T^{(2)\text{eff}}_{ab}$ in Eq. (4.35) to obtain S_{eff} (the effective source inside the world-tube).

4.1.4 Solving the reduced second-order Teukolsky equation with the hyperboloidal method

The reduced second-order Teukolsky equation is solved using a hyperboloidal method [106, 105] by Ben Leather. This method transforms to conformal coordinates on hyperboloidal slices that foliate the spacetime. One advantage of this approach is the boundary conditions can be made trivial in sufficiently regular gauges (as the only

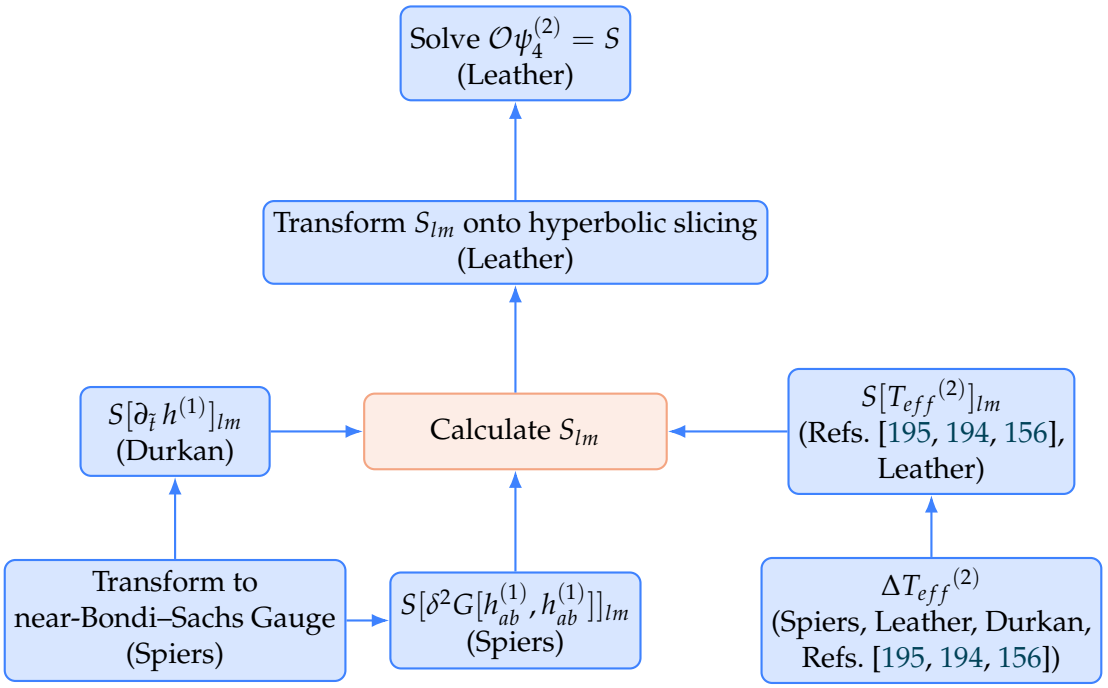

FIGURE 4.1: The stages of solving the reduced second-order Teukolsky equation. In brackets the names of who is responsible for most of that piece of the calculation is shown.

boundary conditions is radiation emanating from future null infinity and out of the horizon, both of which can be set to zero). The coordinates also put the event horizon and $\mathcal{I}^+$at finite coordinate values, making integrating over the whole domain possible and efficient. Finally, a multi-domain spectral method is used with analytic mesh refinement to find a solution in the hyperboloidal coordinates. From the solution Ben Leather obtains $\psi_{4L}^{(2)}$ and will calculate the energy flux for each orbit of radius r_p. Using energy fluxes on a grid of r_p values we will be able to evolve inspirals and generate waveforms.

4.1.5 My role: calculating the source

From the preceding sections, it is clear that solving the reduced second-order Teukolsky equation for quasi-circular orbits in Schwarzschild is a calculation of many parts. In Fig. 4.1, I summarise the various pieces of the calculation and how they fit together in a flow-chart. In the remainder of this section, I summarise my role in the collaboration. In the following section, I present the details of the calculations I made.

My role in this project is calculating various parts of S_{eff} and S_{vac}. Specifically, I derive a (spin-weighted spherical harmonic) mode decomposition for $\mathcal{S}^{\langle 0\rangle}\left[\delta^2 G^{\langle 0\rangle}_{ab}[h^{(1)}_{cd}, h^{(1)}_{cd}]\right]$, $\mathcal{S}^{\langle 0\rangle}\left[\delta G^{\langle 1\rangle}_{ab}[h^{(1)}_{cd}]\right]$ and $\Delta T^{(2)\text{eff}}_{ab}$ in BL coordinates. For $\mathcal{S}^{\langle 0\rangle}\left[\delta^2 G^{\langle 0\rangle}_{ab}[h^{(1)}_{cd}, h^{(1)}_{cd}]\right]$ I also numerically compute data using retarded Lorenz gauge first-order metric perturbation data provided by Niels Warburton as input.

Additionally, I implemented a gauge transformation to *near* the Bondi–Sachs gauge near $\mathcal{I}^+$(but do not fully fix the gauge). This gauge transformation improves the convergence of the source by two orders in r near $\mathcal{I}^+$. Implementing the near Bondi–Sachs transform requires calculating the gauge vector ξ^a using the analysis in Sec. 3.6. Additionally, I produce formulas for the gauge transformation of the slow time derivative of the metric perturbation. Also, as the gauge transformation is implemented at a single r value (at the outer world-tube boundary), a gauge jump in $\psi_{4L}^{(2)}$ occurs. I provide mode decomposition formulas for the jump in $\psi_{4L}^{(2)}$ due to the gauge transformation.

4.2 Calculating the source to the reduced second-order Teukolsky equation

In this section I calculate various parts of the source to the second-order Teukolsky equation. Note, Secs. 4.2.1 and 4.2.3 are applicable for general perturbation in Schwarzschild (in the Carter tetrad). Additionally to working in Schwarzschild in the Carter tetrad, Secs. 4.2.2, 4.2.5 and 4.2.7 specialise to the Lorenz gauge and Secs. 4.2.6 and 4.2.7 specialise to quasi-circular orbits. From this point I will often drop the superscript (1) on $h_{ab}^{(1)}$ for succinctness.

4.2.1 Mode decomposing the source in coordinate form

Obtaining an expression for a mode decomposition of the reduced second-order Teukolsky source (in a coordinate form) involves delicately converting from the GHP formalism into coordinates. It is crucial to maintain the spin-weight property of the GHP quantities, as they are naturally expressed in terms of spin-weighted spherical harmonics (the homogeneous solutions of the angular Teukolsky equation in Schwarzschild). Here, I outline the main steps in calculating a mode decomposed source in coordinate form and discuss how I have improved the compactness of the final expression. I begin by decomposing $\mathcal{S}^{\langle 0\rangle}\Big[-\delta^2 G_{ab}^{\langle 0\rangle}[h_{cd}^{(1)}, h_{cd}^{(1)}]\Big]$ as it is the largest part of the source (note, for here on out I drop $\langle 0\rangle$ labels).

The most prominent obstacle in decomposing the source of the reduced second-order Teukolsky equation is the sheer size of the expression. In GHP form $\mathcal{S}_4$ can be written in two lines, Eq. (3.74) [154]. Similarly, I need to express $\delta^2 G_{ab}$, Eq. (1.19), in GHP form. Each component of $\delta^2 G_{ab}$ in GHP form takes up a page in Latex, so I have not produced them here. Instead, I have included them in the supporting materials accompanying this thesis and will publicly release the expressions as a Mathematica package in the Black Hole Perturbation Toolkit [1] (which will accompany my paper in preparation [175].

Combining the GHP expressions for $\delta^2 G_{ab}$ and $\mathcal{S}_4$ results in an expression for $\mathcal{S}_4[\delta^2 G_{ab}]$ which is monstrous in length. It contains up to four GHP derivatives and is quadratic in $h^{(1)}_{ab}$ (containing ten independent components). Even when simplifying to a Schwarzschild background (i.e., all the spin-coefficients and Ψ_2 are real and $\tau = \tau' = 0$) $\mathcal{S}_4[\delta^2 G_{ab}]$ has ~ 1700 terms in GHP form. Mode decomposing $\mathcal{S}_4[\delta^2 G_{ab}]$ and converting it to coordinates form is only possible by creating a computer algorithm to automate the procedure.

To describe my algorithm to convert each term in $\mathcal{S}_4[\delta^2 G_{ab}]$ to a mode decomposed coordinate form, I select a single term in $\mathcal{S}_4[\delta^2 G_{ab}]$,

$$\mathcal{S}_4[\delta^2 G_{ab}[h^{(1)}_{ab}, h^{(1)}_{ab}]] = \frac{3}{2} h_{n\bar{m}} \rho \eth' \text{Þ}' \text{Þ}' h_{m\bar{m}} + ..., \tag{4.37}$$

to be used as an example. In the following paragraphs, I apply each step of the algorithm to the term in Eq. (4.37), to finally express it in a mode decomposed form:

$$\mathcal{S}_4[\delta^2 G_{ab}[h^{(1)}_{ab}, h^{(1)}_{ab}]] = \sum_{l=2,m}^{\infty} R_{\ell,\mathtt{m}}[r,t] {}_{-2}Y_{\ell,\mathtt{m}}[\theta,\phi], \tag{4.38}$$

in BL coordinates. Additionally, I will express the time dependence as $R_{\ell,\mathtt{m}}[r,t] = R_{\ell,\mathtt{m}}[r] e^{-i\omega t}$. The resulting expression can be converted to the two-timescale framework by converting $e^{-i\omega t} \to e^{-i(k\varphi_r + m\varphi_\phi)}$ followed by $\omega \to k\Omega_r + m\Omega_\phi$ ($\varphi_r = \Omega_r = 0$ for quasi-circular orbits). The resulting expression consists of a separation of variables which is consistent with the separable master Teukolsky equation (Eq. 1.82) in Schwarzschild. By using a spin-weighted spherical harmonic mode decomposition in Eq. (4.38) the angular Teukolsky equation will be solved.

To begin the conversion from GHP to coordinate form, I need to choose a tetrad basis. I choose the Carter tetrad basis to maintain as much symmetry as possible in the tetrad. In BL coordinates, in Schwarzschild, the spin-coefficients in the Carter tetrad take the form [154]

$$\begin{aligned} \rho = -\rho' &= -\frac{1}{r}\sqrt{\frac{f}{2}}, \quad \tau = \tau' = 0 \\ \beta = \beta' &= \frac{\cot(\theta)}{2\sqrt{2}r}, \quad \epsilon = -\epsilon' = \frac{M}{2r^2\sqrt{2f}} \end{aligned} \tag{4.39}$$

where $f = 1 - \frac{2M}{r}$. I will also use $\Psi_2 = -\frac{M}{r^3}$ in Schwarzschild (which is invariant between principle null direction aligned tetrads).

Starting with $\mathcal{S}_4[\delta^2 G_{ab}]$ in GHP notation provides the benefit that in Schwarzschild the GHP derivative $\eth$ and $\eth'$ behave (for any principle-null direction aligned tetrad) as

re-scaled spin-raising/lowering operators [154],

$$\begin{aligned}\eth &= \frac{1}{\sqrt{2}r}\left(\partial_\theta + i\csc(\theta)\partial_\phi - s\cot(\theta)\right) = \frac{1}{\sqrt{2}r}\hat{\eth},\\ \eth' &= \frac{1}{\sqrt{2}r}\left(\partial_\theta - i\csc(\theta)\partial_\phi - s\cot(\theta)\right) = \frac{1}{\sqrt{2}r}\hat{\eth}'.\end{aligned} \tag{4.40}$$

Here $\hat{\eth}'$ and $\hat{\eth}'$ are the spin-raising/lowering operators of the spin-weighted spherical harmonics (${}_sY_{\ell,\mathtt{m}}[\theta,\phi]$) [83] and s is the spin-weight of the object $\hat{\eth}$ or $\hat{\eth}'$ is acting on. Equivalently,

$$\hat{\eth} = (\sin(\theta))^{-s}(\partial_\theta + i\csc(\theta)\partial_\phi)(\sin(\theta))^s. \tag{4.41}$$

From Eq. (4.41) one sees that whilst $\hat{\eth}$ contains purely angular derivatives, for an η which is angular independent, $\hat{\eth}\eta = 0$ only if η has $s = 0$. Nevertheless, an object with no angular dependence is naturally expressed as an $\ell = 0$, $s = 0$ spin-weighted spherical harmonic (rather that any other s-weighted spherical harmonic). Note, all my definitions for $\eth$ differ by a factor of -1 from the conventional definitions in Ref. [83].

As $\hat{\eth}$ and $\hat{\eth}'$ are spin raising and lowering operators respectively, when they act on spin-weighted spherical harmonics they raise and lower the spin as follows [83],

$$\hat{\eth}\,{}_sY_{\ell,\mathtt{m}} = -\sqrt{(l-s)(l+s+1)}\,{}_{s+1}Y_{\ell,\mathtt{m}}, \tag{4.42}$$

$$\hat{\eth}'\,{}_sY_{\ell,\mathtt{m}} = \sqrt{(l+s)(l-s+1)}\,{}_{s-1}Y_{\ell,\mathtt{m}}, \tag{4.43}$$

$$\hat{\eth}'\hat{\eth}\,{}_sY_{\ell,\mathtt{m}} = -(l-s)(l+s+1)\,{}_sY_{\ell,\mathtt{m}}. \tag{4.44}$$

Spin-weighted spherical harmonics also have a useful relation with their complex conjugate,

$${}_s\overline{Y}_{\ell,\mathtt{m}} = (-1)^{s+m}\,{}_{-s}Y_{l,-m}. \tag{4.45}$$

Þ and Þ′ contain no angular derivatives in Schwarzschild. Hence, by expressing any angular dependent quantities in $\mathcal{S}_4[\delta^2 G_{ab}]$ (including the tetrad components of $h^{(1)}_{ab}$) in terms of spin-weighted spherical harmonics, one can avoid explicitly evaluating any θ and ϕ derivatives, instead using the relations in Eqs. (4.42), (4.43) and (4.44) between spin-weighted spherical harmonics.

While Þ and Þ′ are boost raising and lowering operators, there is no known orthogonal basis for boost-weighted functions. Hence, the t and r derivatives appear explicitly in my final coordinate expression. To express these derivatives it is simplest to initially convert the GHP derivatives, Þ and Þ′, to the NP derivatives, D and Δ

(using Eq. (1.76)). This intermediary step effectively implements a half-GHP-half-NP formalism, with the derivatives D, Δ, $\eth$, and $\eth'$ present.

One must take care when implementing half-GHP-half-NP because the NP formalism part introduces quantities (ϵ, ϵ', D, and δ) which do not have a well-defined spin- and boost-weights. This can be problematic as the GHP derivatives, Eq. (1.76) (and the spin raising/lowering operators $\hat{\eth}$ and $\hat{\eth}'$) must act on quantities with well-defined spin/boost weights (to be well defined). This problem can be avoided as it is possible to convert to half-GHP-half-NP whilst maintaining that the GHP operators only act on well-defined spin- and boost-weight quantities. This is achieved in two steps. Firstly, one applies the GHP commutation relations [77] such that no $\eth$ or $\eth'$ acts on a Þ and Þ$'$. For example, applying the appropriate commutation rule [77] twice on Eq. (4.37) results in

$$\frac{3}{2}h_{n\bar{m}}\rho\eth'Þ'Þ'h_{m\bar{m}} = \frac{3}{2}h_{n\bar{m}}\rho\left(Þ'Þ' + \rho^2 - 2\rho'Þ' - (Þ'\rho')\right)\eth' h_{m\bar{m}}. \tag{4.46}$$

I can now convert each Þ and Þ$'$ into NP form (without $\eth$ acting on quantities with an ill-defined spin/boost-weight) using Eq. (1.76). The second critical step is to convert the outermost derivative first to prevent any Þ or Þ$'$ acting on a quantity that does not have well-defined spin/boost weights. For example,

$$\begin{aligned} h_{n\bar{m}}Þ'Þ'\eth' h_{m\bar{m}} =& h_{n\bar{m}}\rho(\Delta Þ' - 2\epsilon'Þ')\eth' h_{m\bar{m}} && (4.47)\\ =& h_{n\bar{m}}\rho(\Delta\Delta - 2\epsilon'\Delta)\eth' h_{m\bar{m}}, && (4.48)\end{aligned}$$

where I have used $\bar{\epsilon}' = \epsilon'$.

Before converting D and Δ to coordinate form, I implement a mode decomposition for the inputs ($h^{(1)}_{ab}, h^{(1)}_{ab}$). Note, it is valid to input two different first-order metric perturbations, such as one puncture and one regular field, so there must be a distinction between the two inputs. I chose the distinction to be present in the choice of ℓ and $\mathtt{m}$ labels. As each term in $\mathcal{S}[\delta^2 G[h^{(1)}_{ab}, h^{(1)}_{ab}]]$ is quadratic in $h^{(1)}_{ab}$ (and its derivatives) I replace one $h_{[a][b]}$ with $h^{\ell_1,\mathtt{m}_1}_{[a][b]s_1}Y_{\ell_1,\mathtt{m}_1}$ and the other $h_{[a][b]}$ with $h^{\ell_2,\mathtt{m}_2}_{[a][b]s_2}Y_{\ell_2,\mathtt{m}_2}$. That is,

$$h_{n\bar{m}}\Delta\Delta\eth' h_{m\bar{m}} = \sum_{\ell_1=1,\mathtt{m}_1}^{\infty}\sum_{\ell_2=1,\mathtt{m}_2}^{\infty} h^{-\ell_1,\mathtt{m}_1}_{n\bar{m}}{}_{-1}Y_{\ell_1,\mathtt{m}_1}\Delta\Delta\eth' h^{\ell_2,\mathtt{m}_2}_{m\bar{m}}{}_0Y_{\ell_2,\mathtt{m}_2}. \tag{4.49}$$

Each $h^{s,\ell,\mathtt{m}}_{[a][b]}$ is a function of r and t. As Eq. (4.49) contains GHP derivatives, the spin and boost weights of the quantities $h^{\ell,\mathtt{m}}_{[a][b]}$ and ${}_sY_{\ell,\mathtt{m}}$ must be defined. As $h_{[a][b]}$ (of spin-weight x and boost weight y) is decomposed into ${}_xY_{\ell,\mathtt{m}}$ and $h^{\ell,\mathtt{m}}_{[a][b]}$, ${}_xY_{\ell,\mathtt{m}}$ has spin-weight x and boost weight 0 and $h^{\ell,\mathtt{m}}_{[a][b]}$ has boost weight y and spin-weight 0. The spin and boost weights of $h_{[a][b]}$ are calculated from the tetrad vectors corresponding to $[a][b]$ (e.g., $h_{[1][3]}$ has $b = 1, s = 1$, see Sec. 1.7.2).

As ð contains purely angular derivatives, and $h^{s,\ell,\mathtt{m}}_{[a][b]}$ only depends on r and t (and has $s = 0$)

$$\text{ð} h^{\ell,\mathtt{m}}_{[a][b]} = 0. \tag{4.50}$$

Hence, each ð only acts on spin-weighted spherical harmonics. Using Eqs. (4.40), (4.42), (4.43), and (4.44) one can replace each ð acting on spin-weighted spherical harmonics with a factor of $\frac{1}{\sqrt{2}r}$ (multiplied a coefficient dependent of l) and a different spin-weighted spherical harmonic[1]. E.g.,

$$h^{-\ell_1,\mathtt{m}_1}_{n\bar{m}}\,{}_{-1}Y_{\ell_1,\mathtt{m}_1}\Delta\Delta\text{ð}'h^{\ell_2,\mathtt{m}_2}_{m\bar{m}}\,{}_0Y_{\ell_2,\mathtt{m}_2} = h^{-\ell_1,\mathtt{m}_1}_{n\bar{m}}\,{}_{-1}Y_{\ell_1,\mathtt{m}_1}\Delta\Delta h^{\ell_2,\mathtt{m}_2}_{m\bar{m}}\frac{\sqrt{\ell_2(\ell_2+1)}}{\sqrt{2}r}\,{}_{-1}Y_{\ell_2,\mathtt{m}_2}, \tag{4.51}$$

The next step is to express the NP derivatives in terms of coordinates. D and Δ convert to coordinate form in the Carter basis (in BL coordinates) straightforwardly,

$$D = \frac{1}{\sqrt{2f}}\partial_t + \sqrt{\frac{f}{2}}\partial_r, \quad \Delta = \frac{1}{\sqrt{2f}}\partial_t - \sqrt{\frac{f}{2}}\partial_r. \tag{4.52}$$

As $h^{(1)}_{ab}$ is assumed to be decomposed into Fourier time-frequency modes, the time dependence of each mode is expressed as

$$h^{s,\ell,\mathtt{m}}_{ab} \propto e^{-i\omega t}; \tag{4.53}$$

this makes the time derivatives trivial. Converting D and Δ to coordinate form results in

$$\begin{aligned} h^{-\ell_1,\mathtt{m}_1}_{n\bar{m}}\,{}_{-1}Y_{\ell_1,\mathtt{m}_1}\Delta\Delta h^{\ell_2,\mathtt{m}_2}_{m\bar{m}}\frac{\sqrt{\ell_2(\ell_2+1)}}{\sqrt{2}r}\,{}_{-1}Y_{\ell_2,\mathtt{m}_2} = \\ -\frac{h^{-\ell_1,\mathtt{m}_1}_{n\bar{m}}\,{}_{-1}Y_{\ell_1,\mathtt{m}_1}\sqrt{\ell_2(\ell_2+1)}}{2\sqrt{2}fr^3}\Big(\omega_2(iM+r^2\omega_2)h_{34}{}^{-2\ell_2,\mathtt{m}_2} \\ -f\big((M+2ir^2\omega_2)h_{34}{}^{-2\ell_2,\mathtt{m}_2}{}_{,r} + fr^2 h_{34}{}^{-2\ell_2,\mathtt{m}_2}{}_{,r,r}\big)\Big)\,{}_{-1}Y_{\ell_2,\mathtt{m}_2}. \end{aligned} \tag{4.54}$$

where the $,r$ subscripts denote a partial derivative with respect to r. The resulting expression for the source are functions of ${}_{s_1}Y_{\ell_1,\mathtt{m}_1}\,{}_{s_2}Y_{\ell_2,\mathtt{m}_2}$. However, to separate the Teukolsky equation, the angular dependence of the source must be expressed as single modes of ${}_{-2}Y_{\ell,\mathtt{m}}$. To achieve this, I re-express two spin-weight spherical harmonics as a

[1]Note, the factor of $\frac{1}{\sqrt{2}r}$ which comes with the conversion of ð to $\hat{\text{ð}}$ has zero spin- and boost-weight.

single spin-(-2)-weight spherical harmonics[2] using

$$ {}_{s_1}Y_{\ell_1,\mathtt{m}_1}\,{}_{s_2}Y_{\ell_2,\mathtt{m}_2} = \sum_{\ell_1=s_1,\mathtt{m}_1}^{\infty}\sum_{\ell_2=s_2,\mathtt{m}_2}^{\infty} C^{\ell,\mathtt{m},-2}_{\ell_1,\mathtt{m}_1,s_1,\ell_2,\mathtt{m}_2,s_2}\,{}_{-2}Y_{\ell,\mathtt{m}}. \tag{4.55} $$

where $C^{\ell,\mathtt{m},s}_{\ell_1,\mathtt{m}_1,s_1,\ell_2,\mathtt{m}_2,s_2}$ is the integral

$$ C^{\ell,\mathtt{m},s}_{\ell_1,\mathtt{m}_1,s_1,\ell_2,\mathtt{m}_2,s_2} = \oint {}_{s}\bar{Y}_{\ell,\mathtt{m}s_1}Y_{\ell_1,\mathtt{m}_1 s_2}Y_{\ell_2,\mathtt{m}_2}. \tag{4.56} $$

These integrals can be evaluated algebraically using 3j symbols [89, 172] (as spin weighted spherical harmonics are related to Wigner-D matrices) through

$$ C^{\ell\mathtt{m}s}_{\ell'\mathtt{m}'s'\ell''\mathtt{m}''s''} = (-1)^{\mathtt{m}+s}\sqrt{\frac{(2\ell+1)(2\ell'+1)(2\ell''+1)}{4\pi}}\begin{pmatrix}\ell & \ell' & \ell''\\ s & -s' & -s''\end{pmatrix}\begin{pmatrix}\ell & \ell' & \ell''\\ -\mathtt{m} & \mathtt{m}' & \mathtt{m}''\end{pmatrix}. \tag{4.57} $$

Hence, $C^{\ell,\mathtt{m},s}_{\ell_1,\mathtt{m}_1,s_1,\ell_2,\mathtt{m}_2,s_2}$ admits the following symmetry,

$$ C^{\ell,\mathtt{m},s}_{\ell_1,\mathtt{m}_1,s_1,\ell_2,\mathtt{m}_2,s_2} = C^{\ell,\mathtt{m},s}_{\ell_2,\mathtt{m}_2,s_2,\ell_1,\mathtt{m}_1,s_1}, \tag{4.58} $$

which can be used to simplify the $\mathcal{S}_4[\delta^2 G_{ab}]$ expression. To achieve maximal cancellations, I chose to apply Eq. (4.58) to each term in $\mathcal{S}_4[\delta^2 G_{ab}]$ such that $s_1 > s_2$, followed by a relabeling of everything in that term with $\ell_1 \to \ell_2, \ell_2 \to \ell_1, \mathtt{m}_1 \to \mathtt{m}_2, \mathtt{m}_2 \to \mathtt{m}_1$. For example,

$$ \frac{\sqrt{\ell_1(\ell_1+1)}}{\sqrt{(\ell_2-1)(\ell_2+2)}}C^{\ell,\mathtt{m},-2}_{\ell_1,\mathtt{m}_1,-2,\ell_2,\mathtt{m}_2,t} \to \frac{\sqrt{\ell_2(\ell_2+1)}}{\sqrt{(\ell_1-1)(\ell_1+2)}}C^{\ell,\mathtt{m},-2}_{\ell_1,\mathtt{m}_1,t,\ell_2,\mathtt{m}_2,-2}. \tag{4.59} $$

As I have labelled the two inputs distinctly, I must also compute the symmetrisation of the entire expression; that is,

$$ \mathcal{S}[\delta^2 G[h^{s_1,\ell_1,\mathtt{m}_1}_{ab}, h^{s_2,\ell_2,\mathtt{m}_2}_{ab}]] = \frac{1}{2}(\mathcal{S}[\delta^2 G[h^{s_1,\ell_1,\mathtt{m}_1}_{ab}, h^{s_2,\ell_2,\mathtt{m}_2}_{ab}]] + \mathcal{S}[\delta^2 G[h^{s_2,\ell_2,\mathtt{m}_2}_{ab}, h^{s_1,\ell_1,\mathtt{m}_1}_{ab}]]). \tag{4.60} $$

The result is a maximally simplified mode decomposition of the source $\mathcal{S}_4[\delta^2 G_{ab}]$ in BL coordinates (for the Carter tetrad). This decomposition technique produces formulas that are consistent for any type of perturbation in Schwarzschild. I will be releasing the decomposition formulas for $\delta^2 G_{ab}[h^{(1)}_{ab}, h^{(1)}_{ab}]$ on the Black Hole Perturbation Theory toolkit [1] shortly and include them in the supporting materials of this thesis.

[2]The two spin-weight spherical harmonics can always be expressed as a spin-(-2)-weight spherical harmonics because $s_1 + s_2 = -2$ as the source is spin-(-2)-weight (this can be used as a consistency check).

4.2.2 Calculating radial derivatives of the metric perturbation analytically in the Lorenz gauge

The expression for $\mathcal{S}_4[\delta^2 G_{ab}]$ requires up to four radial derivatives of h_{ab}. One could calculate the radial derivative numerically; however, numerical derivatives introduce a numerical error and are inefficient. Therefore, it is preferable to calculate the radial derivatives analytically. One can leverage the metric perturbation being a solution to the linearised EFE (Eq. (1.18)) to calculate the second- and higher-order radial derivatives in terms of the first-order derivatives.

To relate the second-order r derivatives to first-order r derivatives requires a coordinate form mode decomposition of the linearised EFE. This can be achieved using the algorithm in Sec. 4.2.1 starting with the linearised EFE in GHP form (which is also given in the supplementary materials [175]).

There are ten components of the second-order radial derivatives of the metric perturbation, and the linearised EFE contains only six linearly independent equations. To achieve linearly independent equations for each $h_{[a][b],r,r}$ component, one must apply additional restrictions. These restrictions account for the gauge freedom in the linearised EFE. The h_{ab} inputs I use are in the Lorenz gauge (i.e., $\bar{h}_{ab;c}{}^{c} = 0$). Applying this condition to the linearised EFE results in ten linearly independent equations for the second-order radial derivative of the first-order metric perturbation. Solving these

equations for $h_{[a][b],r,r}$ gives

$$\begin{aligned}
h^{\ell,\mathrm{m}}_{ll,r,r} &= \frac{1}{f^2r^4}\Big(h_{ll}{}^{\ell_1,\mathrm{m}_1}\big(2f^2r^2+(2M+ir^2\omega_1)^2+fr(4M+r(\mu^{\ell_1}{}_1)^2)\big)\\
&\quad -2fr^2\big(f^{1/2}(-h_{lm}{}^{\ell_1,\mathrm{m}_1}+h_{l\bar{m}}{}^{\ell_1,\mathrm{m}_1})\mu^{\ell_1}{}_1+r^2T_{ll}{}^{\ell_1,\mathrm{m}_1}+Mh_{ll}{}^{\ell_1,\mathrm{m}_1}{}_{,1}+f\big(h_{ln}{}^{\ell_1,\mathrm{m}_1}\\
&\quad +h_{m\bar{m}}{}^{\ell_1,\mathrm{m}_1}+rh_{ll}{}^{\ell_1,\mathrm{m}_1}{}_{,1}\big)\big)\Big), \qquad (4.61)\\
h^{\ell,\mathrm{m}}_{ln,r,r} &= -\frac{1}{f^2r^3}\Big(r^3\omega_1^2h_{ln}{}^{\ell_1,\mathrm{m}_1}+f^{3/2}r(h_{lm}{}^{\ell_1,\mathrm{m}_1}-h_{l\bar{m}}{}^{\ell_1,\mathrm{m}_1}-h_{nm}{}^{\ell_1,\mathrm{m}_1}+h_{n\bar{m}}{}^{\ell_1,\mathrm{m}_1})\mu^{\ell_1}{}_1\\
&\quad +f^2r(h_{ll}{}^{\ell_1,\mathrm{m}_1}-2h_{ln}{}^{\ell_1,\mathrm{m}_1}+h_{nn}{}^{\ell_1,\mathrm{m}_1}-2h_{m\bar{m}}{}^{\ell_1,\mathrm{m}_1}+2rh_{ln}{}^{\ell_1,\mathrm{m}_1}{}_{,1})+f\big(h_{ln}{}^{\ell_1,\mathrm{m}_1}(4M\\
&\quad -r(\mu^{\ell_1}{}_1)^2)+2(2Mh_{m\bar{m}}{}^{\ell_1,\mathrm{m}_1}+r^3T_{m\bar{m}}{}^{\ell_1,\mathrm{m}_1}+Mrh_{ln}{}^{\ell_1,\mathrm{m}_1}{}_{,1})\big)\Big), \qquad (4.62)\\
h^{\ell,\mathrm{m}}_{lm,r,r} &= \frac{1}{f^2r^4}\Big(h_{lm}{}^{\ell_1,\mathrm{m}_1}\big(2f^2r^2+(M+ir^2\omega_1)^2+fr(-4M+r(\mu^{\ell_1}{}_1)^2)\big)\\
&\quad -fr^2\big(f^{1/2}(-h_{ll}{}^{\ell_1,\mathrm{m}_1}\mu^{\ell_1}{}_1+h_{ln}{}^{\ell_1,\mathrm{m}_1}\mu^{\ell_1}{}_1+h_{m\bar{m}}{}^{\ell_1,\mathrm{m}_1}\mu^{\ell_1}{}_1-h_{mm}{}^{\ell_1,\mathrm{m}_1}\mu^{\ell_1}{}_2)\\
&\quad +2(r^2T_{lm}{}^{\ell_1,\mathrm{m}_1}+Mh_{lm}{}^{\ell_1,\mathrm{m}_1}{}_{,1})+2f(h_{nm}{}^{\ell_1,\mathrm{m}_1}+rh_{lm}{}^{\ell_1,\mathrm{m}_1}{}_{,1})\big)\Big), \qquad (4.63)\\
h^{\ell,\mathrm{m}}_{nn,r,r} &= \frac{1}{f^2r^4}\Big(h_{nn}{}^{\ell_1,\mathrm{m}_1}\big(2f^2r^2+(2M-ir^2\omega_1)^2+fr(4M+r(\mu^{\ell_1}{}_1)^2)\big)\\
&\quad -2fr^2\big(f^{1/2}(h_{nm}{}^{\ell_1,\mathrm{m}_1}-h_{n\bar{m}}{}^{\ell_1,\mathrm{m}_1})\mu^{\ell_1}{}_1+r^2T_{nn}{}^{\ell_1,\mathrm{m}_1}+Mh_{nn}{}^{\ell_1,\mathrm{m}_1}{}_{,1}+f\big(h_{ln}{}^{\ell_1,\mathrm{m}_1}\\
&\quad +h_{m\bar{m}}{}^{\ell_1,\mathrm{m}_1}+rh_{nn}{}^{\ell_1,\mathrm{m}_1}{}_{,1}\big)\big)\Big), \qquad (4.64)\\
h^{\ell,\mathrm{m}}_{nm,r,r} &= \frac{1}{f^2r^4}\Big(h_{nm}{}^{\ell_1,\mathrm{m}_1}\big(2f^2r^2+(M-ir^2\omega_1)^2+fr(-4M+r(\mu^{\ell_1}{}_1)^2)\big)\\
&\quad -fr^2\big(f^{1/2}(-h_{ln}{}^{\ell_1,\mathrm{m}_1}\mu^{\ell_1}{}_1+h_{nn}{}^{\ell_1,\mathrm{m}_1}\mu^{\ell_1}{}_1-h_{m\bar{m}}{}^{\ell_1,\mathrm{m}_1}\mu^{\ell_1}{}_1+h_{mm}{}^{\ell_1,\mathrm{m}_1}\mu^{\ell_1}{}_2)\\
&\quad +2(r^2T_{nm}{}^{\ell_1,\mathrm{m}_1}+Mh_{nm}{}^{\ell_1,\mathrm{m}_1}{}_{,1})+2f(h_{lm}{}^{\ell_1,\mathrm{m}_1}+rh_{nm}{}^{\ell_1,\mathrm{m}_1}{}_{,1})\big)\Big), \qquad (4.65)\\
h^{\ell,\mathrm{m}}_{mm,r,r} &= -\frac{1}{f^2r^2}\Big(r^2\omega_1^2h_{mm}{}^{\ell_1,\mathrm{m}_1}-2f^{3/2}(h_{lm}{}^{\ell_1,\mathrm{m}_1}-h_{nm}{}^{\ell_1,\mathrm{m}_1})\mu^{\ell_1}{}_2+2f^2rh_{mm}{}^{\ell_1,\mathrm{m}_1}{}_{,1}\\
&\quad -f\big(h_{mm}{}^{\ell_1,\mathrm{m}_1}(\mu^{\ell_1}{}_2)^2-2(r^2T_{mm}{}^{\ell_1,\mathrm{m}_1}+Mh_{mm}{}^{\ell_1,\mathrm{m}_1}{}_{,1})\big)\Big), \qquad (4.66)\\
h^{\ell,\mathrm{m}}_{m,\bar{m},r,r} &= -\frac{1}{f^2r^3}\Big(r^3\omega_1^2h_{m\bar{m}}{}^{\ell_1,\mathrm{m}_1}+f^{3/2}r(h_{lm}{}^{\ell_1,\mathrm{m}_1}-h_{l\bar{m}}{}^{\ell_1,\mathrm{m}_1}-h_{nm}{}^{\ell_1,\mathrm{m}_1}+h_{n\bar{m}}{}^{\ell_1,\mathrm{m}_1})\mu^{\ell_1}{}_1\\
&\quad +f^2r(h_{ll}{}^{\ell_1,\mathrm{m}_1}-2h_{ln}{}^{\ell_1,\mathrm{m}_1}+h_{nn}{}^{\ell_1,\mathrm{m}_1}-2h_{m\bar{m}}{}^{\ell_1,\mathrm{m}_1}+2rh_{m\bar{m}}{}^{\ell_1,\mathrm{m}_1}{}_{,1})+f\big(4Mh_{ln}{}^{\ell_1,\mathrm{m}_1}\\
&\quad +h_{m\bar{m}}{}^{\ell_1,\mathrm{m}_1}(4M-r(\mu^{\ell_1}{}_1)^2)+2r(r^2T_{ln}{}^{\ell_1,\mathrm{m}_1}+Mh_{m\bar{m}}{}^{\ell_1,\mathrm{m}_1}{}_{,1})\big)\Big), \qquad (4.67)
\end{aligned}$$

where $\mu^{\ell}{}_n = \sqrt{(l-n)(l+n+1)}$. By taking a further r derivative and using these relations iteratively, one can calculate an arbitrarily high number of radial derivatives on h_{ab} in terms of only $h_{[a][b]}$ and $h_{[a][b],r}$.

4.2.3 Converting from the Barack–Lousto–Sago basis to the Carter basis

An additional layer of complexity to this calculation is the h_{ab} I use as input is in the Barack–Lousto–Sago basis [24, 25]. This is due to h_{ab} being calculated by directly

solving the linearised EFE in the Lorenz gauge. To simplify this calculation [24, 25], a Barack–Lousto–Sago basis of modes was chosen, $h^{i,\ell,\mathtt{m}}_{ab}$ (where the i label denotes the Barack–Lousto–Sago mode and runs from one to ten). However, such a basis is not designed for calculations using the Teukolsky formalism. As a preliminary step, I convert the input data, $h^{i,\ell,\mathtt{m}}_{ab}$, into the Carter tetrad modes using [154][3]

$$h^{\ell,\mathtt{m}}_{ll} = \frac{1}{2rf}\left(h^{1\ell,\mathtt{m}} + h^{2\ell,\mathtt{m}}\right) \tag{4.68}$$

$$h^{\ell,\mathtt{m}}_{ln} = \frac{1}{2r}\left(h^{3\ell,\mathtt{m}}\right) \tag{4.69}$$

$$h^{\ell,\mathtt{m}}_{lm} = \frac{-1}{4r\sqrt{f}\mu^{\ell}{}_{1}}\left(h^{4\ell,\mathtt{m}} + h^{5\ell,\mathtt{m}} - i(h^{8\ell,\mathtt{m}} + h^{9\ell,\mathtt{m}})\right) \tag{4.70}$$

$$h^{\ell,\mathtt{m}}_{l\bar{m}} = \frac{1}{4r\sqrt{f}\mu^{\ell}{}_{1}}\left(h^{4\ell,\mathtt{m}} + h^{5\ell,\mathtt{m}} + i(h^{8\ell,\mathtt{m}} + h^{9\ell,\mathtt{m}})\right) \tag{4.71}$$

$$h^{\ell,\mathtt{m}}_{nn} = \frac{1}{2rf}\left(h^{1\ell,\mathtt{m}} - h^{2\ell,\mathtt{m}}\right)\frac{1}{2rf}\left(h^{1\ell,\mathtt{m}} - h^{2\ell,\mathtt{m}}\right) \tag{4.72}$$

$$h^{\ell,\mathtt{m}}_{nm} = \frac{-1}{4r\sqrt{f}\mu^{\ell}{}_{1}}\left(h^{4\ell,\mathtt{m}} - h^{5\ell,\mathtt{m}} - i(h^{8\ell,\mathtt{m}} - h^{9\ell,\mathtt{m}})\right) \tag{4.73}$$

$$h^{\ell,\mathtt{m}}_{n\bar{m}} = \frac{1}{4r\sqrt{f}\mu^{\ell}{}_{1}}\left(h^{4\ell,\mathtt{m}} - h^{5\ell,\mathtt{m}} + i(h^{8\ell,\mathtt{m}} - h^{9\ell,\mathtt{m}})\right) \tag{4.74}$$

$$h^{\ell,\mathtt{m}}_{mm} = \frac{1}{r\mu^{\ell}{}_{2}}\left(h^{7\ell,\mathtt{m}} - ih^{10\ell,\mathtt{m}}\right) \tag{4.75}$$

$$h^{\ell,\mathtt{m}}_{m\bar{m}} = \frac{1}{2r}\left(h^{6\ell,\mathtt{m}}\right) \tag{4.76}$$

$$h^{\ell,\mathtt{m}}_{\bar{m}\bar{m}} = \frac{1}{r\mu^{\ell}{}_{2}}\left(h^{7\ell,\mathtt{m}} - ih^{10\ell,\mathtt{m}}\right). \tag{4.77}$$

$$\tag{4.78}$$

4.2.4 Results: the source for quasi-circular orbits in the Lorenz gauge

To improve efficiency, I convert the formulas for calculating the mode decomposed $\mathcal{S}_4\delta^2 G[h_{ab}, h_{ab}]$ in coordinate form into a C++ code. Efficiency is important for this calculation because to evolve inspirals requires data on $\psi^{(2)}_{4L}$ for a set of r_0 (from the initial geodesic to $r_0 = 2M$ at merger). Also, the input data is large, containing up to $\ell = 50$ modes for ten components of h_{ab} (i.e., there are up to $\mathcal{O}(10^4)$ input modes), and handling this much data in mathematica can cause it to crash. The C++ code allows me to quickly calculate $\mathcal{S}_4\delta^2 G[h_{ab}, h_{ab}]$ for a given r_0.

To calculate the source, I inputted retarded Lorentz gauge h_{ab} data provided by Niels Warburton. To display the behaviour of the source, I present the dominant $\ell = 2, \mathtt{m} = 2$ mode of $\mathcal{S}_4[h_{ab}, h_{ab}]$, with $r_0 = 9M$, in Fig. 4.2. This mode was calculated with input modes up to $\ell_{max} = 10$ input modes.

[3] Here, I reproduce Eq. (118) in Ref. [154], which I independently checked before Ref. [154] was published.

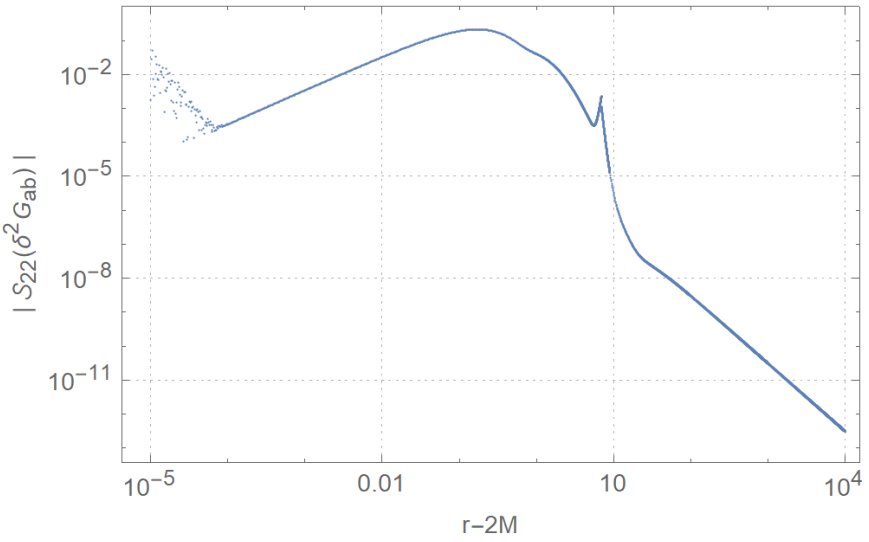

FIGURE 4.2: The $\ell = 2, \mathtt{m} = 2$ mode of $\mathcal{S}_4[\delta^2 G[h_{ab}, h_{ab}]]$ (part of the source to the reduced second-order Teukolsky equation) for $r_0 = 9M$ in the Carter tetrad and BL coordinates. This source has been calculated using up to $\ell_{max} = 10$ input modes of the retarded Lorenz gauge first-order metric perturbation data (provided by Niels Warburton).

In Sec. 3.6.10, I predicted that the behaviour of the reduced second-order Teukolsky source would be $\sim r^{-2}$ near $\mathcal{I}^+$in a generic gauge. As can be seen on the right-hand side of Fig. 4.2, $\mathcal{S}_4[\delta^2 G[h_{ab}, h_{ab}]] \sim r^{-2}$ in agreement with my prediction. All the other Lorenz gauge reduced second-order Teukolsky source modes also behave as $\mathcal{O}(r^{-2})$.

Near the horizon, the source modes behave as $\sim f^1$ (this can be seen on the left-hand side of Fig. 4.2). There is some divergent behaviour for $r - 2M < 10^{-4}M$; this is due to a numerical error not cancelling equivalent terms, a problem that was encountered and well understood in the Lorenz gauge second-order calculation in Refs. [195, 194, 156]. The Carter tetrad being singular at the horizon may be exacerbating this problem. Using a horizon regular tetrad, such as the Hartle–Hawking null tetrad [179], near the horizon may help ameliorate the problem. Close to the horizon we use a near-horizon expansion of $\delta^2 G[h^{(1)}_{ab}, h^{(1)}_{ab}]$ (inherited from the Lorenz-gauge second-order calculations in Refs. [195, 194, 156]), which analytically cancels the spurious divergence near the horizon.

Fig. 4.3 shows how the source converges for an increased number of ℓ_{max} input modes. Note that the convergence is good everywhere except near the worldline ($r = 10M$), where there is no convergence. Fig. 4.4 shows the convergence near the worldline for increasing ℓ_{max} (the number of input modes). One can see that the source diverges on the worldline, and it appears there is no convergence very close to the worldline. The convergence off the worldline is actually exponential. However, for small ℓ_{max}, near the worldline, the behaviour is dominated by a power law divergence (as shown in Fig. 4.3). For sufficiently large ℓ_{max} the exponential convergence will dominate.

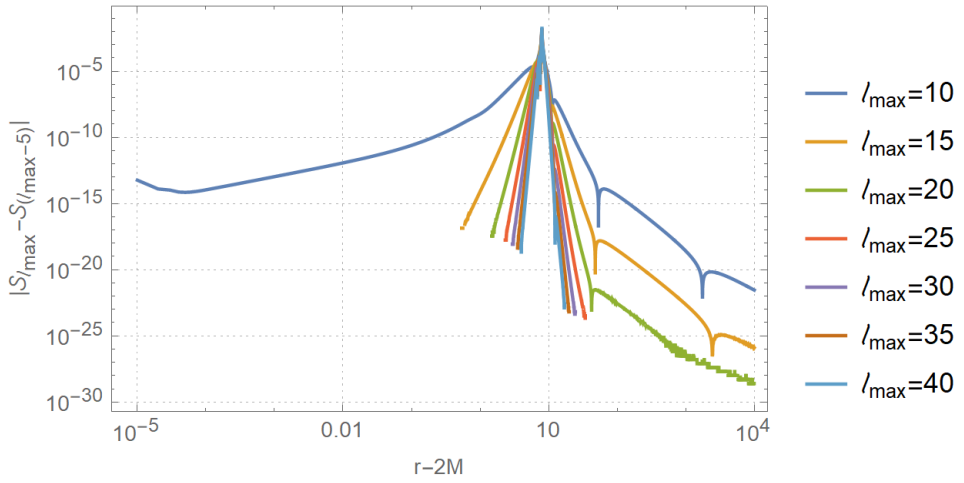

FIGURE 4.3: Convergence test of the $\ell = 2, \mathtt{m} = 2$ mode of $\mathcal{S}_4[\delta^2 G[h_{ab}, h_{ab}]]$ for $r_0 = 10$. The $h^{(1)}_{ab}$ input modes are retarder Lorenz gauge solutions. The multiple curves show how the source converges for higher ℓ_{max} (the maximum number of input modes). The source converges rapidly near the horizon (at $r = 2M$), quickly reaching machine precision except for $|S_{10} - S_5|$. Similarly, the source converges quickly near $\mathcal{I}^+$(right-hand side of the plot). However, near the point-mass (at $r = 10M$) the source converges slowly, and at $r = 10M$ the source diverges.

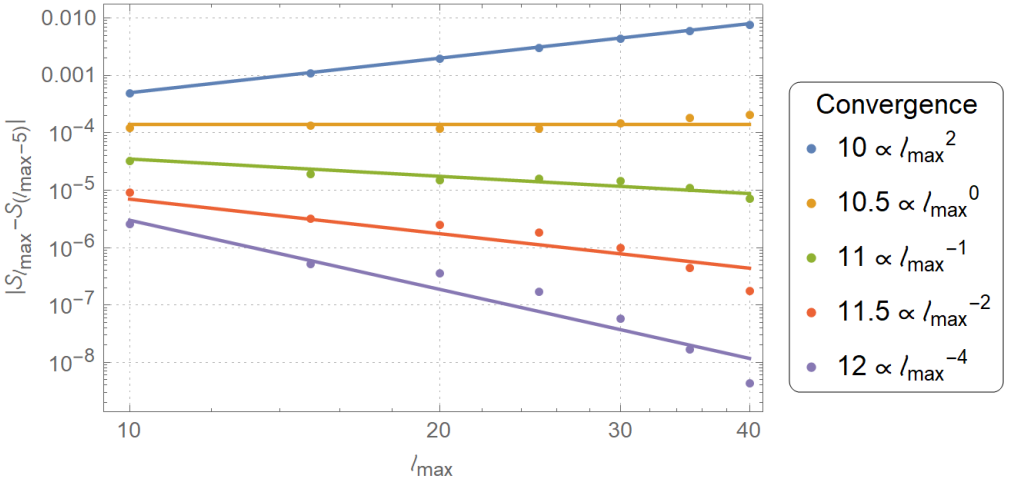

FIGURE 4.4: Convergence test of the $\ell = 2, \mathtt{m} = 2$ mode of $\mathcal{S}_4[\delta^2 G[h_{ab}, h_{ab}]]$ near the point-mass (at $r_0 = 10$). The $h^{(1)}_{ab}$ input modes are retarder Lorenz gauge solutions. The multiple plots show how the source converges for higher ℓ_{max} (the maximum number of input modes) near the point-mass. The lines of best fit have been applied by inspection. The source diverges on the particle and does not converge quickly until at least $2M$ from the particle (for small l_{max}).

The poor convergence is expected [120]; hence, near the worldline, we use an effective source imported from Refs. [156, 195, 194], which overcame the slow convergence using the strategy mentioned in Sec. 4.1.3. Away from the worldline at $r = 12M$, the source converges quickly for an increased number of input modes.

The source I have calculated is consistent with the source calculated by my collaborator Barry Wardell (see Fig. 4.5). He calculates the source using $\delta^2 R_{ab}$ data

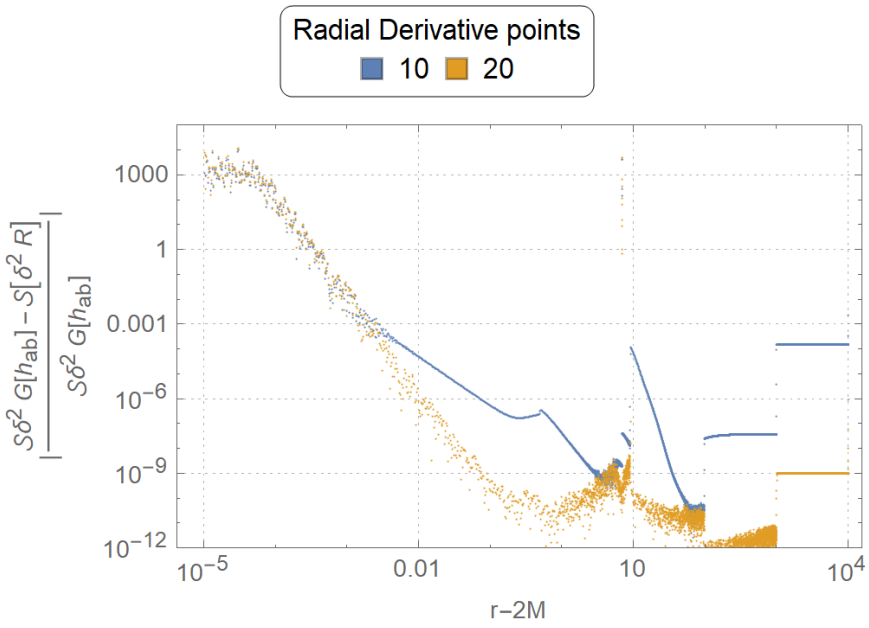

FIGURE 4.5: Fractional disagreement in the $\ell = 2, \mathtt{m} = 2$ mode of $\mathcal{S}_4[\delta^2 G[h_{ab}, h_{ab}]]$ (for $r_0 = 10$ in the Carter tetrad in BL coordinates). One calculation of the source (consistent with Fig. 4.2) has been calculated using up to $\ell = 50$ input modes of the retarded Lorenz gauge first-order metric perturbation (provided by Niels Warburton). The other source has been calculated from the $\delta^2 R_{ab}$ data used in Ref. [194] (with derivatives taken numerically). The blue curve uses a ten-point numerical derivative, whereas the orange plot uses a twenty-point numerical derivative; hence, the plot shows the calculations converge. The reason for disagreement near the horizon is that the radial grid is sparse; hence, the numerical derivatives are inaccurate. Similarly, there is disagreement on the particle (at $r = 7.4$) as there is a jump discontinuity there.

used in Refs. [156, 195, 194]. Wardell acts with $\mathcal{S}$ (Eq. 1.80) on $\delta^2 R_{ab}$ and calculates the radial derivatives numerically. As can be seen in Fig. 4.5, the agreement between our results improves as the number of points Wardell uses in his numerical derivative increases. The disagreement near the horizon is due to Wardell's source behaving poorly near the horizon as the radial grid becomes sparse there, making the numerical derivatives inaccurate.

4.2.5 Transformation to the Bondi–Sachs gauge

To increase the convergence of the source near $\mathcal{I}^+$, I implement a gauge transformation to the Bondi–Sachs gauge. To calculate the gauge transformation I use the procedure described in Sec. 3.6. However, to improve the behaviour of the source by two orders in r near $\mathcal{I}^+$(the maximum possible), it is not necessary to fully transform to the Bondi–Sachs gauge. Instead, it is sufficient to transform to a gauge where the leading (and next-to-leading for h_{ll}) order fall-off of the metric perturbation components is equivalent to the fall-off in the Bondi–Sachs gauge. This also means I do not fully fix the gauge and the resulting $\psi_{4L}^{(2)}$ is not gauge independent.

This can be seen by computing a series expansion of the source $\mathcal{S}_4[\delta^2 G_{ab}[h_{ab}, h_{ab}]]$ in orders of r for a generic asymptotically flat gauge metric perturbation ($h_{ab} = \mathcal{O}(r^{-1})$). The source behaves as

$$\begin{aligned}\mathcal{S}_4[\delta^2 G_{ab}[h_{ab}, h_{ab}]] \propto &(h_{ll}h_{\bar{m}\bar{m}} + h_{l\bar{m}}^2) \\ &+ \big((h_{ll} + h_{ln} + h_{m\bar{m}} + h_{lm} + h_{l\bar{m}})h_{\bar{m}\bar{m}} + (h_{ll} + h_{l\bar{m}})h_{n\bar{m}} + (h_{ln} + h_{m\bar{m}} \\ &+ h_{l\bar{m}})h_{l\bar{m}}\big) + \mathcal{O}(r^{-4}). \end{aligned} \tag{4.79}$$

As $h_{ab} = \mathcal{O}(r^{-1})$, the leading-order behaviour in a generic gauge is $\mathcal{S}_4[\delta^2 G_{ab}] = \mathcal{O}(r^{-2})$, consistent with Sec. 3.6.10. From Eq. (4.79), one can deduce that achieving $\mathcal{S}_4[\delta^2 G_{ab}] = \mathcal{O}(r^{-4})$ requires $h_{ll} = \mathcal{O}(r^{-3})$ and $h_{ln} = h_{lm} = h_{l\bar{m}} = h_{m\bar{m}} = \mathcal{O}(r^{-2})$ (assuming the other components are $\mathcal{O}(r^{-1})$). I.e., it is not necessary to transform the whole metric perturbation to the Bondi–Sachs gauge to achieve $\mathcal{S}_4[\delta^2 G_{ab}] = \mathcal{O}(r^{-4})$, only the leading order (and next to leading order for h_{ll}) in r pieces need to be transformed to Bondi–Sachs form. I call any gauge satisfying $h_{ll} = \mathcal{O}(r^{-3})$ and $h_{ln} = h_{lm} = h_{l\bar{m}} = h_{m\bar{m}} = \mathcal{O}(r^{-2})$ (and the remaining components are $\mathcal{O}(r^{-1})$) *near-Bondi–Sachs*.

The Lorenz gauge is not near-Bondi–Sachs. To see this, I will split the Lorenz gauge metric perturbation into $\mathtt{m} = 0$ and $\mathtt{m} \neq 0$ pieces, the stationary and non-stationary modes, respectively. This split is useful for quasi-circular orbits because the fast-time dependence is purely $e^{-im\phi_p}$. That is, fast-time derivatives annihilate the metric perturbation in the stationary sector, whereas they do not in the non-stationary sector.

For $\mathtt{m} = 0$, the Lorenz gauge applies restrictions on the form of the metric perturbation, $h_{ab} = \mathcal{O}(r^{\ell-1})$ [8]. Hence, for $\ell > 1$ ($\mathtt{m} = 0$) the Lorenz gauge satisfies the *near-Bondi–Sachs* gauge conditions. Similarly, for $\ell = 1$, $h_{ab} = \mathcal{O}(r^{-2})$, and by inspection (of Niels Warburton's h_{ab} data) $h_{ll} = \mathcal{O}(r^{-3})$, so the $\ell = 1$ ($\mathtt{m} = 0$) sector is also *near-Bondi–Sachs*. The only non-*near-Bondi–Sachs* stationary behaviour is in the $\ell = 0$ mode, as $h_{ll} = \mathcal{O}(r^{-1})$.

The $\ell = 0$ mode is the simplest to transform (as $\xi_m = 0$). I calculate the $\ell = 0, \mathtt{m} = 0$ gauge vector next using the analysis in Sec. 3.6 expanded to the required order in r.

To solve for the gauge vector I express Eq. (3.30) in coordinate form, expanded as a series in r (in Schwarzschild),

$$\sqrt{2}\big((1 - \frac{M}{r})\partial_r \xi_l - \frac{M}{r^2}\xi_l + \mathcal{O}(r^{-3}) = -\frac{e^{i\omega r^*} h_{ll}^{1/r}}{r} - \frac{e^{i\omega r^*} h_{ll}^{1/r^2}}{r^2}. \tag{4.80}$$

Here I have also expanded the metric perturbation in orders of r in u-slicing (and converted to t-slicing; that is,

$$h_{ll} = e^{-i\omega u}\left(\frac{h^{1/r}_{ll}}{r} + \frac{h^{1/r^2}_{ll}}{r^2}\right) + \mathcal{O}(r^{-3}) \tag{4.81}$$

$$= e^{-i\omega t}\left(\frac{e^{i\omega r^*}h^{1/r}_{ll}}{r} + \frac{e^{i\omega r^*}h^{1/r^2}_{ll}}{r^2}\right) + \mathcal{O}(r^{-3}) \tag{4.82}$$

(logarithmic terms could also appear in h_{ab}, but to the order in r required they do not appear in the Lorenz gauge h_{ab}). I use an ansatz for ξ_l,

$$\xi_l = \xi_l^{\ln(r)}\ln(r) + \frac{\xi_l^{1/r}}{r} + \frac{\xi_l^{\ln(r)/r}\ln(r)}{r} + \mathcal{O}(r^{-2}). \tag{4.83}$$

Inputting Eq. (4.83) into Eq. (4.80), and solving for each power of r (and $\ln(r)$) gives

$$\xi_l^{\ln(r)} = -\frac{e^{i\omega r^*}h^{1/r}_{ll}}{\sqrt{2}}, \tag{4.84}$$

$$\xi_l^{\ln(r)/r} = \frac{Me^{i\omega r^*}h^{1/r}_{ll}}{\sqrt{2}}, \tag{4.85}$$

$$\xi_l^{1/r} = \frac{e^{i\omega r^*}h^{1/r^2}_{ll}}{\sqrt{2}} + \frac{2Me^{i\omega r^*}h^{1/r}_{ll}}{\sqrt{2}}. \tag{4.86}$$

The next equation to solve is Eq. (3.33a) for ξ_n. Eq. (3.33a) expanded in a series of r (in Schwarzschild) takes the form

$$\sqrt{2}\partial_u\xi_l - \frac{\partial_r(\xi_l - \xi_n)}{\sqrt{2}} + \frac{\sqrt{2}M\partial_u\xi_l}{r} = -\frac{e^{i\omega r^*}h^{1/r}_{ln}}{r} + \mathcal{O}(r^{-2}). \tag{4.87}$$

As $\mathtt{m} = 0$, and time derivatives are $\propto m$ (in the two-timescale framework) the time derivatives annihilate the gauge vector and metric perturbation. Hence, solving Eq. (4.87) for ξ_n (noting $h^{1/r}_{ln} = 0$ for $\ell = 0$ in the Lorenz gauge) gives

$$\xi_n = \xi_l + c + \mathcal{O}(r^{-2}), \tag{4.88}$$

where c is a constant.

The final equation to solve in this sector is Eq. (3.32). Simplifying to $\ell = 0$, in Schwarzschild, in coordinate form, in a large r expansion, Eq. (3.32) is

$$\sqrt{2}\left(\frac{\xi_l - \xi_n}{r}\right) = -\frac{e^{i\omega r^*}h^{1/r}_{m\bar{m}}}{r} + \mathcal{O}(r^{-2}). \tag{4.89}$$

Solving for ξ_n gives

$$\xi_n = \xi_l + e^{i\omega r^*}h^{1/r}_{m\bar{m}} + \mathcal{O}(r^{-2}), \tag{4.90}$$

which is consistent with Eq. (4.88) with $c = e^{i\omega r^*} h^{1/r}_{m\bar{m}}$. This determines the gauge vector in the $\ell = 0, \mathtt{m} = 0$ sector. The gauge vector to take one from the Lorenz gauge to the *near-Bondi–Sachs* gauge (for $\ell = 0, \mathtt{m} = 0$) is

$$\xi_l = e^{i\omega r^*}\left(-\frac{h^{1/r}_{ll}}{\sqrt{2}}\ln(r) + \frac{h^{1/r^2}_{ll} + 2Mh^{1/r}_{ll}}{\sqrt{2}r} + \frac{Mh^{1/r}_{ll}\ln(r)}{\sqrt{2}r}\right), \tag{4.91}$$

$$\xi_n = e^{i\omega r^*}\left(\frac{h^{1/r}_{m\bar{m}}}{\sqrt{2}} - \frac{h^{1/r}_{ll}}{\sqrt{2}}\ln(r) + \frac{h^{1/r^2}_{ll} + 2Mh^{1/r}_{ll}}{\sqrt{2}r} + \frac{Mh^{1/r}_{ll}\ln(r)}{\sqrt{2}r}\right). \tag{4.92}$$

Next, I calculate the gauge vector for the $m \neq 0$ sector. In the Lorenz gauge, for quasi-circular orbits, for $m \neq 0$, the metric perturbation behaves as $h_{ll} = \mathcal{O}(r^{-2})$, $h_{ln} = \mathcal{O}(r^{-1})$, $h_{lm} = \mathcal{O}(r^{-2})$ and $h_{m\bar{m}} = \mathcal{O}(r^{-2})$ (the remaining components are $\mathcal{O}(r^{-1})$). Hence, to transform to the near-Bondi–Sachs gauge I only need to eliminate the $h_{ll} \sim r^{-2}$ and $h_{ln} \sim r^{-1}$ behaviour with a gauge transformation.

In the $m \neq 0$ sector, Eq. 4.80 is unchanged except $h^{1/r}_{ll} = 0$. Hence, the constraints on the ansatz for ξ_l in Eq. (4.84) become

$$\xi_l^{\ln(r)} = 0, \tag{4.93}$$

$$\xi_l^{\ln(r)/r} = 0, \tag{4.94}$$

$$\xi_l^{1/r} = \frac{e^{i\omega r^*} h^{1/r^2}_{ll}}{\sqrt{2}}. \tag{4.95}$$

Eq. (4.87) is also equivalent in the $m \neq 0$ sector; however, the u derivatives now contribute. Hence, inputting Eq. (4.93) for ξ_l, Eq. (4.87) becomes

$$\partial_r \xi_n = \frac{e^{i\omega r^*} h^{1/r}_{ln}}{r} - 2i\omega\frac{\xi_l^{1/r}}{r} + \mathcal{O}(r^{-2}). \tag{4.96}$$

By analysing the retarded Lorenz gauge leading-order-in-r data provided by Niels Warburton, I noted $h^{1/r}_{ln} = +2i\omega\frac{h^{1/r^2}_{ll}}{\sqrt{2}}$. Hence, using Eq. (4.93), Eq. (4.88) becomes

$$\partial_r \xi_n = \mathcal{O}(r^{-2}). \tag{4.97}$$

Therefore,

$$\xi_n = \xi_n^\circ + \mathcal{O}(r^{-2}), \tag{4.98}$$

where ξ_n° is a constant.

The next equation I solve is for the $h'_{lm} = \mathcal{O}(r^{-2})$ component. I simplify Eq. (3.31) to Schwarzschild and compute an expansion in r, giving

$$\frac{(r-M)\partial_r \xi_m}{\sqrt{2}r} - \frac{\xi_m}{\sqrt{2}r} + \frac{\hat{\eth}\xi_l}{\sqrt{2}r} = \mathcal{O}(r^{-2}), \tag{4.99}$$

where I have used $h_{lm} = \mathcal{O}(r^{-2})$ and $\hat{\eth}$ is given in Eq. (4.40). Expanding ξ_l and ξ_m in spin-weighted spherical harmonics, and applying the identity Eq. (4.42), results in

$$\frac{\mu^{\ell}{}_1\xi_l^{1/r\ lm}}{r} = (r-M)\partial_r\xi_m^{lm} - \xi_m^{lm} + \mathcal{O}(r^{-1}), \tag{4.100}$$

where I have also multiplied by $\sqrt{2}r$. Integrating Eq. (4.100), the solution to this equation is

$$\xi_m = \frac{-\mu^{\ell}{}_1\xi_l^{1/r}}{2r} + r\xi_m^r + \mathcal{O}(r^{-2}). \tag{4.101}$$

ξ_m^r is a constant that I set to zero (as this term would produce non-asymptotically flat behaviour in the other metric perturbation components).

The final equation I need to satisfy to eliminate the non-near-Bondi–Sachs behaviour is the $h'_{m\bar{m}} \sim r^{-2}$ component. Expressing Eq. (3.32) as an expansion in r in Schwarzschild gives

$$-\frac{\xi_{\bar{m}}\hat{\eth}\xi_{\bar{m}} + \hat{\eth}'\xi_{\mathtt{m}}}{\sqrt{2}r} + \frac{\sqrt{2}(\xi_l + \xi_n)}{r} = \mathcal{O}(r^{-2}), \tag{4.102}$$

where I have used $h_{m\bar{m}} = \mathcal{O}(r^{-2})$ (in the Lorenz gauge for $m \neq 0$). Inputting Eqs. (4.93), (4.98), and (4.101) for ξ_l, ξ_n, and ξ_m respectively gives

$$\xi_n^{\circ} = 0. \tag{4.103}$$

In summary, the $m \neq 0$ gauge vector takes the form

$$\begin{aligned}
\xi_l &= \sum_{\ell=0,\mathtt{m}}^{\infty} \frac{e^{i\omega r^*} h_{ll}^{1/r^2\,\ell,\mathtt{m}}}{\sqrt{2}r}\,{}_0Y_{\ell,\mathtt{m}} \\
\xi_n &= 0 \\
\xi_m &= \sum_{\ell=1,\mathtt{m}}^{\infty} \frac{-\mu^{\ell}{}_1 e^{i\omega r^*} h_{ll}^{1/r^2\ \ell,\mathtt{m}}}{2\sqrt{2}r}\,{}_1Y_{\ell,\mathtt{m}}.
\end{aligned} \tag{4.104}$$

To calculate the gauge vector in Eqs. (4.91) and (4.104), I use data on the coefficients of the r expansion of the components of $h_{[a][b]}$. These coefficients are provided by Niels Warburton. With the gauge vector and h_{ab} in hand, it is straightforward to compute the near-Bondi–Sachs metric perturbation using $h'_{ab} = h_{ab} + \mathcal{L}_{\xi^c} g_{ab}$.

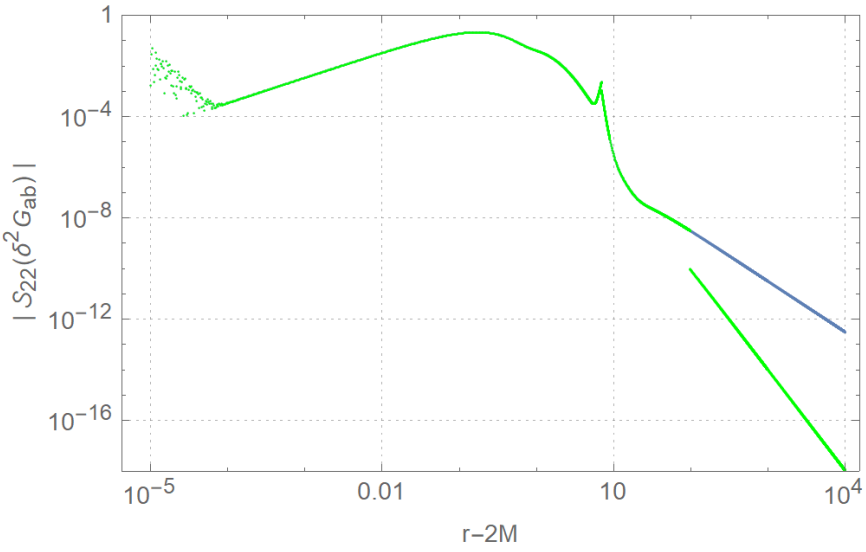

FIGURE 4.6: The $\ell = 2, \mathtt{m} = 2$ mode of $\mathcal{S}_4[\delta^2 G[h_{ab}, h_{ab}]]$ (the source to the reduced second-order Teukolsky equation) for $r_0 = 9M$ in the Carter tetrad and BL coordinates. This source has been calculated using up to $\ell_{max} = 10$ input modes of h_{ab}. The blue line is calculated from retarded Lorenz gauge first-order metric perturbation data (provided by Niels Warburton). The green line is Lorenz gauge until $r = 100M$, where it transforms to the near-Bondi–Sachs gauge.

4.2.5.1 Results: The source for quasi-circular orbits including the near-Bondi–Sachs gauge transform

I implement the near-Bondi–Sachs gauge transformation in my C++ code calculating $\mathcal{S}_4[\delta^2 G_{ab}[h_{ab}, h_{ab}]]$. This allows me to quickly produce source data in the near-Bondi–Sachs gauge near $\mathcal{I}^+$. Fig. 4.6 shows the source where the plot is in the Lorenz gauge on the left side of $r = 100M$. On the right side of $r = 100M$ the line in blue remains in the Lorenz gauge, and the green line is transformed to the near-Bondi–Sachs gauge. The near-Bondi–Sachs gauge source converges two orders in r faster than the Lorenz gauge source (as expected).

In practice, I calculate the near-Bondi–Sachs gauge transformation from the world-tube boundary ($r_0 + 2M$). I then pass this source data to Ben Leather to solve the radial reduced second-order Teukolsky equation. The gauge transform makes the source regular at $\mathcal{I}^+$, allowing Ben Leather to solve for $\psi_{4L}^{(2)}$ using spectral methods without explicitly finding and imposing boundary conditions.

4.2.6 Slow time derivative source decomposition

As a two-timescale approximation is being implemented, there are slow-time derivative contributions to the reduced second-order Teukolsky source, $\mathcal{S}_4[\delta G_{ab}^{\langle 1\rangle}[h_{cd}^{(1)}]]$ in Eq. (4.33). In this section I decompose $\mathcal{S}_4[\delta G_{ab}^{\langle 1\rangle}[h_{cd}^{(1)}]]$ into modes in BL coordinates (for the Carter tetrad).

In practice, $\mathcal{S}_4[\delta G^{\langle 1\rangle}_{ab}[h^{(1)}_{cd}]]$ can be written as two operators, one acting on the slow-time derivative of h_{ab} (see Eq. (4.20)) and the other on the product of the rate of $F^{\{0\}}_{\Omega}$ (see Eq. (4.14)) and $h^{(1)}_{cd}$. That is,

$$\mathcal{S}_4[\delta G^{\langle 1\rangle}_{ab}[h^{(1)}_{cd}]] = X[\vec{\partial}_{\mathcal{V}} h^{(1)}_{cd}] + Y[F^{\{0\}}_{\Omega} h^{(1)}_{cd}]. \tag{4.105}$$

Using Eq. (4.2), $\delta G^{\langle 1\rangle}_{ab}[h^{(1)}_{cd}]$ can be written as

$$\delta G^{\langle 1\rangle}_{ab}[h^{(1)}_{cd}] = \frac{-1}{2} E^{\langle 1\rangle}_{ab}[\bar{h}_{cd}] + \overline{\nabla^{\langle 0\rangle}_{(a} Z^{\langle 1\rangle}_{b)}}[\bar{h}_{cd}] + \overline{\nabla^{\langle 1\rangle}_{(a} Z^{\langle 0\rangle}_{b)}}[\bar{h}_{cd}]. \tag{4.106}$$

Using Eqs.(4.3), (4.19), (4.20), and (4.14), $E^{\langle 1\rangle}_{ab}[\bar{h}_{cd}]$ can be written as

$$E^{\langle 1\rangle}_{ab}[h^{(1)}_{cd}] = \frac{i\mathtt{m} F^{\{0\}}_{\Omega} h^{(1)}_{cd}}{f} + 2t^c \nabla^{\langle 0\rangle}_c \vec{\partial}_{\mathcal{V}} h_{ab}, \tag{4.107}$$

where $\mathtt{m}$ corresponds to the mode of h_{ab}. Similarly, using Eq. (4.1), (4.19), and (4.20),

$$\nabla^{\langle 1\rangle}_a Z^{\langle 0\rangle}_b[h^{(1)}_{cd}] = t_a \vec{\partial}_{\mathcal{V}} Z^{\langle 0\rangle}_b[h^{(1)}_{cd}], \tag{4.108}$$

and

$$Z^{\langle 1\rangle}_a[h^{(1)}_{cd}] = t^c \vec{\partial}_{\mathcal{V}} h_{ac}. \tag{4.109}$$

Hence, inserting Eqs.(4.107), (4.108), and (4.109) into Eq. (4.106) gives

$$\delta G^{\langle 1\rangle}_{ab}[h^{(1)}_{cd}] = \frac{-1}{2}\left(\frac{i\mathtt{m} F^{\{0\}}_{\Omega} h^{(1)}_{cd}}{f} + 2t^c \nabla^{\langle 0\rangle}_c \vec{\partial}_{\mathcal{V}} h_{ab}\right) + + \overline{\nabla^{\langle 0\rangle}_{(a} t^c \vec{\partial}_{\mathcal{V}} \bar{h}_{b)c}} + \overline{t_{(a} \vec{\partial}_{\mathcal{V}} \nabla^c_{\langle 0\rangle} \bar{h}_{b)c}}. \tag{4.110}$$

I then act $\mathcal{S}^{\langle 0\rangle}$ on $\delta G^{\langle 1\rangle}_{ab}[h^{(1)}_{cd}]$ and decompose into modes. For the Carter tetrad in BL coordinates this gives

$$\begin{aligned}
\mathcal{S}^{\langle 0\rangle}\left[\delta G^{\langle 1\rangle}_{ab}[h^{\ell,\mathtt{m}}_{cd}]\right]^{\ell,\mathtt{m}} &= \frac{i\mathtt{m}F^{\{0\}}_{\Omega}}{8r^4f(r)^2}\Bigg(\Big(8M^2-6iMr^2\omega-r^4\omega^2+(-8Mr+6ir^3\omega)f(r)\\
&+4r^2f(r)^2\Big)\bar{h}_{44}{}^{\ell,\mathtt{m}}+2rf(r)^{1/2}\big(-3M+ir^2\omega+3rf(r)\big)\bar{h}_{24}{}^{\ell,\mathtt{m}}\mu^{\ell}{}_2+r^2f(r)\Big(\bar{h}_{22}{}^{\ell,\mathtt{m}}\mu^{\ell}{}_1\mu^{\ell}{}_2\\
&+2rf(r)^{1/2}\mu^{\ell}{}_2\bar{h}_{24}{}^{\ell,\mathtt{m}}{}_{,r}+2(-2M+ir^2\omega)\bar{h}_{44}{}^{\ell,\mathtt{m}}{}_{,r}+rf(r)(6\bar{h}_{44}{}^{\ell,\mathtt{m}}{}_{,r}+r\bar{h}_{44}{}^{\ell,\mathtt{m}}{}_{,r,r})\Big)\Bigg)\\
&+\frac{1}{8r^5f(r)^2}\Bigg((3M-ir^2\omega)f(r)^{1/2}\mu^{\ell}{}_2\big((M+ir^2\omega)\vec{\partial}_{\mathcal{V}}\bar{h}_{14}{}^{\ell,\mathtt{m}}+3(M-ir^2\omega)\vec{\partial}_{\mathcal{V}}\bar{h}_{24}{}^{\ell,\mathtt{m}}\big)\\
&+2r\omega(8iM^2+6Mr^2\omega-ir^4\omega^2)\vec{\partial}_{\mathcal{V}}\bar{h}_{44}{}^{\ell,\mathtt{m}}+rf(r)^{3/2}\mu^{\ell}{}_2(-4ir^2\omega\vec{\partial}_{\mathcal{V}}\bar{h}_{14}{}^{\ell,\mathtt{m}}\\
&-r(\mu^{\ell}{}_1)^2\vec{\partial}_{\mathcal{V}}\bar{h}_{23}{}^{\ell,\mathtt{m}}+4M\vec{\partial}_{\mathcal{V}}\bar{h}_{24}{}^{\ell,\mathtt{m}}+14ir^2\omega\vec{\partial}_{\mathcal{V}}\bar{h}_{24}{}^{\ell,\mathtt{m}}+r(\mu^{\ell}{}_3)^2\vec{\partial}_{\mathcal{V}}\bar{h}_{24}{}^{\ell,\mathtt{m}}-2ir^3\omega\vec{\partial}_{\mathcal{V}}\bar{h}_{14}{}^{\ell,\mathtt{m}}{}_{,r}\\
&-4Mr\vec{\partial}_{\mathcal{V}}\bar{h}_{24}{}^{\ell,\mathtt{m}}{}_{,r}+4ir^3\omega\vec{\partial}_{\mathcal{V}}\bar{h}_{24}{}^{\ell,\mathtt{m}}{}_{,r})+4r^2f(r)^3(2\vec{\partial}_{\mathcal{V}}\bar{h}_{44}{}^{\ell,\mathtt{m}}+r\vec{\partial}_{\mathcal{V}}\bar{h}_{44}{}^{\ell,\mathtt{m}}{}_{,r})\\
&-f(r)\Big(r\mu^{\ell}{}_1\mu^{\ell}{}_2\big(ir^2\omega\vec{\partial}_{\mathcal{V}}\bar{h}_{12}{}^{\ell,\mathtt{m}}+(2M-ir^2\omega)(\vec{\partial}_{\mathcal{V}}\bar{h}_{22}{}^{\ell,\mathtt{m}}-\vec{\partial}_{\mathcal{V}}\bar{h}_{34}{}^{\ell,\mathtt{m}})\big)+\big(4(4M^2\\
&+2iMr^2\omega+3r^4\omega^2)+(2Mr-ir^3\omega)(\mu^{\ell}{}_3)^2\big)\vec{\partial}_{\mathcal{V}}\bar{h}_{44}{}^{\ell,\mathtt{m}}+4r^3\omega(2iM+r^2\omega)\vec{\partial}_{\mathcal{V}}\bar{h}_{44}{}^{\ell,\mathtt{m}}{}_{,r}\Big)\\
&+r^2f(r)^{5/2}\mu^{\ell}{}_2\big(-4\vec{\partial}_{\mathcal{V}}\bar{h}_{14}{}^{\ell,\mathtt{m}}+14\vec{\partial}_{\mathcal{V}}\bar{h}_{24}{}^{\ell,\mathtt{m}}+r(-4\vec{\partial}_{\mathcal{V}}\bar{h}_{14}{}^{\ell,\mathtt{m}}{}_{,r}+8\vec{\partial}_{\mathcal{V}}\bar{h}_{24}{}^{\ell,\mathtt{m}}{}_{,r}-r\vec{\partial}_{\mathcal{V}}\bar{h}_{14}{}^{\ell,\mathtt{m}}{}_{,r,r}\\
&+r\vec{\partial}_{\mathcal{V}}\bar{h}_{24}{}^{\ell,\mathtt{m}}{}_{,r,r})\big)+rf(r)^2\Big(2(4M+6ir^2\omega+r(\mu^{\ell}{}_3)^2)\vec{\partial}_{\mathcal{V}}\bar{h}_{44}{}^{\ell,\mathtt{m}}-r\mu^{\ell}{}_1\mu^{\ell}{}_2\big(-4\vec{\partial}_{\mathcal{V}}\bar{h}_{22}{}^{\ell,\mathtt{m}}\\
&+4\vec{\partial}_{\mathcal{V}}\bar{h}_{34}{}^{\ell,\mathtt{m}}+r(\vec{\partial}_{\mathcal{V}}\bar{h}_{12}{}^{\ell,\mathtt{m}}{}_{,r}-\vec{\partial}_{\mathcal{V}}\bar{h}_{22}{}^{\ell,\mathtt{m}}{}_{,r}+\vec{\partial}_{\mathcal{V}}\bar{h}_{34}{}^{\ell,\mathtt{m}}{}_{,r})\big)+r(8M+12ir^2\omega\\
&+r(\mu^{\ell}{}_3)^2)\vec{\partial}_{\mathcal{V}}\bar{h}_{44}{}^{\ell,\mathtt{m}}{}_{,r}+2ir^4\omega\vec{\partial}_{\mathcal{V}}\bar{h}_{44}{}^{\ell,\mathtt{m}}{}_{,r,r}\Big)\Bigg).
\end{aligned}\tag{4.111}$$

Note, the natural split into a $\vec{\partial}_{\mathcal{V}}\bar{h}_{[a][b]}{}^{\ell,\mathtt{m}}$ piece and a $F^{\{0\}}_{\Omega}\bar{h}_{[a][b]}$ piece.

The dissipative piece of the self force only depends on the fluxes in $h^{(2)}_{\mu\nu}$; that is, only the $m\neq 0$ modes are required. Hence, $F^{\{1\}}_{A}$ can be omitted from $\mathcal{V}_i$ because δM_A only contributes to the $\mathtt{m}=0$ mode of $h^{(1)}_{\mu\nu}$. Therefore,

$$\vec{\partial}_{\mathcal{V}}\to F^{\{0\}}_{\Omega}\frac{\partial}{\partial\Omega}.\tag{4.112}$$

Instead of calculating $\frac{\partial}{\partial\Omega}$ directly, one can calculate r_0 derivatives and use the relation

$$\frac{\partial}{\partial\Omega}=\frac{\partial r_0}{\partial\Omega}\frac{\partial}{\partial r_0}\tag{4.113}$$

where $\frac{\partial r_0}{\partial\Omega}=-\frac{2M^{\frac{1}{3}}}{3\Omega^{\frac{5}{3}}}$.

The data for $\partial_{r_0}\bar{h}_{[a][b]}{}^{\ell,\mathtt{m}}$ is calculated by Leanne Durkan [65] and $F^{\{0\}}_{\Omega}$ is calculated using Ref. [1]. I give Eq. (4.111) to Ben Leather who will add this contribution for the source before solving for $\psi^{(2)\ell,\mathtt{m}}_{4L}$.

Currently, the slow-time derivative contribution to the source is exhibiting singular behaviour near the horizon. This is due to $\mathcal{S}_4[\delta G^{\langle 1\rangle}_{ab}[h^{(1)}_{cd}]]$ being computed on t-slicing. I will re-derive these formulas on s-slicing where the singular will not appear.

4.2.7 Slow time derivative contribution of the Bondi–Sachs gauge transformation

$\mathcal{S}_4[\delta G^{\langle 1\rangle}_{ab}[h^{(1)}_{cd}]]$ is also affected by the near-Bondi–Sachs gauge transform. To account for this contribution, I provide mode decomposed formulas for the correction due to the near-Bondi–Sachs gauge transformation, derived as follows.

In the region where the near-Bondi–Sachs transform is applied, the slow time-derivative of the metric perturbation is transformed as

$$\vec{\partial}_{\mathcal{V}} h'_{ab} = \vec{\partial}_{\mathcal{V}} h_{ab} + \vec{\partial}_{\mathcal{V}} \mathcal{L}_{\xi^c} g_{ab}. \tag{4.114}$$

Hence, the contribution to the slow time derivative due to the near-Bondi–Sachs gauge transform is $\vec{\partial}_{\mathcal{V}} \mathcal{L}_{\xi^c} g_{ab}$. Again, one can use the argument that only the $m \neq 0$ modes are required to calculate the dissipative piece of the second-order self-force. Hence, the only part of the near-Bondi–Sachs gauge transformation that I need to consider is Eq. (4.104).

Using Eq. (4.112), I am interested in the Ω partial derivative of $\left(\mathcal{L}_{\xi^c} g_{ab}\right)^{\ell,\mathtt{m}}_{ll}$. Note, the only pieces of ξ^c (for $m \neq 0$) which are functions of Ω are ω and $h^{1/r^2 \ell,\mathtt{m}}_{ll}$. Hence,

calculating the Ω derivative of the gauge transformation is trivial,

$$
\begin{aligned}
\left(\partial_\Omega \mathcal{L}_{\xi^c} g_{ab}\right)^{\ell,\mathtt{m}}_{ll} &= \frac{e^{i\omega r^*}(M-r)\left(\partial_\Omega h^{1/r^2\ell,\mathtt{m}}_{ll} + i h^{1/r^2\ell,\mathtt{m}}_{ll} r^* \partial_\Omega \omega\right)}{f^{1/2} r^3} \\
\left(\partial_\Omega \mathcal{L}_{\xi^c} g_{ab}\right)^{\ell,\mathtt{m}}_{ln} &= \\
&\frac{e^{i\omega r^*}\left(\left(-3M + r - 2ir^2\omega\right)\partial_\Omega h^{1/r^2\ell,\mathtt{m}}_{ll} + h^{1/r^2\ell,\mathtt{m}}_{ll}\left(-2ir^2 + \left(-3iM + ir + 2r^2\omega\right)r^*\right)\partial_\Omega\omega\right)}{2 f^{1/2} r^3} \\
\left(\partial_\Omega \mathcal{L}_{\xi^c} g_{ab}\right)^{\ell,\mathtt{m}}_{lm} &= \frac{e^{i\omega r^*}(-1+f^{1/2})\mu^\ell{}_1\left(\partial_\Omega h^{1/r^2\ell,\mathtt{m}}_{ll} + i h^{1/r^2\ell,\mathtt{m}}_{ll} r^* \partial_\Omega \omega\right)}{2r^2} \\
\left(\partial_\Omega \mathcal{L}_{\xi^c} g_{ab}\right)^{\ell,\mathtt{m}}_{nn} &= 0 \\
\left(\partial_\Omega \mathcal{L}_{\xi^c} g_{ab}\right)^{\ell,\mathtt{m}}_{nm} &= \\
&\frac{e^{i\omega r^*}\mu^\ell{}_1\left(\left(2M - r + ir^2\omega\right)\partial_\Omega h^{1/r^2\ell,\mathtt{m}}_{ll} + i h^{1/r^2\ell,\mathtt{m}}_{ll}\left(r^2 + \left(2M - r + ir^2\omega\right)r^*\right)\partial_\Omega\omega\right)}{2 f^{1/2} r^3} \\
\left(\partial_\Omega \mathcal{L}_{\xi^c} g_{ab}\right)^{\ell,\mathtt{m}}_{mm} &= \frac{e^{i\omega r^*}(\mu^\ell{}_1)^2\left(\partial_\Omega h^{1/r^2\ell,\mathtt{m}}_{ll} + i h^{1/r^2\ell,\mathtt{m}}_{ll} r^* \partial_\Omega \omega\right)}{2r^2} \\
\left(\partial_\Omega \mathcal{L}_{\xi^c} g_{ab}\right)^{\ell,\mathtt{m}}_{m\bar{m}} &= \frac{e^{i\omega r^*}(2f^{1/2} - (\mu^\ell{}_1)^2)\left(\partial_\Omega h^{1/r^2\ell,\mathtt{m}}_{ll} + i h^{1/r^2\ell,\mathtt{m}}_{ll} r^* \partial_\Omega \omega\right)}{2r^2}.
\end{aligned}
\tag{4.115}
$$

These formulas are given to Ben Leather, who accounts for this contribution (using Eqs. (4.114), (4.112) and (4.113)) using the $\partial_{r_0} h_{ab}$ data provided by Leanne Durkan (noting, $\partial_\Omega \omega$ is trivial).

4.2.8 The Bondi–Sachs gauge jump

In Fig. 4.6, the green line shows a jump discontinuity at $r = 100M$. The discontinuity is due to the data on the left-hand side being in the Lorenz gauge, and on the right-hand side being in the near-Bondi–Sachs gauge. One must account for this jump before integrating over the source. In this section I derive a formula for the jump in $\psi^{(2)}_{4L}$, which can then be used as a junction condition when solving the field equation.

In the new gauge, $\psi^{(2)}_{4L}$ depends on the metric perturbation through

$$
\psi^{(2)\prime}_{4L} := \mathcal{T}_4\left[h^{(2)\prime}_{ab}\right] = \mathcal{T}^{\langle 0\rangle}_4\left[h^{(2)}_{ab} + \mathcal{L}^{\langle 0\rangle}_{\xi^c} h_{ab} + \frac{1}{2}\mathcal{L}^{\langle 0\rangle}_{\xi^c}\mathcal{L}^{\langle 0\rangle}_{\xi^d} g_{ab} + \mathcal{L}^{\langle 1\rangle}_{\xi^d} g_{ab}\right]. \tag{4.116}
$$

That is, the gauge jump ($\Delta\psi^{(2)\prime}_{4L}$) is given by

$$
\Delta\psi^{(2)}_{4L} = \mathcal{T}^{\langle 0\rangle}_4\left[\mathcal{L}^{\langle 0\rangle}_{\xi^c} h_{ab} + \frac{1}{2}\mathcal{L}^{\langle 0\rangle}_{\xi^c}\mathcal{L}^{\langle 0\rangle}_{\xi^d} g_{ab} + \mathcal{L}^{\langle 1\rangle}_{\xi^d} g_{ab}\right]. \tag{4.117}
$$

I express each piece of the jump as a mode-decomposition in BL coordinates (in the Carter tetrad) for the gauge vector in Eq. (4.104). The expression for

$\mathcal{T}_4^{\langle 0\rangle}\left[\mathcal{L}_{\xi^c}^{\langle 0\rangle} h_{ab} + \frac{1}{2}\mathcal{L}_{\xi^c}^{\langle 0\rangle}\mathcal{L}_{\xi^d}^{\langle 0\rangle} g_{ab}\right]$ is too long to be presented here, but is given in a Mathematica booklet in the supporting material of this thesis. The $\mathtt{m} \neq 0$ piece of the slow-time derivative contribution is given by

$$\mathcal{T}_4^{\langle 0\rangle}\left[\mathcal{L}_{\xi^d}^{\langle 1\rangle} g_{ab}\right]_{\mathtt{m}\neq 0} = \frac{e^{i\omega r^*}\mu^\ell{}_1\mu^\ell{}_2}{8fr^4}\Big(2(M - i\omega r^2)\partial_{r_0} h_{ll}^{1/r^2\ell,\mathtt{m}} + h_{ll}^{1/r^2\ell,\mathtt{m}}(-ir^2 + 2(iM + \omega r^2)r^*)\partial_{r_0}\omega\Big), \tag{4.118}$$

where $h_{ll}^{1/r^2\ell,\mathtt{m}}$ has been evaluated in u-slicing (the full expression is still in t-slicing because of the factor of $e^{i\omega r^*}$).

I calculate $\Delta\psi_{4L}^{(2)}$ at the outer world-tube boundary using the gauge vector that takes one from the Lorenz gauge to the near-Bondi-Sachs gauge. I have implemented this calculation in my C++ code and pass the results to Ben Leather, who uses them to account for the jump discontinuity in $\psi_{4L}^{(2)}$.

4.2.9 Decomposing the correction to the effective source

So far, all the contributions to the source I have presented have been for outside the world-tube (or on the world-tube boundary). My final contribution to calculating the source to the reduced second-order Teukolsky equation is inside the world-tube.

Inside the world-tube, the source of the reduced second-order Teukolsky equation is given by Eq. (4.35). The majority of the source is given by $\mathcal{S}^{\langle 0\rangle}$ acting on $\breve{T}_{ab}^{(2)\mathrm{eff}}$. $\breve{T}_{ab}^{(2)\mathrm{eff}}$ is provided by the effective source scheme used in Refs. [195, 194, 156]. The effect of $\mathcal{S}^{\langle 0\rangle}$ acting on $\breve{T}_{ab}^{(2)\mathrm{eff}}$ is calculated numerically by Barry Wardell (using the same code which has been compared to my results in Fig. 4.5).

The additional piece of the source in the world-tube is $\mathcal{S}^{\langle 0\rangle}\left[8\pi\Delta T_{ab}^{(2)\mathrm{eff}}\right]$ (where $\Delta T_{ab}^{(2)\mathrm{eff}}$ is given in Eq. (4.36)). To calculate this contribution we use Barry Wardell's code to act with $\mathcal{S}^{\langle 0\rangle}$ on $\Delta T_{ab}^{(2)\mathrm{eff}}$. To do so requires a formula for $\Delta T_{ab}^{(2)\mathrm{eff}}$. As Barry Wardell's code requires the input to be in the Barack–Lousto–Sago mode basis (see Sec. 4.2.3), I provide a mode decomposition formula for $\Delta T_{ab}^{(2)\mathrm{eff}}$ in this basis.

I calculate the mode decomposition of $\Delta T_{ab}^{(2)\mathrm{eff}}$ from Eq. (4.36) using Eqs. (4.5) and (4.109). I present $\Delta T_{ab}^{(2)\mathrm{eff}}$ in two parts, the first ($\Delta T_{(2)\mathrm{effA}}^{1\ell,\mathtt{m}}$) acts on

slow-time derivatives of the first-order metric perturbation ($\vec{\partial}_v h^{(1)}_{cd}$),

$$\Delta T^{1\ell,\mathtt{m}}_{(2)\mathrm{effA}}[\vec{\partial}_v h^{i\ell,\mathtt{m}}] = -\frac{1}{4f^2r^2}\Big((8M+8fM+2f^2r)\vec{\partial}_v\bar{h}^{2\ell,\mathtt{m}} + 2ifr^2\big(\omega\vec{\partial}_v\bar{h}^{1\ell,\mathtt{m}} + f(\omega\vec{\partial}_v\bar{h}^{3\ell,\mathtt{m}} + i\vec{\partial}_v\bar{h}^{2\ell,\mathtt{m}}{}_{,r})\big)\Big), \tag{4.119}$$

$$\Delta T^{2\ell,\mathtt{m}}_{(2)\mathrm{effA}}[\vec{\partial}_v h^{i\ell,\mathtt{m}}] = -\frac{1}{4fr^2}\Big((8M+2fr)\vec{\partial}_v\bar{h}^{1\ell,\mathtt{m}} + (8M+2ir^2\omega)\vec{\partial}_v\bar{h}^{2\ell,\mathtt{m}} + f\big((4M+2fr)\vec{\partial}_v\bar{h}^{3\ell,\mathtt{m}} - 2r^2(\vec{\partial}_v\bar{h}^{1\ell,\mathtt{m}}{}_{,r} + f\vec{\partial}_v\bar{h}^{3\ell,\mathtt{m}}{}_{,r})\big)\Big), \tag{4.120}$$

$$\Delta T^{3\ell,\mathtt{m}}_{(2)\mathrm{effA}}[\vec{\partial}_v h^{i\ell,\mathtt{m}}] = \frac{2\vec{\partial}_v\bar{h}^{2\ell,\mathtt{m}} - \vec{\partial}_v\bar{h}^{4\ell,\mathtt{m}}}{2fr}, \tag{4.121}$$

$$\Delta T^{4\ell,\mathtt{m}}_{(2)\mathrm{effA}}[\vec{\partial}_v h^{i\ell,\mathtt{m}}] = \frac{r(\mu^{l2}_1)^{)}2(\vec{\partial}_v\bar{h}^{1\ell,\mathtt{m}} + f\vec{\partial}_v\bar{h}^{3\ell,\mathtt{m}}) - (2M+ir^2\omega)\vec{\partial}_v\bar{h}^{4\ell,\mathtt{m}}}{2fr^2}, \tag{4.122}$$

$$\Delta T^{5\ell,\mathtt{m}}_{(2)\mathrm{effA}}[\vec{\partial}_v h^{i\ell,\mathtt{m}}] = -\frac{(4M+4fr)\vec{\partial}_v\bar{h}^{4\ell,\mathtt{m}} - 2r((\mu^{l2}_1)^{)}2\vec{\partial}_v\bar{h}^{2\ell,\mathtt{m}} + fr\vec{\partial}_v\bar{h}^{4\ell,\mathtt{m}}{}_{,r})}{4fr^2}, \tag{4.123}$$

$$\Delta T^{6\ell,\mathtt{m}}_{(2)\mathrm{effA}}[\vec{\partial}_v h^{i\ell,\mathtt{m}}] = \frac{1}{4f^3r^2}\Big((-8M+4fM+2f^2r)\vec{\partial}_v\bar{h}^{2\ell,\mathtt{m}} - 2ifr^2\big(\omega\vec{\partial}_v\bar{h}^{1\ell,\mathtt{m}} + f(\omega\vec{\partial}_v\bar{h}^{3\ell,\mathtt{m}} - i\vec{\partial}_v\bar{h}^{2\ell,\mathtt{m}}{}_{,r})\big)\Big), \tag{4.124}$$

$$\Delta T^{7\ell,\mathtt{m}}_{(2)\mathrm{effA}}[\vec{\partial}_v h^{i\ell,\mathtt{m}}] = \frac{(\mu^{l2}_2)^{)}2\vec{\partial}_v\bar{h}^{4\ell,\mathtt{m}}}{2fr}, \tag{4.125}$$

$$\Delta T^{8\ell,\mathtt{m}}_{(2)\mathrm{effA}}[\vec{\partial}_v h^{i\ell,\mathtt{m}}] = -\frac{(2M+ir^2\omega)\vec{\partial}_v\bar{h}^{8\ell,\mathtt{m}}}{2fr^2}, \tag{4.126}$$

$$\Delta T^{9\ell,\mathtt{m}}_{(2)\mathrm{effA}}[\vec{\partial}_v h^{i\ell,\mathtt{m}}] = -\frac{(4M+4fr)\vec{\partial}_v\bar{h}^{8\ell,\mathtt{m}} - 2fr^2\vec{\partial}_v\bar{h}^{8\ell,\mathtt{m}}{}_{,r}}{4fr^2}, \tag{4.127}$$

$$\Delta T^{10\ell,\mathtt{m}}_{(2)\mathrm{effA}}[\vec{\partial}_v h^{i\ell,\mathtt{m}}] = \frac{(\mu^{l2}_2)^{)}2\vec{\partial}_v\bar{h}^{8\ell,\mathtt{m}}}{2fr}. \tag{4.128}$$

The second part ($\Delta T^{i\ell,\mathrm{m}}_{(2)\mathrm{effB}}$) acts on the second-order puncture ($h^{i\ell,\mathrm{m}}_{(2)\mathcal{P}}$),

$$
\begin{aligned}
\Delta T^{1\ell,\mathrm{m}}_{(2)\mathrm{effB}}[h^{i\ell,\mathrm{m}}_{(2)\mathcal{P}}] &= \frac{1}{2f^2r^3}\Big(4iMr\omega\bar{h}^{2\ell,\mathrm{m}}_{(2)\mathcal{P}} + f\big((4M-r^3\omega^2)\bar{h}^{1\ell,\mathrm{m}}_{(2)\mathcal{P}} - 4M\bar{h}^{5\ell,\mathrm{m}}_{(2)\mathcal{P}} \\
&+ 4Mr(i\omega\bar{h}^{2\ell,\mathrm{m}}_{(2)\mathcal{P}} + \bar{h}^{1\ell,\mathrm{m}}_{(2)\mathcal{P},r})\big) + f^2\big(2M\bar{h}^{1\ell,\mathrm{m}}_{(2)\mathcal{P}} + 2ir^2\omega\bar{h}^{2\ell,\mathrm{m}}_{(2)\mathcal{P}} - (4M+r^3\omega^2)\bar{h}^{3\ell,\mathrm{m}}_{(2)\mathcal{P}} \\
&- ir^2\omega\bar{h}^{4\ell,\mathrm{m}}_{(2)\mathcal{P}} - 2M\bar{h}^{5\ell,\mathrm{m}}_{(2)\mathcal{P}} - 8M\bar{h}^{6\ell,\mathrm{m}}_{(2)\mathcal{P}} + 2Mr\bar{h}^{1\ell,\mathrm{m}}_{(2)\mathcal{P},r} - 4Mr\bar{h}^{3\ell,\mathrm{m}}_{(2)\mathcal{P},r}\big) + f^3r\big(2\bar{h}^{1\ell,\mathrm{m}}_{(2)\mathcal{P}} - 2\bar{h}^{5\ell,\mathrm{m}}_{(2)\mathcal{P}} \\
&+ r(\bar{h}^{5\ell,\mathrm{m}}_{(2)\mathcal{P},r} - r\bar{h}^{1\ell,\mathrm{m}}_{(2)\mathcal{P},r,r})\big) + f^4r\big(-2\bar{h}^{3\ell,\mathrm{m}}_{(2)\mathcal{P}} - 4\bar{h}^{6\ell,\mathrm{m}}_{(2)\mathcal{P}} + r(2\bar{h}^{6\ell,\mathrm{m}}_{(2)\mathcal{P},r} + r\bar{h}^{3\ell,\mathrm{m}}_{(2)\mathcal{P},r,r})\big)\Big) \\
\Delta T^{2\ell,\mathrm{m}}_{(2)\mathrm{effB}}[h^{i\ell,\mathrm{m}}_{(2)\mathcal{P}}] &= \frac{1}{2fr^3}\Big(r\omega\big(4iM\bar{h}^{1\ell,\mathrm{m}}_{(2)\mathcal{P}} + (4iM-r^2\omega)\bar{h}^{2\ell,\mathrm{m}}_{(2)\mathcal{P}}\big) + f\big((4M+2ir^2\omega)\bar{h}^{1\ell,\mathrm{m}}_{(2)\mathcal{P}} \\
&+ 2M\bar{h}^{2\ell,\mathrm{m}}_{(2)\mathcal{P}} + 2iMr\omega\bar{h}^{3\ell,\mathrm{m}}_{(2)\mathcal{P}} - 2M\bar{h}^{4\ell,\mathrm{m}}_{(2)\mathcal{P}} - 4M\bar{h}^{5\ell,\mathrm{m}}_{(2)\mathcal{P}} - ir^2\omega\bar{h}^{5\ell,\mathrm{m}}_{(2)\mathcal{P}} + 4Mr\bar{h}^{1\ell,\mathrm{m}}_{(2)\mathcal{P},r} \\
&+ 2Mr\bar{h}^{2\ell,\mathrm{m}}_{(2)\mathcal{P},r}\big) - f^2\big(4M\bar{h}^{3\ell,\mathrm{m}}_{(2)\mathcal{P}} + (8M+2ir^2\omega)\bar{h}^{6\ell,\mathrm{m}}_{(2)\mathcal{P}} + r(-2\bar{h}^{2\ell,\mathrm{m}}_{(2)\mathcal{P}} + 2\bar{h}^{4\ell,\mathrm{m}}_{(2)\mathcal{P}} + 4M\bar{h}^{3\ell,\mathrm{m}}_{(2)\mathcal{P},r} \\
&+ 2ir^2\omega\bar{h}^{3\ell,\mathrm{m}}_{(2)\mathcal{P},r} - r\bar{h}^{4\ell,\mathrm{m}}_{(2)\mathcal{P},r} + r^2\bar{h}^{2\ell,\mathrm{m}}_{(2)\mathcal{P},r,r})\big)\Big) \\
\Delta T^{3\ell,\mathrm{m}}_{(2)\mathrm{effB}}[h^{i\ell,\mathrm{m}}_{(2)\mathcal{P}}] &= \frac{1}{2fr^2}\Big(-ir\omega(2\bar{h}^{2\ell,\mathrm{m}}_{(2)\mathcal{P}} - \bar{h}^{4\ell,\mathrm{m}}_{(2)\mathcal{P}}) + 2f^2(\bar{h}^{3\ell,\mathrm{m}}_{(2)\mathcal{P}} + 2\bar{h}^{6\ell,\mathrm{m}}_{(2)\mathcal{P}} + r\bar{h}^{3\ell,\mathrm{m}}_{(2)\mathcal{P},r}) \\
&+ f(-2\bar{h}^{1\ell,\mathrm{m}}_{(2)\mathcal{P}} + 4\bar{h}^{5\ell,\mathrm{m}}_{(2)\mathcal{P}} - \bar{h}^{7\ell,\mathrm{m}}_{(2)\mathcal{P}} + \bar{h}^{6\ell,\mathrm{m}}_{(2)\mathcal{P}}({\mu^\ell}_1)^2 - 2r\bar{h}^{1\ell,\mathrm{m}}_{(2)\mathcal{P},r} + r\bar{h}^{5\ell,\mathrm{m}}_{(2)\mathcal{P},r})\Big) \\
\Delta T^{4\ell,\mathrm{m}}_{(2)\mathrm{effB}}[h^{i\ell,\mathrm{m}}_{(2)\mathcal{P}}] &= \frac{1}{8fr^3}\Big(2f^2r(\bar{h}^{4\ell,\mathrm{m}}_{(2)\mathcal{P}} + i\bar{h}^{8\ell,\mathrm{m}}_{(2)\mathcal{P}}) - 4r\omega\big((-2iM+r^2\omega)\bar{h}^{4\ell,\mathrm{m}}_{(2)\mathcal{P}} \\
&+ ir\bar{h}^{1\ell,\mathrm{m}}_{(2)\mathcal{P}}({\mu^\ell}_1)^2\big) + f\big(8(2M+ir^2\omega)\bar{h}^{5\ell,\mathrm{m}}_{(2)\mathcal{P}} - 8M\bar{h}^{7\ell,\mathrm{m}}_{(2)\mathcal{P}} - 4ir^2\omega\bar{h}^{7\ell,\mathrm{m}}_{(2)\mathcal{P}} + 4iM\bar{h}^{8\ell,\mathrm{m}}_{(2)\mathcal{P}} \\
&- 4r\bar{h}^{2\ell,\mathrm{m}}_{(2)\mathcal{P}}({\mu^\ell}_1)^2 - 4ir^2\omega\bar{h}^{3\ell,\mathrm{m}}_{(2)\mathcal{P}}({\mu^\ell}_1)^2 + 8M\bar{h}^{6\ell,\mathrm{m}}_{(2)\mathcal{P}}({\mu^\ell}_1)^2 + 4ir^2\omega\bar{h}^{6\ell,\mathrm{m}}_{(2)\mathcal{P}}({\mu^\ell}_1)^2 \\
&- ir\bar{h}^{8\ell,\mathrm{m}}_{(2)\mathcal{P}}({\mu^\ell}_1)^2 + ir\bar{h}^{8\ell,\mathrm{m}}_{(2)\mathcal{P}}({\mu^\ell}_2)^2 + \bar{h}^{4\ell,\mathrm{m}}_{(2)\mathcal{P}}(4M + 3r({\mu^\ell}_1)^2 + r({\mu^\ell}_2)^2) - 4r^2({\mu^\ell}_1)^2\bar{h}^{2\ell,\mathrm{m}}_{(2)\mathcal{P},r} \\
&+ 8Mr\bar{h}^{5\ell,\mathrm{m}}_{(2)\mathcal{P},r} + 4ir^3\omega\bar{h}^{5\ell,\mathrm{m}}_{(2)\mathcal{P},r}\big)\Big) \\
\Delta T^{5\ell,\mathrm{m}}_{(2)\mathrm{effB}}[h^{i\ell,\mathrm{m}}_{(2)\mathcal{P}}] &= \frac{1}{8fr^3}\Big(-4ir\omega(-2M\bar{h}^{4\ell,\mathrm{m}}_{(2)\mathcal{P}} + r\bar{h}^{2\ell,\mathrm{m}}_{(2)\mathcal{P}}({\mu^\ell}_1)^2) + f\Big(\bar{h}^{5\ell,\mathrm{m}}_{(2)\mathcal{P}}(4M + 3r({\mu^\ell}_1)^2 \\
&+ r({\mu^\ell}_2)^2) + i\Big(\bar{h}^{9\ell,\mathrm{m}}_{(2)\mathcal{P}}(4M - r({\mu^\ell}_1)^2 + r({\mu^\ell}_2)^2) + 4r\big(i\bar{h}^{1\ell,\mathrm{m}}_{(2)\mathcal{P}}({\mu^\ell}_1)^2 + r(2\omega\bar{h}^{4\ell,\mathrm{m}}_{(2)\mathcal{P}} \\
&+ i({\mu^\ell}_1)^2\bar{h}^{1\ell,\mathrm{m}}_{(2)\mathcal{P},r} - r\omega\bar{h}^{4\ell,\mathrm{m}}_{(2)\mathcal{P},r})\big)\Big)\Big) + 2f^2r(13\bar{h}^{5\ell,\mathrm{m}}_{(2)\mathcal{P}} - 6\bar{h}^{7\ell,\mathrm{m}}_{(2)\mathcal{P}} + i\bar{h}^{9\ell,\mathrm{m}}_{(2)\mathcal{P}} + 2\bar{h}^{3\ell,\mathrm{m}}_{(2)\mathcal{P}}({\mu^\ell}_1)^2 \\
&+ 10\bar{h}^{6\ell,\mathrm{m}}_{(2)\mathcal{P}}({\mu^\ell}_1)^2 + 2r({\mu^\ell}_1)^2\bar{h}^{3\ell,\mathrm{m}}_{(2)\mathcal{P},r} - 2r({\mu^\ell}_1)^2\bar{h}^{6\ell,\mathrm{m}}_{(2)\mathcal{P},r} + 2r\bar{h}^{7\ell,\mathrm{m}}_{(2)\mathcal{P},r} - 2r^2\bar{h}^{5\ell,\mathrm{m}}_{(2)\mathcal{P},r,r})\Big) \\
\Delta T^{6\ell,\mathrm{m}}_{(2)\mathrm{effB}}[h^{i\ell,\mathrm{m}}_{(2)\mathcal{P}}] &= \frac{1}{2f^3r^3}\Big(4iMr\omega\bar{h}^{2\ell,\mathrm{m}}_{(2)\mathcal{P}} + f\big((4M-r^3\omega^2)\bar{h}^{1\ell,\mathrm{m}}_{(2)\mathcal{P}} - 2M(ir\omega\bar{h}^{2\ell,\mathrm{m}}_{(2)\mathcal{P}} + 2\bar{h}^{5\ell,\mathrm{m}}_{(2)\mathcal{P}} \\
&- 2r\bar{h}^{1\ell,\mathrm{m}}_{(2)\mathcal{P},r})\big) - f^2\big((4M+r^3\omega^2)\bar{h}^{3\ell,\mathrm{m}}_{(2)\mathcal{P}} + 8M\bar{h}^{6\ell,\mathrm{m}}_{(2)\mathcal{P}} + r(ir\omega\bar{h}^{4\ell,\mathrm{m}}_{(2)\mathcal{P}} - 2ir^2\omega\bar{h}^{2\ell,\mathrm{m}}_{(2)\mathcal{P},r} \\
&+ 4M\bar{h}^{3\ell,\mathrm{m}}_{(2)\mathcal{P},r})\big) - f^3\big(2M\bar{h}^{3\ell,\mathrm{m}}_{(2)\mathcal{P}} + 4M\bar{h}^{6\ell,\mathrm{m}}_{(2)\mathcal{P}} + r(2\bar{h}^{1\ell,\mathrm{m}}_{(2)\mathcal{P}} - 2\bar{h}^{5\ell,\mathrm{m}}_{(2)\mathcal{P}} + 2M\bar{h}^{3\ell,\mathrm{m}}_{(2)\mathcal{P},r} + r\bar{h}^{5\ell,\mathrm{m}}_{(2)\mathcal{P},r} \\
&- r^2\bar{h}^{1\ell,\mathrm{m}}_{(2)\mathcal{P},r,r})\big) + f^4r\big(2\bar{h}^{3\ell,\mathrm{m}}_{(2)\mathcal{P}} + 4\bar{h}^{6\ell,\mathrm{m}}_{(2)\mathcal{P}} - r(2\bar{h}^{6\ell,\mathrm{m}}_{(2)\mathcal{P},r} + r\bar{h}^{3\ell,\mathrm{m}}_{(2)\mathcal{P},r,r})\big)\Big)
\end{aligned}
\tag{4.129}
$$

and

$$\Delta T^{7\ell,\mathtt{m}}_{(2)\text{effB}}[h^{i\ell,\mathtt{m}}_{(2)\mathcal{P}}] = \frac{1}{4fr^3}\Big(4f^2r(\bar{h}^{7\ell,\mathtt{m}}_{(2)\mathcal{P}} + i\bar{h}^{10\ell,\mathtt{m}}_{(2)\mathcal{P}}) - 2ir^2\omega\bar{h}^{4\ell,\mathtt{m}}_{(2)\mathcal{P}}(\mu^\ell{}_2)^2 + f\big(i\bar{h}^{10\ell,\mathtt{m}}_{(2)\mathcal{P}}(8M - r(\mu^\ell{}_2)^2 + r(\mu^\ell{}_3)^2) + \bar{h}^{7\ell,\mathtt{m}}_{(2)\mathcal{P}}(8M + r(\mu^\ell{}_2)^2 + r(\mu^\ell{}_3)^2) - 2r(\mu^\ell{}_2)^2(2\bar{h}^{5\ell,\mathtt{m}}_{(2)\mathcal{P}} + \bar{h}^{6\ell,\mathtt{m}}_{(2)\mathcal{P}}(\mu^\ell{}_1)^2 + r\bar{h}^{5\ell,\mathtt{m}}_{(2)\mathcal{P},r})\big)\Big)$$

$$\Delta T^{8\ell,\mathtt{m}}_{(2)\text{effB}}[h^{i\ell,\mathtt{m}}_{(2)\mathcal{P}}] = \frac{1}{8fr^3}\Big(-4r\omega(-2iM + r^2\omega)\bar{h}^{8\ell,\mathtt{m}}_{(2)\mathcal{P}} + 2f^2r(-i\bar{h}^{4\ell,\mathtt{m}}_{(2)\mathcal{P}} + \bar{h}^{8\ell,\mathtt{m}}_{(2)\mathcal{P}}) + f\big(-i\bar{h}^{4\ell,\mathtt{m}}_{(2)\mathcal{P}}(4M - r(\mu^\ell{}_1)^2 + r(\mu^\ell{}_2)^2) + \bar{h}^{8\ell,\mathtt{m}}_{(2)\mathcal{P}}(4M - r(\mu^\ell{}_1)^2 + r(\mu^\ell{}_2)^2) + 4(2M + ir^2\omega)(2\bar{h}^{9\ell,\mathtt{m}}_{(2)\mathcal{P}} - \bar{h}^{10\ell,\mathtt{m}}_{(2)\mathcal{P}} + r\bar{h}^{9\ell,\mathtt{m}}_{(2)\mathcal{P},r})\big)\Big)$$

$$\Delta T^{9\ell,\mathtt{m}}_{(2)\text{effB}}[h^{i\ell,\mathtt{m}}_{(2)\mathcal{P}}] = \frac{1}{8fr^3}\Big(8iMr\omega 1\bar{h}^{8\ell,\mathtt{m}}_{(2)\mathcal{P}} + f\big(-i\bar{h}^{5\ell,\mathtt{m}}_{(2)\mathcal{P}}(4M - r(\mu^\ell{}_1)^2 + r(\mu^\ell{}_2)^2) + \bar{h}^{9\ell,\mathtt{m}}_{(2)\mathcal{P}}(4M - r(\mu^\ell{}_1)^2 + r(\mu^\ell{}_2)^2) - 4ir^2\omega 1(-2\bar{h}^{8\ell,\mathtt{m}}_{(2)\mathcal{P}} + r\bar{h}^{8\ell,\mathtt{m}}_{(2)\mathcal{P},r})\big) - 2f^2r(i\bar{h}^{5\ell,\mathtt{m}}_{(2)\mathcal{P}} - 13\bar{h}^{9\ell,\mathtt{m}}_{(2)\mathcal{P}} + 6\bar{h}^{10\ell,\mathtt{m}}_{(2)\mathcal{P}} - 2r\bar{h}^{10\ell,\mathtt{m}}_{(2)\mathcal{P},r} + 2r^2\bar{h}^{9\ell,\mathtt{m}}_{(2)\mathcal{P},r,r})\Big)$$

$$\Delta T^{10\ell,\mathtt{m}}_{(2)\text{effB}}[h^{i\ell,\mathtt{m}}_{(2)\mathcal{P}}] = \frac{1}{4fr^3}\Big(4f^2r(-i\bar{h}^{7\ell,\mathtt{m}}_{(2)\mathcal{P}} + \bar{h}^{10\ell,\mathtt{m}}_{(2)\mathcal{P}}) - 2ir^2\omega\bar{h}^{8\ell,\mathtt{m}}_{(2)\mathcal{P}}(\mu^\ell{}_2)^2 + f\big(-i\bar{h}^{7\ell,\mathtt{m}}_{(2)\mathcal{P}}(8M - r(\mu^\ell{}_2)^2 + r(\mu^\ell{}_3)^2) + \bar{h}^{10\ell,\mathtt{m}}_{(2)\mathcal{P}}(8M + r(\mu^\ell{}_2)^2 + r(\mu^\ell{}_3)^2) - 2r(\mu^\ell{}_2)^2(2\bar{h}^{9\ell,\mathtt{m}}_{(2)\mathcal{P}} + r\bar{h}^{9\ell,\mathtt{m}}_{(2)\mathcal{P},r})\big)\Big). \tag{4.130}$$

The total $\Delta T^{1\ell,\mathtt{m}}_{(2)\text{eff}}$ is

$$\Delta T^{1\ell,\mathtt{m}}_{(2)\text{eff}} = \Delta T^{1\ell,\mathtt{m}}_{(2)\text{effA}} + \Delta T^{1\ell,\mathtt{m}}_{(2)\text{effB}}. \tag{4.131}$$

I give these expressions to Ben Leather, who uses Barry Wardell's code to calculate $\mathcal{S}[\Delta T^{(2)\text{eff}}_{ab}]$. The input $\vec{\partial}_{\mathcal{V}}h^{i\ell,\mathtt{m}}$ is provided by Leanne Durkan. $h^{i\ell,\mathtt{m}}_{(2)\mathcal{P}}$ is provided by the data used in the calculation in Refs. [195, 194, 156].

This completes the source calculation in the world-tube. Except, there are some delta functions on the particle which we have missed. These arise due to the derivatives in $\mathcal{S}_4$ acting on C^0 content in $\delta^2 G[h^{\mathcal{P}}_{ab}, h^{\mathcal{R}}_{ab}]$. We are currently calculating this contribution and will add it to the source shortly.

4.3 Current status of the source to the reduced second-order Teukolsky equation

I have described and derived many parts of the source to the reduced second-order Teukolsky equation. These pieces need to be put together and transformed to hyperboloidal coordinates in order for Ben Leather to solve for $\psi_{4L}^{(2)\ell,\mathtt{m}}$ using spectral methods [105, 106].

Fig. 4.7 shows the parts of the source currently working in hyperboloidal coordinates. Outside of the world-tube ($\sigma_- < \sigma < \sigma_+$) the source is calculated using the mode decomposition formula derived in Sec. 4.2.1. Also, a transformation to the near-Bondi– Sachs gauge has been implemented on the left-hand side of Fig. 4.7. Note that the source converges due to this gauge transformation. Inside the world-tube, the effective source [120] from Refs. [195, 194, 156] has been used, plus the correction to the effective source given in Sec. 4.2.9.

There is, however, a distributional piece that we have not yet accounted for in the effective source. Formulas have been derived for this piece and will be added shortly. Finally, the slow-time derivative contribution needs to be added. The slow-time derivative contribution currently contains divergent behaviour near the horizon. This is due to my formulas being derived on t-slicing. I will re-derive the formulas for the slow-time derivative contribution on s-slicing and this will remove the divergent behaviour.

With the complete source to the reduced second-order Teukolsky equation, Ben Leather will account for the jumps on the world-tube boundaries caused by switching to the effective source and the gauge transformation to the Bondi–Sachs gauge (given in Sec. 4.2.8). He will then solve for $\psi_{4L}^{(2)\ell,\mathtt{m}}$ using spectral methods. We will then extract the energy flux from $\psi_{4L}^{(2)\ell,\mathtt{m}}$ and compare the results to Ref. [195]. Once we have completed this procedure on a grid of r_0 values we can generate first-post-adiabatic waveforms. In the near future, waveforms like these will be used to help inform models used to detect IMRIs in LIGO/Virgo/KAGRA data analysis.

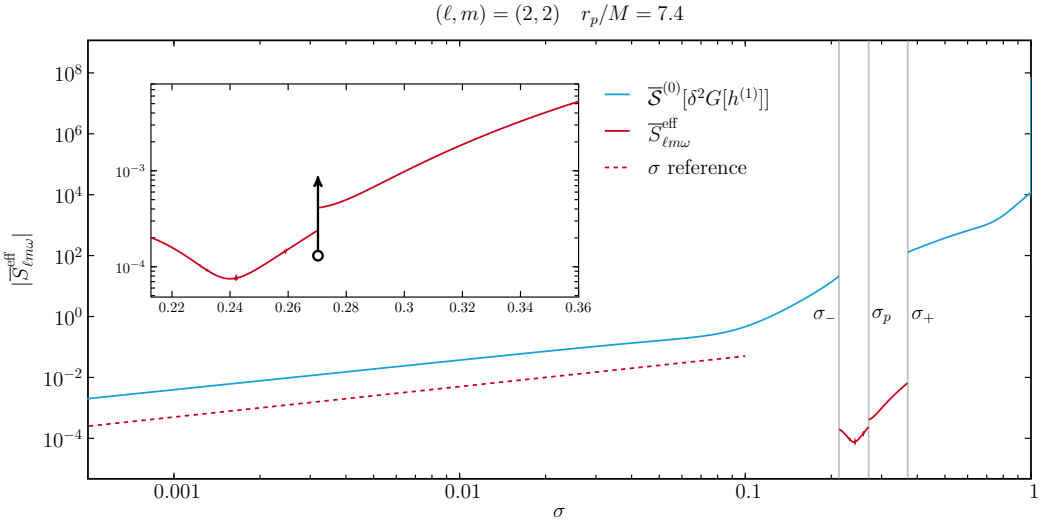

FIGURE 4.7: A plot of the $\ell = 2, \mathtt{m} = 2$ mode of the source in hyperboloidal slicing. The Bondi–Sachs gauge has been implemented near future null infinity (the left-hand side of the plot), causing the source to converge. Inside the world-tube, $\sigma_- < \sigma < \sigma_+$, the effective source (from Refs. [120, 195, 194, 156]) has been used. Note how the source is regular on the worldline. Two pieces are missing from this source, a distributional piece on the worldline and a slow-time derivative contribution. Plot courtesy of Ben Leather.

Chapter 5

GHZ Metric Reconstruction and Self-Force Calculations

Recently, Green, Hollands, and Zimmerman (GHZ) [86] presented a method for calculating non-vacuum metric perturbations in Kerr; here, I shall call this procedure *GHZ metric reconstruction*. This publication was a momentous step forward in black hole perturbation theory as it provided a method for calculating non-linear metric perturbations in Kerr.

Here, I summarise how GHZ extended CCK metric reconstruction to non-vacuum perturbations and discuss this method's potential for extending self-force calculations to second order. Following, in Sec. 5.2, I implement GHZ metric reconstruction for a perturbation produced by a stationary point mass in a flat background spacetime. The toy model provided crucial insights used to formulate a metric reconstruction scheme for self-force calculations. This scheme can calculate a sufficiently regular first-order metric perturbation to source second-order self-force calculations [183]. This work was completed in collaboration with V. Toomani, P. Zimmerman, S. Hollands, A. Pound, and S. Green, and forms part of our paper Ref. [183].

5.1 A summary of GHZ metric reconstruction

GHZ showed that any metric perturbation to a Kerr background spacetime can be written as

$$h^{(n)}_{ab} = x_{ab} + \dot{g}_{ab} + \mathrm{Re}[\mathcal{S}_0^\dagger \Phi]_{ab}, \tag{5.1}$$

where x_{ab} is known as a *corrector tensor*, $\dot{g}_{ab} := \frac{d}{ds} g^{M(s),a(s)}_{ab}|_{s=0}$ (a perturbation to another metric in the Kerr family), and Φ is, again, a Hertz potential. Eq. (5.1) is in an

outgoing radiation gauge ($h^{(n)}_{ab} l^a = 0$), a key property in the derivation of this method. Note, as discussed in Sec. 1.8.1, any metric perturbation can be put into the outgoing radiation gauge [158].

The GHZ method built on CCK metric reconstruction (see Sec. 1.8). The $\mathrm{Re}[\mathcal{S}_0^\dagger \Phi]_{ab}$ piece of Eq. (5.1) is equivalent to CCK metric reconstruction. CCK showed that their method was consistent in vacuum. GHZ showed that CCK metric reconstruction can be made consistent for non-vacuum perturbations with the inclusion of a corrector tensor (x_{ab}).

As a preliminary step, before describing how GHZ extended CCK metric reconstruction to non-vacuum, first I note, CCK metric reconstruction produces a metric perturbation in the trace-free radiation gauge ($h_{la} = h_{m\bar{m}} = 0$, see Sec. 1.8.1). Price, Shankar, and Whiting [158] showed that any metric perturbation of a Petrov type II (and type D) background spacetime, where $T^{(1)}_{ll} = 0$, can be expressed in a trace-free radiation gauge. However, this is not sufficient to show CCK metric reconstruction holds for any perturbation with $T^{(1)}_{ll} = 0$.

To describe how GHZ showed (in Kerr) that the validity of CCK metric reconstruction extends beyond vacuum perturbations, I will outline their proof in reverse order of how they present it in their paper. Firstly, GHZ showed CCK metric reconstruction alone extends beyond vacuum perturbations. For a perturbation with a smooth source of compact support, if the condition on the stress-energy tensor $T^{(1)}_{la} = 0$ is satisfied, the metric perturbation can be written as $h_{ab} = \mathrm{Re}[\mathcal{S}_0^\dagger \Phi]_{ab}$ (up to perturbations to another Kerr solution).

I will now outline how GHZ showed $h_{ab} = \mathrm{Re}[\mathcal{S}_0^\dagger \Phi]_{ab}$ when $T^{(1)}_{la} = 0$. First note, $T^{(1)}_{ll} = 0$; therefore, according to Ref. [158], a trace-free radiation metric perturbation exists. The CCK metric perturbation ($h_{ab} = \mathrm{Re}[\mathcal{S}_0^\dagger \Phi]_{ab}$) trivially satisfies the trace-free radiation gauge condition as $\mathcal{S}^\dagger_{0\, l[a]} = \mathcal{S}^\dagger_{0\, m\bar{m}} = 0$ (see. Eq. (1.93)). The remaining components of the trace-free radiation gauge metric perturbation are the nn, nm and mm components (and their complex conjugates). GHZ showed that any trace-free radiation gauge metric perturbation satisfying $\mathcal{E}[h_{ab}]_{l\bar{m}} = 0$ and $\mathcal{E}[h_{ab}]_{ln} = 0$ can be written as $h_{ab} = \mathrm{Re}[\mathcal{S}_0^\dagger \Phi]_{ab}$[1] up to gauge[2]. By analysing each non-trivial component, h_{nn}, h_{nm}, and h_{mm} (and their complex conjugates) GHZ showed there exists a Φ such that $h_{ab} = \mathrm{Re}[\mathcal{S}_0^\dagger \Phi]_{ab}$ (up to gauge).

A keen reader will have noticed $\mathcal{E}[\mathcal{S}_0^\dagger \Phi]_{m\bar{m}} = 0$.

[1] This proof uses $(\mathcal{E}\mathcal{S}_0^\dagger \Phi)_{l\bar{m}} = (\mathcal{E}\mathcal{S}_0^\dagger \Phi)_{ln} = 0$ for any Φ, which is trivial when considering $\mathcal{T}_0^\dagger \mathcal{O}_0^\dagger = \mathcal{E}\mathcal{S}_0^\dagger$ and $\mathcal{T}^\dagger_{l\bar{m}} = \mathcal{T}^\dagger_{ln} = 0$ by definition.

[2] The proof also uses the residual freedom in the trace free radiation gauge. The resulting gauge also appears to be not unique, there exists a residual gauge vector $\zeta^a = -\zeta^\circ_n l^a$ (using Held's notation [90] where the superscript circle denotes that such a quantity is annihilated by Þ). This can concluded from ζ°_n not appearing in Eq (77) of Ref. [86].

This can be seen by considering $\mathcal{T}_0^\dagger \mathcal{O}_0^\dagger = \mathcal{E}\mathcal{S}_0^\dagger$ and $\mathcal{T}_0^\dagger{}_{m\bar{m}} = 0$ by definition [154]. Hence, $T^{(1)}_{m\bar{m}} = 0$. This may seem problematic for GHZ metric reconstruction because it does not explicitly state the assumption $T^{(1)}_{m\bar{m}} = 0$ for CCK metric reconstruction to be consistent. However, this condition holds due to the other assumptions for which CCK metric reconstruction is consistent; that is, $T^{(1)}_{m\bar{m}} = 0$ for any $T^{(1)}_{ab}$ which satisfies $\nabla^a T^{(1)}_{ab} = 0$ and $T^{(1)}_{la} = 0$ [183].

GHZ also showed that Φ relates to ψ_4 through the conventional CCK metric reconstruction equation (Eq. (1.91)). A crucial difference to the CCK metric reconstruction is Φ satisfies $\mathcal{O}\Phi = \eta$ (rather than $\mathcal{O}\Phi = 0$ in the vacuum case). η is a complex scalar that can be calculated from the stress energy tensor T_{ab}, as I will describe shortly. Hence, it is possible to construct a metric without calculating ψ_4 directly.

The second leap forward made by GHZ [86] was extending metric reconstruction to include perturbations which do not satisfy $T^{(1)}_{la} = 0$. They achieved this by introducing a so-called corrector tensor (x_{ab}) to handle the $T_{la} \neq 0$ part of the source. By using the ansatz,

$$x_{ab} = 2m_{(a}\bar{m}_{b)}x_{m\bar{m}} - 2l_{(a}\bar{m}_{b)}x_{nm} - 2l_{(a}m_{b)}x_{n\bar{m}} + l_a l_a x_{nn}, \tag{5.2}$$

they showed x_{ab} could be calculated by solving three hierarchical ODEs aligned with outgoing null rays. The three hierarchical ODEs are obtained by contracting l^a, m^a and n^a, respectively, with

$$\mathcal{E}[x_{cd}]_{la} = T_{la}. \tag{5.3}$$

The ODEs are given in Eqs. (56), (57) and (58) of Ref. [86]; for example,

$$(\text{Þ}(\text{Þ} - \rho - \bar{\rho}) + 2\rho\bar{\rho})\, x_{m\bar{m}} = T_{ll}, \tag{5.4}$$

where the thorns simplify to radial derivatives in the Kinnersley tetrad in Kerr–Newman coordinates (see Appendix B of Ref. [86]).

Having calculated x_{ab}, one can find an effective metric perturbation, $\tilde{h}_{ab} := h_{ab} - x_{ab}$, which satisfies

$$\mathcal{E}[\tilde{h}_{cd}]_{la} = \tilde{T}_{ab} := T_{ab} - \mathcal{E}x_{ab}. \tag{5.5}$$

As $\tilde{T}_{la} = 0$ (by the definition of x_{ab}), $\tilde{h}_{ab}$ can be found using CCK metric reconstruction using the appropriate Hertz potential. The Hertz potential can be calculated from the CCK inversion relation,

$$-\frac{1}{4}\text{Þ}^4\bar{\Phi} = \psi_0. \tag{5.6}$$

The CCK metric reconstruction inversion relation is consistent in $\tilde{T}_{la} = 0$ because $\mathcal{T}_0[x_{ab}] = 0$ (by the ansatz used for x_{ab}).

Alternatively, one can calculate the Hertz potential from η. Having calculated x_{ab}, one can calculate η using

$$Re[\mathcal{T}'^{\dagger}\eta]_{ab} = T_{ab} - \mathcal{E}[x_{cd}]_{ab}. \tag{5.7}$$

For example, taking the $\bar{m}\bar{m}$ component of Eq. (5.7) gives

$$\frac{1}{4}(\text{Þ} - \rho)(\text{Þ} - \rho)\eta = T_{\bar{m}\bar{m}} - \mathcal{E}[x_{cd}]_{\bar{m}\bar{m}}, \tag{5.8}$$

which can be solved for η. From η one can calculate the Hertz potential using

$$\mathcal{O}\Phi = \eta. \tag{5.9}$$

$\tilde{h}_{ab}$ is then given by

$$\tilde{h}_{ab} = \text{Re}[\mathcal{S}_0^{\dagger}\Phi]_{ab}. \tag{5.10}$$

The full metric perturbation is $h_{ab} = \tilde{h}_{ab} + x_{ab}$ and satisfies the non-vacuum linearised Einstein field equation in Kerr (for a smooth source of compact support). The final piece to add to the metric perturbation is $\dot{g}_{ab}$, a vacuum perturbation to another Kerr solution (known as the completion piece, see Sec. 1.8.2), which can be calculated using techniques developed in Ref. [117]. $\dot{g}_{ab}$ is actually redundant in GHZ metric reconstruction as x_{ab} contains this piece of the perturbation, as I show in Sec. 5.2.

5.1.1 Discussion: prospect for using GHZ metric reconstruction for self-force calculations

When Ref. [86] was first published, an open question was how it could be utilized to help self-force calculations. One problem facing self-force is obtaining a sufficiently regular first-order metric perturbation to source second-order calculations. Can GHZ metric reconstruction be utilized to find a sufficiently regular metric perturbation?

As discussed in Sec. 1.8.1, CCK metric reconstruction in the self-force problem produces string singularities emanating from the particle (to either the horizon, out to asymptotic infinity, or both), or singularities on a sphere containing the particle, see Fig. 3.1. Second-order calculations are sourced by quadratic operators acting on the first-order metric perturbation. When inputting the CCK metric perturbation, the resulting second-order source contains products of delta functions, which are not well defined.

GHZ is similar to CCK metric reconstruction, but can the additional information it offers help to regularise the metric perturbation? Off the particle, CCK metric reconstruction can recover the whole metric perturbation as the perturbation is vacuum. However, on the sphere containing the particle CCK metric reconstruction breaks down (as the perturbation is non-vacuum). Hence, CCK metric reconstruction cannot recover the entire metric perturbation on this sphere. In practice, in the CCK no-string solution there is missing the radial delta function coefficient on the sphere [155]. Our collaboration conjectured, by using GHZ metric reconstruction, these coefficients could be calculated. In Sec. 5.2 I show how GHZ recovers the whole metric perturbation for the flat spacetime example.

Our collaboration also conjectured that it would be easier to regularise the metric perturbation with the whole metric perturbation. In Sec. 5.3, I summarise the punctured shadowless gauge formalism. This formalism uses GHZ metric reconstruction, gauge transformations, and a puncture scheme to ameliorate singularities in the radiation gauge. When implemented, the resulting metric perturbation will be sufficiently regular to source second-order calculations. The formalism would not be possible without obtaining the whole metric perturbation with GHZ metric reconstruction. Implementation of this formalism in Kerr is in the planning stages.

There is another possible utility in GHZ metric reconstruction for self-force calculations: calculating $h^{(2)}_{ab}$. Eq. (5.1) can be used to calculate a metric perturbation to any perturbative order (given the source is constructed from the lower order metric perturbations). Ref. [86] does discuss how the current proof is limited to a source of compact support whereas perturbations beyond the linear order are sourced by all preceding perturbations, so are non-compact. However, this seems to be an overly conservative constraint. Ref. [86] states that they expect this issue can be overcome and will be addressed in a forthcoming paper.

GHZ metric reconstruction is not the only hope for second-order calculations. Ref. [10] provides identities for linearised gravity in Kerr which can be used for non-vacuum metric reconstruction. This method has been used in combination with a gauge transformation to the Lorenz gauge to produce a Lorenz gauge metric reconstruction technique [64].

5.1.2 The reduced second-order Teukolsky equation and GHZ metric reconstruction

The reduced second-order Teukolsky equation appears implicitly in GHZ metric reconstruction [86]. There are multiple routes to implementing second-order GHZ metric reconstruction, and one involves solving the reduced second-order Teukolsky

equation, Eq. (2.20). As discussed in section 5 of Ref. [86], $T_{ab} = T^{(2)}_{ab} - \delta^2 G[h^{(1)}_{ab}]$ at second order (though they omit $T^{(2)}_{ab}$, which must be included for self-force calculations). Hence, Eq. (98) in Ref. [86] becomes the spin +2 reduced second-order Teukolsky equation. That is, the second-order form of Eq. (98) in Ref. [86] solves for $\psi^{(2)}_{0L}$. This distinction, that only the linear piece of the Weyl scalar is solved for (and the existence of the reduced-nth-order Teukolsky equation), is not stated explicitly in Ref. [86], but is an implicit result of their method.

Returning to the goal of calculating first-post-adiabatic EMRI models, full second-order GHZ metric reconstruction may be unnecessary. Calculating $\psi^{(2)}_{4L}$ (or $\psi^{(2)}_{0L}$) may be sufficient, as only the dissipative second-order self-force is required. As $\psi^{(2)}_{4L}$ contains the information of the gravitational waves being dissipated away from the system, it is reasonable to expect the dissipative second-order self-force could be extracted from $\psi^{(2)}_{4L}$. However, (as discussed in Sec. 1.7.4) this will require balance laws (in a usable form) relating the orbital energy, angular momentum, and Carter constant to the emitted gravitational wave fluxes. Hence, for EMRI models calculating $h^{(2)}_{ab}$ (and therefore second-order GHZ metric reconstruction) may be unnecessary.

An advantage of only solving the reduced second-order Teukolsky equation (Eq. (2.20)) is that it involves solving fewer differential equations numerically (and hence is faster) than full GHZ metric reconstruction. Looking away from the motivation of modelling EMRIs, calculating the second-order metric perturbation will have other benefits in self-force. Information about the conservative second-order self-force will allow comparison with high-order post-Newtonian and post-Minkowski terms and help calibrate effective one-body theory [57]. In these cases implementing GHZ metric reconstruction at second order would be advantageous, as it can be used to calculate both the dissipative and conservative second-order self-force. Also, for third- and higher-order calculations obtaining the full $h^{(2)}_{ab}$ will be required.

5.2 GHZ metric reconstruction for a toy model

Here I implement first-order GHZ metric reconstruction for a perturbation produced by a stationary point mass in a flat background spacetime. Throughout, I compare the results to Ref. [155] (which solved the same problem with CCK metric reconstruction) and discuss the new information provided by GHZ metric reconstruction.

5.2.1 GHP quantities in flat spacetime for a stationary point mass perturbation

Before I begin constructing a metric perturbation in flat spacetime, I first give an overview of the GHP formalism (see Sec. 5.1) in flat spacetime. I also summarise the

stress-energy tensor produced by a stationary point-mass perturbation. Note, for this chapter only, I work in the $(+---)$ signature and absorb a factor of 8π into the stress-energy tensor and mass of the compact object,

$$8\pi T_{ab} \to T_{ab}, \quad 8\pi\mu \to \mu, \tag{5.11}$$

as to be consistent with Refs. [86, 183].

Here, I work in retarded time coordinates, $\{u, r, \theta, \phi\}$ ($u := t - r$ in flat space), and in the Kinnersley tetrad. In flat spacetime, the Kinnersley tetrad expressed in retarded time coordinates is

$$l^\mu = (0,1,0,0),\, n^\mu = (1,-\frac{1}{2},0,0),\, m^\mu = \frac{1}{\sqrt{2}r}(0,0,1,i\sin[\theta]). \tag{5.12}$$

In this tetrad and coordinate scheme, the zeroth-order GHP spin coefficients take the form

$$\kappa = \kappa' = \sigma = \sigma' = \epsilon = \epsilon' = \tau = \tau' = 0 \tag{5.13}$$

$$\rho = -\frac{1}{r},\, \rho' = \frac{1}{2r},\, \beta = \beta' = \frac{\cot[\theta]}{2\sqrt{2}r}. \tag{5.14}$$

As no curvature is present in flat spacetime, the zeroth-order Weyl scalars are zero,

$$\psi_0 = \psi_1 = \psi_2 = \psi_3 = \psi_4 = 0. \tag{5.15}$$

The GHP derivative operators, assuming a stationary perturbation (i.e., all t derivatives are zero), are given as

$$\begin{aligned} \text{Þ} &= l^\mu\partial_\mu = \partial_r, & \text{Þ}' &= n^\mu\partial_\mu = -\frac{1}{2}\partial_r, \\ \eth &= m^\mu\partial_\mu - s\beta = \frac{1}{\sqrt{2}r}\hat{\eth}, & \eth' &= \overline{m}^\mu\partial_\mu + s\beta = \frac{1}{\sqrt{2}r}\hat{\eth}', \end{aligned} \tag{5.16}$$

where $\hat{\eth}$ and $\hat{\eth}'$ are spin raising and spin lowering operators acting on a spin-weight s object defined in Eq. (4.41). The spin raising/lowering operators obey the relations of Eqs. (4.42), (4.43), and (4.44) when acting on spin-weighted spherical harmonics. I will also use the complex conjugate relation for spin-weighted spherical harmonics given by Eq. (4.45).

I will use the stress-energy of point mass perturbation (of mass μ), given by,

$$\begin{aligned} T^{\alpha\beta}_{(1)} := T^{\alpha\beta} =& \mu u^\alpha u^\beta \delta^3[\vec{x} - \vec{x}_p] \\ =& \mu\delta^\alpha_u\delta^\beta_u\delta^3[\vec{x} - \vec{x}_p], \end{aligned} \tag{5.17}$$

where the four-velocity $u^\alpha = \delta^\alpha_u$ (δ^α_β is the Kronecker delta function) as the particle is stationary.

I will use the boundary conditions that $x_{ab} = 0$ and $\eta = 0$ for $r < r_p$, as to generate a half-string solution (one could alternatively set $x_{ab} = 0$ and $\eta = 0$ for $r > r_p$ to generate another half-string solution).

5.2.2 Calculating the corrector tensor x_{ab}

The first step in GHZ metric reconstruction is calculating the corrector tensor x_{ab} using the ansatz

$$x_{ab} = 2m_{(a}\bar{m}_{b)}x_{m\bar{m}} - 2l_{(a}\bar{m}_{b)}x_{nm} - 2l_{(a}m_{b)}x_{n\bar{m}} + l_a l_b x_{nn}. \tag{5.18}$$

Following GHZ's prescribed method, I calculating each component of x_{ab} in an iterative manner.

5.2.2.1 Calculating $x_{m\bar{m}}$

I begin by solving Eq. (56) in Ref. [86] for $x_{m\bar{m}}$. In flat spacetime this can be written as

$$\begin{aligned} &\big(\text{Þ}(\text{Þ} - \rho - \bar{\rho}) + 2\rho\bar{\rho}\big)x_{m\bar{m}} = T_{ll} \\ \Rightarrow &\big(\partial_r^2 + \frac{2}{r}\partial_r\big)x_{m\bar{m}} = \frac{\mu}{r_p^2}\delta^2[\theta^A - \theta_p^A]\delta[r - r_p], \end{aligned} \tag{5.19}$$

where I have inputted Eq. (5.17) for the stress-energy tensor. This equation can be solved for $x_{m\bar{m}}$, giving

$$x_{m\bar{m}} = \mu\frac{r - r_p}{rr_p}\Theta[r - r_p]\delta^2[\theta^A - \theta_p^A] + \frac{a}{r} + b, \tag{5.20}$$

where $\Theta[r - r_p]$ is a Heaviside function and a and b are functions independent of r. Imposing the boundary condition that $x_{ab} = 0$ for $r < r_p$ results in $a = b = 0$. This gives

$$x_{m\bar{m}} = \mu\frac{r - r_p}{rr_p}\Theta[r - r_p]\delta^2[\theta^A - \theta_p^A]. \tag{5.21}$$

5.2.2.2 Calculating x_{nm}

Next, I turn my attention to calculating x_{nm}. I need to solve Eq. (57) in Ref. [86],

$$\frac{1}{2}\big(\text{Þ}(\text{Þ}-2\rho)+2\bar{\rho}(\rho-\bar{\rho})\big)x_{nm} = T_{lm} - \frac{1}{2}\big((\text{Þ}+\rho-\bar{\rho})(\eth+\bar{\tau}'-\tau)) + 2\bar{\tau}'(\text{Þ}-2\rho) - (\eth-\tau-\bar{\tau}')\bar{\rho}+2\rho\tau\big)x_{m\bar{m}} \tag{5.22}$$

In a stationary flat spacetime, inputting $T_{lm}=0$ and Eq. (5.21) for $x_{m\bar{m}}$, this simplifies to

$$\left(\partial_r^2+\frac{2}{r}\partial_r-\frac{2}{r}\right)x_{nm} = -\frac{\mu}{\sqrt{2}rr_p}\hat{\eth}\delta^2[\theta^A-\theta_p^A]\;\partial_r\left(\frac{r-r_p}{r}\Theta[r-r_p]\right). \tag{5.23}$$

Solving for x_{nm} gives

$$x_{nm} = -\frac{\mu}{\sqrt{2}}\frac{(r-r_p)^2(r+2r_p)}{6r^2r_p^2}\Theta[r-r_p]\;\hat{\eth}\delta^2[\theta^A-\theta_p^A]+ar+\frac{b}{r^2}, \tag{5.24}$$

where a and b are independent of r. Again, imposing the boundary condition $x_{ab}=0$ for $r<r_p$ gives $a=b=0$. Additionally, I calculate a mode decomposition. A mode decomposition of the angular Dirac delta function is

$$\delta^2[\theta^A-\theta_p^A] = \sum_{\ell=0,m}^{\infty}\overline{Y}_{\ell,\mathtt{m}}[\theta_p^A]\;Y_{\ell,\mathtt{m}}[\theta^A]. \tag{5.25}$$

Inputting this into Eq. (5.24) results in (with $a=b=0$)

$$x_{nm} = \sum_{\ell=1,m}^{\infty}\frac{\mu}{\sqrt{2}}\frac{(r-r_p)^2(r+2r_p)}{6r^2r_p^2}\Theta[r-r_p]\sqrt{\ell(\ell+1)}\overline{Y}_{\ell,\mathtt{m}}[\theta_p^A]\;{}_1Y_{\ell,\mathtt{m}}[\theta^A], \tag{5.26}$$

where the sum runs from $\ell=1$ because spin weighted spherical harmonics exist for $\ell\geq|s|$ (the m sum always runs from $-\ell$ to ℓ, but I omit this label for brevity).

5.2.2.3 Calculating x_{nn}

Finally, I turn my attention to calculating x_{nn}. Eq. (58) in Ref. [86] is

$$\begin{aligned}\frac{1}{2}\big(\rho(\text{Þ}-\rho)+\bar{\rho}(\text{Þ}-\bar{\rho})\big)x_{nn} &= T_{ln} - \frac{1}{2}\big((\eth'+\tau'-\bar{\tau})(\eth-\tau+\bar{\tau}')\\ &+(\eth'\eth-\tau\tau'-\bar{\tau}\bar{\tau}'+\tau\bar{\tau})-(\psi_2+\bar{\psi}_2)+(\text{Þ}'-2\rho')\bar{\rho}+(\text{Þ}-2\bar{\rho})\rho'+\rho(3\text{Þ}'-2\bar{\rho}')\\ &+\bar{\rho}'(3\text{Þ}-2\rho)-2\text{Þ}'\text{Þ}+2\rho\bar{\rho}'+2\eth'(\tau)-\tau\bar{\tau}\big)x_{m\bar{m}}-\frac{1}{2}\big((\text{Þ}-2\rho)(\eth'-\bar{\tau})\\ &+(\tau'+\bar{\tau})(\text{Þ}+\bar{\rho})-2(\eth'-\tau')\rho-2\bar{\tau}\text{Þ}\big)x_{nm}-\frac{1}{2}\big((\text{Þ}-2\bar{\rho})(\eth-\tau)+(\bar{\tau}'+\tau)(\text{Þ}+\rho)\\ &-2(\eth-\bar{\tau}')\bar{\rho}-2\tau\text{Þ}\big)x_{n\bar{m}}.\end{aligned} \tag{5.27}$$

For a stationary perturbation in flat spacetime, this simplifies to

$$\frac{2}{r}\left[\partial_r+\frac{1}{r}\right]x_{nn}=-\frac{\mu}{r_p^2}\delta[r-r_p]\delta^2[\theta^A-\theta_p^A]+\left[\frac{1}{r^2}\hat{\eth}'\hat{\eth}+\partial_r^2+\frac{4}{r}\partial_r+\frac{2}{r^2}\right]x_{m\bar{m}}$$
$$+\frac{1}{\sqrt{2}}\left[\frac{1}{r}+\frac{3}{r^2}\right]\left(\hat{\eth}'x_{nm}+\hat{\eth}x_{n\bar{m}}\right). \tag{5.28}$$

Inputting Eqs. (5.24) and (5.21) for x_{nm} and $x_{m\bar{m}}$ respectively, one can solve for x_{nn}, giving

$$x_{nn}=-\frac{\mu(r-r_p)^3}{6r^2r_p^2}\Theta[r-r_p]\hat{\eth}'\hat{\eth}\delta^2[\theta^A-\theta_p^A]+\frac{\mu(r-r_p)}{rr_p}\Theta[r-r_p]\delta^2[\theta^A-\theta_p^A]+\frac{a}{r}, \tag{5.29}$$

where a is independent of r. Again, I apply the boundary condition $x_{ab}=0$ for $r<r_p$; hence, $a=0$. Decomposing Eq. (5.29) gives

$$x_{nn}=\sum_{\ell=0,m}^{\infty}\mu\left[\frac{(r-r_p)^3}{6r^2r_p^2}\ell(\ell+1)+\frac{(r-r_p)}{rr_p}\right]\Theta[r-r_p]\overline{Y}_{\ell,\mathtt{m}}[\theta_p^A]Y_{\ell,\mathtt{m}}[\theta^A]. \tag{5.30}$$

5.2.3 The metric reconstruction source

I have calculated the corrector tensor x_{ab}, which accounts for the T_{la} piece of the source. Therefore, I can now calculate the CCK metric reconstruction piece using a Hertz potential. Instead of calculating a Weyl scalar to source the Hertz potential, I will instead use η (see Sec. 5.1), which, as described by Ref. [86], can be calculated in a multitude of ways (of which I will use two to provide a consistency check).

5.2.3.1 Calculating η

The most direct method of calculating η is by solving Eq. (99a) of Ref. [86],

$$-\frac{1}{4}\left(\text{Þ}^2-4(\rho+\bar{\rho})\text{Þ}+12\rho\bar{\rho}\right)\text{Þ}^2\bar{\eta}=T_0, \tag{5.31}$$

where T_0 is the source to the spin 2 Teukolsky equation, $\mathcal{O}^\dagger(\psi_0)=T_0$. That is,

$$T_0:=\mathcal{S}_0[T_{ab}]=(\eth-\bar{\tau}'-4\tau)\left((\text{Þ}-2\bar{\rho})T_{lm}-(\eth-\bar{\tau}')T_{ll}\right)$$
$$+(\text{Þ}-\bar{\rho}-4\rho)\left((\eth-2\bar{\tau}')T_{lm}-(\text{Þ}-\bar{\rho})T_{mm}\right). \tag{5.32}$$

Note, T_0 can be calculated from T_{ab} or $\tilde{T}_{ab}:=T_{ab}-\mathcal{E}x_{ab}$ as $\mathcal{S}_0[\mathcal{E}x_{ab}]=0$ (this can be seen more clearly from $\mathcal{T}_0[x_{ab}]=0$ and using $\mathcal{O}_0\mathcal{T}_0=\mathcal{S}_0\mathcal{E}$). This is an important conclusion because it means that the GHZ Hertz potential is identical to the CCK

Hertz potential (if you assume CCK is consistent in non-vacuum) as used by Ori in Ref. [135]. Hence, one can use the results of Ref. [135] for the Hertz potential in Kerr.

Using the stationary point particle stress-energy, Eq. (5.17), T_0 simplifies to

$$T_0 = -\frac{\mu\delta[r-r_p]}{2r_p^4}\hat{\eth}^2[\delta^2[\theta^A-\theta_p^A]]. \tag{5.33}$$

Simplifying Eq. (5.31) to flat spacetime and inputting the flat space T_0, gives

$$-\frac{1}{4}\big(\partial_r^4+\frac{8}{r}\partial_r^3+\frac{12}{3}\partial_r^2\big)\bar{\eta} = -\frac{\mu\delta[r-r_p]}{2r_p^4}\hat{\eth}^2[\delta^2[\theta^A-\theta_p^A]]. \tag{5.34}$$

This can be solved for $\bar{\eta}$, giving

$$\bar{\eta} = A+Br+\frac{C}{r}+\frac{D}{r^2}+\frac{\mu(r-r_p)^3}{3r_p^2r^2}\Theta[r-r_p]\Big(\hat{\eth}^2\delta^2[\theta^A-\theta_p^A]\Big). \tag{5.35}$$

I use a familiar boundary condition that $\eta = 0$ for $r < r_p$; this sets $A = B = C = D = 0$. Applying the complex conjugate operation gives

$$\eta = \frac{\mu(r-r_p)^3}{3r_p^2r^2}\Theta[r-r_p]\Big(\hat{\eth}'^2\delta^2[\theta^A-\theta_p^A]\Big). \tag{5.36}$$

As a consistency check, I calculate η from Eq. (5.8) [86]. This gives

$$\begin{aligned}\frac{1}{4}(\text{Þ}-\rho)(\text{Þ}-\rho)\eta = T_{\tilde{m}\tilde{m}} - \big((\text{Þ}-\rho)(\eth'-\bar{\tau})-(\eth'-\bar{\tau}-\tau')\rho-\bar{\tau}(\text{Þ}+\bar{\rho})\\ +\tau'(\text{Þ}-\bar{\rho}+\rho)\big)x_{n\tilde{m}} - \big((\text{Þ}-2\rho)\sigma'+(\bar{\tau}+\tau')\eth'+(\bar{\tau}-\tau')^2\big)x_{m\tilde{m}}.\end{aligned} \tag{5.37}$$

In stationary flat space (with $T_{\tilde{m}\tilde{m}} = 0$) this simplifies to

$$\frac{1}{4}\big(\partial_r^2+\frac{2}{r}\partial_r\big)\eta = -\big(\frac{1}{r}\partial_r+\frac{1}{r^2}\big)x_{n\tilde{m}}. \tag{5.38}$$

Inputting the complex-conjugate of Eq. (5.24) for $x_{n\tilde{m}}$, and solving for η, gives

$$\eta = a+\frac{b}{r}+\frac{\mu(r-r_p)^3}{3r_p^2r^2}\Theta[r-r_p]\Big(\hat{\eth}'^2\delta^2[\theta^A-\theta_p^A]\Big). \tag{5.39}$$

Where again, I have use the boundary condition $\eta = 0$ for $r < r_p$ which sets $a = b = 0$. This η is identical to Eq. (5.36).

To calculate the Hertz potential from η, I require a mode decomposition. Using Eq. (4.43) gives

$$\eta = \sum_{\ell=2,m}^{\infty} \frac{\mu(r-r_p)^3}{3r_p^2 r^2}\Theta[r-r_p]\lambda_2\, \overline{Y}_{\ell,\mathtt{m}}[\theta^A_p]\ {}_{-2}Y_{\ell,\mathtt{m}}[\theta^A], \tag{5.40}$$

where $\lambda_p := \sqrt{\frac{(\ell+p)!}{(\ell-p)!}}$.

5.2.3.2 Calculating the Hertz potential

The next step is calculating the Hertz potential using Eq (86) in Ref. [86]. That is, I need to solve a sourced Teukolsky equation for the Hertz potential (Φ),

$$\mathcal{O}_4(\Phi) = \eta, \tag{5.41}$$

where $\mathcal{O}_4$ takes the form

$$\begin{aligned}\mathcal{O}_4(\Phi) =& 2\big((\text{Þ}' - \rho')(\text{Þ} + 3\rho) - (\eth' - \tau')(\eth + 3\tau) - 3\psi_2\big)\Phi \\ =& 2\big(-\frac{1}{2}\partial_r^2 + \frac{1}{r}\partial_r - \eth'\eth\big)\Phi,\end{aligned} \tag{5.42}$$

where, on the second line I have simplified to flat spacetime.

Initially, this does not appear to be a radial ODE, due to the presence of the $\eth$ and $\eth'$ derivatives. However, in flat spacetime it simplifies greatly by expanding Φ in spin -2 (as the Hertz potential is a solution to the spin -2 Teukolsky equation) spin-weighted spherical harmonics, $\Phi = \sum_{\ell,\mathtt{m}}^{\infty} \Phi_{\ell,\mathtt{m}}\ {}_{-2}Y_{\ell,\mathtt{m}}[\theta^A]$. Hence,

$$\begin{aligned}-\eth'\eth\Phi &= -\frac{1}{2r^2}\hat{\eth}'\hat{\eth}\Phi \\ &= \sum_{\ell=2,m}^{\infty} -\Phi_{\ell,\mathtt{m}}\frac{1}{2r^2}\hat{\eth}'\hat{\eth}\ {}_2Y_{\ell,\mathtt{m}}[\theta^A] \\ &= \sum_{\ell=2,m}^{\infty} \Phi_{\ell,\mathtt{m}}\frac{(\ell+2)(\ell-1)}{2r^2}\ {}_2Y_{\ell,\mathtt{m}}[\theta^A],\end{aligned} \tag{5.43}$$

where $\Phi_{\ell,\mathtt{m}}$ is a function of r. Here, I have used the fact that $\hat{\eth}'\hat{\eth}$ is the Laplace operator on the unit 2-sphere [83], see Eq. (4.44).

I can input the new form for $-\eth'\eth\Phi$ (Eq. (5.43)) into Eq. (5.41), along with the mode decomposition of η (Eq. (5.40)). This gives

$$\sum_{\ell=2,m}^{\infty}\left(2\Big(-\frac{1}{2}\partial_r^2+\frac{1}{r}\partial_r+\frac{(\ell+2)(\ell-1)}{2r^2}\Big)\Phi_{\ell,\mathtt{m}}\right){}_{-2}Y_{\ell,\mathtt{m}}[\theta^A]$$
$$=\sum_{\ell=2,m}^{\infty}\frac{\mu(r-r_p)^3}{6r_p^2r^2}\Theta[r-r_p]\lambda_2\,\overline{Y}_{\ell,\mathtt{m}}[\theta_p^A]\;{}_{-2}Y_{\ell,\mathtt{m}}[\theta^A]. \tag{5.44}$$

This is a radial ODE which can be solved for each mode of Φ. The general solution is

$$\Phi^{r<r_p}=\sum_{\ell=2,m}^{\infty}\left(A_{\ell,\mathtt{m}}r^{\ell+2}+B_{\ell,\mathtt{m}}r^{1-l}\right){}_{-2}Y_{\ell,\mathtt{m}}[\theta^A], \tag{5.45}$$

$$\begin{aligned}\Phi^{r\geq r_p}=\sum_{\ell=2,m}^{\infty}&A_{\ell,\mathtt{m}}r^{\ell+2}+B_{\ell,\mathtt{m}}r^{1-l}+\mu\Big(-\frac{2}{(2\ell+1)\lambda_2}\frac{r^{\ell+2}}{r_p^{\ell+1}}+\frac{2}{(2\ell+1)\lambda_2}\frac{r_p^{\ell}}{r^{\ell-1}}\\&+\lambda_2\big(\frac{r^3}{3(\ell-1)(\ell+2)r_p^2}-\frac{r^2}{\ell(\ell+1)r_p}+\frac{r}{\ell(\ell+1)}\\&-\frac{r_p}{3(\ell-1)(\ell+2)}\big)\Big)\,\overline{Y}_{\ell,\mathtt{m}}[\theta_p^A]\;{}_{-2}Y_{\ell,\mathtt{m}}[\theta^A],\end{aligned} \tag{5.46}$$

where $\Phi^{r<r_p}$ and $\Phi^{r\geq r_p}$ are defined as Φ for $r<r_p$ and $r\geq r_p$ respectively. Assuming regularity at the origin for Eq. (5.45) sets $B_{\ell,\mathtt{m}}=0$. To eliminate the most divergent term in Eq. (5.46) as $r\to\infty$, I choose $A_{\ell,\mathtt{m}}=\frac{2\mu}{(2\ell+1)\lambda_2}\frac{1}{r_p^{\ell+1}}\overline{Y}_{\ell,\mathtt{m}}[\theta_p^A]$. I can justify these boundary conditions as they produce the same results as solving for Φ by integration of its source against the retarded Green's function. Hence, Eqs. (5.45) and (5.46) simplify to

$$\Phi^{r<r_p}=\sum_{\ell=2,m}^{\infty}\frac{2\mu}{(2\ell+1)\lambda_2}\frac{r^{\ell+2}}{r_p^{\ell+1}}\,\overline{Y}_{\ell,\mathtt{m}}[\theta_p^A]\;{}_{-2}Y_{\ell,\mathtt{m}}[\theta^A], \tag{5.47}$$

$$\begin{aligned}\Phi^{r\geq r_p}=\sum_{\ell=2,m}^{\infty}&\mu\Big(\frac{2}{(2\ell+1)\lambda_2}\frac{r_p^{\ell}}{r^{\ell-1}}+\lambda_2\big(\frac{r^3}{3(\ell-1)(\ell+2)r_p^2}\\&-\frac{r^2}{\ell(\ell+1)r_p}+\frac{r}{\ell(\ell+1)}-\frac{r_p}{3(\ell-1)(\ell+2)}\big)\Big)\,\overline{Y}_{\ell,\mathtt{m}}[\theta_p^A]\;{}_{-2}Y_{\ell,\mathtt{m}}[\theta^A].\end{aligned} \tag{5.48}$$

Here, one sees the structure of the Hertz potential splits into Coulombic terms (which are $\propto r^{\ell}$ or $\propto r^{-l}$) and polynomial in r terms. Eqs. (5.47) and (5.48) are consistent with the Hertz potential derived in Ref. [155].

5.2.4 The CCK metric reconstruction piece

Now I use the standard CCK metric reconstruction formula $h^{rec}_{ab} = \mathrm{Re}[\mathcal{S}_0^\dagger \Phi]$ to calculate part of the metric perturbation. $\mathcal{S}_0^\dagger$ is defined as [86]

$$\begin{aligned}\mathcal{S}_0^\dagger[\Phi]_{ab} =& \Big(- l_a l_b(\eth - \tau)(\eth + 3\tau) - m_a m_b(\text{Þ} - \rho)(\text{Þ} + 3\rho) \\ &+ l_{(a}m_{b)}\big\{(\text{Þ} - \rho + \bar{\rho})(\eth + 3\tau) + (\eth - \tau + \bar{\tau}')(\text{Þ} + 3\rho)\big\}\Big)\Phi. \end{aligned} \tag{5.49}$$

Simplifying to flat space gives

$$\mathrm{Re}[\mathcal{S}_0^\dagger \Phi]_{ab} = \frac{1}{2}\Big(- \frac{l_a l_b}{2r}\hat{\eth}\hat{\eth} - m_a m_b(\partial_r + \frac{1}{r})(\partial_r - \frac{3}{r}) + l_{(a}m_{b)}\sqrt{2}\Big(\frac{1}{r}\partial_r - \frac{2}{r^2}\Big)\hat{\eth}\Big)\Phi + c.c, \tag{5.50}$$

where *c.c.* denotes the complex conjugate. From Eq. (5.50), one can write

$$h^{rec}_{nn} = -\frac{1}{4r^2}\Big(\hat{\eth}\hat{\eth}\Phi + \hat{\eth}'\hat{\eth}'\bar{\Phi}\Big), \tag{5.51}$$

$$h^{rec}_{\bar{m}\bar{m}} = -\frac{1}{2}\Big(\partial_r^2 - \frac{2}{r}\partial_r\Big)\Phi, \tag{5.52}$$

$$h^{rec}_{n\bar{m}} = -\frac{\sqrt{2}}{4}\Big(\frac{1}{r}\partial_r - \frac{2}{r^2}\Big)\hat{\eth}\Phi. \tag{5.53}$$

To calculate the full metric perturbation (up to gauge) one simply has to add the corrector tensor,

$$h_{ab} = h^{rec}_{ab} + x_{ab}. \tag{5.54}$$

Using the $r < r_p$ and $r > r_p$ split for Φ, I shall calculate the $r < r_p$ and $r > r_p$ parts of h^{rec}_{ab} separately (labelled $h^{rec<}_{ab}$ and $h^{rec>}_{ab}$ respectively). The $r = r_p$ part of h^{rec}_{ab} will be calculated in Sec. 5.2.4.5 (which is non-trivial due to the Heaviside function in Φ at $r = r_p$).

5.2.4.1 Calculating h^{rec}_{nn} and h_{nn}

First, I calculate $h^{rec<}_{nn}$ from Eq. (5.51) by inputting Eq. (5.47) for Φ. This gives

$$h^{rec<}_{nn} = \sum_{\ell=2,m}^{\infty} - \frac{\mu}{2(2\ell+1)\lambda_2}\frac{r^\ell}{r_p^{\ell+1}}\Big(\hat{\eth}\hat{\eth}\overline{Y}_{\ell,\mathtt{m}}[\theta^A_p]\ {}_{-2}Y_{\ell,\mathtt{m}}[\theta^A] + \hat{\eth}'\hat{\eth}'Y_{\ell,\mathtt{m}}[\theta^A_p]\ {}_{-2}\overline{Y}_{\ell,\mathtt{m}}[\theta^A]\Big). \tag{5.55}$$

Using the definition Eq. (4.45), I can write

$$\begin{aligned} Y_{\ell,\mathtt{m}}[\theta_p^A]\ {}_{-2}\overline{Y}_{\ell,\mathtt{m}}[\theta^A] &= (-1)^m \overline{Y}_{l,-m}[\theta_p^A](-1)^{m-2}\ {}_2Y_{l,-m}[\theta^A] \\ &= \overline{Y}_{l,-m}[\theta_p^A]\ {}_2Y_{l,-m}[\theta^A]. \end{aligned} \tag{5.56}$$

Hence,

$$\begin{aligned} \hat{\eth}\hat{\eth}\overline{Y}_{\ell,\mathtt{m}}[\theta_p^A]\ {}_{-2}Y_{\ell,\mathtt{m}}[\theta^A] &= \hat{\eth}'\hat{\eth}' Y_{\ell,\mathtt{m}}[\theta_p^A]\ {}_{-2}\overline{Y}_{\ell,\mathtt{m}}[\theta^A] \\ &= \lambda_2 \overline{Y}_{\ell,\mathtt{m}}[\theta_p^A]\ Y_{\ell,\mathtt{m}}[\theta^A]. \end{aligned} \tag{5.57}$$

After using a change of labels $-m \to m$ (only where the $-m$ labels occur), Eq. (5.55) simplifies to

$$h_{nn}^{rec<} = \sum_{\ell=2,m}^{\infty} -\frac{\mu}{2\ell+1}\frac{r^\ell}{r_p^{\ell+1}}\overline{Y}_{\ell,\mathtt{m}}[\theta_p^A]\ Y_{\ell,\mathtt{m}}[\theta^A]. \tag{5.58}$$

Note, for $r < r_p$ $x_{ab} = 0$; therefore,

$$\begin{aligned} h_{nn}^{<} &= h_{nn}^{rec<} \\ &= \sum_{\ell=2,m}^{\infty} -\frac{\mu}{2\ell+1}\frac{r^\ell}{r_p^{\ell+1}}\overline{Y}_{\ell,\mathtt{m}}[\theta_p^A]\ Y_{\ell,\mathtt{m}}[\theta^A]. \end{aligned} \tag{5.59}$$

Using that the complex and angular part of $\Phi^{r>r_p}$ and $\Phi^{r<r_p}$ take the same form, taking Eq. (5.51) and input Eq. (5.48) for Φ, I can use the same arguments to calculate $h_{nn}^{rec>}$, finding

$$\begin{aligned} h_{nn}^{rec>} = \sum_{\ell=2,m}^{\infty} -\mu\Big(&\frac{1}{2\ell+1}\frac{r_p^\ell}{r^{\ell+1}} + \ell(\ell+1)\frac{r^3-r_p^3}{6r_p r^2} \\ &- (\ell-1)(\ell+2)\frac{r-r_p}{2rr_p}\Big)\overline{Y}_{\ell,\mathtt{m}}[\theta_p^A]\ Y_{\ell,\mathtt{m}}[\theta^A]. \end{aligned} \tag{5.60}$$

Adding the corrector tensor to calculate the full metric perturbation gives

$$\begin{aligned} h_{nn}^{>} &= h_{nn}^{rec>} + x_{nn} \\ &= \sum_{\ell=0,m}^{\infty} \mu\Big(\frac{r-r_p}{rr_p} + \ell(\ell+1)\frac{(r-r_p)^3}{6r^2r_p^2}\Big)\overline{Y}_{\ell,\mathtt{m}}[\theta_p^A]\ Y_{\ell,\mathtt{m}}[\theta^A] \\ &\quad + \sum_{\ell=2,m}^{\infty}\Bigg\{-\mu\Big(\frac{1}{2\ell+1}\frac{r_p^\ell}{r^{\ell+1}} + \ell(\ell+1)\frac{r^3-r_p^3}{6r_p r^2} \\ &\quad - (\ell-1)(\ell+2)\frac{r-r_p}{2rr_p}\Big)\Bigg\}\overline{Y}_{\ell,\mathtt{m}}[\theta_p^A]\ Y_{\ell,\mathtt{m}}[\theta^A]. \end{aligned} \tag{5.61}$$

The polynomial in r terms cancel (apart from the $\ell = \{0, 1\}$ terms), giving

$$h^{>}_{nn} = \sum_{\ell=0,m}^{1} \mu\Big(\frac{r - r_p}{r r_p} + \ell(\ell+1)\frac{(r-r_p)^3}{6r^2 r_p^2}\Big)\overline{Y}_{\ell,\mathtt{m}}[\theta^A_p]\; Y_{\ell,\mathtt{m}}[\theta^A] + \sum_{\ell=2,m}^{\infty} \frac{-\mu}{2\ell+1}\frac{r_p^\ell}{r^{\ell+1}}\overline{Y}_{\ell,\mathtt{m}}[\theta^A_p]\; Y_{\ell,\mathtt{m}}[\theta^A]. \tag{5.62}$$

5.2.4.2 Calculating $h^{rec}_{\bar{m}\bar{m}}$ and $h_{\bar{m}\bar{m}}$

Now I calculate $h^{rec<}_{\bar{m}\bar{m}}$ using Eq. (5.52), inputting Eq. (5.47) for Φ, which gives

$$h^{rec<}_{\bar{m}\bar{m}} = \sum_{\ell=2,m}^{\infty} -\frac{\mu(\ell+2)(\ell-1)}{(2\ell+1)\lambda_2}\frac{r^\ell}{r_p^{\ell+1}}\;\overline{Y}_{\ell,\mathtt{m}}[\theta^A_p]\;{}_{-2}Y_{\ell,\mathtt{m}}[\theta^A]. \tag{5.63}$$

Again, as $x_{ab} = 0$ for $r < r_p$,

$$\begin{aligned} h^{<}_{\bar{m}\bar{m}} &= h^{rec<}_{\bar{m}\bar{m}} \\ &= \sum_{\ell=2,m}^{\infty} -\frac{\mu(\ell+2)(\ell-1)}{(2\ell+1)\lambda_2}\frac{r^\ell}{r_p^{\ell+1}}\;\overline{Y}_{\ell,\mathtt{m}}[\theta^A_p]\;{}_{-2}Y_{\ell,\mathtt{m}}[\theta^A]. \end{aligned} \tag{5.64}$$

Putting Eq. (5.48) into Eq. (5.52) gives

$$h^{rec>}_{\bar{m}\bar{m}} = \sum_{\ell=2,m}^{\infty} -\mu\left(\frac{(\ell+2)(\ell-1)}{(2\ell+1)\lambda_2}\frac{r_p^\ell}{r^{\ell+1}} + \sqrt{\frac{(\ell+2)(\ell-1)}{\ell(\ell+1)}}\frac{r-r_p}{r r_p}\right)\overline{Y}_{\ell,\mathtt{m}}[\theta^A_p]\;{}_{-2}Y_{\ell,\mathtt{m}}[\theta^A]. \tag{5.65}$$

As $x_{\bar{m}\bar{m}} = 0$,

$$\begin{aligned} h^{>}_{\bar{m}\bar{m}} &= h^{rec>}_{\bar{m}\bar{m}} \\ &= \sum_{\ell=2,m}^{\infty} -\mu\left(\frac{(\ell+2)(\ell-1)}{(2\ell+1)\lambda_2}\frac{r_p^\ell}{r^{\ell+1}} + \sqrt{\frac{(\ell+2)(\ell-1)}{\ell(\ell+1)}}\frac{r-r_p}{r r_p}\right)\overline{Y}_{\ell,\mathtt{m}}[\theta^A_p]\;{}_{-2}Y_{\ell,\mathtt{m}}[\theta^A]. \end{aligned} \tag{5.66}$$

5.2.4.3 Calculating $h^{rec}_{n\bar{m}}$ and $h_{n\bar{m}}$

Using Eq. (5.53) and inputting Eq. (5.47) for Φ gives

$$\begin{aligned} h^{rec<}_{n\bar{m}} &= \sum_{\ell=2,m}^{\infty} -\frac{\mu\sqrt{2}}{2(2\ell+1)\lambda_2}\frac{r^\ell}{r_p^{\ell+1}}\hat{\eth}\;\overline{Y}_{\ell,\mathtt{m}}[\theta^A_p]\;{}_{-2}Y_{\ell,\mathtt{m}}[\theta^A] \\ &= \sum_{\ell=2,m}^{\infty} \frac{\mu\sqrt{2}l}{2(2\ell+1)\sqrt{\ell(\ell+1)}}\frac{r^\ell}{r_p^{\ell+1}}\overline{Y}_{\ell,\mathtt{m}}[\theta^A_p]\;{}_{-1}Y_{\ell,\mathtt{m}}[\theta^A], \end{aligned} \tag{5.67}$$

where I have used Eq. (4.42). Again, as $x_{ab} = 0$ for $r < r_p$,

$$\begin{aligned} h^{<}_{n\bar{m}} =& h^{rec<}_{n\bar{m}} \\ =& \sum_{\ell=2,m}^{\infty} \frac{\mu\sqrt{2}l}{2(2\ell+1)\sqrt{\ell(\ell+1)}} \frac{r^\ell}{r_p^{\ell+1}} \, \overline{Y}_{\ell,\mathtt{m}}[\theta^A_p] \, {}_{-1}Y_{\ell,\mathtt{m}}[\theta^A]. \end{aligned} \tag{5.68}$$

Inputting Eq. (5.48) into Eq. (5.52), and again using Eq. (4.42), gives

$$\begin{aligned} h^{rec>}_{n\bar{m}} =& \sum_{\ell=2,m}^{\infty} \frac{\sqrt{2}\mu}{4} \left(\frac{-2(\ell+1)}{(2\ell+1)(\lambda_2)^2} \frac{r_p^\ell}{r^{\ell+1}} + \frac{r^3+2r_p^3}{3(\ell-1)(\ell+2)r^2 r_p^2} - \frac{1}{\sqrt{(\ell+1)}r} \right) \\ & \sqrt{(\ell+2)(\ell-1)}\lambda_2 \, \overline{Y}_{\ell,\mathtt{m}}[\theta^A_p] \, {}_{-1}Y_{\ell,\mathtt{m}}[\theta^A]. \end{aligned} \tag{5.69}$$

Calculating the full metric perturbation by adding the corrector tensor gives

$$\begin{aligned} h^{>}_{n\bar{m}} =& h^{rec>}_{n\bar{m}} + x_{n\bar{m}} \\ =& h^{rec>}_{n\bar{m}} - \sqrt{2}\frac{(r-r_p)^2(r+2r_p)}{12r^2r_p^2}\sqrt{\ell(\ell+1)} \, \overline{Y}_{\ell,\mathtt{m}}[\theta^A_p] \, {}_{-1}Y_{\ell,\mathtt{m}}[\theta^A] \\ =& \sum_{m=-1}^{1} \mu \frac{(r-r_p)^2(r+2r_p)}{6r^2r_p} \overline{Y}_{1,m}[\theta^A_p] \, {}_{-1}Y_{1,m}[\theta^A] \\ & + \sum_{\ell=2,m}^{\infty} \frac{-\sqrt{2}\mu}{2} \left(\frac{(\ell+1)}{(2\ell+1)\sqrt{\ell(\ell+1)}} \frac{r_p^\ell}{r^{\ell+1}} - \frac{1}{\sqrt{(\ell+1)}} \frac{1}{r} \right) \overline{Y}_{\ell,\mathtt{m}}[\theta^A_p] \, {}_{-1}Y_{\ell,\mathtt{m}}[\theta^A], \end{aligned} \tag{5.70}$$

where I have used Eq. (5.26) to input $x_{n\bar{m}}$ (and most of the polynomial terms have cancelled, apart from the $\ell = \{0, 1\}$ terms).

5.2.4.4 Calculating $h_{m\bar{m}}$

The CCK metric reconstruction does not contribute to $h_{m\bar{m}}$. That is,

$$h_{m\bar{m}} = x_{m\bar{m}}. \tag{5.71}$$

Hence, using Eq. (5.21),

$$\begin{aligned} h^{<}_{m\bar{m}} &= 0, \\ h^{>}_{m\bar{m}} &= \mu \frac{r-r_p}{rr_p} \delta^2[\theta^A - \theta^A_p]. \end{aligned} \tag{5.72}$$

5.2.4.5 Calculating h^{rec}_{ab} on the sphere $r = r_p$

In the analysis above I have ignored h^{rec}_{ab} at $r = r_p$ (which I label $h^{rec,r=r_p}_{ab}$) as to make the equations more easy to handle. Now I will calculate h^{rec}_{ab} at $r = r_p$. CCK metric

reconstruction involves taking radial derivatives of Φ. As the expression for Φ is currently split up into $\Phi^{<}$ for $r < r_p$ and $\Phi^{>}$ for $r > r_p$, I cannot directly calculate the radial derivative of Φ at $r = r_p$ until I re-express Φ in a manner which is consistent at $r = r_p$. By combining Eqs. (5.47) and (5.48) using Heaviside functions, I can write

$$\begin{aligned}\Phi = \sum_{\ell=2,m}^{\infty} \mu \Bigg(& \frac{2}{(2\ell+1)\lambda_2} \frac{r^{\ell+2}}{r_p^{\ell+1}} + \Theta[r-r_p] \Bigg(\frac{-2}{(2\ell+1)\lambda_2} \frac{r^{\ell+2}}{r_p^{\ell+1}} + \frac{2}{(2\ell+1)\lambda_2} \frac{r_p^{\ell}}{r^{\ell-1}} \\ & + \lambda_2 \Bigg(\frac{r^3}{3(\ell-1)(\ell+2)r_p^2} - \frac{r^2}{\ell(\ell+1)r_p} + \frac{r}{\ell(\ell+1)} \\ & - \frac{r_p}{3(\ell-1)(\ell+2)} \Bigg) \Bigg) \Bigg) \, \overline{Y}_{\ell,\mathtt{m}}[\theta_p^A] \, {}_{-2}Y_{\ell,\mathtt{m}}[\theta^A]. \end{aligned} \tag{5.73}$$

I shall label the radial function inside the large circular brackets in Eq. (5.73) as $F(r)$ (the radial coefficient of the Heaviside function). $F(r)$ can provide an extra contribution to Φ at $r = r_p$ when the radial derivative acts on the Heaviside function. Note, in Eq. (5.51) there are no radial derivatives, so there are no additional terms in h^{rec}_{nn} at $r = r_p$. That is, $h^{rec,r=r_p}_{nn} = h^{rec>}_{nn}(r = r_p)$.

For $h^{rec}_{n\bar{m}}$, in Eq. (5.53) there is one radial derivative acting on Φ. Acting with a radial derivative on the Heaviside function in Eq. (5.73) contributes $\delta[r-r_p]F(r)|_{r=r_p}$. However, as $F(r_p) = 0$, $\delta[r-r_p]F(r)|_{r=r_p} = 0$. Hence, there are no additional terms in $h^{rec}_{n\bar{m}}$ at $r = r_p$. That is, $h^{rec,r=r_p}_{n\bar{m}} = h^{rec>}_{n\bar{m}}(r = r_p)$. Note, $h^{rec}_{n\bar{m}}$ is discontinuous at $r = r_p$.

Finally, for $h^{rec}_{\bar{m}\bar{m}}$, Eq. (5.52) contains a two radial derivatives acting on Φ. The single derivatives do not contribute using the same argument as for $h^{rec,r=r_p}_{\bar{m}\bar{m}}$. When the double radial derivative acts on the Heaviside function twice, the $F(r_p) = 0$ coefficient, again, results in no contribution. I next investigate the final possible contribution, when one radial derivative acts on the Heaviside function and one acts on $F(r)$. As

$$\begin{aligned}\partial_r F(r)|_{r=r_p} = & -\frac{2(\ell+2)}{(2\ell+1)\lambda_2} \frac{r^{\ell+1}}{r_p^{\ell+1}} + \frac{2(1-l)}{(2\ell+1)\lambda_2} \frac{r_p^{\ell}}{r^{\ell}} \\ & + \lambda_2 \Bigg(\frac{r^2}{(\ell-1)(\ell+2)r_p^2} - \frac{2r}{\ell(\ell+1)r_p} + \frac{1}{\ell(\ell+1)} \Bigg)|_{r=r_p} \\ = & 0, \end{aligned} \tag{5.74}$$

this term also does not contribute. That is, $h^{rec,r=r_p}_{\bar{m}\bar{m}} = h^{rec>}_{\bar{m}\bar{m}}(r = r_p)$. Therefore, it is consistent to write the $h^{rec>}_{ab}$ and $h^{>}_{ab}$ I calculated in the previous subsection as $h^{rec\geq}_{ab}$ and $h^{\geq}_{ab}$ respectively (as they are both consistent at $r = r_p$).

5.2.5 A summary of the half-string metric perturbation

I have calculated the half-string metric perturbation using the GHZ metric reconstruction formula,

$$h_{ab} = h^{rec}_{ab} + x_{ab}, \tag{5.75}$$

in flat spacetime for a stationary point mass perturbation. Here is a summary of the results:

First I note, as $x_{ab} = 0$ for $r < r_p$, $h^{<}_{ab} = h^{rec<}_{ab}$; that is,

$$h^{<}_{nn} = \sum_{\ell=2,m}^{\infty} -\frac{\mu}{2\ell+1}\frac{r^\ell}{r_p^{\ell+1}}\,\overline{Y}_{\ell,\mathtt{m}}[\theta^A_p]\;Y_{\ell,\mathtt{m}}[\theta^A], \tag{5.76}$$

$$h^{<}_{\bar{m}\bar{m}} = \sum_{\ell=2,m}^{\infty} -\frac{\mu(\ell+2)(\ell-1)}{(2\ell+1)\lambda_2}\frac{r^\ell}{r_p^{\ell+1}}\,\overline{Y}_{\ell,\mathtt{m}}[\theta^A_p]\;{}_{-2}Y_{\ell,\mathtt{m}}[\theta^A], \tag{5.77}$$

$$h^{<}_{mm} = \sum_{\ell=2,m}^{\infty} -\frac{\mu(\ell+2)(\ell-1)}{(2\ell+1)\lambda_2}\frac{r^\ell}{r_p^{\ell+1}}\,\overline{Y}_{\ell,\mathtt{m}}[\theta^A_p]\;{}_{2}Y_{\ell,\mathtt{m}}[\theta^A], \tag{5.78}$$

$$h^{<}_{n\bar{m}} = \sum_{\ell=2,m}^{\infty} -\frac{\mu\sqrt{2}l}{2(2\ell+1)\sqrt{\ell(\ell+1)}}\frac{r^\ell}{r_p^{\ell+1}}\,\overline{Y}_{\ell,\mathtt{m}}[\theta^A_p]\;{}_{-1}Y_{\ell,\mathtt{m}}[\theta^A], \tag{5.79}$$

$$h^{<}_{nm} = \sum_{\ell=2,m}^{\infty} \frac{\mu\sqrt{2}l}{2(2\ell+1)\sqrt{\ell(\ell+1)}}\frac{r^\ell}{r_p^{\ell+1}}\,\overline{Y}_{\ell,\mathtt{m}}[\theta^A_p]\;{}_{1}Y_{\ell,\mathtt{m}}[\theta^A]. \tag{5.80}$$

All other components of h_{ab} equal zero for $r < r_p$. The solution for h_{ab} in Eq. (5.80) is manifestly smooth for $r < r_p$ because the factors of $(r/r_p)^\ell$ ensures the sum converges exponentially with ℓ.

For $r \geq r_p$ the metric perturbation takes the form

$$h^{\geq}_{nn} = \sum_{\ell=0,m}^{1} \mu\Big(\frac{r-r_p}{rr_p} + \ell(\ell+1)\frac{(r-r_p)^3}{6r^2r_p^2}\Big)\overline{Y}_{\ell,\mathtt{m}}[\theta^A_p]\; Y_{\ell,\mathtt{m}}[\theta^A] + \sum_{\ell=2,m}^{\infty} \frac{-\mu}{2\ell+1}\frac{r_p^\ell}{r^{\ell+1}}\overline{Y}_{\ell,\mathtt{m}}[\theta^A_p]\; Y_{\ell,\mathtt{m}}[\theta^A], \tag{5.81}$$

$$h^{\geq}_{\bar{m}\bar{m}} = \sum_{\ell=2,m}^{\infty} -\mu\left(\frac{(\ell+2)(\ell-1)}{(2\ell+1)\lambda_2}\frac{r_p^\ell}{r^{\ell+1}} + \sqrt{\frac{(\ell+2)(\ell-1)}{\ell(\ell+1)}}\frac{r-r_p}{rr_p}\right)\overline{Y}_{\ell,\mathtt{m}}[\theta^A_p]\; {}_{-2}Y_{\ell,\mathtt{m}}[\theta^A], \tag{5.82}$$

$$h^{\geq}_{mm} = \sum_{\ell=2,m}^{\infty} -\mu\left(\frac{(\ell+2)(\ell-1)}{(2\ell+1)\lambda_2}\frac{r_p^\ell}{r^{\ell+1}} + \sqrt{\frac{(\ell+2)(\ell-1)}{\ell(\ell+1)}}\frac{r-r_p}{rr_p}\right)\overline{Y}_{\ell,\mathtt{m}}[\theta^A_p]\; {}_{2}Y_{\ell,\mathtt{m}}[\theta^A], \tag{5.83}$$

$$h^{\geq}_{n\bar{m}} = \sum_{m=-1}^{1} \mu\frac{(r-r_p)^2(r+2r_p)}{6r^2r_p}\overline{Y}_{1,m}[\theta^A_p]\; {}_{-1}Y_{1,m}[\theta^A] + \sum_{\ell=2,m}^{\infty} \frac{-\sqrt{2}\mu}{2}\left(\frac{(\ell+1)}{(2\ell+1)\sqrt{\ell(\ell+1)}}\frac{r_p^\ell}{r^{\ell+1}} - \frac{1}{\sqrt{(\ell+1)}}\frac{1}{r}\right)\overline{Y}_{\ell,\mathtt{m}}[\theta^A_p]\; {}_{-1}Y_{\ell,\mathtt{m}}[\theta^A], \tag{5.84}$$

$$h^{\geq}_{nm} = \sum_{m=-1}^{1} -\mu\frac{(r-r_p)^2(r+2r_p)}{6r^2r_p}\overline{Y}_{1,m}[\theta^A_p]\; {}_{-1}Y_{1,m}[\theta^A] + \sum_{\ell=2,m}^{\infty} \frac{\sqrt{2}\mu}{2}\left(\frac{(\ell+1)}{(2\ell+1)\sqrt{\ell(\ell+1)}}\frac{r_p^\ell}{r^{\ell+1}} - \frac{1}{\sqrt{(\ell+1)}}\frac{1}{r}\right)\overline{Y}_{\ell,\mathtt{m}}[\theta^A_p]\; {}_{-1}Y_{\ell,\mathtt{m}}[\theta^A], \tag{5.85}$$

$$h^{\geq}_{m\bar{m}} = \mu\frac{r-r_p}{rr_p}\delta^2[\theta^A - \theta^A_p]. \tag{5.86}$$

All other components of h_{ab} equal zero for $r \geq r_p$.

The form of the metric perturbation for $r \geq r_p$ splits into three pieces: Coulombic terms which fall off as $(r_p/r)^\ell$ at large r (and as such, converge exponentially quickly as $r < r_p$); mass and dipole moment terms which contribute the $\ell < 2$ terms; and polynomial in r terms (e.g., $h^{\geq}_{m\bar{m}} = \mu\frac{r-r_p}{rr_p}\delta^2[\theta^A - \theta^A_p]$). The polynomial in r terms give the solution its string like nature. As the polynomial in r do not converge as a series for large ℓ, except as distributions (see Appendix D of Ref. [183]), these terms are problematic. Similarly, the metric perturbation is singular in the $h^{\geq}_{m\bar{m}}$ component as it contains an angular delta function for $r \geq r_p$. Hence, such a metric perturbation is said to be in a *half-string* radiation gauge.

The $\ell < 2$ terms are equivalent to $\dot{g}_{ab}$, which appears in Eq. (5.1). However, the $\ell < 2$ terms have been contributed directly from the corrector tensor (x_{ab}). That is, $\dot{g}_{ab}$ in Eq. (5.1) is redundant (and this property extends to Kerr [183]).

5.2.6 The no-string gauge solution

To isolate the singular nature of the metric perturbation to a finite surface, one can transform to a no-string radiation gauge. This involves using a gauge transform to eliminate the string singularities emanating from r_p out to future null infinity. One finds that it is possible to gauge away the singular terms proportional to polynomials in r (i.e., the Coulombic $\sim r^\ell$ cannot be gauged away) for $\ell \geq 2$. However, the resulting transformation introduces a sphere of singularities with radius r_p. I compute this gauge transform and compare the results with Ref. [155]. Ref. [155] derived the no-string solution using two alternative methods. Firstly, by constructing the solution out of the two regular halves of two half-string solutions (plus adding a completion $\ell < 2$ piece). Secondly, by transforming directly to the no-string gauge from the Lorenz gauge solution (locally near the particle).

To gauge away the half-string singularities I use the gauge transformation equation,

$$h'_{ab} = h_{ab} + \mathcal{L}_{\vec{\xi}} g_{ab} = h_{ab} + 2\xi^c_{;(a} g_{b)c}. \tag{5.87}$$

By solving for ξ^c, such that the string singularities are gauged away, one finds that all the ($\ell \geq 2$) polynomial string terms can be eliminated using the gauge vector

$$\xi^l = \sum_{\ell=2,m}^{\infty} \frac{-\mu}{\ell(\ell+1)} \Theta[r - r_p] \overline{Y}_{\ell,\mathtt{m}}[\theta^A_p] \; Y_{\ell,\mathtt{m}}[\theta^A], \tag{5.88}$$

$$\xi^n = \sum_{\ell=2,m}^{\infty} \frac{-\mu}{2\ell(\ell+1)} \Theta[r - r_p] \overline{Y}_{\ell,\mathtt{m}}[\theta^A_p] \; Y_{\ell,\mathtt{m}}[\theta^A], \tag{5.89}$$

$$\xi^m = \sum_{\ell=2,m}^{\infty} \frac{-\mu}{\sqrt{2\ell(\ell+1)}} \frac{r - r_p}{r_p} \Theta[r - r_p] \overline{Y}_{\ell,\mathtt{m}}[\theta^A_p] \; {}_1Y_{\ell,\mathtt{m}}[\theta^A]. \tag{5.90}$$

Acting with this gauge transformation on the metric perturbation in Sec. 5.2.4.5 results in a no-string gauge solution, h'_{ab}, of the form

$$h'_{ll} = \sum_{\ell=2,m}^{\infty} \frac{-\mu}{\ell(\ell+1)} \delta[r-r_p] \overline{Y}_{\ell,\mathtt{m}}[\theta_p^A]\ Y_{\ell,\mathtt{m}}[\theta^A], \tag{5.91}$$

$$h'_{ln} = 0, \tag{5.92}$$

$$h'_{lm} = 0, \tag{5.93}$$

$$\begin{aligned} h'_{nn} = &\sum_{\ell=0,m}^{1} \mu\Big(\frac{r-r_p}{rr_p} + \ell(\ell+1)\frac{(r-r_p)^3}{6r^2r_p^2}\Big)\Theta[r-r_p]\overline{Y}_{\ell,\mathtt{m}}[\theta_p^A]\ Y_{\ell,\mathtt{m}}[\theta^A] + \\ &\sum_{\ell=2,m}^{\infty} -\mu\Big(\frac{1}{2\ell+1}\Big(\frac{r^\ell}{r_p^{\ell+1}}\Theta[r_p-r] + \frac{r_p^\ell}{r^{\ell+1}}\Theta[r-r_p]\Big) \\ &\quad + \frac{1}{2\ell(\ell+1)}\delta[r-r_p]\Big)\overline{Y}_{\ell,\mathtt{m}}[\theta_p^A]\ Y_{\ell,\mathtt{m}}[\theta^A], \end{aligned} \tag{5.94}$$

$$\begin{aligned} h'_{nm} = &\sum_{m=-1}^{1} -\mu\frac{(r-r_p)^2(r+2r_p)}{6r^2r_p^2}\Theta[r-r_p]\overline{Y}_{1,m}[\theta_p^A]\ {}_{-1}Y_{1,m}[\theta^A] + \\ &\sum_{\ell=2,m}^{\infty}\frac{\mu\sqrt{2}}{2(2\ell+1)\sqrt{\ell(\ell+1)}}\Big(\frac{lr^\ell}{r_p^{\ell+1}}\Theta[r_p-r] + \frac{(\ell+1)r_p^\ell}{r^{\ell+1}}\Theta[r-r_p]\Big)\overline{Y}_{\ell,\mathtt{m}}[\theta_p^A]\ {}_1Y_{\ell,\mathtt{m}}[\theta^A], \end{aligned} \tag{5.95}$$

$$h'_{m\bar{m}} = \sum_{\ell=0,m}^{1} \mu\frac{r-r_p}{rr_p}\Theta[r-r_p]\overline{Y}_{\ell,\mathtt{m}}[\theta_p^A]\ Y_{\ell,\mathtt{m}}[\theta^A] \tag{5.96}$$

$$\begin{aligned} h'_{mm} = &\sum_{\ell=2,m}^{\infty}\frac{-\mu}{2(2\ell+1)}\sqrt{\frac{(\ell+2)(\ell-1)}{\ell(\ell+1)}}\Big(\frac{r^\ell}{r_p^{\ell+1}}\Theta[r_p-r] \\ &\quad + \frac{r_p^\ell}{r^{\ell+1}}\Theta[r-r_p]\Big)\overline{Y}_{\ell,\mathtt{m}}[\theta_p^A]\ {}_2Y_{\ell,\mathtt{m}}[\theta^A]. \end{aligned} \tag{5.97}$$

The no-string metric perturbation can also be written as the sum of three pieces. Firstly, a Coulombic piece, h'^{C}_{ab} (which is invariant between the half-string and no

string solution; i.e., $h^C_{ab} = h'^C_{ab}$),

$$h^C_{ll} = h'^C_{ll} = 0, \tag{5.98}$$

$$h^C_{ln} = h'^C_{ln} = 0, \tag{5.99}$$

$$h^C_{lm} = h'^C_{lm} = 0, \tag{5.100}$$

$$h^C_{nn} = h'^C_{nn} = \sum_{\ell=2,m}^{\infty} -\mu\left(\frac{1}{2\ell+1}\left(\frac{r^\ell}{r_p^{\ell+1}}\Theta[r_p - r] + \frac{r_p^\ell}{r^{\ell+1}}\Theta[r - r_p]\right)\right)\overline{Y}_{\ell,\mathtt{m}}[\theta^A_p]\; Y_{\ell,\mathtt{m}}[\theta^A], \tag{5.101}$$

$$h^C_{nm} = h'^C_{nm} = \sum_{\ell=2,m}^{\infty} \frac{\mu\sqrt{2}}{2(2\ell+1)\sqrt{\ell(\ell+1)}}\left(\frac{lr^\ell}{r_p^{\ell+1}}\Theta[r_p - r] + \frac{(\ell+1)r_p^\ell}{r^{\ell+1}}\Theta[r - r_p]\right)\overline{Y}_{\ell,\mathtt{m}}[\theta^A_p]\; {}_1Y_{\ell,\mathtt{m}}[\theta^A], \tag{5.102}$$

$$h^C_{m\bar{m}} = h'^C_{m\bar{m}} = 0 \tag{5.103}$$

$$h^C_{mm} = h'^C_{mm} = \sum_{\ell=2,m}^{\infty} \frac{-\mu}{2(2\ell+1)}\sqrt{\frac{(\ell+2)(\ell-1)}{\ell(\ell+1)}}\left(\frac{r^\ell}{r_p^{\ell+1}}\Theta[r_p - r] + \frac{r_p^\ell}{r^{\ell+1}}\Theta[r - r_p]\right)\overline{Y}_{\ell,\mathtt{m}}[\theta^A_p]\; {}_2Y_{\ell,\mathtt{m}}[\theta^A]. \tag{5.104}$$

Secondly, a $\ell \geq 2$ "polynomial" piece $h'^{P,\ell\geq 2}_{ab}$,

$$h'^{P,\ell\geq 2}_{ll} = \sum_{\ell=2,m}^{\infty} \frac{-\mu}{\ell(\ell+1)}\delta[r - r_p]\overline{Y}_{\ell,\mathtt{m}}[\theta^A_p]\; Y_{\ell,\mathtt{m}}[\theta^A], \tag{5.105}$$

$$h'^{P,\ell\geq 2}_{ln} = 0, \tag{5.106}$$

$$h'^{P,\ell\geq 2}_{lm} = 0, \tag{5.107}$$

$$h'^{P,\ell\geq 2}_{nn} = \sum_{\ell=2,m}^{\infty} \frac{-\mu}{2\ell(\ell+1)}\delta[r - r_p]\overline{Y}_{\ell,\mathtt{m}}[\theta^A_p]\; Y_{\ell,\mathtt{m}}[\theta^A], \tag{5.108}$$

$$h'^{P,\ell\geq 2}_{nm} = 0, \tag{5.109}$$

$$h'^{P,\ell\geq 2}_{m\bar{m}} = 0, \tag{5.110}$$

$$h'^{P,\ell\geq 2}_{mm} = 0. \tag{5.111}$$

This piece is confined to delta functions on the surface of a sphere radius $r = r_p$, and as such, is not a polynomial in r; however, it arose from the polynomial piece in the half-string gauge, so I call it the $\ell \geq 2$ "polynomial" piece. Note, the surface of the sphere is not in the radiation gauge as $h'^{P,\ell\geq 2}_{ll} \neq 0$. Finally, there is a $\ell = \{0, 1\}$

polynomial piece, $h'^{P,\ell<2}_{ab}$, that takes the form

$$h'^{P,\ell<2}_{ll} = 0, \tag{5.112}$$
$$h'^{P,\ell<2}_{ln} = 0, \tag{5.113}$$
$$h'^{P,\ell<2}_{lm} = 0, \tag{5.114}$$
$$h'^{P,\ell<2}_{nn} = \sum_{\ell=0,m}^{1} \mu\Big(\frac{r-r_p}{rr_p} + \ell(\ell+1)\frac{(r-r_p)^3}{6r^2r_p^2}\Big)\Theta[r-r_p]\overline{Y}_{\ell,\mathtt{m}}[\theta^A_p]\ Y_{\ell,\mathtt{m}}[\theta^A], \tag{5.115}$$
$$h'^{P,\ell<2}_{nm} = \sum_{m=-1}^{1} \mu\frac{(r-r_p)^2(r+2r_p)}{6r^2r_p^2}\Theta[r-r_p]\overline{Y}_{1,m}[\theta^A_p]\ {}_{-1}Y_{1,m}[\theta^A], \tag{5.116}$$
$$h'^{P,\ell<2}_{m\bar{m}} = \sum_{\ell=0,m}^{1} \mu\frac{r-r_p}{rr_p}\Theta[r-r_p]\overline{Y}_{\ell,\mathtt{m}}[\theta^A_p]\ Y_{\ell,\mathtt{m}}[\theta^A] \tag{5.117}$$
$$h'^{P,\ell<2}_{mm} = 0. \tag{5.118}$$

The full no-string metric perturbation, Eq. (5.91), is given by $h'_{ab} = h'^{C}_{ab} + h'^{P,\ell\geq 2}_{ab} + h'^{P,\ell<2}_{ab}$. This solution is equivalent to the solution given in Ref. [155].

5.2.6.1 The no-string $\ell < 2$ piece

Whilst I have successful gauged away the singular string extending out to $\mathcal{I}^+$, there remains non-asymptotically flat behaviour in the $\ell < 2$ piece of the metric perturbation (Eqs. (5.112) to (5.118)). The $\sim r^0$ behaviour in the nn, nm and $m\bar{m}$ components and the $\sim r^1$ behaviour in the nn and nm components are non-asymptotically flat. In this section, I eliminate this poor behaviour with a gauge transform.

Whilst the non-asymptotically flat behaviour must be pure gauge, not all the $\ell < 2$ sector is pure gauge. There is physical information in the $\ell < 2$ modes of the metric perturbation: a mass perturbation and a dipole moment caused by the centre of mass not being at the origin. These contributions are asymptotically flat, so I will not attempt to gauge away the entire $\ell < 2$ metric perturbation. I restrict the gauge transform to remaining in the radiation gauge (except on the sphere of radius r_p centred on the origin). It will also become apparent that the asymptotically flat $\ell < 2$ piece of the metric perturbation is the so-called "completion piece" [155] and the gauge transformation to eliminate the non-asymptotically flat $\ell < 2$ piece is the so-called "gauge completion piece" [187].

Next, I eliminate the remaining non-asymptotically flat terms with a gauge transform. As I show, this requires an additional degree of care compared to the gauge transforms used in the $\ell \geq 2$ sector. The gauge vector required has linear and quadratic dependencies on time. I shall derive the gauge vector for $\ell = 0$ and $\ell = 1$ separately.

In the $\ell = 0$ sector, attempting to eliminate the $\sim r^0$ and $\sim r^1$ behaviour in Eq. (5.115) with a gauge transform results in a hierarchical list of equations for the gauge vector,

$$\text{Þ}'\xi_n = -\tfrac{1}{2}x_{nn}^{\ell=0}, \tag{5.119a}$$

$$\xi_l = -\frac{1}{2\rho'}\left(x_{m\bar{m}} + 2\rho\xi_n\right), \tag{5.119b}$$

where I have used that $h_{ab} = x_{ab}$ in the $\ell < 2$ sector. Solving these equations gives

$$(\xi_l)_{00} = -\frac{\mu\overline{Y}_{0,0}[\theta_p^A]}{2r_p}u, \tag{5.120a}$$

$$(\xi_n)_{00} = \left(\frac{u}{r_p} - \frac{r}{2r_p} - \Theta[r - r_p]\right)\frac{\mu\overline{Y}_{0,0}[\theta_p^A]}{2}. \tag{5.120b}$$

Similarly, for the $\ell = 1$ sector, one solves the hierarchical equations

$$\text{Þ}'\xi_n = -\tfrac{1}{2}x_{nn}, \tag{5.121a}$$

$$(\eth' + \bar{\rho}')\xi_{\bar{m}} = -\left(x_{nm} + \eth'\xi_n\right), \tag{5.121b}$$

$$\xi_l = -\frac{1}{2\rho'}\left(x_{m\bar{m}} + 2\,\mathrm{Re}[\eth\xi_{\bar{m}}] + 2\rho\xi_n\right), \tag{5.121c}$$

giving

$$(\xi_l)_{1\mathtt{m}} = \frac{\mu u^2\overline{Y}_{1,\mathtt{m}}[\theta_p^A]}{12{r_p}^2}, \tag{5.122a}$$

$$(\xi_n)_{1\mathtt{m}} = -\left(\frac{u^2}{12{r_p}^2} + \frac{ur}{3{r_p}^2} + \Theta[r - r_p]\right)\frac{\mu\overline{Y}_{1,\mathtt{m}}[\theta_p^A]}{2}, \tag{5.122b}$$

$$(\xi_{\bar{m}})_{1\mathtt{m}} = \left(\frac{r}{r_p} + \frac{ur}{3{r_p}^2} + \frac{u^2}{6{r_p}^2}\right)\frac{\mu\overline{Y}_{1,\mathtt{m}}[\theta_p^A]}{2}. \tag{5.122c}$$

the u dependence of the gauge vector is required to eliminate the non-asymptotically flat behaviour in the metric perturbation. As I do not want to include a u dependence in the resulting metric perturbation, these parts of the gauge vector do not have a Heaviside function coefficient. That is, I extend the contribution to the metric perturbation from the u dependent gauge vector down to the origin. The resulting terms in the metric perturbation are regular at the origin, so this extension is permissible. The resulting no-string metric perturbation is

$$\tilde{h}_{ab} = h_{ab}^C + \tilde{h}_{ab}^{\delta}\,\delta[r - r_p] + \tilde{h}_{ab}^{\ell=0,1}, \tag{5.123}$$

with

$$\tilde{h}^{\delta}_{ll} = \sum_{\ell=2,m}^{\infty} \frac{-\mu}{\ell(\ell+1)} \overline{Y}_{\ell,\mathtt{m}}[\theta^A_p] Y_{\ell,\mathtt{m}}[\theta^A], \tag{5.124a}$$

$$\tilde{h}^{\delta}_{ln} = -\frac{\mu}{2}\left(\frac{1}{4\pi} + \sum_{m=-1}^{1} \overline{Y}_{1,\mathtt{m}}[\theta^A_p] Y_{1,\mathtt{m}}[\theta^A]\right), \tag{5.124b}$$

$$\tilde{h}^{\delta}_{nn} = \frac{\mu}{2}\left(\frac{1}{4\pi} - \sum_{m=-1}^{1} \overline{Y}_{1,\mathtt{m}}[\theta^A_p] Y_{1,\mathtt{m}}[\theta^A] - \sum_{\ell=2,m}^{\infty} \frac{1}{\ell(\ell+1)} \overline{Y}_{\ell,\mathtt{m}}[\theta^A_p] Y_{\ell,\mathtt{m}}[\theta^A]\right), \tag{5.124c}$$

and

$$\tilde{h}^{\ell=0,1}_{nn} = -\mu\left(\frac{1}{4\pi}\left(\frac{\Theta[r-r_p]}{r} + \frac{\Theta[r_p-r]}{r_p}\right) + \sum_{m=-1}^{1} \frac{\Theta[r-r_p] r_p}{3r^2} \overline{Y}_{1,\mathtt{m}}[\theta^A_p] Y_{1,\mathtt{m}}[\theta^A]\right), \tag{5.125a}$$

$$\tilde{h}^{\ell=0,1}_{m\bar{m}} = -\mu\Theta[r_p-r]\left(\frac{1}{4\pi r_p} + \sum_{m=-1}^{1} \frac{1}{r_p} \overline{Y}_{1,\mathtt{m}}[\theta^A_p] Y_{1,\mathtt{m}}[\theta^A]\right), \tag{5.125b}$$

$$\tilde{h}^{\ell=0,1}_{n\bar{m}} = \sum_{m=-1}^{1} \mu\left(\frac{\Theta[r_p-r] r}{6 {r_p}^2} - \frac{\Theta[r-r_p] r_p}{3r^2}\right) \overline{Y}_{1,\mathtt{m}}[\theta^A_p]_{-1} Y_{1,\mathtt{m}}[\theta^A]. \tag{5.125c}$$

The requirements that the metric perturbation is regular at the origin, asymptotically flat at $\mathcal{I}^+$, and contains no linear or quadratic u dependencies produces a gauge transformation that is the so-called "gauge completion piece". This method for including the gauge completion piece is simpler than previously used methods and is derived from more physical motivations. Previously, the gauge completion piece has been determined by imposing the continuity of certain metric components at $r = r_p$ [104, 169, 31, 183].

The gauge-invariant completion piece has also been included by the inclusion of the corrector tensor. The $\frac{\mu}{4\pi r}$ behaviour (for $r > r_p$) in $h^{\ell=0,1}_{nn}$ in Eq. (5.125) is a perturbation towards a Schwarzschild solution, the completion piece one expects from a stationary point mass perturbation. The $\mathcal{O}(r^{-2})$ behaviour (for $r > r_p$) in $h^{\ell=0,1}_{ab}$ is the result of a change in the centre of mass of the system away from the origin. In Kerr or Schwarzschild, the change in the centre of mass is pure gauge due to the non-zero mass of the background spacetime.

5.3 Extension to Kerr and regularisation: the punctured shadowless gauge

The motivation for the flat space toy model was to check if the GHZ procedure is consistent with previous self-force results, understand how it differs from CCK metric reconstruction, and recognize how to best attempt GHZ metric reconstruction in Kerr.

In Ref. [183], I (with collaborators) presented the flat-spacetime implementation of GHZ metric reconstruction. We then used the experience gained in flat spacetime to streamline the application of GHZ metric reconstruction in Kerr. Finally, we produced a formalism for calculating a regular first-order metric perturbation for the self-force problem in Kerr by combining GHZ metric reconstruction, gauge transformations, and a puncture scheme. Here, I summarise the construction of this formalism, pointing out how the flat space toy model informed its formation.

As noted in Sec. 5.2.3.1, part of the GHZ metric reconstruction calculation in Kerr is already in the literature. Ref. [135] calculates a Hertz potential which is consistent with the CCK piece of GHZ metric reconstruction. The original motivation for Ref. [135] was to achieve metric reconstruction in non-vacuum, but the metric perturbation it produces does not satisfy the linearised EFE. GHZ metric reconstruction provides the missing piece (the corrector tensor) to satisfy the linearised EFE.

Ref. [183] streamlines the GHZ approach by using the Held formalism [90]. The Held formalism allows the equations in GHZ metric reconstruction to be expressed in a series expansion of ρ (to positive and negative powers). The expansion allows many equations to be solved for each power in ρ separately. This reduces GHZ metric reconstruction to finding a finite set of ρ-independent quantities (A_i).

The direct application of GHZ metric reconstruction in Ref. [86] for a point-particle source puts one in the half-string radiation gauge. Ref. [183] reformulates GHZ metric reconstruction such that it results in a no-string radiation gauge. Our reformulation of GHZ metric reconstruction to include the gauge transformation automatically is straightforward as the gauge vector that takes one from the half-string radiation gauge to the no-string radiation gauge can be written in terms of A_i. As the flat space example illustrates, GHZ metric reconstruction recovers the full metric perturbation in the half- and no-string gauge. This includes coefficients of delta functions on the sphere containing the particle which are not recovered with CCK metric reconstruction.

The completion piece and gauge completion piece arise naturally (in x_{ab}) in the Kerr calculation as they did in flat space. By transforming the GHZ metric reconstruction to the no-string gauge while requiring that the solution is regular at the horizon, asymptotically flat at $\mathcal{I}^+$, and contains no linear or quadratic u dependencies, the completion piece and gauge completion piece are spontaneously included in the solution.

Ref. [183] then generalizes the point particle no-string gauge solution to an extended source shadowless gauge solution. When applying GHZ metric reconstruction to an extended source, a shadow emanates out to $\mathcal{I}^+$, similarly to the string singularity in the half-string gauge. The half-shadow gauge solution is similarly problematic for a singular source as it requires many ℓ-modes to resolve and is not asymptotically flat.

One can treat the half-shadow gauge similarly to the half-string gauge; that is, one can transform to a shadowless gauge (akin to a no-string gauge). The shadowless gauge contains a spherical shell region (containing the extended source), which can be a non-vacuum solution, akin to the spherical singular region in the no-string gauge. Our metric construction formalism in the shadowless gauge can be applied to any spatially compact source.

Due to the singular nature of the point particle, applying the shadowless gauge directly to the self-force problem recovers the no-string solution used previously in the literature (and calculated in the flat spacetime toy model in Sec. 5.2.6). To produce a formalism for calculating a sufficiently regular first-order metric perturbation for second-order self-force calculations, Ref. [183] formulates a puncture scheme *within* the shadowless gauge. In essence, this formalism puts the puncture into a sufficiently regular gauge that one can solve for the residual field using our shadowless metric reconstruction formalism. Putting the most singular part of the field (the puncture) in a more regular gauge prevents the strong singularities that extend off the particle. This is achieved by taking the puncture to sufficiently high orders in $\mathbf{r}$, such that the singular nature of the point particle is removed from the calculation (see Sec. 1.6.3.5). Hence, applying the shadowless gauge to the punctured self-force problem produces a regular (residual) metric perturbation. There are plans to implement the punctured shadowless gauge as part of the plan to produce the first second-order self-force calculations in Kerr.

The primary motivation for developing this metric reconstruction scheme was to calculate a sufficiently regular metric perturbation to source second-order calculations. This work has other advantages and applications. As the formalism can handle extended sources, it could be used for eccentric orbits without relying on the method of extended homogeneous solutions [114]. The formalism also obtains the regular metric perturbation directly, so there is no requirement for further regularisation [114].

Chapter 6

Conclusions

Second-order black hole perturbation theory is an emerging field of research with recent successes. Self-force waveform models to first-post-adiabatic accuracy have recently produced exciting results in Schwarzschild [156, 195, 194]. The resulting waveforms show remarkable agreement with Numerical Relativity waveforms even in the $\epsilon \sim \frac{1}{10}$ regime. The dissipative piece of the second-order self-force is a crucial contribution to these results.

A significant motivation for first-post-adiabatic modelling [69] is the observation of EMRIs (and IMRIs). For these systems, the spin of the massive black hole is expected to be significant [38, 160]. Hence, calculations in a Kerr background are required. Generic (eccentric and inclined orbit) EMRI waveform templates to first-post-adiabatic accuracy will enable precise parameter extraction from LISA measurements. For data analysis, it is not only necessary to be able to compute first-post-adiabatic waveforms but to do so efficiently. That is, for LISA science, efficient dissipative second-order self-force calculations (for generic orbits in Kerr) are necessary[1].

The current method of calculating the second-order self-force (used in Refs. [156, 195, 194]) relies on the separability of the EFE in Schwarzschild (in the Lorenz gauge). In Kerr, the EFE are non-separable. Hence, a new, efficient method of calculating the second-order self-force is required that applies to Kerr. This thesis has extended some black hole perturbation theory methods to second order in Kerr and implemented a selection of these methods in Schwarzschild.

At first order in Kerr, the non-separability of the EFE has been avoided by solving the Teukolsky equation [177, 178]. The Teukolsky equation is a separable PDE for a curvature scalar ($\psi_4^{(1)}$). An extension of the Teukolsky equation to second order exists in the literature [45], which I call the *Campanelli–Lousto–Teukolsky equation*. The

[1] Additional first-post adiabatic contributions, such as the secondary spin and resonances are also necessary, but these effects are beyond the scope of this thesis.

Campanelli–Lousto–Teukolsky equation is a PDE for a second-order vacuum curvature scalar $\psi_4^{(2)}$. In Sec. 2.2.2 I show that, in general, the source to this equation is not well defined in the second-order self-force problem (unless a puncture scheme is used). In summary, products of the first-order metric perturbation and first-order stress-energy tensor appear in the source. In the self-force problem, the first-order metric perturbation is singular, and the first-order stress-energy contains a Dirac delta function on the worldline. Hence, their product (and the source) is not well defined as a distribution. This problem could be avoided using a puncture scheme. But, using the Campanelli–Lousto–Teukolsky equation for second-order metric reconstruction will be less straightforward as the equation does not appear naturally in the GHZ metric reconstruction scheme [86].

I found an alternative extension of the Teukolsky equation to second order (see, Sec. 2.3), which I call the *reduced second-order Teukolsky equation*. This equation is distinct from the Campanelli–Lousto–Teukolsky equation, solving for $\psi_{4L}^{(2)}$, a quantity purely dependent on $h_{ab}^{(2)}$. The reduced second-order Teukolsky equation is derived by applying the Wald identity [190] on $h_{ab}^{(2)}$. The equation also appears implicitly in GHZ metric reconstruction [86]'s extension to non-linear orders. Importantly, in Sec. 2.3.2 I show that the source of the reduced second-order Teukolsky equation is well defined for self-force calculations in a highly regular gauge [151, 185]. I also show that $\psi_{4L}^{(2)}$ is infinitesimal tetrad rotation invariant, unlike $\psi_4^{(2)}$.

The existence of a well-defined separable second-order equation in the self-force problem in Kerr is a significant advancement in the prospect of calculating generic EMRI waveform templates for LISA. Similarly, the reduced second-order Teukolsky equation could be employed to help produce first-post-adiabatic IMRI (and $\epsilon \sim \frac{1}{10}$ binary) models for black holes with spin. These systems are beginning to be observable with ground-based gravitational-wave detectors [11, 4]. They are also significant sources for future ground and space-based detectors.

The reduced second-order Teukolsky equation also has utility for investigating second-order quasi-normal mode calculations in Kerr [102]. Numerical Relativity ringdown calculations have been shown to be well modelled using linear black hole perturbation theory [78, 93]. This interesting phenomenon may be due to most of the non-linear behaviour being hidden behind the event-horizon of the merged black hole [133]. As gravitational wave detectors improve [20], second-order quasi-normal mode contributions will likely become detectable [168]. Non-linear quasi-normal modes of black holes is already an area of active research [102, 163, 168].

In Chapter 3, I amended the adverse property that $\psi_{4L}^{(2)}$ (like $\psi_4^{(2)}$) is not gauge invariant. I achieve this by constructing a gauge-invariant version ($\psi_{4L}'^{(2)}$) using first-order gauge fixing. Re-expressing the reduced second-order Teukolsky equation

in a gauge fixed form, Eq. (3.4), solves for $\psi_{4L}^{\prime(2)}$ directly. I presented two practical methods for first-order gauge fixing to calculate the required inputs for Eq. (3.4).

The first gauge-fixing scheme fixes to the *"fully constrained Chandrasekhar-like"* algebraically. Sec. 3.5 gives a method for calculating the gauge vector to the *"fully constrained Chandrasekhar-like"* class of gauges from any gauge. The gauge vector is solved for algebraically. I also found that the *"fully constrained Chandrasekhar-like"* class of gauges are generally not asymptotically flat.

The second gauge-fixing method fixes to an asymptotically flat gauge but requires solving ODEs. Sec. 3.6 gives a method for calculating the gauge vector to the Bondi–Sachs gauge (from a generic gauge). To constrain the residual gauge freedom of the Bondi–Sachs gauge (the BMS freedoms), I gave a method for constraining the BMS freedoms for perturbations to Kerr (in Sec. 3.6.6). These methods can be used in Eq. (3.4) to solve for an asymptotically flat second-order gauge-invariant $\psi_{4L}^{\prime(2)}$. The asymptotically flat nature of the Bondi–Sachs gauge is useful for avoiding infrared divergences near $\mathcal{I}^+$, which arise from the slow falloff of second-order sources in generic gauges [156].

Both gauge fixing schemes fully fix the gauge up to residual gauge freedom along the Killing vectors of Kerr spacetime. Hence, $\psi_{4L}^{\prime(2)}$ is gauge invariant up to these Killing symmetries. I plan to constrain the remaining degrees of freedom using the gauge transformation of the first-order stress-energy tensor, Eq. (3.3).

I also gave a method for calculating a local gauge transform to a highly regular gauge (from the Lorenz gauge) near the worldline (Sec. 3.7) in Fermi–Walker coordinates. This gauge transformation is necessary to make the source of the reduced second-order Teukolsky equation well defined. The method needs to be converted to practical coordinates for implementation (work currently being carried out by Sam Upton).

A collaboration is being set up to implement the techniques in Chaps. 2 and 3 in Kerr. However, new insights and progress can be made by implementing these techniques in Schwarzschild in preparation for Kerr. My current collaboration with Ben Leather, Leanne Durkan, Sam Upton, Barry Wardell, Niels Warburton, and Adam Pound is solving the reduced second-order Teukolsky equation for quasi-circular orbits in Schwarzschild.

My role in this calculation is producing various formulas for the reduced second-order Teukolsky source and the source data that can be integrated numerically. My leading contribution is calculating a mode decomposition of $\mathcal{S}[\delta^2 G[h_{ab}^{(1)}, h_{ab}^{(1)}]]$. The decomposition is valid for any perturbation to Schwarzschild (in the Carter tetrad), even outside of the self-force context. I first express $\mathcal{S}[\delta^2 G[h_{ab}^{(1)}, h_{ab}^{(1)}]]$ in GHP form. I then used the Carter tetrad [46] to convert $\mathcal{S}[\delta^2 G[h_{ab}^{(1)}, h_{ab}^{(1)}]]$ to BL coordinates. I

express all the angular dependence in $\mathcal{S}[\delta^2 G[h^{(1)}_{ab}, h^{(1)}_{ab}]]$ using spin-weighted spherical harmonics, the eigenbasis of the master Teukolsky equation in Schwarzschild. Using this formula, I calculate the source data (see Fig. 4.2) using retarded Lorenz gauge $h^{(1)}_{ab}$ data from Niels Warburton, which allows one to solve the radial Teukolsky equation for $\psi^{(2)}_{4L}$. That is, I give the source data to Ben Leather, who numerically solves the radial Teukolsky equation for each $\ell, \mathtt{m}$ mode $\psi^{(2)\ell,\mathtt{m}}_{4L}$.

The retarded Lorenz gauge source contains a slow fall-off near $\mathcal{I}^+$, which results in an infrared divergence in the retarded solution. To ameliorate this divergence, I applied the methods in Sec. 3.6.4 to transform to the Bondi–Sachs gauge. Upon analysis of the source, it is clear that a complete transformation to the Bondi–Sachs gauge is unnecessary to reduce the divergence by two orders in r. Instead, it is only necessary to transform the leading-order in r (and next-to-leading-order for $h^{(1)}_{ll}$) behaviour of $h^{(1)}_{ab}$, such that, it is equivalent to the leading order behaviour in the Bondi–Sachs gauge. I calculated the gauge transformation and found the source does converge two orders in r faster, eliminating the infrared divergence (see Fig. 4.6). This convergence allows Ben Leather to solve the radial Teukolsky equation with simple boundary conditions (outgoing radiation at $\mathcal{I}^+$and ingoing radiation at the horizon).

There are additional parts to the source of the reduced second-order Teukolsky equation. To achieve first-post adiabatic accuracy, a two-timescale approximation is implemented. Hence, there is a slow-time derivative contribution to the source at second-order ($\delta G^{\langle 1\rangle}_{ab}[h^{(1)}_{cd}]$). I calculated a formula for $\mathcal{S}[\delta G^{\langle 1\rangle}[\partial_{\mathcal{V}} h^{(1)}_{ab}]]$. The slow-time derivative data ($\partial_{\mathcal{V}} h^{(1)}_{ab}$) is provided by Leanne Durkan. Additionally, as I have implemented a transformation to the *near* Bondi–Sachs gauge, this needs to be accounted for in $\partial_{\mathcal{V}} h^{(1)}_{ab}$. I provide Leanne with formulas for the correction to $\partial_{\mathcal{V}} h^{(1)}_{ab}$ due to the near Bondi–Sachs transformation.

The sum for each $(\ell, \mathtt{m})$ mode of $\mathcal{S}[\delta^2 G[h^{(1)}_{ab}, h^{(1)}_{ab}]]$ does not converge near the worldline for increased number of ℓ_{max} input modes (of $h^{(1)}_{ab}$). Additionally, there is singular behaviour in $\mathcal{S}[\delta^2 G[h^{(1)}_{ab}, h^{(1)}_{ab}]]$ and $T^{(2)}_{ab}$ that makes the source of the reduced second-order Teukolsky equation singular. An effective source (with a puncture scheme) is used to avoid these divergences. That is, in a world-tube containing the worldline we solve Eq. (4.32), rather than Eq. (4.33). This requires an effective source (S_{eff}). It is possible to construct S_{eff} from the effective source used in Refs. [156, 195, 194]. However, a correction term, Eq. (4.36), is required. I provide formulas for a mode decomposition of Eq. (4.36). The correction requires inputs for $h^{(2)\mathcal{P}}_{cd}$ (provided by the calculation in Refs. [156, 195, 194]) and $\partial_{\mathcal{V}} h^{(1)}_{cd}$.

My final contribution to this collaborative effort is the jump in $\psi^{(2)}_{4L}$ due to the near-Bondi–Sachs gauge transformation. I implement the near-Bondi–Sachs transformation on the $\mathcal{I}^+$side of the world-tube. Hence, the source (and $\psi^{(2)}_{4L}$) is discontinuous at this side of the world-tube boundary. To account for this

discontinuity, I calculate data on the jump in $\psi^{(2)}_{4L}$ due to the gauge transform (including contributions from the gauge transformation of the slow-time derivatives). Ben Leather then includes this jump as a junction condition when solving the radial Teukolsky equation for $\psi^{(2)}_{4L}$.

In Sec. 4.3, I presented the working parts of the source to the reduced second-order Teukolsky equation. There remains a missing distributional piece on the worldline, which will be added shortly. Also, the slow-time derivative contribution needs to be added, which is currently exhibiting unexpected singular behaviour at the horizon. The singular behaviour is due to the slow-time derivatives contribution being calculated on t-slicing. I will re-derive the formulas in Sec. 4.2.6 on s-slicing and this will avoid the singular behaviour at the horizon.

After obtaining the full source, Ben Leather will solve the radial Teukolsky equation for $\psi^{(2)}_{4L}$. To do so, Leather transforms to hyperboloidal slicing with a compactified radial coordinate. Leather will then use spectral methods with analytic mesh refinement to solve for $\psi^{(2)}_{4L}$ [106, 105]. From $\psi^{(2)}_{4L}$, our collaboration will extract energy fluxes for quasi-circular orbits in Schwarzschild. Accurate flux data on a dense grid of r_0 values will allow us to generate waveforms to first-post-adiabatic accuracy. These waveforms will be compared with Refs. [156, 195, 194] (which will soon be used to help inform models used for LIGO data analysis).

There are many advantages to our reduced second-order Teukolsky calculation compared to the methods used in Refs. [156, 195, 194]. Firstly, the equation solved is simpler. The Teukolsky equation solves for one complex scalar. Whereas the linearised EFE solved in Refs. [156, 195, 194] are ten real equations, six of which are evolution, four of which are constraints. Hence, solving the reduced second-order Teukolsky is more efficient. Additionally, solving a single equation will simplify the extension to eccentric orbits. The most important advantage is that the reduced second-order Teukolsky calculation is extendable to Kerr.

Our calculation in Schwarzschild shows encouraging progress, but for realistic EMRI models calculations must be in Kerr. Plans to implement a reduced second-order Teukolsky calculation in Kerr have begun. An initial hurdle to this implementation is obtaining a sufficiently regular first-order metric perturbation to construct a well-defined second-order source. The metric perturbation used to calculate first-order self-force effects in Kerr contains gauge singularities on a sphere containing the compact object. Inputting these singularities into the quadratic source operator produces an ill-defined source. In Ref. [183] I (with collaborators) produced a formalism for calculating a regular first-order metric perturbation. This formalism combines GHZ metric reconstruction [86], a shadowless gauge (similar to the no-string gauge but with an extended source), and a puncture scheme. I give a summary of GHZ metric reconstruction and the regularisation formalism in Sec 5.1.

My contribution to Ref. [183] was computing the first implementation of GHZ metric reconstruction. To have maximum analytical control, the implementation was made for a stationary point-mass perturbation in flat spacetime. This implementation gave valuable insights into how GHZ compares to CCK metric reconstruction. During the implementation, we realised that the Hertz potential in GHZ already exists in the literature. That is, one can use the results of Ref. [135] for the Hertz potential (in Kerr). Implementing a transformation to the no-string gauge in the flat spacetime model also revealed that the perturbation to another Kerr solution is contained in the corrector tensor. Similarly, the gauge completion piece can be included by gauge transforming the no-string solution such that the final solution is asymptotically flat, regular at the origin (or horizon), and ensuring the metric perturbation contains no linear or quadratic growth in time. This method includes the completion piece in a more direct manner and provides a simpler, more physically motivated method for including the gauge completion piece than previous calculations [187, 104, 169, 31, 183]. Finally, I compared the flat spacetime string and no-string radiation gauge metric perturbations obtained using GHZ and found them to be consistent with Ref. [155] (which used CCK metric reconstruction). The flat spacetime model helped us understand how to efficiently implement GHZ metric reconstruction and formulate ideas for the regularisation scheme in Kerr.

6.1 Comments on future work

There are many projects and routes for progress in second-order self-force. An obvious improvement to the quasi-circular orbit waveform in Schwarzschild is the extension to eccentric orbits. Ref. [100] contains an effective-source approach which is designed to handle eccentric orbits for second-order equations like the reduced second-order Teukolsky equation. Implementing this method would produce the primary first-post adiabatic waveforms for eccentric orbits. It is expected that adding eccentricity will produce waveforms carrying more information [122], allowing tighter constraints on EMRI parameter measurements.

Adding the secondary spin is another method for making the waveforms more astrophysically realistic. Waveforms for quasi-circular orbits in Schwarzschild with the spinning secondary contribution have recently been published [112]. It would be straightforward to add this analysis to the reduced second-order Teukolsky scheme.

The next frontier of second-order self-force and first-post-adiabatic waveforms is Kerr. The methods developed in this thesis will provide a roadmap to the first second-order calculation in Kerr. Unforeseen problems may appear, but the consensus of our collaboration is that a quasi-circular evolution is feasible in the next few years. One foreseen problem is separating the source of the Teukolsky equation in Kerr; to solve

the reduced second-order Teukolsky equation in a separable manner its source must be decomposed into spin-weighted spheroidal harmonics [177]. This problem is highly non-trivial as spin-weighted spheroidal harmonics are not known in a closed form and background quantities in Kerr mix the angular and radial coordinate.

Another challenge to second-order calculations in Kerr is obtaining the effective source near the worldline efficiently. There are currently methods for calculating the second-order effective source which are extendable to Kerr [153, 120]. These methods have been implemented in Schwarzschild [156, 195, 194] and used in the second-order calculation in Chap. 4 in Schwarzschild. However, this method is very inefficient and a bottleneck to calculations in Schwarzschild. In Kerr, the problem will be worse. Using current methods, calculating the effective source for generic orbits in Kerr is unfeasible with current technology on the time frame of LISA's planned launch. New methods, significant efficiency savings and exponential growth in computing resources might be required. Nevertheless, the current methods will be capable of calculating the effective source and completing a second-order calculation for quasi-circular orbits in Kerr in the next couple of years.

One method of ameliorating the singularity on the worldline is transforming to a highly regular gauge. My colleague Sam Upton has begun implementing the transformation from the Lorenz gauge to the highly regular gauge. He is converting the Fermi–Walker expression in Eq. (3.85) in Schwarzschild for quasi-circular orbits to BL coordinates and decomposing into modes (spin-weighted spherical harmonics). It has turned out to be a challenging calculation; however, we expect to be able to implement it in the reduced second-order Teukolsky equation scheme soon. This will reduce the singular nature of the source and make it well defined as a distribution without using a puncture scheme. However, using a puncture scheme in conjunction with the highly regular gauge will still be advantageous because it will make the source (and solution) converge faster for higher ℓ_{max}.

Additionally, one may want to calculate gauge invariants associated to the highly regular gauge. The highly regular gauge transform given in Eq. (3.85) is not fully fixed and requires that one starts in the Lorenz gauge. One could attempt to fully fix the highly regular gauge similarly to how I fixed the BMS freedoms in the Bondi–Sachs gauge (in Sec. 3.6.7). One would also need to extend the method for calculating the gauge vector to the highly regular gauge such that one can start in any initial gauge. The resulting gauge fixing scheme could be used with Eq. (3.1) to calculate a gauge invariant $\psi'^{(2)}_{4L}$ associated with the highly regular gauge. An additional problem with the highly regular gauge vector in Eq. (3.85) is that it only calculates the gauge transform from the Lorenz gauge to the highly regular gauge. To implement a gauge transform to the highly regular gauge from the metric perturbation obtained by the formalism described in Sec. 5.3 [183] will require a gauge vector from the shadowless gauge to a highly regular gauge.

A further region where gauge fixing to a *good* gauge is desirable is near the horizon. Such gauges are called *horizon regular*. To produce a formalism for finding such a gauge vector, one could repeat the analysis used to find a gauge transformation to the Bondi–Sachs like gauge but near the horizon (similarly to Sec. 3.6). Additionally, one would likely want to fix additional freedoms relating to isometries of the horizon (like the BMS freedoms near $\mathcal{I}^+$).

Balance laws have been used to evolve the quasi-circular inspiral from the fluxes extracted at $\mathcal{I}^+$and $\mathcal{H}^+$ in Schwarzschild [156, 195, 194]. However, in Kerr, second-order balance laws are not readily available for generic orbits. There has been progress in deriving second-order balance laws for the energy and angular-momentum fluxes, but they are not yet in a practical form [123]. The evolution of the Carter constant at second order is an open problem. The Carter constant evolution is more challenging as there is not strictly a balance law at first order (the averaged rate of change of the Carter constant is expressed in terms of the amplitudes of $\psi_4^{(1)}$ at the horizon and $\mathcal{I}^+$, but unlike $\dot{E}$ and $\dot{L}$, it also involves quantities at the particle [134, 68]). Nevertheless, deriving practical balance laws at second-order will lead to faster calculations.

Rather than using balance laws, it is possible to calculate the second-order self-force using the metric perturbation at the particle. However, this will require second-order metric reconstruction. GHZ metric reconstruction [86] is applicable at second order. Nevertheless, implementing second-order GHZ metric reconstruction will be a significant project and less efficient than directly calculating fluxes from $\psi_{4L}^{(2)}$. However, calculating the conservative self-force will benefit synergies with post-Newtonian theory, post-Minkowskian theory, and the effective one-body formalism.

Another effect that becomes significant for generic inspirals in Kerr is resonances [70, 29, 186]. Modelling resonances is an open problem, but there has been progress on methods which could be used in the gravitational case in Kerr [130]. One issue with modelling resonances is that the two-timescale approximation breaks down. Another area where the two-timescale approximation breaks down is the transition to plunge, plunge, and quasi-normal mode ringdown. These parts of the waveform need to be modelled and then attached (using a matching scheme) to the end of the two-timescale waveform to achieve a complete binary merger waveform.

One of the primary goals of LISA is to test General Relativity and the Standard Model of particle physics. To do so, waveform templates in General Relativity alone are not sufficient. Waveform templates for alternative theories of gravity and beyond the Standard Model will be required. One can then use data analysis with LISA measurements to assess which theory best matches observations. Maximising the precision of potential measurements will require the waveforms in alternative theories

to achieve first-post-adiabatic in accuracy. Calculating such waveforms will be a massive task. The formulation of first-post-adiabatic methods and implementation of self-force methods in alternate theories [199] will be required. Nevertheless, the two-timescale framework in black hole perturbation theory is built to add small perturbations to our models. Hence, it should be possible to introduce small deviations from General Relativity (the regime of alternative theories that has not yet been constrained) into the two-timescale framework. However, the scope and breadth of alternative theories of gravity, plus the challenging nature of self-force calculations in general, will make producing accurate waveforms in alternative theories of gravity and beyond the Standard Model a mighty task.

Appendix A

Perturbing NP Quantities

In this appendix, I define the perturbed NP quantities (spin coefficients and Weyl scalars) using the method prescribed by Chrzanowski [51]. This method begins by finding a perturbed tetrad. I then use this tetrad to calculate the perturbed NP quantities. I compare the perturbed NP quantities to Campanelli and Lousto's results [45], finding discrepancies. The results in this appendix were calculated in collaboration with Jordan Moxon [72] and independently checked with Beatrice Bonga and Nicholas P. Loutrel [102].

A.1 Calculating the perturbed tetrad and their parallel derivatives

Before discussing Chrzanowski's method [51], I first note that his results stem from a metric with a negative signature. Here I adapt his results to be consistent with a positive metric signature. Also, in this appendix, I write the perturbation operator (δ in Eq. (1.15)) as $\mathcal{D}$ as to not confuse it with the NP derivative δ.

Ref. [51] begins by defining a perturbed tetrad in total generality [51],

$$\begin{aligned}
\mathcal{D}[l_\mu] &= l_\mu^{(1)} = q l_\mu + u n_\mu + R m_\mu + \bar{R}\bar{m}_\mu \\
\mathcal{D}[n_\mu] &= n_\mu^{(1)} = s l_\mu + t n_\mu + U m_\mu + \bar{U}\bar{m}_\mu \\
\mathcal{D}[m_\mu] &= m_\mu^{(1)} = V l_\mu + W n_\mu + X m_\mu + Y \bar{m}_\mu,
\end{aligned} \tag{A.1}$$

where the lower-case Latin letters (without indices) are real functions and the upper-case Latin letters are complex functions. The goal of this calculation is to determine these functions in terms of the metric perturbation $h_{ab}^{(1)}$.

Following Ref. [51], by using the infinitesimal tetrad rotations and relabelling, I can simplify Eq. (A.1), giving

$$\begin{aligned} l^{(1)}_\mu &= a n_\mu \\ n^{(1)}_\mu &= b l_\mu + c n_\mu \\ m^{(1)}_\mu &= D l_\mu + E n_\mu + f m_\mu + G \bar{m}_\mu. \end{aligned} \tag{A.2}$$

The metric perturbation can be defined as

$$\mathcal{D}(g_{\mu\nu}) = \mathcal{D}(-2 l_{(\mu} n_{\nu)} + 2 m_{(\mu} \bar{m}_{\nu)}) \tag{A.3}$$

$$\Rightarrow h_{\mu\nu} = -2 l^{(1)}_{(\mu} n_{\nu)} - 2 l_{(\mu} n^{(1)}_{\nu)} + 2 m^{(1)}_{(\mu} \bar{m}_{\nu)} + 2 m_{(\mu} \bar{m}^{(1)}_{\nu)}. \tag{A.4}$$

By contracting Eq. (A.3) with every combination of tetrad vectors one finds the functions (a, b, c, D, E, f, G) in Eq. (A.2) in terms of $h^{(1)}_{ab}$. The resulting perturbed tetrad is

$$\begin{aligned} l^{(1)}_\mu &= -h^{(1)}_{ll} n_\mu \\ n^{(1)}_\mu &= -\frac{1}{2} h^{(1)}_{nn} l_\mu - h^{(1)}_{nl} n_\mu \\ m^{(1)}_\mu &= -h^{(1)}_{nm} l_\mu - h^{(1)}_{lm} n_\mu + \frac{1}{2} h^{(1)}_{m\bar{m}} m_\mu + \frac{1}{2} h^{(1)}_{mm} \bar{m}_\mu. \end{aligned} \tag{A.5}$$

So far, the only difference from the perturbed tetrad in Ref. [51] is due to the signature of the metric. Next, Chrzanowski uses gauge transformations to simplify Eq. (A.5); here, I choose to preserve the gauge degrees of freedom.

Chrzanowski's next paragraph alludes to the ability to repeat the above analysis with raised indices using a simple rule. He states

> "Since the contravariant components of the perturbed metric satisfy $g^{\mu\nu} = g^{(0)\mu\nu} - h^{\mu\nu}_{(1)}$, the contravariant components of the perturbed tetrad vectors are opposite in sign to the covariant components, e.g., $n^{(1)\mu} = -g^{\mu\nu} n^{(1)}_\nu$ so that $\Delta^{(1)} = -\frac{1}{2} h^{(1)}_{nn} D$."

That is, to raise the indices, all that is required is a sign change. The reasoning for this statement may not be obvious. Conventionally, raising the index of a perturbation could be construed as having two possible meanings:

$$l^{(1)\mu} = g^{(0)\mu\nu} l^{(1)}_\nu \tag{A.6}$$

or

$$\mathcal{D}(l^\mu) = g^{\mu\nu} l_\nu = (g^{(0)\mu\nu} - h^{\mu\nu}_{(1)})(l^{(0)}_\nu + l^{(1)}_\nu) + \mathcal{O}(\varepsilon^2) \tag{A.7}$$

$$= l^{(1)\mu} - h^{\mu l} + \mathcal{O}(\varepsilon^2). \tag{A.8}$$

Eq. (A.6) is simply the index of the one-form $l^{(1)}_{\nu}$ being raised by the background metric. Eq. (A.7) is the first-order perturbation of the tetrad basis vector l^{μ}. Note that these two definitions are distinct, but also neither satisfy $l^{(1)\mu} = -g^{\mu\nu}l^{(1)}_{\nu}$ in Chrzanowski's statement.

However, the statement $l^{(1)\mu} = -g^{\mu\nu}l^{(1)}_{\nu}$ is consistent if one repeats the analysis of Eqs. (A.1) to (A.5) with all the indices up. This is shown by first noting that as $g^{\mu\nu} = g^{(0)\mu\nu} - h^{\mu\nu}_{(1)}$, Eq. (A.10) becomes

$$\mathcal{D}(g^{\mu\nu}) = \mathcal{D}(-2l^{(\mu}n^{\nu)} + 2m^{(\mu}\bar{m}^{\nu)}) \tag{A.9}$$

$$\Rightarrow -h^{\mu\nu}_{(1)} = -2l^{(\mu}_{(1)}n^{\nu)} - 2l^{(\mu}n^{\nu)}_{(1)} + 2m^{(\mu}_{(1)}\bar{m}^{\nu)} + 2m^{(\mu}\bar{m}^{\nu)}_{(1)}. \tag{A.10}$$

The method is nearly identical and hence the analysis produces contravariant components of the perturbed tetrad vectors which are opposite in sign to the covariant components of my initial analysis (Eq. (A.5)). There is, however, one subtlety: the infinitesimal tetrad transformations in Eq. (A.2) are different when simplifying the perturbed contravariant basis vectors to when one is simplifying the perturbed covariant basis vectors. This can be seen by noting that if $l^{(1)}_{\mu} = -h^{(1)}_{ll}n_{\mu}$, then the corresponding perturbed contravariant basis vector takes the form

$$\mathcal{D}(l^{\mu}) = \mathcal{D}(g^{\mu\nu}l_{\nu}) \tag{A.11}$$

$$= g^{(0)\mu\nu}l^{1}_{\nu} - h^{\mu\nu}_{(1)}l_{\nu} \tag{A.12}$$

$$= -h^{(1)}_{ll}n^{\mu} - h^{\mu l}_{(1)} \tag{A.13}$$

$$\neq h_{ll}n^{\mu} \tag{A.14}$$

Here one finds that $l^{\mu}_{(1)} \neq -g^{(0)\mu\nu}l^{(1)}_{\nu}$. However, by using infinitesimal tetrad transformations, one finds $\mathcal{D}(l_{\mu}) = -h^{(1)}_{ll}n^{\mu} - h^{\mu l}_{(1)}$ can be transformed into $\mathcal{D}(l_{\mu}) = h^{(1)}_{ll}n^{\mu}$. Hence, in Ref. [51] the perturbed tetrad with indices up is a different tetrad to the perturbed tetrad with indices down. Nevertheless, either tetrad is valid.

The next step in the Chrzanowski method [51] is to use the expressions for the perturbed tetrad contravariant vectors to express the perturbed parallel derivatives (Eq. (1.58)),

$$D^{(1)} = \frac{1}{2}h^{(1)}_{ll}\Delta \tag{A.15}$$

$$\Delta^{(1)} = \frac{1}{2}h^{(1)}_{nn}D + h^{(1)}_{nl}\Delta \tag{A.16}$$

$$\delta^{(1)} = h^{(1)}_{nm}D + h^{(1)}_{lm}\Delta - \frac{1}{2}h^{(1)}_{m\bar{m}}\delta - \frac{1}{2}h^{(1)}_{mm}\bar{\delta}_{\mu}. \tag{A.17}$$

Note that these equations are only consistent when acting on scalars. This is because when a tetrad parallel derivative (Eq. (1.58)) acts on a tensor of a higher rank, the

perturbation of the connection (spin coefficients) contributes, and Eqs. (A.15), (A.16), and (A.17) no longer hold.

A.1.1 Calculating the perturbed NP quantities

Now that I have equations for the perturbations of the contravariant tetrad legs and their parallel derivatives, I can attempt to derive the perturbations of the NP scalars. To calculate the perturbed NP spin coefficients, I perturb the NP commutation relations [48]

$$\Delta D - D\Delta = (\gamma + \bar{\gamma})D + (\epsilon + \bar{\epsilon})\Delta - (\pi + \bar{\tau})\delta - (\bar{\pi} + \tau)\bar{\delta}, \tag{A.18}$$

$$\delta D - D\delta = (\bar{\alpha} + \beta - \bar{\pi})D + \kappa\Delta - (\bar{\rho} + \epsilon - \bar{\epsilon})\delta - \sigma\bar{\delta}, \tag{A.19}$$

$$\delta\Delta - \Delta\delta = -\bar{\nu}D + (\tau - \bar{\alpha} - \beta)\Delta + (\mu - \gamma + \bar{\gamma})\delta + \bar{\lambda}\bar{\delta}, \tag{A.20}$$

$$\bar{\delta}\delta - \delta\bar{\delta} = (-\mu + \bar{\mu})D + (-\rho + \bar{\rho})\Delta + (\alpha - \bar{\beta})\delta + (-\bar{\alpha} + \beta)\bar{\delta}. \tag{A.21}$$

After perturbing these equations, I can input the definitions for the perturbed parallel derivatives, Eq. (A.17). By using the zeroth-order commutation relations, one can obtain equations for the twelve NP spin coefficients (in Petrov type-D spacetimes) by

reading off the coefficients for each zeroth-order tetrad parallel derivatives. This gives

$$\begin{aligned}\kappa^{(1)} = &-\kappa h^{(1)}_{ln} - \tfrac{1}{2}\kappa h^{(1)}_{m\bar{m}} - \tfrac{1}{2}\bar{\kappa} h^{(1)}_{mm} - (D - 2\varepsilon - \bar{\rho}) h^{(1)}_{lm} + \sigma h^{(1)}_{l\bar{m}} \\ &- (\bar{\alpha} + \beta - \tfrac{1}{2}\bar{\pi} - \tfrac{1}{2}\tau - \tfrac{1}{2}\delta) h^{(1)}_{ll},\end{aligned} \tag{A.22}$$

$$\sigma^{(1)} = -\tfrac{1}{2}\bar{\lambda} h^{(1)}_{ll} - (\tfrac{1}{2}D - \varepsilon + \bar{\varepsilon} + \tfrac{1}{2}\rho - \tfrac{1}{2}\bar{\rho}) h^{(1)}_{mm} - (-\bar{\pi} - \tau) h^{(1)}_{lm}, \tag{A.23}$$

$$\begin{aligned}\nu^{(1)} = &\lambda h^{(1)}_{nm} - (-\Delta - 2\gamma - \bar{\mu}) h^{(1)}_{n\bar{m}} + \nu h^{(1)}_{ln} - \tfrac{1}{2}\nu h^{(1)}_{m\bar{m}} - \tfrac{1}{2}\bar{\nu} h^{(1)}_{\bar{m}\bar{m}} \\ &- (\alpha + \bar{\beta} - \tfrac{1}{2}\pi - \tfrac{1}{2}\bar{\tau} + \tfrac{1}{2}\bar{\delta}) h^{(1)}_{nn},\end{aligned} \tag{A.24}$$

$$\lambda^{(1)} = \lambda h^{(1)}_{ln} - (-\tfrac{1}{2}\Delta - \gamma + \bar{\gamma} + \tfrac{1}{2}\mu - \tfrac{1}{2}\bar{\mu}) h^{(1)}_{\bar{m}\bar{m}} - \tfrac{1}{2}\bar{\sigma} h^{(1)}_{nn} - (-\pi - \bar{\tau}) h^{(1)}_{n\bar{m}}, \tag{A.25}$$

$$\begin{aligned}\mu^{(1)} = &-(-\tfrac{1}{2}\mu - \tfrac{1}{2}\bar{\mu}) h^{(1)}_{ln} - (-\tfrac{1}{2}\Delta + \tfrac{1}{2}\mu - \tfrac{1}{2}\bar{\mu}) h^{(1)}_{m\bar{m}} - (-\tfrac{1}{2}\delta - \beta - \tfrac{1}{2}\tau) h^{(1)}_{n\bar{m}} \\ &- (\tfrac{1}{2}\bar{\delta} + \bar{\beta} - \pi - \tfrac{1}{2}\bar{\tau}) h^{(1)}_{nm} + \tfrac{1}{2}\nu h^{(1)}_{lm} - \tfrac{1}{2}\bar{\nu} h^{(1)}_{l\bar{m}} - \tfrac{1}{2}\rho h^{(1)}_{nn},\end{aligned} \tag{A.26}$$

$$\begin{aligned}\rho^{(1)} = &\tfrac{1}{2}\kappa h^{(1)}_{n\bar{m}} - \tfrac{1}{2}\bar{\kappa} h^{(1)}_{nm} - \tfrac{1}{2}\mu h^{(1)}_{ll} - (\tfrac{1}{2}\bar{\delta} - \alpha - \tfrac{1}{2}\pi) h^{(1)}_{lm} - (\tfrac{1}{2}\rho - \tfrac{1}{2}\bar{\rho}) h^{(1)}_{ln} \\ &- (\tfrac{1}{2}D + \tfrac{1}{2}\rho - \tfrac{1}{2}\bar{\rho}) h^{(1)}_{m\bar{m}} - (-\tfrac{1}{2}\delta + \bar{\alpha} - \tfrac{1}{2}\bar{\pi} - \tau) h^{(1)}_{l\bar{m}},\end{aligned} \tag{A.27}$$

$$\begin{aligned}\varepsilon^{(1)} = &\tfrac{1}{4}\kappa h^{(1)}_{n\bar{m}} - \tfrac{1}{4}\bar{\kappa} h^{(1)}_{nm} - (-\tfrac{1}{4}\Delta + \tfrac{1}{2}\bar{\gamma} + \tfrac{1}{4}\mu - \tfrac{1}{4}\bar{\mu}) h^{(1)}_{ll} - (\tfrac{1}{2}D + \tfrac{1}{4}\rho - \tfrac{1}{4}\bar{\rho}) h^{(1)}_{ln} \\ &- (\tfrac{1}{4}\rho - \tfrac{1}{4}\bar{\rho}) h^{(1)}_{m\bar{m}} + \tfrac{1}{4}\sigma h^{(1)}_{\bar{m}\bar{m}} - \tfrac{1}{4}\bar{\sigma} h^{(1)}_{mm} - (-\tfrac{1}{4}\delta + \tfrac{1}{2}\bar{\alpha} - \tfrac{1}{4}\bar{\pi} - \tfrac{1}{2}\tau) h^{(1)}_{l\bar{m}} \\ &- (\tfrac{1}{4}\bar{\delta} - \tfrac{1}{2}\alpha - \tfrac{3}{4}\pi - \tfrac{1}{2}\bar{\tau}) h^{(1)}_{lm},\end{aligned} \tag{A.28}$$

$$\begin{aligned}\pi^{(1)} = &\tfrac{1}{2}\lambda h^{(1)}_{lm} - (-\tfrac{1}{2}\Delta + \bar{\gamma} - \tfrac{1}{2}\bar{\mu}) h^{(1)}_{l\bar{m}} - (-\tfrac{1}{2}D - \varepsilon + \tfrac{1}{2}\rho) h^{(1)}_{n\bar{m}} - \tfrac{1}{2}\bar{\sigma} h^{(1)}_{nm} \\ &+ \tfrac{1}{2}\tau h^{(1)}_{\bar{m}\bar{m}} - (\tfrac{1}{2}\bar{\delta} + \tfrac{1}{2}\pi + \tfrac{1}{2}\bar{\tau}) h^{(1)}_{ln} + \tfrac{1}{2}\bar{\tau} h^{(1)}_{m\bar{m}},\end{aligned} \tag{A.29}$$

$$\begin{aligned}\tau^{(1)} = &-\tfrac{1}{2}\bar{\lambda} h^{(1)}_{l\bar{m}} - (\tfrac{1}{2}\Delta - \gamma + \tfrac{1}{2}\mu) h^{(1)}_{lm} + \tfrac{1}{2}\pi h^{(1)}_{mm} + \tfrac{1}{2}\bar{\pi} h^{(1)}_{m\bar{m}} \\ &- (\tfrac{1}{2}D + \bar{\varepsilon} - \tfrac{1}{2}\bar{\rho}) h^{(1)}_{nm} + \tfrac{1}{2}\sigma h^{(1)}_{n\bar{m}} - (-\tfrac{1}{2}\delta - \tfrac{1}{2}\bar{\pi} - \tfrac{1}{2}\tau) h^{(1)}_{ln},\end{aligned} \tag{A.30}$$

$$\begin{aligned}\alpha^{(1)} = &-\tfrac{1}{4}\bar{\kappa} h^{(1)}_{nn} + \tfrac{3}{4}\lambda h^{(1)}_{lm} - (-\tfrac{1}{4}\Delta - \gamma + \tfrac{1}{2}\bar{\gamma} + \tfrac{1}{2}\mu - \tfrac{1}{4}\bar{\mu}) h^{(1)}_{l\bar{m}} - \tfrac{1}{4}\nu h^{(1)}_{ll} \\ &- (\tfrac{1}{4}D - \tfrac{1}{2}\varepsilon - \tfrac{1}{4}\rho - \tfrac{1}{2}\bar{\rho}) h^{(1)}_{n\bar{m}} - \tfrac{1}{4}\bar{\sigma} h^{(1)}_{nm} - (-\tfrac{1}{4}\delta + \tfrac{1}{2}\bar{\alpha} - \tfrac{1}{4}\bar{\pi} - \tfrac{1}{4}\tau) h^{(1)}_{\bar{m}\bar{m}} \\ &- (\tfrac{1}{4}\bar{\delta} - \tfrac{1}{4}\pi - \tfrac{1}{4}\bar{\tau}) h^{(1)}_{ln} - (\tfrac{1}{4}\bar{\delta} + \tfrac{1}{2}\alpha - \tfrac{1}{4}\pi - \tfrac{1}{4}\bar{\tau}) h^{(1)}_{m\bar{m}},\end{aligned} \tag{A.31}$$

$$\begin{aligned}\beta^{(1)} = &-\tfrac{1}{4}\kappa h^{(1)}_{nn} - \tfrac{1}{4}\bar{\lambda} h^{(1)}_{l\bar{m}} - (-\tfrac{1}{4}\Delta - \tfrac{1}{2}\gamma - \tfrac{1}{4}\mu - \tfrac{1}{2}\bar{\mu}) h^{(1)}_{lm} - \tfrac{1}{4}\bar{\nu} h^{(1)}_{ll} \\ &- (\tfrac{1}{4}D - \varepsilon + \tfrac{1}{2}\bar{\varepsilon} + \tfrac{1}{2}\rho - \tfrac{1}{4}\bar{\rho}) h^{(1)}_{nm} + \tfrac{3}{4}\sigma h^{(1)}_{n\bar{m}} - (\tfrac{1}{4}\delta - \tfrac{1}{4}\bar{\pi} - \tfrac{1}{4}\tau) h^{(1)}_{ln} \\ &- (-\tfrac{1}{4}\delta + \tfrac{1}{2}\beta - \tfrac{1}{4}\bar{\pi} - \tfrac{1}{4}\tau) h^{(1)}_{m\bar{m}} - (\tfrac{1}{4}\bar{\delta} + \tfrac{1}{2}\bar{\beta} - \tfrac{1}{4}\pi - \tfrac{1}{4}\bar{\tau}) h^{(1)}_{mm},\end{aligned} \tag{A.32}$$

$$\begin{aligned}\gamma^{(1)} = &\tfrac{1}{4}\lambda h^{(1)}_{mm} - \tfrac{1}{4}\bar{\lambda} h^{(1)}_{\bar{m}\bar{m}} - (\tfrac{1}{4}\mu - \tfrac{1}{4}\bar{\mu}) h^{(1)}_{m\bar{m}} - (-\gamma + \tfrac{1}{4}\mu - \tfrac{1}{4}\bar{\mu}) h^{(1)}_{ln} + \tfrac{1}{4}\nu h^{(1)}_{lm} - \tfrac{1}{4}\bar{\nu} h^{(1)}_{l\bar{m}} \\ &- (\tfrac{1}{4}D + \tfrac{1}{2}\bar{\varepsilon} + \tfrac{1}{4}\rho - \tfrac{1}{4}\bar{\rho}) h^{(1)}_{nn} - (-\tfrac{1}{4}\delta - \tfrac{1}{2}\beta - \tfrac{1}{2}\bar{\pi} - \tfrac{3}{4}\tau) h^{(1)}_{n\bar{m}} \\ &- (\tfrac{1}{4}\bar{\delta} + \tfrac{1}{2}\bar{\beta} - \tfrac{1}{2}\pi - \tfrac{1}{4}\bar{\tau}) h^{(1)}_{nm}.\end{aligned} \tag{A.33}$$

The perturbed Weyl scalars can be calculated by perturbing the Ricci identities (e.g., for ψ_0 I use Eq. (1.71)). This gives

$$\begin{aligned}\Psi_0^{(1)} &= (-3\epsilon^{(1)} + \bar{\epsilon}^{(1)} - \rho^{(1)} - \bar{\rho}^{(1)})\sigma + (-3\epsilon + \bar{\epsilon} - \rho - \bar{\rho})\sigma^{(1)} \\ &\quad + \kappa^{(1)}(\bar{\alpha} + 3\beta - \bar{\pi} + \tau) + \kappa(\bar{\alpha}^{(1)} + 3\beta^{(1)} - \bar{\pi}^{(1)} + \tau^{(1)}) - \\ &\quad h_{nm}^{(1)} D\kappa + D\sigma^{(1)} - h_{lm}^{(1)}\Delta\kappa + \tfrac{1}{2}h_{ll}^{1}\Delta\sigma + \tfrac{1}{2}h_{n\bar{m}}^{(1)}\delta\kappa - \delta\kappa^{(1)} + \tfrac{1}{2}h_{mm}^{(1)}\bar{\delta}\kappa, \end{aligned} \tag{A.34}$$

$$\begin{aligned}\Psi_1^{(1)} &= \kappa^{(1)}(\gamma + \mu) + \kappa(\gamma^{(1)} + \mu^{(1)}) + \epsilon^{(1)}(\bar{\alpha} - \bar{\pi}) + \epsilon(\bar{\alpha}^{(1)} - \bar{\pi}^{(1)}) + \beta^{(1)}(\bar{\epsilon} - \bar{\rho}) \\ &\quad + \beta(\bar{\epsilon}^{(1)} - \bar{\rho}^{(1)}) + (-\alpha^{(1)} - \pi^{(1)})\sigma + (-\alpha - \pi)\sigma^{(1)} \\ &\quad + D\beta^{(1)} - h_{nm}^{(1)} D\epsilon + \tfrac{1}{2}h_{ll}^{(1)}\Delta\beta - h_{lm}^{(1)}\Delta\epsilon + \tfrac{1}{2}h_{n\bar{m}}^{(1)}\delta\epsilon - \delta\epsilon^{(1)} + \tfrac{1}{2}h_{mm}^{(1)}\bar{\delta}\epsilon, \end{aligned} \tag{A.35}$$

$$\begin{aligned}\Psi_2^{(1)} &= \tfrac{1}{3}\big(\bar{\epsilon}^{(1)}\mu + \bar{\epsilon}\mu^{(1)} + \epsilon^{(1)}(\bar{\gamma} + 2\mu - \bar{\mu}) + \epsilon(2\gamma^{(1)} + \bar{\gamma}^{(1)} + 2\mu^{(1)} - \bar{\mu}^{(1)}) \\ &\quad + 2\kappa^{(1)}\nu + 2\kappa\nu^{(1)} + \bar{\alpha}^{(1)}\pi + \bar{\alpha}\pi^{(1)} + \alpha^{(1)}(\bar{\alpha} - \bar{\pi}) - \pi^{(1)}\bar{\pi} - \pi\bar{\pi}^{(1)} \\ &\quad + (\gamma^{(1)} + \mu^{(1)})\rho + \mu\rho^{(1)} + \gamma^{(1)}(\bar{\epsilon} - \bar{\rho}) - \mu^{(1)}\bar{\rho} + \gamma(2\epsilon^{(1)} + \bar{\epsilon}^{(1)} + \rho^{(1)} - \bar{\rho}^{(1)}) \\ &\quad - \mu\bar{\rho}^{(1)} - 2\lambda^{(1)}\sigma - 2\lambda\sigma^{(1)} + (-\alpha^{(1)} - \pi^{(1)})\tau + \alpha(\bar{\alpha}^{(1)} - 2\beta^{(1)} - \bar{\pi}^{(1)} - \tau^{(1)}) \\ &\quad - \pi\tau^{(1)} + \beta^{(1)}(\bar{\beta} - 2\pi - \bar{\tau}) + \beta(-2\alpha^{(1)} + \bar{\beta}^{(1)} - 2\pi^{(1)} - \bar{\tau}^{(1)}) \\ &\quad - h_{nm}^{(1)} D\alpha + h_{n\bar{m}}^{(1)} D\beta - \tfrac{1}{2}h_{nn}^{(1)} D\epsilon + D\gamma^{(1)} + D\mu^{(1)} - h_{nm}^{(1)} D\pi - h_{lm}^{(1)}\Delta\alpha \\ &\quad + h_{l\bar{m}}^{(1)}\Delta\beta - h_{ln}^{(1)}\Delta\epsilon - \Delta\epsilon^{(1)} + \tfrac{1}{2}h_{ll}^{(1)}\Delta\gamma + \tfrac{1}{2}h_{ll}^{(1)}\Delta\mu - h_{lm}^{(1)}\Delta\pi \\ &\quad + \tfrac{1}{2}h_{n\bar{m}}^{(1)}\delta\alpha - \delta\alpha^{(1)} - \tfrac{1}{2}h_{\bar{m}\bar{m}}^{(1)}\delta\beta + \tfrac{1}{2}h_{n\bar{m}}^{(1)}\delta\pi - \delta\pi^{(1)} + \tfrac{1}{2}h_{mm}^{(1)}\bar{\delta}\alpha \\ &\quad - \tfrac{1}{2}h_{n\bar{m}}^{(1)}\bar{\delta}\beta + \bar{\delta}\beta^{(1)} + \tfrac{1}{2}h_{mm}^{(1)}\bar{\delta}\pi\big), \end{aligned} \tag{A.36}$$

$$\begin{aligned}\Psi_3^{(1)} &= \alpha^{(1)}(\bar{\gamma} - \bar{\mu}) + \alpha(\bar{\gamma}^{(1)} - \bar{\mu}^{(1)}) + \nu^{(1)}(\epsilon + \rho) + \nu(\epsilon^{(1)} + \rho^{(1)}) + \lambda^{(1)}(-\beta - \tau) \\ &\quad + \lambda(-\beta^{(1)} - \tau^{(1)}) + \gamma^{(1)}(\bar{\beta} - \bar{\tau}) + \gamma(\bar{\beta}^{(1)} - \bar{\tau}^{(1)}) - \tfrac{1}{2}h_{nn}^{(1)} D\alpha + h_{n\bar{m}}^{(1)} D\gamma \\ &\quad - h_{ln}^{(1)}\Delta\alpha - \Delta\alpha^{(1)} + h_{l\bar{m}}^{(1)}\Delta\gamma - \tfrac{1}{2}h_{\bar{m}\bar{m}}^{(1)}\delta\gamma - \tfrac{1}{2}h_{43}^{(1)}\bar{\delta}\gamma + \bar{\delta}\gamma^{(1)}, \end{aligned} \tag{A.37}$$

$$\begin{aligned}\Psi_4^{(1)} &= -\lambda^{(1)}(3\gamma - \bar{\gamma} + \mu + \bar{\mu}) - \lambda(3\gamma^{(1)} - \bar{\gamma}^{(1)} + \mu^{(1)} + \bar{\mu})^{(1)} \\ &\quad - \nu^{(1)}(-3\alpha - \bar{\beta} - \pi + \bar{\tau}) - \nu(-3\alpha^{(1)} - \bar{\beta}^{(1)} - \pi^{(1)} + \bar{\tau})^{(1)} \\ &\quad - \tfrac{1}{2}h_{nn}^{(1)} D\lambda + h_{n\bar{m}}^{(1)} D\nu - h_{ln}^{(1)}\Delta\lambda - \Delta\lambda^{(1)} + h_{l\bar{m}}^{(1)}\Delta\nu - \tfrac{1}{2}h_{\bar{m}\bar{m}}^{(1)}\delta\nu \\ &\quad - \tfrac{1}{2}h_{m\bar{m}}^{(1)}\bar{\delta}\nu + \bar{\delta}\nu^{(1)}. \end{aligned} \tag{A.38}$$

The equations for the perturbed NP spin coefficients and Weyl scalars (Eqs. (A.22) to (A.38)) are consistent with Refs. [72] and [102] (and have also been checked against the unpublished results of Béatrice Bonga). The perturbed NP spin coefficients (Eq. (A.33)) include some minor corrections to Ref. [45].

Appendix B

Transformation to a Bondi-Sachs Gauge in Coordinate Form

Here I give a method for calculating the gauge vector ξ^a which takes one from any gauge to the Bondi–Sachs gauge. The calculation for ξ^a reduces to solving a hierarchical set of ODEs along outgoing radial null rays. The resulting metric perturbation, $\hat{h}_{ab} = h_{ab} + 2\nabla_{(a}\xi_{b)}$, is fully gauge fixed up to the BMS freedoms (which I fix in Sec. 3.6.7). The results in this appendix were obtained by Jordan Moxon (and will be published in Ref. [174]) and reproduced here to provide context for the Bond–Sachs gauge fixing method in NP form in Sec. 3.6.

I assume that $g^{(0)}_{ab}$ is expressed in a Bondi-Sachs gauge, which I review in Sec. 3.6.6 for Kerr spacetimes.

To derive equations for ξ^a from the Bondi-Sachs gauge conditions, I work with the index-up version of the metric. The perturbative expansion of the index-up metric takes the form

$$g^{ab} = g^{ab}_{(0)} - h^{ab}_{(1)} + \mathcal{O}(\varepsilon^2), \tag{B.1}$$

and the index-up Bondi-Sachs metric (the inverse of Eq. (3.23)) has components

$$g^{\alpha\beta}_{(0)} = \begin{bmatrix} 0 & -e^{-2\beta} & 0^A \\ -e^{-2\beta} & \frac{e^{-2\beta}V}{\hat{r}} & -e^{-2\beta}U^A \\ 0^b & -e^{-2\beta}U^B & \hat{r}^{-2}f^{AB} \end{bmatrix}. \tag{B.2}$$

I write the decomposition of the gauge vector into ξ^u, ξ^r and ξ^A pieces as

$$\xi^a = \begin{bmatrix} a \\ b \\ c^A \end{bmatrix}. \tag{B.3}$$

The gauge conditions $\hat{h}^{uu} = 0$ and $\hat{h}^{uA} = 0$ simplify to a hierarchical pair of radial ordinary differential equations,

$$\partial_{\hat{r}} a = -e^{2\beta} h^{uu}, \tag{B.4a}$$

$$\partial_{\hat{r}} c^A = -e^{2\beta} U^A h^{uu} + \frac{1}{\hat{r}^2} e^{2\beta} h^{AB} \partial_B a + h^{uA}. \tag{B.4b}$$

The equations (B.4) determine the gauge components a and c up to an integration constant which corresponds to choosing a and c^A on a single $r =$ constant surface. I choose this surface to be $\mathcal{I}^+$.

The u dependence of a and c^A (at $\mathcal{I}^+$) is constrained by the asymptotic falloff conditions $\lim_{r\to\infty} \hat{h}^{\hat{r}u} = 0$ and $\lim_{r\to\infty} \hat{h}^{\hat{r}A} = 0$. These produce the evolution equations

$$\partial_u a|_{\mathcal{I}^+} = -h^{ru}|_{\mathcal{I}^+}, \tag{B.5a}$$

$$\partial_u c^A|_{\mathcal{I}^+} = -h^{rA}|_{\mathcal{I}^+}. \tag{B.5b}$$

The RHS of these equations is zero if the original gauge is asymptotically flat. This fixes the remaining freedom of a and c^A at $\mathcal{I}^+$, up to choosing an initial a and c^A on a single sphere at constant u (at $\mathcal{I}^+$). When working in the frequency domain, the above equations constrain the oscillatory part of the gauge vector, and the zero frequency contribution remains unfixed (corresponding to the initial data).

I must also apply the condition $\hat{h}^{AB} \to 0$ at $\mathcal{I}^+$. This constraint will be used to constrain the traceless part of $\hat{h}^{AB}$ (the trace piece is constrained by Eq. (B.7)). This condition can be expressed as

$$(D^A c^B - \frac{1}{2} q^{AB} D_C c^C)|_{\mathcal{I}^+} = (h^{AB} - q^{AB} h_A{}^A)|_{\mathcal{I}^+}. \tag{B.6}$$

Eq. (B.6) fixes the initial data of c^A up to a $\ell = 1$ vector harmonic contribution. Eq. (B.6) must hold over the entirety of $\mathcal{I}^+$. This may appear problematic when simultaneously imposing the evolution condition (B.5). However, Ref. [124] demonstrated that $\hat{h}^{AB} \to 0$ at $\mathcal{I}^+$ is ensured by consistency with the EFE (provided it is successfully imposed for a single initial hypersurface). In the frequency domain,

this is equivalent to the nonzero frequency conditions being imposed by the EFE (provided the zero frequency part is in the Bondi-Sachs gauge). The remaining freedom is choosing a on a sphere of constant u at $\mathcal{I}^+$, and the vector harmonic $\ell = 1$ piece of c^A. These freedoms both correspond to the perturbative BMS freedoms.

Finally, imposing the gauge condition condition $q_{AB}\hat{h}^{AB} = 0$ (equivalent to ensuring r is the areal coordinate of the perturbed metric) constrains the remaining gauge vector component (b). This results in

$$b = \frac{\hat{r}}{4} D_A c^A - \frac{e^{2\beta}\hat{r}^3}{4} U^A h_{AB} \partial_{\hat{r}} c^B. \tag{B.7}$$

As this equation is algebraic (given c^A is known), it determines b entirely. Note, the condition that $\hat{h}^{\hat{r}\hat{r}} \to 0$ at $\mathcal{I}^+$is satisfied by consistency with the EFE when the above conditions are also satisfied.

Hence, by solving this hierarchical differential equation, one can calculate the gauge vector ξ to the Bondi–Sachs gauge. In summary, and in a practical order for calculating a, b, and c:

1. Choose initial data for a on a single cut of $\mathcal{I}^+$, then determine initial data for c on that same cut using Eq. (B.6).
2. Use Eq. (B.5) to calculate a and c on the whole of $\mathcal{I}^+$.
3. Use Eq. (B.4) to extend a, then c^A into the spacetime, on each hypersurface, given their values at $\mathcal{I}^+$.
4. Use Eq. (B.7) to calculate b given a and c^A on each hypersurface.

To fully constrain the gauge, one can derive the initial data using the BMS frame fixing method in Sec. 3.6.7.

Appendix C

Deriving the Local Gauge Transform to a Highly Regular Gauge

Here, I present the full derivation of the gauge vector (ξ^a) which takes one from the Lorenz gauge to a highly regular gauge near the worldline (as summarised in Sec. 3.7). I shall write $\xi^a[x^\mu]$ (at point x with coordinates x^μ) as a function of the difference in coordinates from a point on the worldline (x' with coordinates $x^{\mu'}$) to x, $\Delta x^\mu[x^\mu] = x^\mu - x^{\mu'}$. $x^{\mu'}$ and x^μ are connected by a future-directed null geodesic β_{x^μ} (on the background spacetime). For each x^μ there is a unique β_{x^μ} that connects to the worldline. Hence, for each x^μ there is a unique $x^{\mu'}$ and Δx^μ.

As I am interested in calculating $\xi^a[x^\mu]$ near γ, I will express $\xi^a[x^\mu]$ as an expansion in the distance from the worldline. First, I must define the distance from the worldline. As Δx^μ is the difference between two points on a null geodesic, to zeroth-order, it is a null vector; hence, Δx^μ is null in length. However, one can isolate the spatial part of Δx^μ, which I denote as λ. λ will be an appropriate measure for distance from the worldline. Later I shall derive a precise way of extracting the spatial piece of Δx^μ, defining λ. But for now, I use λ only to denote the order of expansion. I intend to define $\xi^a[x^\mu]$ to $\mathcal{O}(\lambda^0)$ as this should be sufficient for eliminating the most singular term in $h^{(1)}_{ab}$ on the worldline.

To calculate the gauge vector to a highly regular gauge, I first must analyse what makes a gauge highly regular. The highly regular gauge condition is

$$h^{HR}_{ab}k^a = 0. \tag{C.1}$$

Where h^{HR}_{ab} is the metric perturbation in the highly regular gauge and k^a is the set of null vectors corresponding to the set of future-directed null geodesics, β, emanating from the worldline (i.e., the compact object's future directed light cone, see Fig. C.1). Note that β_{x^μ} is a member of the set β. Therefore, a gauge transform from a generic

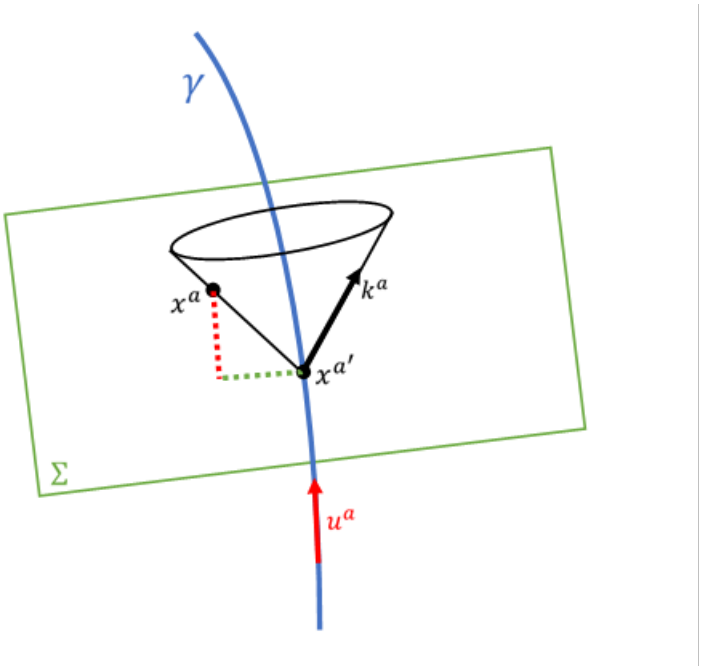

FIGURE C.1: A light-cone extending from the retarded position of the compact object, $x^{\mu'}$ (on the geodesic γ), with a retarded time t_{ret}. The null vectors tangent to the generators of the light cone are labeled k^a. The green rectangular plane represents the spacelike hyperspace (Σ) orthogonal to the objects four-velocity ($u^{a'}$) containing x', on which each point x^a can be projected (see the green dashed line which is tangent to the green spacelike hyperspace, the red dashed line is tangent to u^a). Similarly, the null vector k^a can be projected onto the spacelike hyperspace.

gauge into a highly regular gauge is given by

$$(h_{ab} + \mathcal{L}_{\xi^a} g_{ab}) k^a = 0. \tag{C.2}$$

I wish to find the gauge vector ξ^a, specializing to the case that the initial metric perturbation is in the Lorenz gauge. To achieve this, first, I must express the set of null vectors k^a as an expansion in the distance from the worldline λ.

C.1 Expanding k^a in orders of distance from the worldline

Here I set out a method for defining an expansion for k^a in order of distance from γ, up to $\mathcal{O}(\lambda^0)$. Expressly, given a point x in the neighbourhood of γ, I will derive an equation for k^a written as a function of x^μ and $u^a[x']$ (the four-velocity of γ). I shall achieve this by splitting k^a into a timelike piece, tangent to u^a, and a spacelike piece, orthogonal to u^a. Note that all quantities with primed indices are evaluated at x', and those with indices without a prime are evaluated at x.

k^a is defined as the null vector (see Fig. C.1) associated with the unique null geodesic β connecting point x to x'. However, during this derivation, I relax this definition as I

only require calculating k^a up to $\mathcal{O}(\lambda^0)$. Many of these simplifications would have to be reconsidered if one were to attempt a higher-order expansion.

First, I split k^a locally into a timelike piece and a spacelike piece using Fermi-Walker coordinates (which, at leading order, are indistinguishable from Fermi normal coordinates). This method is consistent with any global coordinate scheme as I shall construct a local basis defined with respect to the global coordinate system. Fermi normal coordinates are constructed from an orthonormal basis that is parallel propagated along γ [140]. For the timelike basis vector, I use u^a (appropriate as γ is a timelike geodesic). The spacelike basis vectors are labelled $e_i^{(1)}$, $e_i^{(2)}$ and $e_i^{(3)}$ and are tangent to the hypersurface Σ (which is orthogonal to u^a, see Fig. C.1). To obtain the basis vectors for all proper times on γ, the basis vectors are parallel transported along γ. Note, as I have not specified the coordinate basis of u^a, it is independent of the global coordinate system. This method allows us to work within Σ covariantly.

In this basis I can write $u^{a'} = (1, 0^i)$, where $i \in \{1, 2, 3\}$. I can also write k^a as $k^a = (k^\tau, k^i)$, where τ is a time coordinate (on x' τ is the proper time of γ), and k^τ and k^i denote the timelike and spacelike part of k^a respectively. As k^a is a null vector, the scaling of its components is arbitrary (as long as it remains future directed). Hence, I can fix $k^\tau = 1$ for simplicity (rescaling k^i), making $k^a = (1, k^i)$.

Next, I want to express k^i near the point x' as an expansion in orders of distance from the worldline. As k^a is a null vector, the expansion must satisfy $g_{ab}k^a k^b = 0$. In Fermi coordinates, the metric components on γ reduce to the Minkowski metric [140]. Hence, on γ, the null vector condition takes the simple form

$$\begin{aligned} & \eta_{ab}k^a k^b = 0, \\ \Rightarrow \quad & -1 + \delta_{ij}k^i k^j = 0, \end{aligned} \tag{C.3}$$

where η_{ab} is the Minkowski metric. Therefore, locally $\delta_{ij}k^i k^j = 1$. That is, k^i is a spacelike unit three-vector.

The choice of Fermi normal coordinates has naturally partitioned k^a into a timelike piece (k^τ) and a spacelike piece (k^i); however, I wish to represent the split of k^a in terms of four-vectors. On the worldline, the timelike piece is tangent to $u^{a'}$, and the spacelike piece is orthogonal to $u^{a'}$. At this point I need to define u^a off of the worldline. This can be achieved by parallel transporting $u^{a'}$. I use the bi-tensor of parallel transport [143], $g^a{}_{b'}$, to define $u^a := g^a_{a'}u^{a'}$. Therefore, with the inclusion of the

transport tensor, the tangent piece ($k^a_{\parallel}$) to u^a is given by

$$\begin{aligned} k^a_{\parallel} &= -g^a{}_{c'} g^b{}_{d'} u^{c'} u^{d'} g_{cb} k^c, \\ &= -(\delta^a{}_{c'} + \mathcal{O}(\lambda))(\delta^b{}_{d'} + \mathcal{O}(\lambda)) u^{c'} u^{d'} (\eta_{cb} + \mathcal{O}(\lambda)) k^c, \\ &= -u^a u^b \eta_{cb} k^c + \mathcal{O}(\lambda), \\ &= u^a k^\tau + \mathcal{O}(\lambda), \\ &= u^a + \mathcal{O}(\lambda), \qquad \text{(C.4)} \\ &= (1, 0^i) + \mathcal{O}(\lambda), \qquad \text{(C.5)} \end{aligned}$$

where I have used $g^c{}_{c'} = \delta^c{}_{c'} + \mathcal{O}(\lambda)$ [143] and $g_{ab} = \eta_{ab} + \mathcal{O}(\lambda)$. From here on out I use $u^a = \delta^a{}_{c'} u^{c'} + \mathcal{O}(\lambda)$. This results in a simple equation for the tangent piece of k^a to u^a (Eq. (C.5)).

The orthogonal piece of k^a to u^a ($k^a_{\perp}$) can be obtained by using the projection operator $P_{ab} = g_{ab} + u_a u_b$. Hence,

$$\begin{aligned} k^a_{\perp} &= P^a{}_b k^b \\ &= k^a - u^a + \mathcal{O}(\lambda) \\ &= (0, k^i) + \mathcal{O}(\lambda). \qquad \text{(C.6)} \end{aligned}$$

From this point, I can drop the specialisation to Fermi-Walker coordinates and produce equations defined in arbitrary coordinate schemes. I need to express k^i as a function of x^α and u^a. In Fermi normal coordinates, spacetime is locally flat. Therefore, to calculate k^i, I can simplify the definition of k^a by noting that in flat spacetime, geodesics are straight lines. That is, the direction of k^a must be equivalent to the direction of the vector connecting points x and x', $k^a \propto \Delta x^a := x^a - x^\alpha$. In the flat-spacetime approximation, one can consider Δx^a as a tensorial object; however, in curved spacetime, conducting covariant calculations requires replacing the role of Δx^a with Synge's world-function $\sigma(x, x')$ [143]. Note, in flat spacetime one can consider Δx^a as a bivector as it is evaluated at two points simultaneously (x and x').

To isolate the piece of Δx^a orthogonal u^a, I again use the projection operator,

$$k^a_{\perp} \propto P^a{}_b \Delta x^b + \mathcal{O}(\lambda). \qquad \text{(C.7)}$$

As k^i is required to be a unit vector (see Eq. (C.3)), I must re-normalise for the magnitude of $P^a{}_b \Delta x^b$. As $P^a{}_b P_{ac} = P_{cb}$, this gives

$$k^a_{\perp} = \frac{P^a{}_b \Delta x^b}{\sqrt{P_{cd} \Delta x^c \Delta x^d}} + \mathcal{O}(\lambda), \qquad \text{(C.8)}$$

a function for $k^a_\perp$ in terms of Δx^a and P_{ab}. Summing $k^a_\parallel$ and $k^a_\perp$ gives k^a,

$$k^a = k^a_\parallel + k^a_\perp = u^a + \frac{P^a{}_b \Delta x^b}{\sqrt{P_{cd}\Delta x^c \Delta x^d}} + \mathcal{O}(\lambda). \tag{C.9}$$

C.2 Approximating x'

I have found an expression for k^a (Eq. (C.9)), but I am not finished because Δx^a and $u^a = g^a_{c'} u^{c'}$ are both functions of x'. As x' is defined as the point on γ which connects to x with a unique null geodesic β, calculating x' exactly is challenging. Instead, I will find a sufficiently accurate approximation by expanding $x^{a'}$ in orders of λ.

Finding x' for a given x is a non-trivial problem. To begin, I approximate x' using $\hat{x}$, the point on γ with the same coordinate time as point x. I can then expand around $\hat{x}$ in orders of λ to approximate x'. Tensors evaluated at $\hat{x}$ have indices with a hat.

First I evaluate if the projection operator (arising in Eq. (C.9)) can be approximated by setting $\hat{x} = x'$. As I am working in approximately flat spacetime, γ is a straight line. Hence, $u^{a'} = u^{\hat{a}} + \mathcal{O}(\lambda)$. Using the transport tensor ($g^a_{\hat{a}}$) [143], I define $\hat{u}^a := g^a_{\hat{a}} u^{\hat{a}} = \delta^a_{\hat{a}} u^{\hat{a}} + \mathcal{O}(\lambda)$. Also, in the flat space approximation $g_{a'b'} = g_{\hat{a}\hat{b}} + \mathcal{O}(\lambda)$. Therefore, the projection operator at $\hat{x}$ is equivalent to the projection operator at x' up to $\mathcal{O}(\lambda)$. That is, $P_{ab} = P_{\hat{a}\hat{b}} + \mathcal{O}(\lambda)$.

Next, I must show that $\Delta x^{\hat{\alpha}} := x^\alpha - x^{\hat{\alpha}}$ (where $x^{\hat{\alpha}}$ is the coordinates of $\hat{x}$) sufficiently approximates Δx^a. $x^{\alpha'}$ and $x^{\hat{\alpha}}$ both sit on γ; given $\Delta\tau$ ($x^{\tau'} - x^{\hat{\tau}} := \Delta\tau$), the difference between $x^{\alpha'}$ and $x^{\hat{\alpha}}$ is $\Delta\tau u^{a'} + \mathcal{O}(\lambda^2)$ which is $\mathcal{O}(\lambda)$. Hence,

$$x^{\hat{\alpha}} = x^{\alpha'} + \mathcal{O}(\lambda). \tag{C.10}$$

Therefore,

$$\Delta x^{\hat{\alpha}} = \Delta x^{\alpha'} + \mathcal{O}(\lambda). \tag{C.11}$$

Hence, using Eq. (C.8), all corrections to $k_\perp$ and $k_\parallel$ are $\mathcal{O}(\lambda)$ when one uses $\hat{x}$ in place of x'. Therefore, I can write k^a as

$$k^a = u^{\hat{a}} + \frac{P^{\hat{a}}{}_{\hat{b}} \Delta x^{\hat{a}}}{\sqrt{\hat{P}_{\hat{c}\hat{d}}\Delta x^{\hat{c}} \Delta x^{\hat{d}}}} + \mathcal{O}(\lambda). \tag{C.12}$$

C.3 Obtaining an expansion for ξ^a

Returning to Eq. (C.2), by writing the Lie derivative in terms of covariant derivatives, one obtains

$$\begin{aligned}(h_{ab} + \xi^c{}_{;a} g_{cb} + \xi^c{}_{;b} g_{ac}) k^a = 0,\\ \Rightarrow (h_{ab} + \xi_{b;a} + \xi_{a;b}) k^a = 0,\end{aligned} \tag{C.13}$$

where I have used the fact $g_{ab;c} = 0$. With my expansion for k^a (Eq. (C.12)) to hand, and assuming that h_{ab} is known (in the Lorenz gauge), I am now prepared to solve Eq. (C.13) for ξ^a.

I shall begin with an ansatz for the form of ξ_a as an expansion up to $\mathcal{O}(\lambda)$,

$$\xi_a = g^{\hat{a}}{}_a \left[X_{\hat{a}} \log[\rho] + Y_{\hat{a}} + Z_{\hat{a}\hat{b}} \frac{\Delta x^{\hat{b}}}{\rho} \right] + \mathcal{O}(\lambda), \tag{C.14}$$

$$\Rightarrow \xi_a = g^{\hat{a}}{}_a \xi_{\hat{a}} + \mathcal{O}(\lambda), \tag{C.15}$$

with

$$\xi_{\hat{a}} := X_{\hat{a}} \log[\rho] + Y_{\hat{a}} + Z_{\hat{a}\hat{b}} \frac{\Delta x^{\hat{b}}}{\rho}, \tag{C.16}$$

where $X_{\hat{a}}$, $Y_{\hat{a}}$ and $Z_{\hat{a}\hat{b}}$ are coefficients independent of λ (which are all evaluated at $\hat{x}$) and $\rho := \sqrt{P_{\hat{c}\hat{d}} \Delta x^{\hat{c}} \Delta x^{\hat{d}}} \sim \lambda$.

Eq. (C.13) contains the covariant derivative of ξ_a only. To find $\xi_{a;b}$ I act with the covariant derivative on (C.16), giving

$$\xi_{a;b} = g^{\hat{a}}{}_{a;b} \xi_{\hat{a}} + g^{\hat{a}}{}_a \xi_{\hat{a};b}, \tag{C.17}$$

$$\Rightarrow \xi_{a;b} = g^{\hat{a}}{}_a \xi_{\hat{a};b} + \mathcal{O}(\lambda), \tag{C.18}$$

where I have used $g^{\hat{a}}{}_{a;b} = \mathcal{O}(\lambda)$ [143]. Let Eq. (C.18) define $\xi_{\hat{a};b}$. Taking the covariant derivative of Eq. (C.16), one can show $\xi_{\hat{a};b}$ is given by

$$\xi_{\hat{a};b} = X_{\hat{a}} \frac{P_{\hat{c}\hat{d}} \Delta x^{\hat{c}}{}_{;b} \Delta x^{\hat{d}}}{\rho^2} + Z_{\hat{a}\hat{b}} \left[\frac{\Delta x^{\hat{b}}{}_{;b}}{\rho} - \frac{\Delta x^{\hat{b}} P_{\hat{e}\hat{f}} \Delta x^{\hat{e}}{}_{;b} \Delta x^{\hat{f}}}{\rho^{\frac{3}{2}}} \right] + \mathcal{O}(\lambda^0), \tag{C.19}$$

as the coefficients (such as $X_{\hat{a}}$) are evaluated at $\hat{x}$, their covariant derivative at x are suppressed by an $\mathcal{O}(\lambda^1)$ (i.e., $X_{\hat{a};b} = \mathcal{O}(\lambda^1)$).

I now find an expression for $\Delta x^{\hat{a}}{}_{;b}$,

$$\Delta x^{\hat{a}}{}_{;b} = \Delta x^{\hat{a}}{}_{,b} - \Gamma^{\hat{a}}{}_{b\hat{c}}\Delta x^{\hat{c}} \tag{C.20}$$
$$= \Delta x^{\hat{a}}{}_{,b} + \mathcal{O}(\lambda), \tag{C.21}$$
$$= x^{a}{}_{,b} - x^{\hat{a}}{}_{,b} + \mathcal{O}(\lambda), \tag{C.22}$$
$$= \frac{\partial x^a}{\partial x^b} - \frac{\partial x^{\hat{a}}}{\partial x^b} + \mathcal{O}(\lambda), \tag{C.23}$$
$$= \delta^a_b + \mathcal{O}(\lambda), \tag{C.24}$$

where I have used $\frac{\partial x^{\hat{c}}}{\partial x^b} = 0$, $\Delta x^{\hat{a}} = \mathcal{O}(\lambda)$ and $\Gamma^{\hat{a}}{}_{b\hat{c}} = \mathcal{O}(\lambda^0)$. I can now write Eq. (C.19) as

$$\xi_{\hat{a};b} = X_{\hat{a}}\frac{P_{c\hat{d}}\delta^c{}_b\Delta x^{\hat{d}}}{\rho^2} + Z_{\hat{a}\hat{b}}\left[\frac{\delta^{\hat{b}}_b}{\rho} - \frac{\Delta x^{\hat{b}}P_{e\hat{f}}\delta^e{}_b\Delta x^{\hat{f}}}{\rho^3}\right] + \mathcal{O}(\lambda^0), \tag{C.25}$$

Before inputting the form for $\xi_{\hat{a};b}$ into Eq. (C.13), I rewrite it as

$$g^{\hat{b}}{}_d(\delta^{\hat{a}}_{\hat{b}}\delta^b_a + \delta^{\hat{a}}_a\delta^b_{\hat{b}})\xi_{\hat{a};b}k^a = h_{ad}k^a, \tag{C.26}$$
$$\Rightarrow (\delta^{\hat{a}}_d\delta^b_a + \delta^{\hat{a}}_a\delta^b_d)\xi_{\hat{a};b}k^a + \mathcal{O}(\lambda) = h_{ad}k^a, \tag{C.27}$$

Inputting Eq. (C.19) gives

$$(\delta^{\hat{a}}_d\delta^b_a + \delta^{\hat{a}}_a\delta^b_d)\left(X_{\hat{a}}\frac{P_{c\hat{d}}\delta^c{}_b\Delta x^{\hat{d}}}{\rho^2} + Z_{\hat{a}\hat{b}}\left[\frac{\delta^{\hat{b}}_b}{\rho} - \frac{\Delta x^{\hat{b}}P_{e\hat{f}}\delta^e{}_b\Delta x^{\hat{f}}}{\rho^3}\right]\right)k^a + \mathcal{O}(\lambda^0) = h_{ad}k^a, \tag{C.28}$$

Contracting the Kronecker delta (which are zeroth-order transportation tensors) and using Eq. (C.9) for k^a gives

$$\left(\frac{X_dP_{a\hat{d}}\Delta x^{\hat{d}} + X_aP_{d\hat{d}}\Delta x^{\hat{d}}}{\rho^2} + \frac{Z_{da} + Z_{ad}}{\rho}\right.$$
$$\left. - \frac{Z_{d\hat{b}}\Delta x^{\hat{b}}P_{a\hat{f}}\Delta x^{\hat{f}} + Z_{a\hat{b}}\Delta x^{\hat{b}}P_{d\hat{f}}\Delta x^{\hat{f}}}{\rho^3}\right)\left(u^a + \frac{P^a{}_{\hat{a}}\Delta x^{\hat{a}}}{\rho}\right) + \mathcal{O}(\lambda^0) = h_{ad}k^a. \tag{C.29}$$

My analysis produced some ambiguity on where $P_{a\hat{d}}$ is evaluated; but note, that as I am working in approximately flat spacetime $P_{a\hat{d}} \approx P_{ab} \approx P_{\hat{a}\hat{d}}$ (any difference is $\mathcal{O}(\lambda)$). As I am expanding functions at x around their values at $\hat{x}$ I evaluate $P_{a\hat{d}}$ at $\hat{x}$.

I now need to obtain a form of the RHS of Eq. (C.29) which allows the coefficients (X_a, Y_a and Z_{ab}) to be derived. To do this, I assume h_{ab} is in the Lorentz gauge. Therefore,

the metric perturbation near the worldline takes the form [143]

$$h_{ab} = \frac{2\mu}{\rho} g_a^{\hat{a}} g_b^{\hat{b}} (g_{\hat{a}\hat{b}} + 2u_{\hat{a}} u_{\hat{b}}) + \mathcal{O}(\lambda^0), \tag{C.30}$$

$$= \frac{2\mu}{\rho} (g_{ab} + 2u_a u_b) + \mathcal{O}(\lambda^0). \tag{C.31}$$

Hence,

$$h_{ad}k^a = \frac{2\mu}{\rho} (g_{ab} + 2u_a u_b) \left(u^a + \frac{P^a{}_{\hat{a}} \Delta \hat{x}^{\hat{a}}}{\rho} \right) + \mathcal{O}(\lambda^0), \tag{C.32}$$

$$h_{ad}k^a = \frac{2\mu}{\rho} \left(- u_d + \frac{P_{da} \Delta x^a}{\rho} \right) + \mathcal{O}(\lambda^0). \tag{C.33}$$

Putting the LHS and RHS of Eq. (C.29) together gives

$$\left(\frac{X_d P_{a\hat{d}} \Delta x^{\hat{d}} + X_a P_{d\hat{d}} \Delta x^{\hat{d}}}{\rho^2} + \frac{Z_{da} + Z_{ad}}{\rho} \right.$$
$$\left. - \frac{Z_{d\hat{b}} \Delta x^{\hat{b}} P_{a\hat{f}} \Delta x^{\hat{f}} + Z_{a\hat{b}} \Delta x^{\hat{b}} P_{d\hat{f}} \Delta x^{\hat{f}}}{\rho^3} \right) \left(u^a + \frac{P^a{}_{\hat{a}} \Delta \hat{x}^{\hat{a}}}{\rho} \right) + \mathcal{O}(\lambda^0) = \frac{2\mu}{\rho} \left(- u_d + \frac{P_{da} \Delta x^a}{\rho} \right). \tag{C.34}$$

A short investigation reveals that the choice $X_a = -2\mu u_a$ and $Z_{ab} = A P_{ab}$ (where A is an arbitrary function independent of λ) satisfies the above equation. Therefore, ξ_a takes the form

$$\xi_a = g^{\hat{a}}{}_a \Big[- 2\mu u_{\hat{a}} \log[\rho] + Y_{\hat{a}} + A P_{ab} \Big] + \mathcal{O}(\lambda), \tag{C.35}$$

$$\xi_a = - 2\mu \hat{u}_a \log[\hat{\rho}] + Y_a + A P_{ab} \frac{\Delta \hat{x}^b}{\hat{\rho}} + \mathcal{O}(\lambda), \tag{C.36}$$

where Y_a is an arbitrary set of four functions independent of λ. For simplicity, one can freely set $Y_a = 0_a$ and $A = 0$, which gives

$$\xi_a[x^{\hat{c}}] = - 2\mu \hat{u}_a \log[\hat{\rho}] + \mathcal{O}(\lambda). \tag{C.37}$$

This gauge vector takes one locally from the Lorenz gauge to a highly regular gauge, which is useful for second-order SF calculations, such as solving Eq. (2.20). The main advantage is the source in the highly regular gauge is well defined as a distribution on the worldline. The source is also more regular than in generic gauges, making integration easier. However, this gauge vector does not fully fix the gauge, requires that one starts in the Lorenz gauge, and is only calculated up to leading order in the distance from the worldline.

References

[1] Black Hole Perturbation Toolkit. (bhptoolkit.org).

[2] J. Aasi, B. Abbott, R. Abbott, T. Abbott, M. Abernathy, K. Ackley, C. Adams, T. Adams, P. Addesso, R. Adhikari, et al. Advanced ligo. *Classical and quantum gravity*, 32(7):074001, 2015.

[3] B. P. Abbott, R. Abbott, T. Abbott, M. Abernathy, F. Acernese, K. Ackley, C. Adams, T. Adams, P. Addesso, R. Adhikari, et al. Observation of gravitational waves from a binary black hole merger. *Physical review letters*, 116 (6):061102, 2016.

[4] R. Abbott, T. Abbott, S. Abraham, F. Acernese, K. Ackley, C. Adams, R. Adhikari, V. Adya, C. Affeldt, M. Agathos, et al. GW190814: gravitational waves from the coalescence of a 23 solar mass black hole with a 2.6 solar mass compact object. *The Astrophysical Journal Letters*, 896(2):L44, 2020.

[5] R. Abbott, T. Abbott, S. Abraham, F. Acernese, K. Ackley, A. Adams, C. Adams, R. Adhikari, V. Adya, C. Affeldt, et al. Population properties of compact objects from the second LIGO–Virgo gravitational-wave transient catalog. *The Astrophysical journal letters*, 913(1):L7, 2021.

[6] R. Abbott, T. Abbott, F. Acernese, K. Ackley, C. Adams, N. Adhikari, R. Adhikari, V. Adya, C. Affeldt, D. Agarwal, et al. GWTC-3: compact binary coalescences observed by LIGO and Virgo during the second part of the third observing run. *arXiv preprint arXiv:2111.03606*, 2021.

[7] V. Acquaviva, N. Bartolo, S. Matarrese, and A. Riotto. Gauge-invariant second-order perturbations and non-gaussianity from inflation. *Nuclear Physics B*, 667(1-2):119–148, 2003.

[8] S. Akcay. Fast frequency-domain algorithm for gravitational self-force: Circular orbits in Schwarzschild spacetime. *Physical Review D*, 83(12):124026, 2011.

[9] K. Akiyama, A. Alberdi, W. Alef, J. C. Algaba, R. Anantua, K. Asada, R. Azulay, U. Bach, A.-K. Baczko, D. Ball, et al. First sagittarius A* event horizon telescope

results. i. the shadow of the supermassive black hole in the center of the Milky Way. *The Astrophysical Journal Letters*, 930(2):L12, 2022.

[10] S. Aksteiner, L. Andersson, and T. Bäckdahl. New identities for linearized gravity on the Kerr spacetime. *Physical Review D*, 99(4):044043, 2019.

[11] P. Amaro-Seoane. Detecting intermediate-mass ratio inspirals from the ground and space. *Physical Review D*, 98(6):063018, 2018.

[12] P. Amaro-Seoane. X-mris: Extremely large mass-ratio inspirals. *arXiv preprint arXiv:1903.10871*, 2019.

[13] P. Amaro-Seoane, J. R. Gair, A. Pound, S. A. Hughes, and C. F. Sopuerta. Research update on extreme-mass-ratio inspirals. In *Journal of Physics: Conference Series*, volume 610, page 012002. IOP Publishing, 2015.

[14] P. Amaro-Seoane, J. Andrews, M. A. Sedda, A. Askar, R. Balasov, I. Bartos, S. S. Bavera, J. Bellovary, C. P. Berry, E. Berti, et al. Astrophysics with the laser interferometer space antenna. *arXiv preprint arXiv:2203.06016*, 2022.

[15] N. Andersson. *Gravitational-Wave Astronomy: Exploring the Dark Side of the Universe*. Oxford Graduate Texts, 2019.

[16] M. Armano, H. Audley, G. Auger, J. Baird, P. Binetruy, M. Born, D. Bortoluzzi, N. Brandt, A. Bursi, M. Caleno, et al. The lisa pathfinder mission. In *Journal of Physics: Conference Series*, volume 610, page 012005. IOP Publishing, 2015.

[17] R. Arnowitt, S. Deser, and C. W. Misner. Republication of: The dynamics of general relativity. *General Relativity and Gravitation*, 40(9):1997–2027, 2008.

[18] K. Arun, E. Belgacem, R. Benkel, L. Bernard, E. Berti, G. Bertone, M. Besancon, D. Blas, C. G. Böhmer, R. Brito, et al. New horizons for fundamental physics with LISA. *Living Reviews in Relativity*, 25(1):1–148, 2022.

[19] S. Bai, Z. Cao, X. Gong, Y. Shang, X. Wu, and Y. Lau. Light cone structure near null infinity of the Kerr metric. *Physical Review D*, 75(4):044003, 2007.

[20] M. Bailes, B. Berger, P. Brady, M. Branchesi, K. Danzmann, M. Evans, K. Holley-Bockelmann, B. Iyer, T. Kajita, S. Katsanevas, et al. Gravitational-wave physics and astronomy in the 2020s and 2030s. *Nature Reviews Physics*, 3(5): 344–366, 2021.

[21] L. Barack. Lectures on black-hole perturbation theory. Presentation slides, http://www.ctc.cam.ac.uk/activities/rise/slides/barack.pdf, 2019. Kavli-RISE Summer School on Gravitational Waves.

[22] L. Barack and C. O. Lousto. Perturbations of Schwarzschild black holes in the Lorenz gauge: Formulation and numerical implementation. *Physical Review D*, 72(10):104026, 2005.

[23] L. Barack and A. Pound. Self-force and radiation reaction in general relativity. *Reports on Progress in Physics*, 82(1):016904, 2018.

[24] L. Barack and N. Sago. Gravitational self-force on a particle in circular orbit around a Schwarzschild black hole. *Physical Review D*, 75(6):064021, 2007.

[25] L. Barack and N. Sago. Gravitational self-force on a particle in eccentric orbit around a Schwarzschild black hole. *Physical Review D*, 81(8):084021, 2010.

[26] L. Barack, A. Ori, and N. Sago. Frequency-domain calculation of the self-force: The high-frequency problem and its resolution. *Physical Review D*, 78(8):084021, 2008.

[27] E. Barausse, E. Berti, T. Hertog, S. Huhes, P. Jetzer, P. Pani, T. Sotiriou, N. Tamanini, H. Witek, K. Yagi, et al. Prospects for fundamental physics with LISA. *arXiv preprint arXiv:2001.09793*, 2020.

[28] G. Barnich and C. Troessaert. BMS charge algebra. *Journal of High Energy Physics*, 2011(12):1–22, 2011.

[29] C. P. Berry, R. H. Cole, P. Canizares, and J. R. Gair. Importance of transient resonances in extreme-mass-ratio inspirals. *Physical Review D*, 94(12):124042, 2016.

[30] D. Bertacca, N. Bartolo, M. Bruni, K. Koyama, R. Maartens, S. Matarrese, M. Sasaki, and D. Wands. Galaxy bias and gauges at second order in General Relativity. *Classical and Quantum Gravity*, 32(17):175019, 2015.

[31] D. Bini and A. Geralico. Gauge-fixing for the completion problem of reconstructed metric perturbations of a Kerr spacetime. *arXiv preprint arXiv:1908.03191*, 2019.

[32] D. Bini, T. Damour, and A. Geralico. Binary dynamics at the fifth and fifth-and-a-half post-Newtonian orders. *Physical Review D*, 102(2):024062, 2020.

[33] N. T. Bishop and L. R. Venter. Kerr metric in Bondi–Sachs form. *Physical Review D*, 73(8):084023, 2006.

[34] L. Blanchet. Gravitational radiation from post-newtonian sources and inspiralling compact binaries. *Living Reviews in Relativity*, 17(1):2, 2014.

[35] L. Blanchet and T. Damour. Radiative gravitational fields in general relativity i. general structure of the field outside the source. *Philosophical Transactions of the Royal Society of London. Series A, Mathematical and Physical Sciences*, 320(1555): 379–430, 1986.

[36] H. Bondi, M. G. J. Van der Burg, and A. Metzner. Gravitational waves in general relativity, vii. waves from axi-symmetric isolated system. *Proceedings of the Royal Society of London. Series A. Mathematical and Physical Sciences*, 269(1336):21–52, 1962.

[37] R. Bonetto, A. Pound, and Z. Sam. Deformed Schwarzschild horizons in second-order perturbation theory: Mass, geometry, and teleology. *Physical Review D*, 105(2):024048, 2022.

[38] L. Brenneman, C. Reynolds, M. Nowak, R. Reis, M. Trippe, A. Fabian, K. Iwasawa, J. Lee, J. Miller, R. Mushotzky, et al. The spin of the supermassive black hole in NGC 3783. *The Astrophysical Journal*, 736(2):103, 2011.

[39] D. Brizuela, J. M. Martin-Garcia, and G. A. M. Marugán. Second-and higher-order perturbations of a spherical spacetime. *Physical Review D*, 74(4): 044039, 2006.

[40] D. Brizuela, J. M. Martin-Garcia, and M. Tiglio. Complete gauge-invariant formalism for arbitrary second-order perturbations of a Schwarzschild black hole. *Physical Review D*, 80(2):024021, 2009.

[41] D. Brizuela, J. M. Martin-Garcia, U. Sperhake, and K. D. Kokkotas. High-order perturbations of a spherical collapsing star. *Physical Review D*, 82(10):104039, 2010.

[42] M. Bruni, S. Matarrese, S. Mollerach, and S. Sonego. Perturbations of spacetime: gauge transformations and gauge invariance at second order and beyond. *Classical and Quantum Gravity*, 14(9):2585, 1997.

[43] A. Buonanno and T. Damour. Effective one-body approach to general relativistic two-body dynamics. *Physical Review D*, 59(8):084006, 1999.

[44] R. H. C. C J Moore and C. P. L. Berry. Gravitational-wave sensitivity curves. *Classical and Quantum Gravity*, 32(1):015014, 2014.

[45] M. Campanelli and C. O. Lousto. Second order gauge invariant gravitational perturbations of a Kerr black hole. *Physical Review D*, 59(12):124022, 1999.

[46] B. Carter. Global structure of the Kerr family of gravitational fields. *Physical Review*, 174(5):1559, 1968.

[47] B. Carter and J. B. Hartle. *Gravitation in Astrophysics: Cargèse 1986*, volume 156. Springer Science & Business Media, 2012.

[48] S. Chandrasekhar. *The Mathematical Theory of Black Holes*. Clarendon Press Oxford, 1992. reprint: 2009.

[49] C. Cheung, I. Z. Rothstein, and M. P. Solon. From scattering amplitudes to classical potentials in the post-Minkowskian expansion. *Physical Review Letters*, 121(25):251101, 2018.

[50] P. L. Chrzanowski. Vector potential and metric perturbations of a rotating black hole. *Physical Review D*, 11(8):2042, 1975.

[51] P. L. Chrzanowski. Applications of metric perturbations of a rotating black hole: Distortion of the event horizon. *Physical Review D*, 13(4):806, 1976.

[52] A. J. Chua, C. J. Moore, and J. R. Gair. Augmented kludge waveforms for detecting extreme-mass-ratio inspirals. *Physical Review D*, 96(4):044005, 2017.

[53] J. M. Cohen and L. S. Kegeles. Space-time perturbations. *Physics Letters A*, 54(1): 5–7, 1975.

[54] E. H. T. Collaboration et al. First M87 event horizon telescope results. i. the shadow of the supermassive black hole. *arXiv preprint arXiv:1906.11238*, 2019.

[55] G. Compère. *Advanced lectures on general relativity*, volume 952. Springer, 2019.

[56] L. Consortium et al. LISA: A proposal in response to the ESA call for L3 mission concepts. *arXiv preprint arXiv:1702.00786*, 2017.

[57] T. Damour. Gravitational scattering, post-Minkowskian approximation, and effective-one-body theory. *Physical Review D*, 94(10):104015, 2016.

[58] K. Danzmann. The ESA website, the laser interferometer space antenna. https://www.elisascience.org/articles/lisa-mission, 2019.

[59] S. Detweiler. Radiation reaction and the self-force for a point mass in general relativity. *Physical review letters*, 86(10):1931, 2001.

[60] S. Detweiler. Perspective on gravitational self-force analyses. *Classical and Quantum Gravity*, 22(15):S681, 2005.

[61] S. Detweiler. Gravitational radiation reaction and second-order perturbation theory. *Physical Review D*, 85(4):044048, 2012.

[62] S. Detweiler and B. F. Whiting. Self-force via a Green's function decomposition. *Physical Review D*, 67(2):024025, 2003.

[63] P. A. M. Dirac. Classical theory of radiating electrons. *Proceedings of the Royal Society of London. Series A. Mathematical and Physical Sciences*, 167(929):148–169, 1938.

[64] S. R. Dolan, C. Kavanagh, and B. Wardell. Gravitational perturbations of rotating black holes in Lorenz gauge. *Physical Review Letters*, 128(15):151101, 2022.

[65] L. Durkan and N. Warburton. Slow evolution of the metric perturbation due to a quasicircular inspiral into a Schwarzschild black hole. *arXiv preprint arXiv:2206.08179*, 2022.

[66] A. Einstein. Näherungsweise integration der feldgleichungen der gravitation. *Albert Einstein: Akademie-Vorträge: Sitzungsberichte der Preußischen Akademie der Wissenschaften 1914–1932*, pages 99–108, 2005.

[67] A. Einstein. Approximate integration of the field equations of gravitation. *Albert Einstein: Academy Lecturesäge: Meeting Reports of the Prussian Academy of Sciences 1914–1932*, pages 99–108, 2005.

[68] E. E. Flanagan and T. Hinderer. Evolution of the carter constant for inspirals into a black hole: Effect of the black hole quadrupole. *Physical Review D*, 75(12): 124007, 2007.

[69] E. E. Flanagan and T. Hinderer. Two-timescale analysis of extreme mass ratio inspirals in Kerr spacetime Orbital motion. *Physical Review D*, 78(6):064028, 2008.

[70] E. E. Flanagan and T. Hinderer. Transient resonances in the inspirals of point particles into black holes. *Physical review letters*, 109(7):071102, 2012.

[71] E. E. Flanagan and D. A. Nichols. Conserved charges of the extended Bondi-Metzner-Sachs algebra. *Physical Review D*, 95(4):044002, 2017.

[72] E. E. Flanagan, T. Hinderer, J. Moxon, and A. Pound. The two body problem in general relativity in the extreme mass ratio limit via multiscale expansions. II. dynamics of the strong-filed region. Yet to be published.

[73] S. J. Fletcher and A. W.-C. Lun. The Kerr spacetime in generalized Bondi–Sachs coordinates. *Classical and Quantum Gravity*, 20(19):4153, 2003.

[74] F. G. Friedlander, G. Friedlander, M. S. Joshi, M. Joshi, and M. C. Joshi. *Introduction to the Theory of Distributions*. Cambridge University Press, 1998.

[75] J. R. Gair, L. Barack, T. Creighton, C. Cutler, S. L. Larson, E. S. Phinney, and M. Vallisneri. Event rate estimates for LISA extreme mass ratio capture sources. *Classical and Quantum Gravity*, 21(20):S1595, 2004.

[76] A. Geller. Masses in the stellar graveyard. https://ligo.northwestern.edu/media/mass-plot/index.html, 2022.

[77] R. Geroch, A. Held, and R. Penrose. A space-time calculus based on pairs of null directions. *Journal of Mathematical Physics*, 14(7):874–881, 1973.

[78] M. Giesler, M. Isi, M. A. Scheel, and S. A. Teukolsky. Black hole ringdown: the importance of overtones. *Physical Review X*, 9(4):041060, 2019.

[79] R. J. Gleiser, C. O. Nicasio, R. H. Price, and J. Pullin. Colliding black holes: How far can the close approximation go? *Physical Review Letters*, 77(22):4483, 1996.

[80] R. J. Gleiser, C. O. Nicasio, R. H. Price, and J. Pullin. Second-order perturbations of a Schwarzschild black hole. *Classical and Quantum Gravity*, 13(10):L117, 1996.

[81] R. J. Gleiser, C. O. Nicasio, R. H. Price, and J. Pullin. Gravitational radiation from Schwarzschild black holes: the second-order perturbation formalism. *Physics Reports*, 325(2):41–81, 2000.

[82] J. Goldberg and R. Sachs. Republication of: A theorem on Petrov types. *General Relativity and Gravitation*, 41(2):433–444, 2009.

[83] J. N. Goldberg, A. J. MacFarlane, E. T. Newman, F. Rohrlich, and E. G. Sudarshan. Spin-s spherical harmonics and ð. *Journal of Mathematical Physics*, 8 (11):2155–2161, 1967.

[84] S. E. Gralla. Second-order gravitational self-force. *Physical Review D*, 85(12): 124011, 2012.

[85] S. E. Gralla and R. M. Wald. A rigorous derivation of gravitational self-force. *Classical and Quantum Gravity*, 25(20):205009, 2008.

[86] S. R. Green, S. Hollands, and P. Zimmerman. Teukolsky formalism for nonlinear Kerr perturbations. *Classical and Quantum Gravity*, 37(7):075001, 2020.

[87] S. W. Hawking and J. Hartle. Energy and angular momentum flow into a black hole. *Communications in mathematical physics*, 27(4):283–290, 1972.

[88] K. Hecht. Sudden and adiabatic approximations. In *Quantum Mechanics*, pages 561–571. Springer, 2000.

[89] K. T. Hecht. *Quantum mechanics*. Springer Science & Business Media, 2012.

[90] A. Held. A formalism for the investigation of algebraically special metrics. i. *Communications in Mathematical Physics*, 37(4):311–326, 1974.

[91] D. E. Holz and S. A. Hughes. Using gravitational-wave standard sirens. *The Astrophysical Journal*, 629(1):15, 2005.

[92] K. Ioka and H. Nakano. Second-and higher-order quasinormal modes in binary black-hole mergers. *Physical Review D*, 76(6):061503, 2007.

[93] M. Isi, M. Giesler, W. M. Farr, M. A. Scheel, and S. A. Teukolsky. Testing the no-hair theorem with GW150914. *Physical Review Letters*, 123(11):111102, 2019.

[94] L. S. Kegeles and J. M. Cohen. Constructive procedure for perturbations of spacetimes. *Physical Review D*, 19(6):1641, 1979.

[95] T. S. Keidl, J. L. Friedman, and A. G. Wiseman. Finding fields and self-force in a gauge appropriate to separable wave equations. *Physical Review D*, 75(12): 124009, 2007.

[96] T. S. Keidl, A. G. Shah, J. L. Friedman, D.-H. Kim, and L. R. Price. Gravitational self-force in a radiation gauge. *Physical Review D*, 82(12):124012, 2010.

[97] R. P. Kerr. Gravitational field of a spinning mass as an example of algebraically special metrics. *Physical review letters*, 11(5):237, 1963.

[98] J. Kevorkian and J. Cole. The method of multiple scales for ordinary differential equations. In *Multiple Scale and Singular Perturbation Methods*, pages 267–409. Springer, 1996.

[99] W. Kinnersley. Type D vacuum metrics. *Journal of Mathematical Physics*, 10(7): 1195–1203, 1969.

[100] B. Leather and N. Warburton. Applying the effective-source approach to frequency-domain self-force calculations for eccentric orbits. in preparation.

[101] C. O. Lousto and H. Nakano. Regular second-order perturbations of binary black holes in the extreme mass ratio regime. *Classical and Quantum Gravity*, 26 (1):015007, 2008.

[102] N. Loutrel, J. L. Ripley, E. Giorgi, and F. Pretorius. Second-order perturbations of Kerr black holes: Formalism and reconstruction of the first-order metric. *Physical Review D*, 103(10):104017, 2021.

[103] J. Luo, L.-S. Chen, H.-Z. Duan, Y.-G. Gong, S. Hu, J. Ji, Q. Liu, J. Mei, V. Milyukov, M. Sazhin, et al. Tianqin: a space-borne gravitational wave detector. *Classical and Quantum Gravity*, 33(3):035010, 2016.

[104] M. M van De Meent. The mass and angular momentum of reconstructed metric perturbations. *Classical and Quantum Gravity*, 34(12):124003, 2017.

[105] R. P. Macedo. Hyperboloidal framework for the Kerr spacetime. *Classical and Quantum Gravity*, 37(6):065019, 2020.

[106] R. P. Macedo, B. Leather, N. Warburton, B. Wardell, and A. Zenginoğlu. Hyperboloidal method for frequency-domain self-force calculations. *arXiv preprint arXiv:2202.01794*, 2022.

[107] T. Mädler and J. Winicour. Bondi-Sachs formalism. *arXiv preprint arXiv:1609.01731*, 2016.

[108] K. Martel and E. Poisson. Gravitational perturbations of the Schwarzschild spacetime: a practical covariant and gauge-invariant formalism. *Physical Review D*, 71(10):104003, 2005.

[109] K. Martel and E. Poisson. Gravitational perturbations of the Schwarzschild spacetime: A practical covariant and gauge-invariant formalism. *Physical Review D*, 71(10):104003, 2005.

[110] J. M. Martín-García et al. xAct: Efficient tensor computer algebra for mathematica. *URl: http://xact. es/(c it. on pp. 12, 13)*, 2002.

[111] S. Matarrese, S. Mollerach, and M. Bruni. Relativistic second-order perturbations of the Einstein–de Sitter universe. *Physical Review D*, 58(4):043504, 1998.

[112] J. Mathews, A. Pound, and B. Wardell. Self-force calculations with a spinning secondary. *Physical Review D*, 105(8):084031, 2022.

[113] M. V. D. Meent. Gravitational self-force on eccentric equatorial orbits around a Kerr black hole. *Physical Review D*, 94(4):044034, 2016.

[114] M. V. D. Meent. Gravitational self-force on generic bound geodesics in Kerr spacetime. *Physical Review D*, 97(10):104033, 2018.

[115] M. V. D. Meent and A. G. Shah. Metric perturbations produced by eccentric equatorial orbits around a Kerr black hole. *Physical Review D*, 92(6):064025, 2015.

[116] A. P. C. Merlin and L. Barack. Gravitational self-force from radiation-gauge metric perturbations. *Physical Review D*, 89(2):024009, 2014.

[117] C. Merlin, A. Ori, L. Barack, A. Pound, and M. van de Meent. Completion of metric reconstruction for a particle orbiting a Kerr black hole. *Physical Review D*, 94(10):104066, 2016.

[118] C. Merlin, A. Ori, L. Barack, A. Pound, and M. van de Meent. Completion of metric reconstruction for a particle orbiting a kerr black hole. *Physical Review D*, 94(10):104066, 2016.

[119] J. Miller and A. Pound. Two-timescale evolution of extreme-mass-ratio inspirals: waveform generation scheme for quasicircular orbits in Schwarzschild spacetime. *arXiv preprint arXiv:2006.11263*, 2020.

[120] J. Miller, B. Wardell, and A. Pound. Second-order perturbation theory: the problem of infinite mode coupling. *Physical Review D*, 94(10):104018, 2016.

[121] C. W. Misner, K. S. Thorne, and J. A. Wheeler. Gravitation WH Freeman and Co. *San Francisco*, page 660, 1973.

[122] B. Moore and N. Yunes. Data analysis implications of moderately eccentric gravitational waves. *Classical and Quantum Gravity*, 37(22):225015, 2020.

[123] J. Moxon, E. E. Flanagan, A. Pound, Z. Sam, and J. E. Thompson. Energy and angular momentum balance laws in second-order self-force theory. in preparation.

[124] J. Moxon, M. A. Scheel, and S. A. Teukolsky. Improved Cauchy-characteristic evolution system for high-precision numerical relativity waveforms. *Physical Review D*, 102(4):044052, 2020.

[125] V. F. Mukhanov, L. R. W. Abramo, and R. H. Brandenberger. Backreaction problem for cosmological perturbations. *Physical Review Letters*, 78(9):1624, 1997.

[126] K. Nakamura. Gauge invariant variables in two-parameter nonlinear perturbations. *Progress of Theoretical Physics*, 110(4):723–755, 2003.

[127] K. Nakamura. Gauge-invariant formulation of second-order cosmological perturbations. *Physical Review D*, 74(10):101301, 2006.

[128] K. Nakamura. Second-order gauge invariant cosmological perturbation theory: —Einstein equations in terms of gauge invariant variables—. *Progress of theoretical physics*, 117(1):17–74, 2007.

[129] H. Nakano and K. Ioka. Second-order quasinormal mode of the Schwarzschild black hole. *Physical Review D*, 76(8):084007, 2007.

[130] Z. Nasipak and C. R. Evans. Resonant self-force effects in extreme-mass-ratio binaries: A scalar model. *Physical Review D*, 104(8):084011, 2021.

[131] E. Newman and R. Penrose. An approach to gravitational radiation by a method of spin coefficients. *Journal of Mathematical Physics*, 3(3):566–578, 1962.

[132] C. O. Nicasio, R. Gleiser, and J. Pullin. Second order perturbations of a Schwarzschild black hole: inclusion of odd parity perturbations. *General Relativity and Gravitation*, 32(10):2021–2042, 2000.

[133] M. Okounkova. Revisiting non-linearity in binary black hole mergers. *arXiv preprint arXiv:2004.00671*, 2020.

[134] A. Ori. Radiative evolution of the carter constant for generic orbits around a Kerr black hole. *Physical Review D*, 55(6):3444, 1997.

[135] A. Ori. Reconstruction of inhomogeneous metric perturbations and electromagnetic four-potential in Kerr spacetime. *Physical Review D*, 67(12): 124010, 2003.

[136] T. Osburn and N. Nishimura. New self-force method via elliptic pdes for Kerr inspiral models. *arXiv preprint arXiv:2206.07031*, 2022.

[137] R. Penrose. Asymptotic properties of fields and space-times. *Phys. Rev. Lett.*, 10: 66–68, Jan 1963. . URL https://link.aps.org/doi/10.1103/PhysRevLett.10.66.

[138] R. Penrose. Zero rest-mass fields including gravitation: asymptotic behaviour. *Proceedings of the Royal Society of London. Series A. Mathematical and physical sciences*, 284(1397):159–203, 1965.

[139] C. Pitrou, X. Roy, and O. Umeh. xpand: An algorithm for perturbing homogeneous cosmologies. *Classical and Quantum Gravity*, 30(16):165002, 2013.

[140] E. Poisson. *The Relativist's Toolkit*. Cambridge University Press, 2004.

[141] E. Poisson and I. Vlasov. Geometry and dynamics of a tidally deformed black hole. *Physical Review D*, 81(2):024029, 2010.

[142] E. Poisson and C. M. Will. *Gravity: Newtonian, post-newtonian, relativistic*. Cambridge University Press, 2014.

[143] E. Poisson, A. Pound, and I. Vega. Living rev. *Relativity*, 14(7), 2011.

[144] A. Pound. Self-consistent gravitational self-force. *Physical Review D*, 81(2): 024023, 2010.

[145] A. Pound. Nonlinear gravitational self-force: Field outside a small body. *Physical Review D*, 86(8):084019, 2012.

[146] A. Pound. Second-order gravitational self-force. *Physical Review Letters*, 109(5): 051101, 2012.

[147] A. Pound. Motion of small objects in curved spacetimes: An introduction to gravitational self-force. In *Equations of Motion in Relativistic Gravity*, pages 399–486. Springer, 2015.

[148] A. Pound. Gauge and motion in perturbation theory. *Physical Review D*, 92(4): 044021, 2015.

[149] A. Pound. Second-order perturbation theory: problems on large scales. *Physical Review D*, 92(10):104047, 2015.

[150] A. Pound. Nonlinear gravitational self-force: second-order equation of motion. *Physical Review D*, 95(10):104056, 2017.

[151] A. Pound. Nonlinear gravitational self-force: second-order equation of motion. *Physical Review D*, 95(10):104056, 2017.

[152] A. Pound. Nonlinear gravitational self-force: second-order equation of motion. *Physical Review D*, 95(10):104056, 2017.

[153] A. Pound and J. Miller. Practical, covariant puncture for second-order self-force calculations. *Physical Review D*, 89(10):104020, 2014.

[154] A. Pound and B. Wardell. Black hole perturbation theory and gravitational self-force. *arXiv preprint arXiv:2101.04592*, 2021.

[155] A. Pound, C. Merlin, and L. Barack. Gravitational self-force from radiation-gauge metric perturbations. *Physical Review D*, 89(2):024009, 2014.

[156] A. Pound, B. Wardell, N. Warburton, and J. Miller. Second-order self-force calculation of gravitational binding energy in compact binaries. *Physical Review Letters*, 124(2):021101, 2020.

[157] A. N. Pressley. *Elementary differential geometry*. Springer Science & Business Media, 2010.

[158] L. R. Price, K. Shankar, and B. F. Whiting. On the existence of radiation gauges in Petrov type II spacetimes. *Classical and Quantum Gravity*, 24(9):2367, 2007.

[159] T. C. Quinn and R. M. Wald. Axiomatic approach to electromagnetic and gravitational radiation reaction of particles in curved spacetime. *Physical Review D*, 56(6):3381, 1997.

[160] C. S. Reynolds. The spin of supermassive black holes. *Classical and Quantum Gravity*, 30(24):244004, 2013.

[161] D. Richstone, E. Ajhar, R. Bender, G. Bower, A. Dressler, S. Faber, A. Filippenko, K. Gebhardt, R. Green, L. Ho, et al. Supermassive black holes and the evolution of galaxies. *arXiv preprint astro-ph/9810378*, 1998.

[162] A. G. Riess, S. Casertano, W. Yuan, L. M. Macri, and D. Scolnic. Large magellanic cloud cepheid standards provide a 1% foundation for the determination of the hubble constant and stronger evidence for physics beyond λcdm. *The Astrophysical Journal*, 876(1):85, 2019.

[163] J. L. Ripley, N. Loutrel, E. Giorgi, and F. Pretorius. Numerical computation of second-order vacuum perturbations of Kerr black holes. *Physical Review D*, 103 (10):104018, 2021.

[164] E. Rosenthal. Second-order gravitational self-force. *Physical Review D*, 74(8): 084018, 2006.

[165] W.-H. Ruan, Z.-K. Guo, R.-G. Cai, and Y.-Z. Zhang. Taiji program: Gravitational-wave sources. *International Journal of Modern Physics A*, 35(17): 2050075, 2020.

[166] R. Sachs. Asymptotic symmetries in gravitational theory. *Physical Review*, 128(6): 2851, 1962.

[167] R. K. Sachs. Gravitational waves in general relativity viii. waves in asymptotically flat space-time. *Proceedings of the Royal Society of London. Series A. Mathematical and Physical Sciences*, 270(1340):103–126, 1962.

[168] L. Sberna, P. Bosch, W. E. East, S. R. Green, and L. Lehner. Nonlinear effects in the black hole ringdown: Absorption-induced mode excitation. *Physical Review D*, 105(6):064046, 2022.

[169] A. G. Shah and A. Pound. Linear-in-mass-ratio contribution to spin precession and tidal invariants in Schwarzschild spacetime at very high post-newtonian order. *Physical Review D*, 91(12):124022, 2015.

[170] A. G. Shah, T. S. Keidl, J. L. Friedman, D.-H. Kim, and L. R. Price. Conservative, gravitational self-force for a particle in circular orbit around a Schwarzschild black hole in a radiation gauge. *Physical Review D*, 83(6):064018, 2011.

[171] A. G. Shah, J. L. Friedman, and T. S. Keidl. Extreme-mass-ratio inspiral corrections to the angular velocity and redshift factor of a mass in circular orbit about a Kerr black hole. *Physical Review D*, 86(8):084059, 2012.

[172] M. Shiraishi. *Probing the early universe with the CMB scalar, vector and tensor bispectrum*. Springer Science & Business Media, 2013.

[173] C. F. Sopuerta, M. Bruni, and L. Gualtieri. Nonlinear n-parameter spacetime perturbations: Gauge transformations. *Physical Review D*, 70(6):064002, 2004.

[174] A. Spiers, J. Moxon, and A. Pound. Second-order Teukolsky formalism with applications to gravitational self-force theory. in preparation, .

[175] A. Spiers, A. Pound, and B. Wardell. Second-order perturbation theory in Schwarzschild spacetime. in preparation, .

[176] A. Spiers, S. Upton, and A. Pound. Prospective second-order gravitational self-force methods in Kerr and the highly regular gauge. Presentation, GR22 Valencia, 2019.

[177] S. A. Teukolsky. Rotating black holes: Separable wave equations for gravitational and electromagnetic perturbations. *Physical Review Letters*, 29(16): 1114, 1972.

[178] S. A. Teukolsky. Perturbations of a rotating black hole. 1. fundamental equations for gravitational electromagnetic and neutrino field perturbations. *Astrophys. J.*, 185:635–647, 1973.

[179] S. A. Teukolsky and W. Press. Perturbations of a rotating black hole. iii-interaction of the hole with gravitational and electromagnetic radiation. *The Astrophysical Journal*, 193:443–461, 1974.

[180] K. Tomita. On the non-linear behavior of nonspherical perturbations in relativistic gravitational collapse. *Progress of Theoretical Physics*, 52(4):1188–1204, 1974.

[181] K. Tomita. Relativistic second-order perturbations of nonzero-λ flat cosmological models and CMB anisotropies. *Physical Review D*, 71(8):083504, 2005.

[182] K. Tomita and N. Tajima. Nonlinear behavior of nonspherical perturbations of the Schwarzschild metric. *Progress of Theoretical Physics*, 56(2):551–560, 1976.

[183] V. Toomani, P. Zimmerman, A. Spiers, S. Hollands, A. Pound, and S. R. Green. New metric reconstruction scheme for gravitational self-force calculations. *Classical and Quantum Gravity*, 39(1):015019, 2021.

[184] C. Uggla and J. Wainwright. Simple expressions for second order density perturbations in standard cosmology. *Classical and Quantum Gravity*, 31(10): 105008, 2014.

[185] S. D. Upton and A. Pound. Second-order gravitational self-force in a highly regular gauge. *Physical Review D*, 103(12):124016, 2021.

[186] M. van de Meent. Conditions for sustained orbital resonances in extreme mass ratio inspirals. *Physical Review D*, 89(8):084033, 2014.

[187] M. Van De Meent. Self-force corrections to the periapsis advance around a spinning black hole. *Physical review letters*, 118(1):011101, 2017.

[188] M. van de Meent and H. P. Pfeiffer. Intermediate mass-ratio black hole binaries: Applicability of small mass-ratio perturbation theory. *arXiv preprint arXiv:2006.12036*, 2020.

[189] R. M. Wald. On perturbations of a Kerr black hole. *Journal of Mathematical Physics*, 14(10):1453–1461, 1973.

[190] R. M. Wald. Construction of solutions of gravitational, electromagnetic, or other perturbation equations from solutions of decoupled equations. *Physical Review Letters*, 41(4):203, 1978.

[191] R. M. Wald. *General Relativity*. The University of Chicago Press, 1984.

[192] N. Warburton, S. Akcay, L. Barack, J. R. Gair, and N. Sago. Evolution of inspiral orbits around a Schwarzschild black hole. *Physical Review D*, 85(6):061501, 2012.

[193] N. Warburton, T. Osburn, and C. R. Evans. Evolution of small-mass-ratio binaries with a spinning secondary. *Physical Review D*, 96(8):084057, 2017.

[194] N. Warburton, A. Pound, B. Wardell, J. Miller, and L. Durkan. Gravitational-wave energy flux for compact binaries through second order in the mass ratio. *Physical review letters*, 127(15):151102, 2021.

[195] B. Wardell, A. Pound, N. Warburton, J. Miller, L. Durkan, and A. L. Tiec. Gravitational waveforms for compact binaries from second-order self-force theory. *arXiv preprint arXiv:2112.12265*, 2021.

[196] A. Wolfe and G. Burbidge. Black holes in elliptical galaxies. *The Astrophysical Journal*, 161:419, 1970.

[197] M. S. Y Mino and T. Tanaka. Gravitational radiation reaction to a particle motion. *Physical Review D*, 55(6):3457, 1997.

[198] H. Yang, F. Zhang, S. R. Green, and L. Lehner. Coupled oscillator model for nonlinear gravitational perturbations. *Physical Review D*, 91(8):084007, 2015.

[199] P. Zimmerman. Gravitational self-force in scalar-tensor gravity. *Physical Review D*, 92(6):064051, 2015.